UNITED STATES DEPARTMENT OF THE INTERIOR
GEOLOGICAL SURVEY

Electrical Survey of the Honey Lake Valley, Lassen County, California and Washoe County, Nevada

by

Herbert A. Pierce and Donald B. Hoover[1]

Open-File Report 88-668
1988

[1]U.S. Geological Survey, Box 25046, MS 964, DFC, Lakewood, CO 80225

Introduction

During April 1988 the U.S. Geological Survey (USGS) performed a series of electrical soundings and telluric traverses in and north of Honey Lake Valley (fig. 1). Seventeen multi-frequency audio-magnetotelluric (AMT) and seventeen magnetotelluric (MT) soundings were recorded as well as two telluric traverses (TT-1 and TT-2, fig. 1) to define the resistivities and changes in resistivity in and near the basin. The work was done to help determine subsurface geology and thickness of basin fill. The information will eventually be integrated into ground water flow models.

The area includes part of northeastern California and northwestern Nevada in the Basin and Range province. The area is near the boundary between the northern Sierra Nevada Range, the southern Cascades and the Basin and Range provinces.

Four USGS-built instruments were used in this survey: the multi-frequency AMT receiver (4.5 to 27kHz), an experimental "suitcase" MT receiver (.001 to 0.5 Hz), the multi-frequency telluric traverse receiver (4.5 to 14kHz), and the 0.025 Hz telluric traverse receiver. The AMT and MT systems measure naturally occurring electric and magnetic fields from which apparent resistivities at several frequencies are calculated. The frequency versus apparent resistivity curves may be inverted to give a resistivity curve as a function of depth. The telluric systems only measure the natural electric fields within their frequency range, which indicate relative differences in resistivity along the traverse. To provide resistivity data on the telluric lines, three AMT soundings coincident with the telluric lines were measured, allowing ratioed electric field data to be converted to apparent resistivities.

The main objectives were to map depth-to-basement and ascertain thickness of some of the volcanic flows. It was hoped that shallow and deep resistivity boundaries could be modeled by combining the high (14kHz to 4.5Hz) and low (.5Hz to .001Hz) frequency data sets and performing joint inversions.

Magnetotelluric and Audio-magnetotelluric Methods

The MT method is an electromagnetic sounding method that measures variations in earth resistivity as a function of depth (Keller and Frischknecht, 1966). The soundings are obtained by measuring the earth's surface electromagnetic fields at different frequencies. Because lower frequency electromagnetic waves penetrate further into the earth than higher frequency waves, measurement of the electromagnetic fields over a broad frequency range gives information on differences in resistivity with depth. The audio-magnetotelluric (AMT) method samples the electric and magnetic fields in the audio-frequency range, about 1 Hz to 27 kHz. This method is discussed in detail by Strangway and others (1973); the application and details of the USGS AMT system are given by Hoover and others (1976; 1978) and Hoover and Long (1976).

Apparent resistivities are calculated from AMT measurements by a method similar to MT measurements. The AMT system measures both the electric field (E-field) and the magnetic field (H-field) at each frequency. Amplitudes of

corresponding electric and magnetic field pulses are digitized and apparent resistivities are calculated using the following Cagniard (1953) equation:

$$\rho a = 1/5f[E/H]^2 \qquad (1)$$

where ρa is apparent resistivity in ohm-m, and f is frequency in Hz. E is the E-field magnitude in mV/km and H is the H-field in gammas.

The depth of exploration of the AMT and MT methods is not only a function of frequency, but also of the resistivity of the volume of earth sampled. For a homogeneous earth the maximum depth of exploration (D) in meters can be approximated by a relationship given by Bostik (1977).

$$D = 355\sqrt{\rho a/f} \qquad (2)$$

where ρa is the half-space resistivity in ohm-m, and f is the frequency in Hz.

All sounding techniques measure the earth laterally as well as vertically below the measuring station. Thus, in areas of complex geology, one-dimensional model interpretations may be significantly biased and may not be accurate representations of the vertical distribution of resistivity beneath the sounding site.

Sources of the MT signals are the time-varying portion of the earth's natural magnetic field which induces current flow in the earth (Keller and Frischknecht, 1966). Sources of the AMT signals may be either artificial or natural. The USGS equipment used in this survey is designed for use with natural sources. The principal source of natural electromagnetic energy in the audio-magnetotelluric frequency range is electrical discharge during lightning storms. Typically, the signal strength is low except when generated by local storms. The low signal strength can result in poor quality data, especially in the 1 kHz to 4 kHz frequency range where the energy is attenuated by propagation in the earth-ionosphere waveguide. Figure 2 shows some of the frequencies and amplitudes for the bands sampled by the four geophysical receivers. Figure 2 shows a second area of low signal strength at around 1 Hz. The limitations of natural source AMT exploration are discussed more fully by Hoover and others (1978).

The AMT soundings used 25 m-long telluric dipoles, and the MT soundings used 75 m-long telluric dipoles. Both the MT and AMT induction sensors and receiving systems were built by the USGS geophysics instrument laboratory in Denver, Colorado.

Telluric traverse method

The telluric traverse (TT) method employs natural earth currents (telluric currents) at different frequencies to measure, indirectly, changes in earth resistivity along a traverse. It was used as early as 1921 (Leonardon, 1928) by C. Schlumberger, but until recently has not been used very much in the United States. Beyer (1977) discusses the method in detail and presents a series of curves computed for two-dimensional structures. He concludes that the method is well suited for rapid reconnaissance in regions of several hundred square-kilometers when searching for targets such as hydrothermal systems. The method also should be suitable for locating fossil

hydrothermal systems and related mineral deposits, because rock alteration remains after hydrothermal convection has ceased. We have found that the technique is also useful in mapping faults and other geologic boundaries.

In applying the technique, a receiving array of three equidistant, in-line electrodes is used. This array represents two colinear dipoles sharing a common central electrode. The potential difference across each dipole is proportional to the component of the telluric field in the direction of the array. This configuration permits the simultaneous measurement of the telluric field at two dipoles in the direction of the traverse. The traverse is extended by moving the three-electrode array forward one dipole length so that the forward electrode site becomes the center electrode site for the next two measurements. This process is repeated for as long as desired.

Telluric measurements are made in a narrow frequency band typically using micropulsations with periods of about 30 seconds (0.033 Hz), but may be made over a wide range of frequencies. Because lower frequency electromagnetic signals penetrate deeper than higher frequency signals, one can, to some extent, select a maximum depth of exploration. The formula for maximum depth of exploration is the same as for AMT work (equation 2). Frequencies selected for this survey were 0.025, 7.5, 27, and 270 Hz. The telluric receivers used were designed and manufactured by USGS.

Combined telluric and resistivity methods

After the telluric ratios are calculated and the apparent resistivities are calculated from the corresponding AMT and MT soundings, resistivity values can be assigned to the telluric ratios and an electrical cross section constructed. If the traverse is run in the transverse magnetic (TM) mode, that is, if the profile is perpendicular to the geologic strike and the structures are assumed to be two-dimensional, then the apparent resistivities are proportional to the square of the telluric ratios along the traverse.

Data discussion

The data consist of two telluric traverses, and 17 MT and AMT stations. For each location (fig. 1), an AMT and an MT sounding were made in two orthogonal directions (typically north-south and east-west). Soundings are made in 2 directions because real earth resistivities near structures or other inhomogeneities vary with measurement direction. Presentation of the data will be MT, AMT, Telluric traverses, and electrical cross sections.

MT data

The scheme for numbering the station locations is MTHOXX. The alpha characters, MT, designate a magnetotelluric data set, HO stands for Honey Lake, and XX is a sequential number assigned to the station. Most of the experimental MT data sets in this study contain large errors in apparent resistivities, phase, and skew, partly as a result of failed individual components of the receiver-coils, coaxial lead-in cables, and magnetic induction pre-amplifiers. Previous MT soundings (Lassen 2 and 4, fig. 1) supplied by Dal Stanley, U.S. Geological Survey (written communication, 1988) suggest that noise in these soundings has decreased the apparent resistivities by an order of magnitude and rendered them unusable (Figure 3).

Appendix 1 shows the rotated (tensor) computer results for the 17 MT stations and the smoothed AMT values plotted with the MT data. MT data include apparent resistivities, phase, Z-maximum direction, and skew. Confidence intervals for all values are shown by error bars. The "X" data points and associated error bars for apparent resistivity, phase, and Z-maximum direction are for the north-south electric line (dipole) orientation. The phase values for a layered one-dimensional model generally fall on the 45 degree line, less than 45 degrees indicates more conductive rocks and more than 45 degrees more resistive rocks. The tensor results show the "X" data point rotated in the strike direction.

Appendix 2 contains the unrotated MT data and the actual resistivity values for the two AMT sounding directions (X=electric field line oriented north-south, Y=electric field line oriented east-west). The Z-maximum directions for the various frequencies are zero because the orthogonal soundings are not rotated in the strike direction.

Sounding MTH001 is about 100 m north of the Don Dow well (Sect. 36, T29N R14E). Significant contrast between the resistivities of the sediments and the basement rocks is necessary in order to map depth-to-basement. Resistivities of the sediments at MTH001 are about 3 to 18 ohm-m (from AMTH001, Appendix 3) and resistivities of the basement rocks 10 to 15 ohm-m (from Wellex log). The small contrast is easily masked by the 4000 feet (1219 m) of conductive sediments. The Wellex log only penetrated the basement rocks 160 feet (49 m) and most of that probably is in the weathered zone. Using equation 2, assuming an average resistivity of 10 ohm-m for the 1219 m of valley sediments and solving for frequency, the highest frequency that should sense the top of the basement is .85 Hz. For this study, however, the frequency range from 0.1 to 1.0 Hz was unreliable for all 17 MT stations for reasons discussed previously.

Dal Stanley's MT sounding Lassen 2 (figure 3) is a good sounding to compare with sounding MTH004 (Appendix 3). Lassen 2 shows a curve that becomes resistive with lower frequencies whereas MTH004 remains conductive (<10 ohm-m). Lassen 2 shows about 1725 m (5660 feet) of sediments atop the resistive basement rocks near MTH004. MTH004, however, shows conductive sediments to the maximum depth of penetration 35,000 feet (10.6 km). This is inconsistent with known Basin and Range geology.

AMT data

Appendix 3 contains the scalar AMT sounding curves. The station numbering scheme is the same for the MT stations except that AMT proceeds the H0XX characters. The apparent resistivities range from about 2 ohm-m to more than 3200 ohm-m at depth. Generally the curves from Honey Lake Valley display flat and conductive (about 10 ohm-m) apparent resistivities. The sounding curves for AMTH003 and AMTH006 located on volcanic rocks display apparent resistivities of about 30 ohm-m. The sounding curves located on the granites of the Fort Sage Mountains (AMTH011) are the most resistive (400 to >2000 ohm-m). AMTH012, on the volcanic rocks near Fish Springs Ranch, displays apparent resistivities of about 60 ohm-m.

Telluric traverses

Two north-south trending telluric traverses were recorded with the multi-frequency telluric receiver and the 0.25 Hz telluric receiver. The ratios are tabulated in appendix 4 and the relative telluric voltages are plotted together on figures 4 and 5 for TT-1 and TT-2 respectively.

Telluric traverse number 1 (TT-1, fig. 4) shows more than 10 to 1 change in relative voltage from the Fort Sage Mountains on the south to the sediments in the Honey Lake Valley. The steep gradient from station 0 to 1000 reflects the fault contact. From station 1000 to 3000 the slope of the curves is not as great. This gradual slope has four possible causes: a gradual coarse-to fine-grained rock sequence from the topographically higher mountains north into the valley, a dilution of conductive saline water in the valley by a tongue of fresh water from the higher granites, a dry alluvial fan at the base of the range front, or a "step" in the fault contact at depth that changes the slope because its expression is masked by conductive alluvial cover. Most probable is a combination of fresh water from the slopes of the granites in the coarse-to-fine grained alluvial fan at the base of the mountains. This interpretation will be discussed further in the electrical cross section. Probably the most intriguing feature of TT-1 is the moderately sharp rise in the 0.025 Hz curve between stations 8000 and 8500. This suggests a fault in the basement 8 km north of the range front fault. The fault is probably the north boundary of a graben structure about 7 km wide. Another interesting feature seen in the higher frequency curves (7.5, 27, and 270 Hz) is that the lowest points on the three curves, measuring only valley fill at maximum sounding depth of exploration, are directly over the step in the basement. This suggests some alteration of the valley fill, probably saline fluids circulating upward from the fault. These fluids may be circulating currently or may be the remnant of a circulating cell. Another possibility is a hydrothermal system, though the data do not confirm this interpretation.

Telluric traverse number 2 (TT-2, fig. 5), located just east of Fish Springs Ranch, shows the electrical response across a small resistive volcanic outcrop, a drop into the conductive alkali flat sediments, and a possible graben structure at depth. The volcanic rocks appear to continue to about station 2500 with gradually increasing amounts of conductive cover. The graben structure located between stations 2500 and 6000 is about 3.5 km wide. As in TT-1, the lowest ratios recorded for the 7.5, 27, and 270 Hz curves are atop the northern step in the graben structure (between stations 5000 and 7000), suggesting saline fluids mixing in the sediments.

Electrical cross-sections

The electrical cross section for telluric traverse number 1 (fig. 6) runs north-south along the Cal-Neva road in California. It starts on the granites of the Fort Sage Mountains and proceeds north 9.5 km onto the Honey Lake Valley sediments. From stations -250 to 0 the resistive (>1800 ohm-m) granites are evident. The steep gradient between stations 0 to 500 represents the range front fault. An interesting feature is the resistive (320 ohm-m) closed anomaly about 325 m (1000') deep centered between stations 1500 to 2000. The top of the anomaly is about 175 m (500') below the surface and the bottom appears to be near 475 m (1500') below the surface, based on the 56 ohm-m contour. The anomaly appears to tongue out from the granites and pinch

out near station 3000. The graben feature defined by the relative voltage changes (figure 3, 0.025 Hz curve) is not seen in the resistivity section because reliable MT resistivities at 0.025 Hz were not available.

The electrical cross section for telluric traverse number 2 (fig. 7) runs north from the Fish Springs Ranch with station 0 near the 90 degree bend in the road. The entrance road to the Fish Springs Ranch house is near station 500. The resistive volcanic rocks near the ranch are roughly outlined by the 56 ohm-m line, stations -500 to 1500. As on TT-1, figure 6, a resistive anomaly extends some distance out into the alkali flat area beneath conductive overburden to station 2500. Either the volcanics finger out into the sediments, or fresh water may be entering the saline basin sediments here with a depth from the surface to the top of the 56 ohm-m line of about 160 m (500 feet). This resistive zone pinches out towards the basin. The graben feature between stations 2500 and 6000 indicated on the relative voltage plots (fig. 5) is expressed in the AMT section as a conductive zone between stations 2500 and 6000 roughly outlined by the 18 ohm-m line. The graben structure appears to be slightly wider than 3 km.

Figure 8 is the electrical cross section constructed from the AMT data starting at the Don Dow well and proceeding north up Highway 395 towards Karlo. The line crosses volcanic rocks near Viewland that have an apparent thickness of about 600 m (1970 feet). The north end in the mud flat area and south end in the Honey Lake Valley are in basins that contain conductive sediments.

Figure 9 is the electrical cross section constructed from the AMT data only. The section is roughly parallel to the general strike of the valley. Station 6 shows a thin 45 m (150 feet) thick layer of volcanic rocks over sediments. Station 3 in the east-west orientation shows volcanics to a depth of 250 m (820 feet), assuming that the 32 ohm-m line coincides with the extent of the volcanics. Stations 16 and 17 show a general thickening of the volcanic cover to 450 m (1500 feet) and station 16 with 550 m (1800 feet) of volcanic cover. Between stations 16 and 17 the volcanic cover thins to 225 m (740 feet). This thinning may be due to a fault, a change in lithology, or simply less volcanics. Stations 15 and 14 are located in the valley fill and show low resistivities (3 to 10 ohm-m) typical of fine grained sediments.

Figure 10 is the north-south electrical cross section of the eastern part of the Honey Lake Valley in Nevada. Stations 14 and 13 are located on the conductive sediments. Station 12 is located south of the Fish Springs Ranch due east of Willow Springs. Resistivities at station 12 imply volcanics at the maximum depth of exploration, about 450 m (1480 feet). From this data set, thickness of the volcanics at station 12 is determined to be greater than 450 meters, but the total thickness cannot be calculated.

Figure 11 is the AMT electrical cross section north-to-south along the Cal-Neva road. Station 7 is on volcanic rocks. Stations 8, 9, and 10 are in the valley fill. Station 11 is on the granites of the Fort Sage Mountains and displays the most resistive vertical distribution.

Conclusions

Thickness of volcanic rocks in several parts of the basin were calculated from models based on the results of this study. However, depth to basement could not be determined because of technical problems encountered with our new experimental "suitcase" MT receiver.

The telluric methods were used to generally outline the basement and changes in the fill. Basement depths cannot be calculated from only the relative telluric voltage changes at 0.025 Hz. The telluric data (electric field data) suggest that the problem is solvable. In this environment, an MT data set obtained at the previously occupied 17 sounding sites would give accurate depth-to-basement values.

Acknowledgments

We would like to thank Doug Maurer (WRD Carson City) for assisting in the field work, for supplying gravity and magnetic models of the area, and for supplying the Don Dow Wellex logs. We give special thanks to Dal Stanley, USGS, for modeling and for supplying unpublished MT data that served as a critical check on the experimental "suitcase" MT system.

References

Beyer, J. H., 1977, Telluric and d.c. resistivity techniques applied to the geophysical investigation of Basin and Range geothermal systems, Part 1: The E-field ratio Telluric Method, LBL-6325-1/3: Lawrence Berkeley Laboratory, University of California, Berkeley.

Bostik, F. X., Jr., 1977, A simple and almost exact method of MT analysis. Geothermal Workshop Report, University of Utah, U.S. Geological Survey Contract 14-08-0001-6-359, p. 175-177.

Cagniard, Louis, 1953, Basic theory of the magnetotelluric method of geophysical prospecting: Geophysics, v. 18, p. 605-635.

Hoover, D. B., Frischknecht, F. C., Tippens, C. L., 1976, Audio-magnetotelluric soundings as a reconnaissance exploration technique in Long Valley, California. Journal of Geophysical Research, v. 81, p. 801-809.

Hoover, D. B., and Long, C. L., 1976, Audio-magnetotelluric methods in reconnaissance geothermal exploration. Proceedings, 2nd U.N. Symposium, Developmental geothermal Resources, p. 1059-1064.

Hoover, D. B., Long, C. L., Senterfit, R. M., 1978, Some results from audio-magnetotelluric investigations in geothermal areas. Geophysics, v. 43, p. 1501-1514.

Keller, G. V., and Frischknecht, F. C., 1966, Electrical methods in geophysical prospecting. New York Pergamon Press, p. 197-350.

Leonardon, E. G., 1928, Source observations upon telluric currents and their applications to electrical prospecting. Terrestral Magnetism, v. 33, no. 2, p. 91-94.

Strangway, D. W., Swift, C. M., Jr., and Holmer, R. C., 1973, The application of audio-frequency magnetotelluric (AMT) to mineral exploration: Geophysics, v. 39, p. 1159-1175.

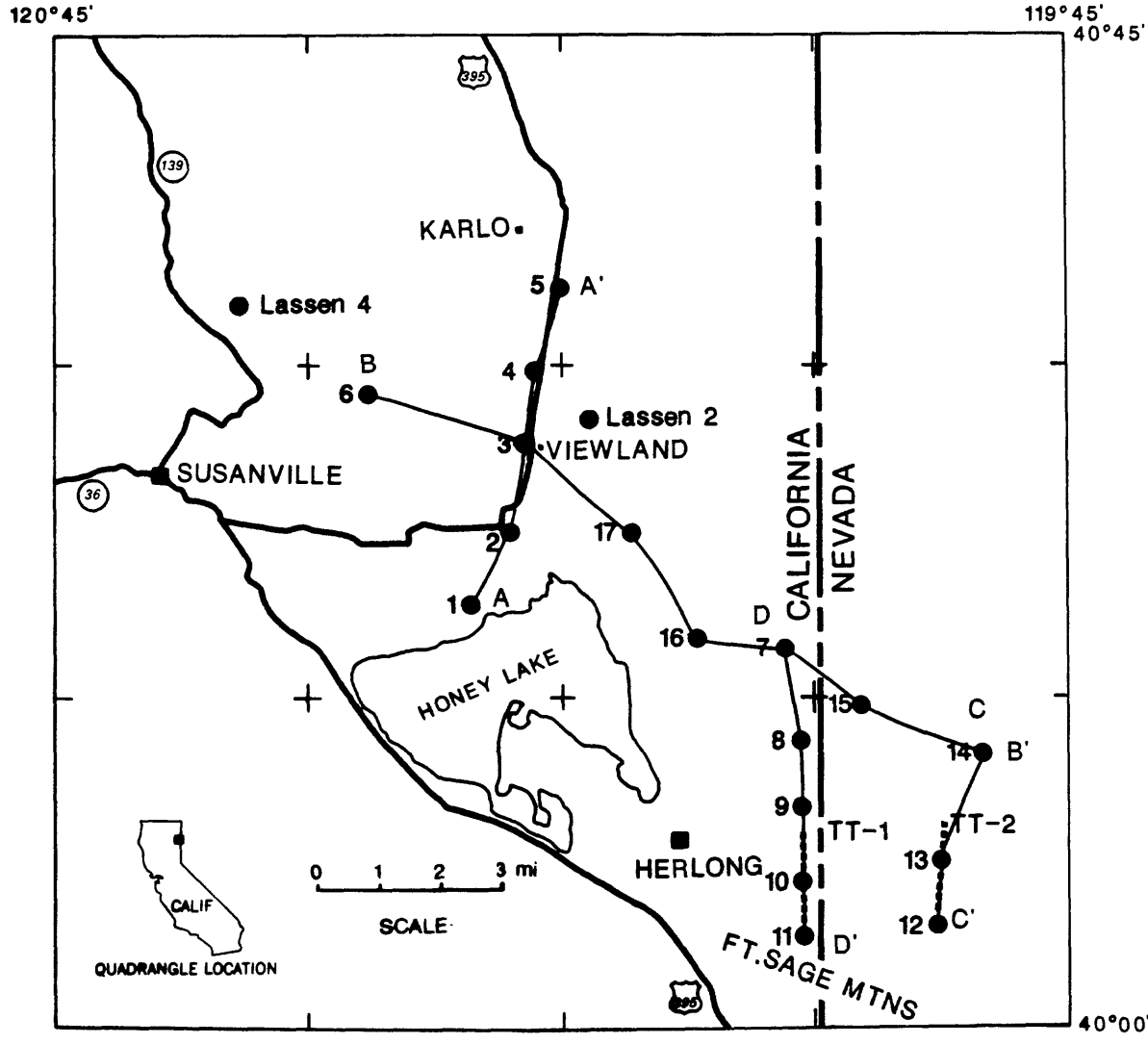

Figure 1. Location map for the MT, AMT, telluric traverses, and resistivity sections. Dots are AMT and MT stations. Dashed lines are telluric traverses. Thin lines between capitalized letters, i.e., A-A', are the end points for the electrical cross section.

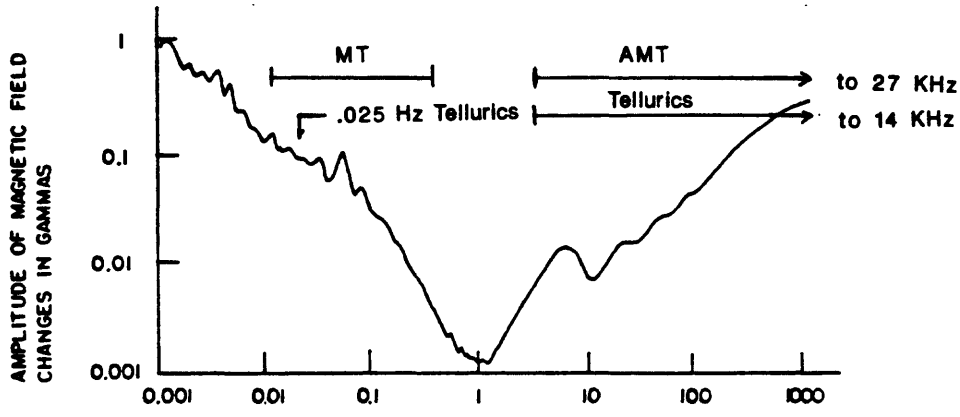

Figure 2. Typical spectrum of amplitudes of electromagnetic noise in the extremely low frequency (ELF) range (from Keller and Frischknecht, 1966. Partial frequency ranges of the MT, AMT and TT equipment are also shown.

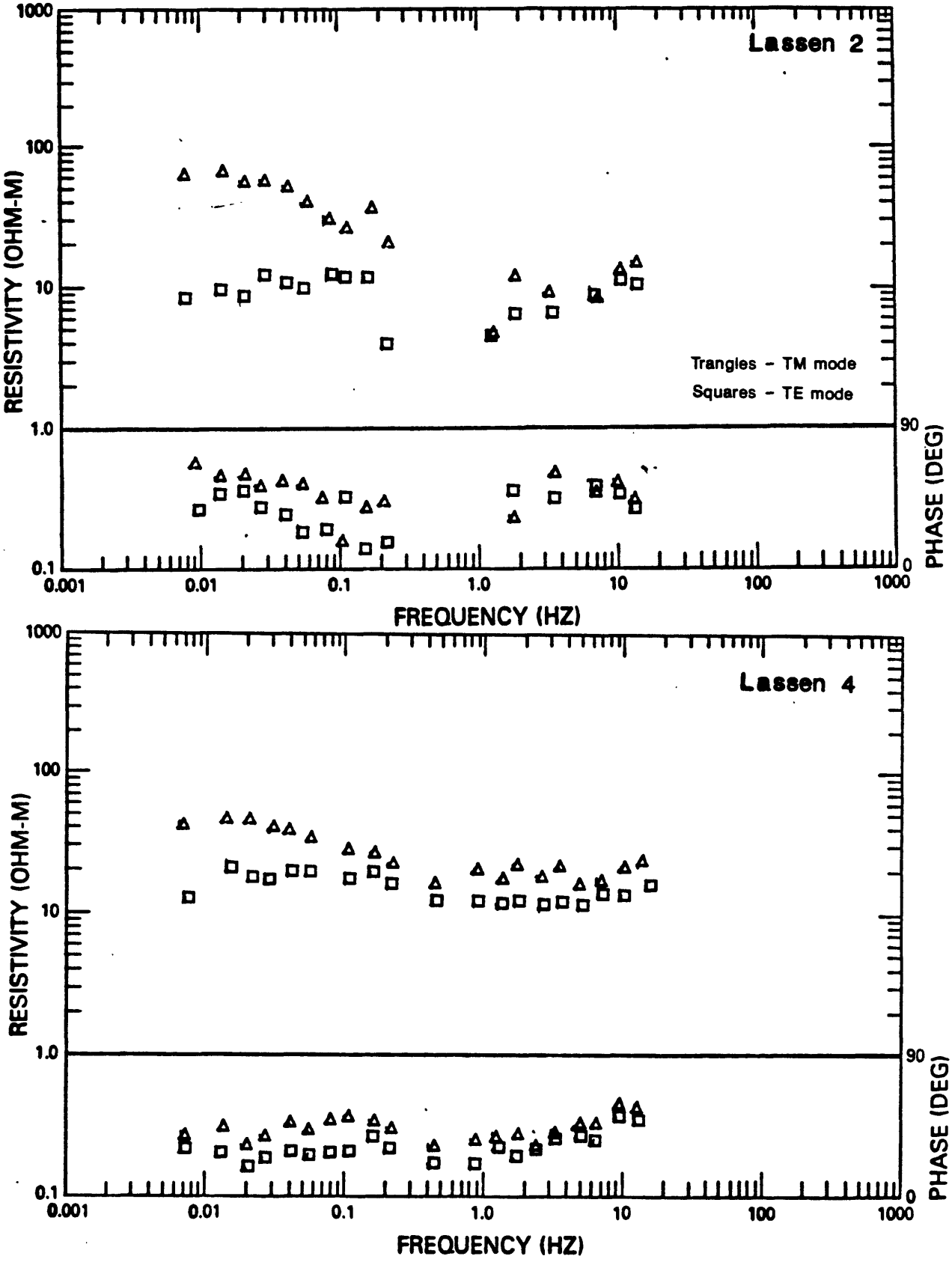

Figure 3. MT Soundings Lassen 2 and 4 from unpublished data collected by Dal Stanley (U.S. Geological Survey, written communication, 1988). These two soundings were used to check the experimental "suitcase" MT soundings in appendix 1 and 2.

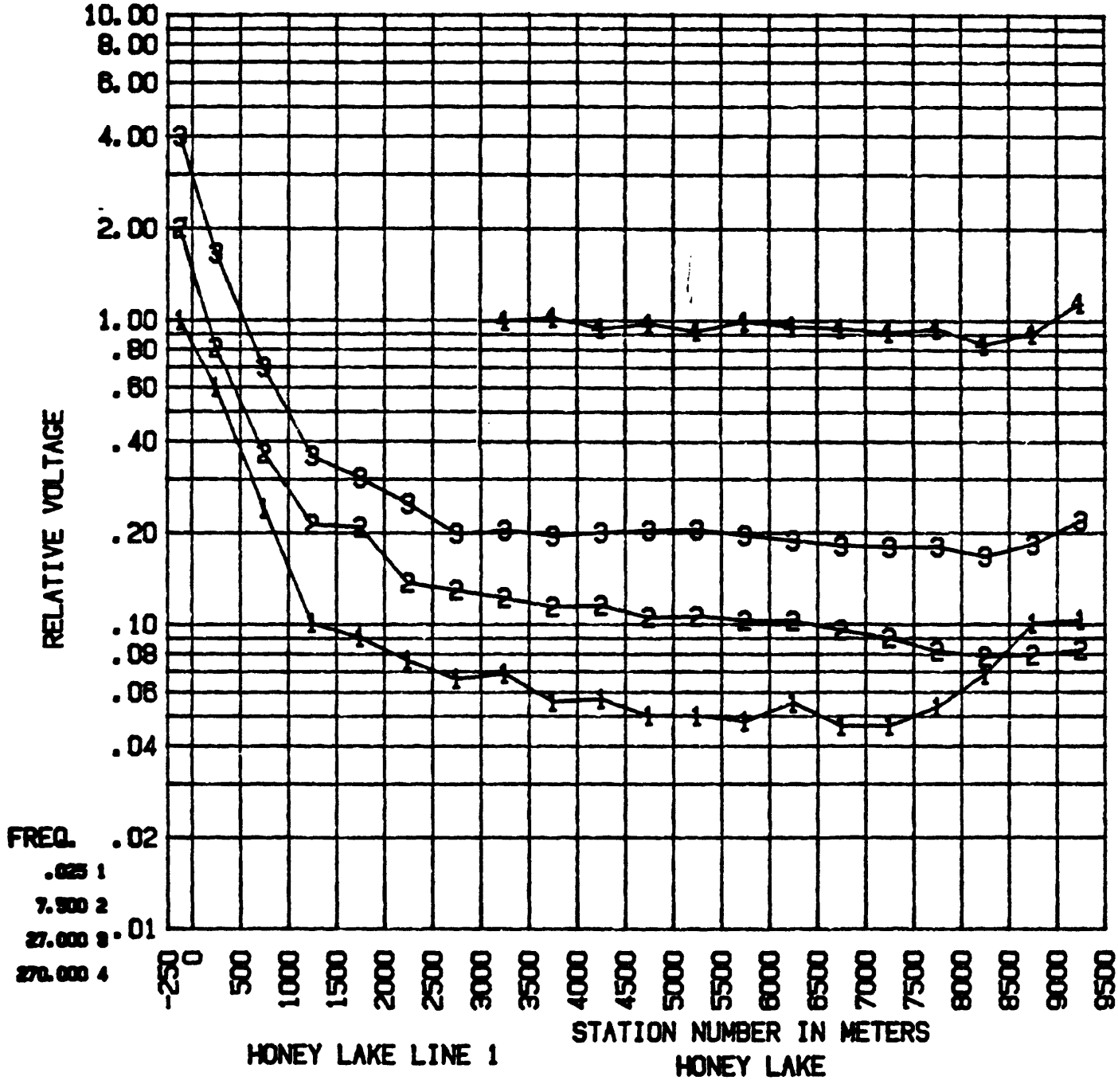

Figure 4. Telluric traverse 1 (TT-1) with sequential frequency offset by a factor of 2 to allow discrimination of the curves. Data for the 270 Hz curve was not recorded until station 3000-3500.

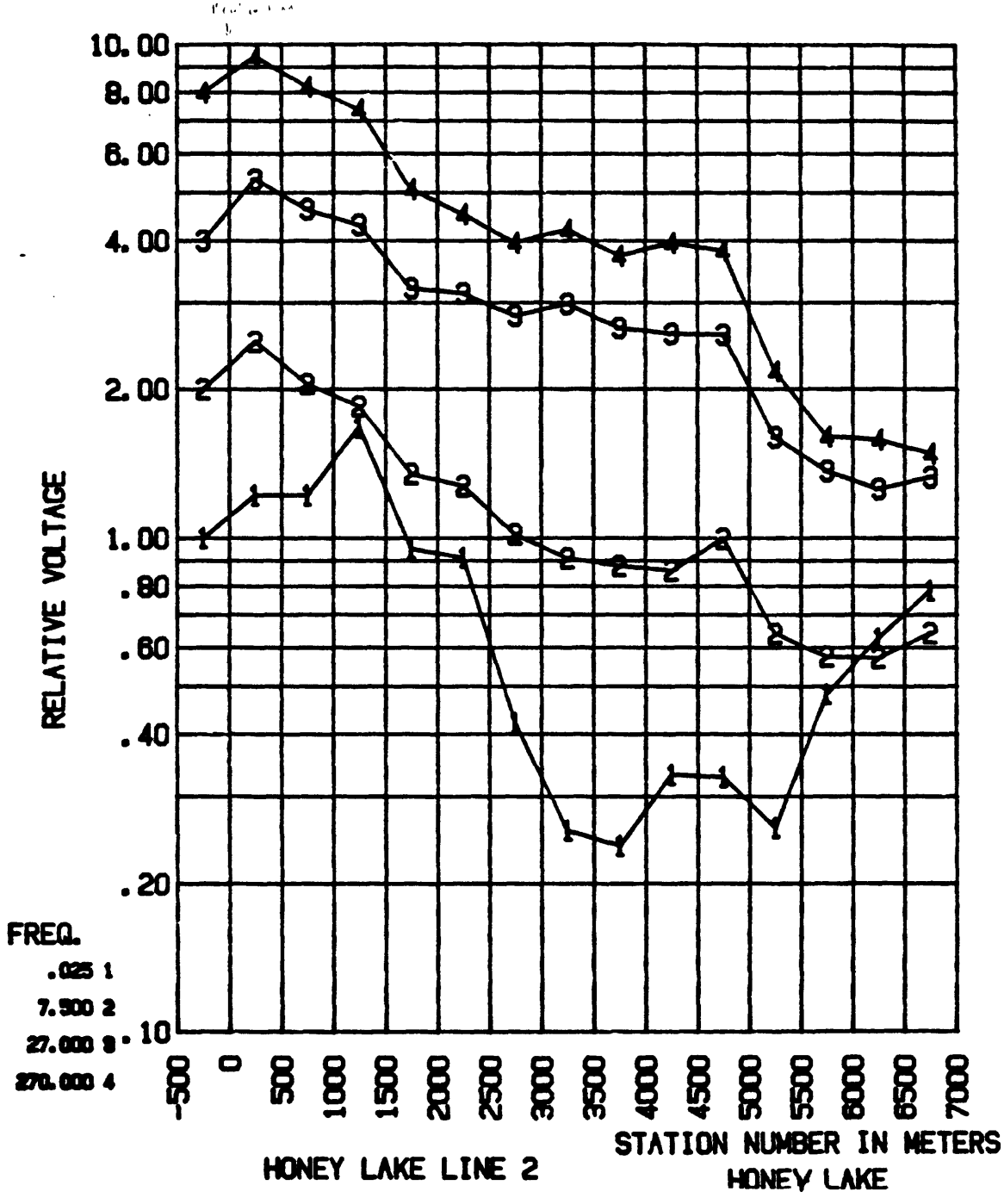

Figure 5. Telluric traverse 2 (TT-2) with sequential frequency offset by a factor of 2 to allow discrimination of the curves. Note the graben feature between stations 2500 and 6000 on the .025 Hz curve.

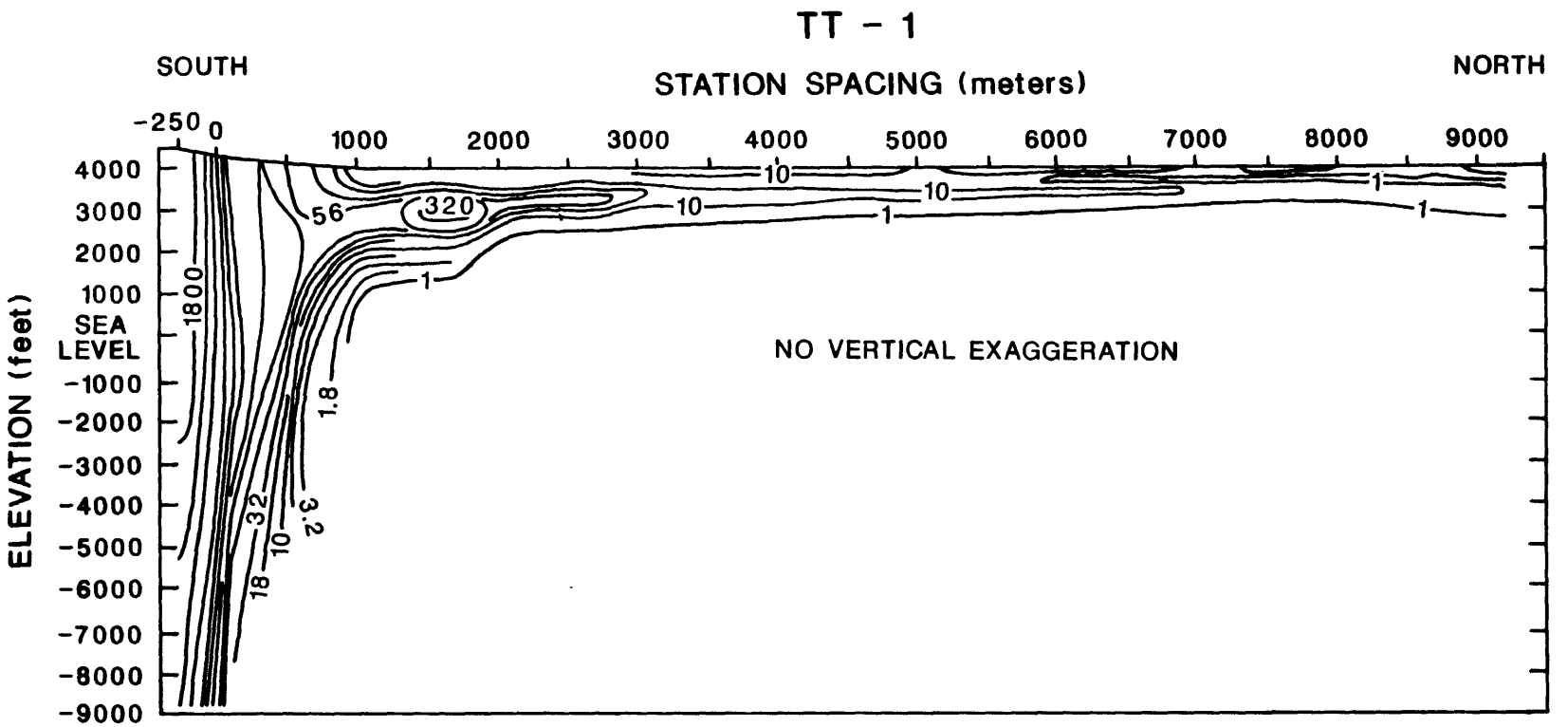

Figure 6. Electrical cross section along TT-1 contours are a logarythmic interval of four divisions per decade in ohm-m (10, 18, 32, 56, 100....),

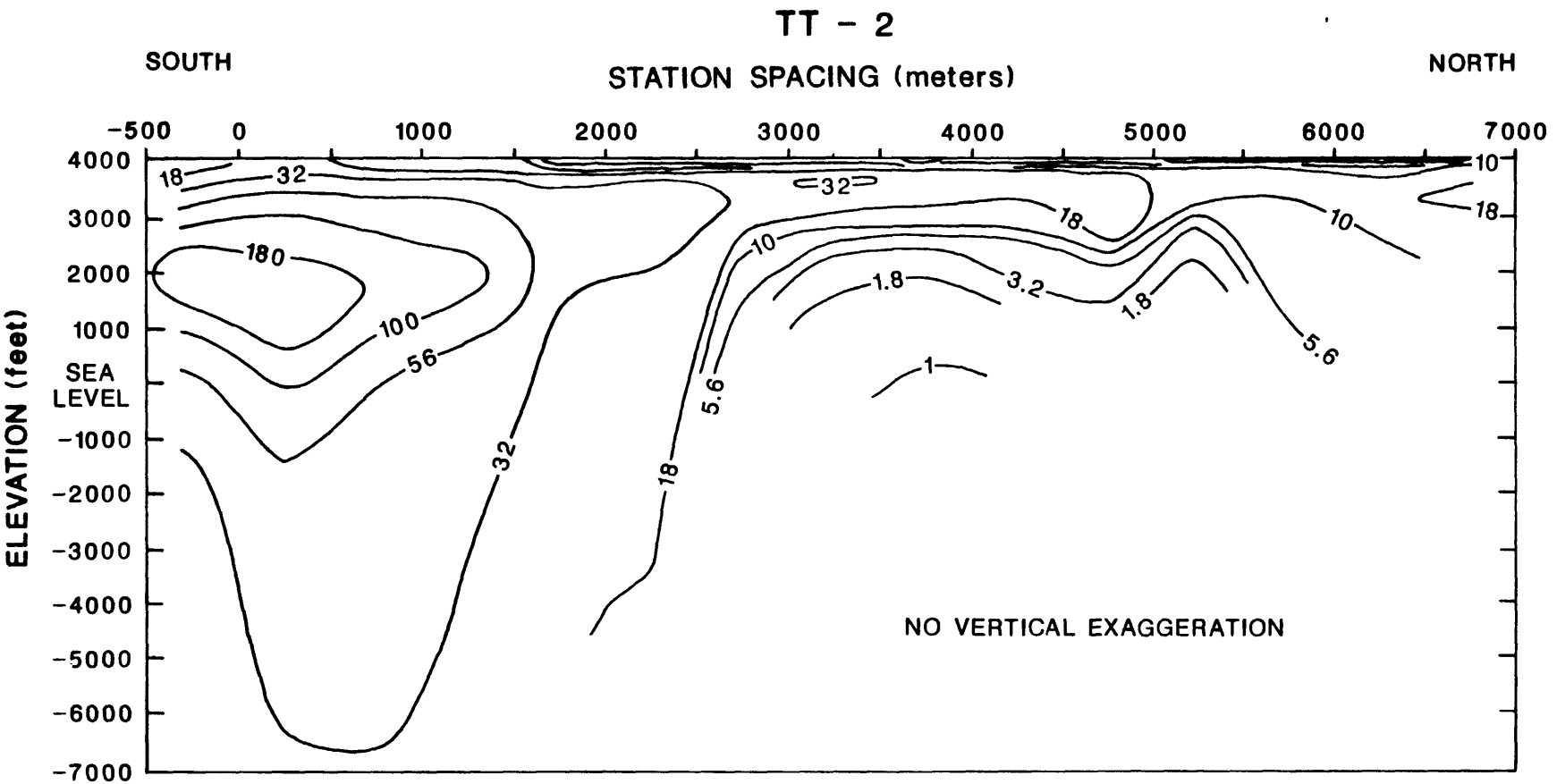

Figure 7. Electrical cross section along TT-2 contours are a logarythmic interval of four divisions per decade in ohm-m (10, 18, 32, 56, 100....).

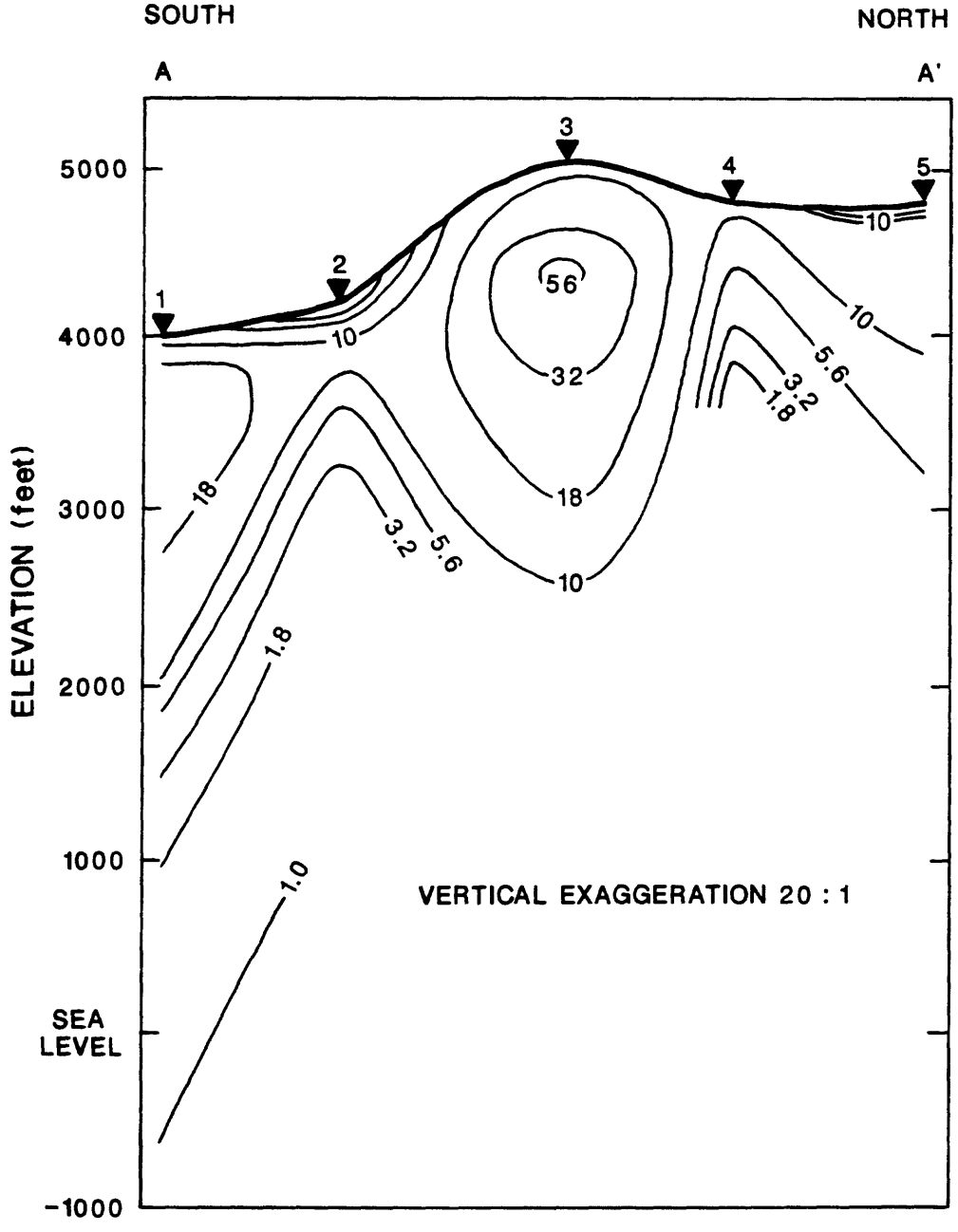

Figure 8. Electrical cross section from the Don Dow well north towards Karlo (A-A', fig. 1). Contours are a logarythmic interval of four divisions per decade in ohm-m (10, 18, 32, 56, 100....).

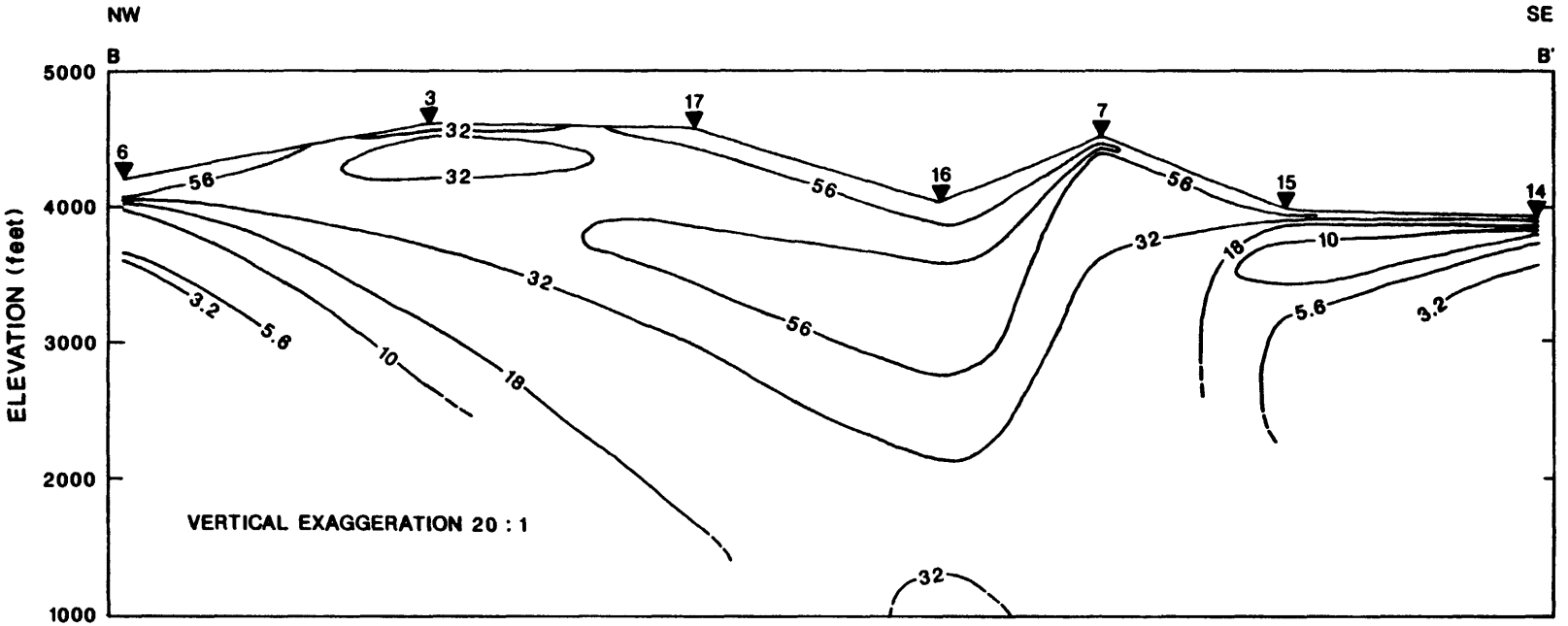

Figure 9. Electrical cross section roughly northwest to southeast (B-B', fig. 1) along the north side of Honey Lake Valley. Contours are logarythmic apparent resistivities in ohm-m from inverted AMT dat, 4 to a decade (10, 18, 32, 56, 100....).

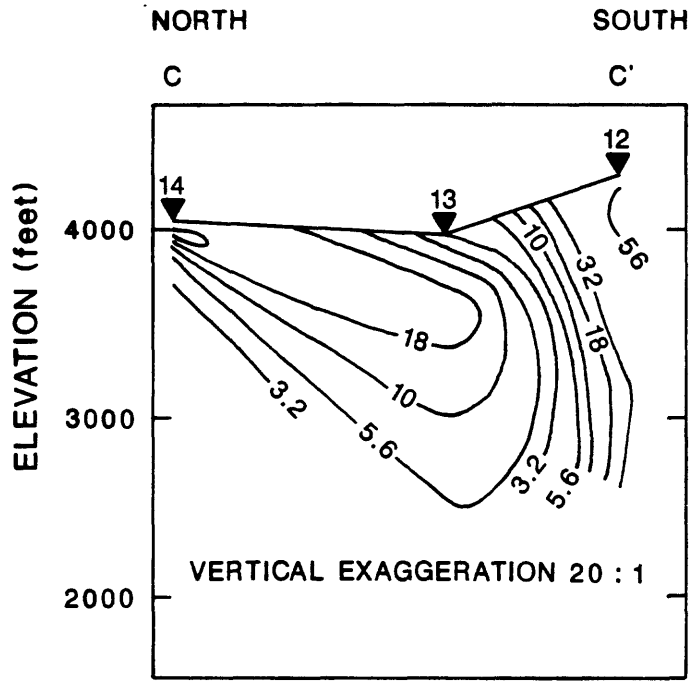

Figure 10. Electrical cross section along the eastern side of Honey Lake Valley from inverted AMT data (C-C', fig. 1). Contours are a logarythmic interval of four divisions per decade in ohm-m (10, 18, 32, 56, 100....).

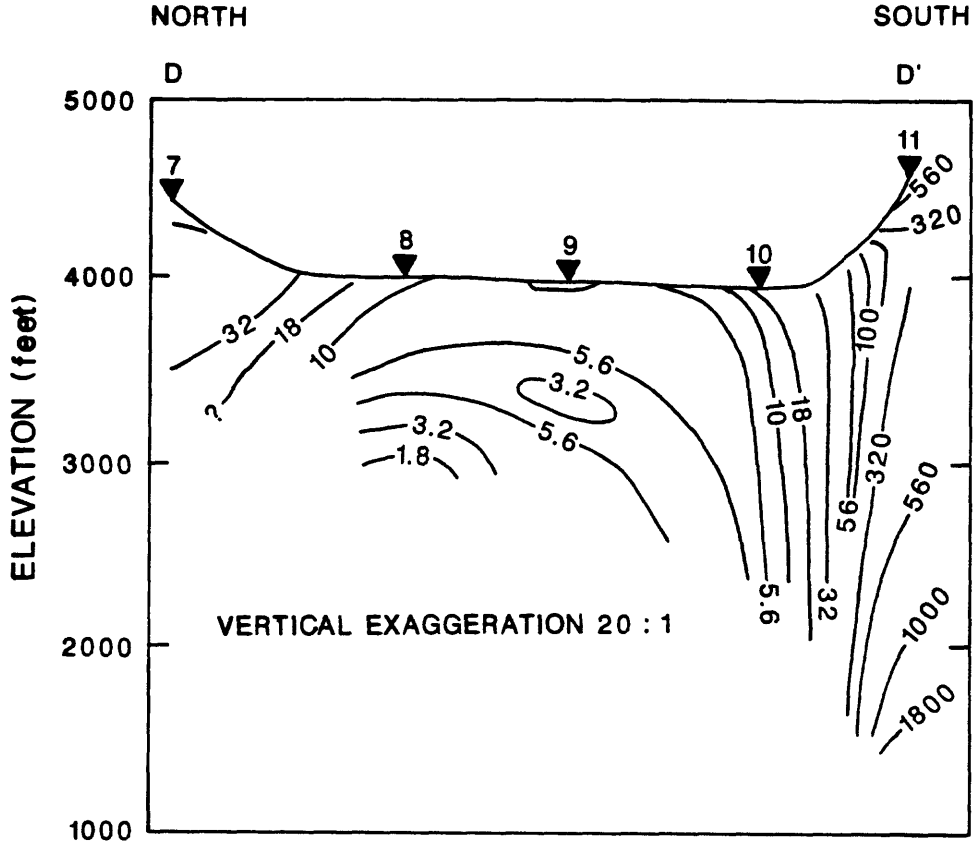

Figure 11. Electrical cross section across the Honey Lake Valley roughly parallel to the Cal-Neva road from inverted AMT data (D-D', fig. 1). Contours are a logarythmic interval of four divisions per decade in ohm-m (10, 18, 32, 56, 100....).

Appendix 1

MTH001 LOCAL H-ref 21:33:03 12 May 1988
APPARENT RESISTIVITY

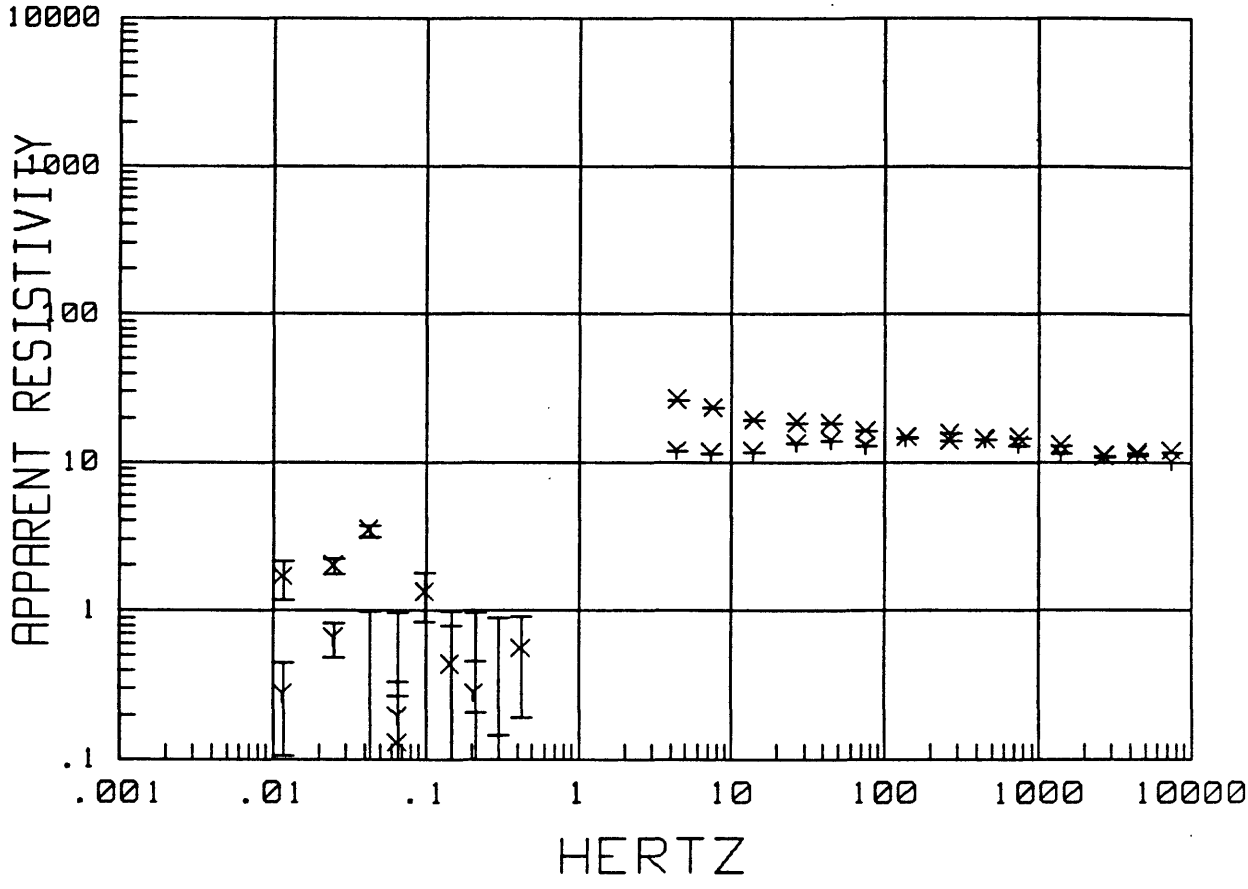

MTH001 LOCAL H-ref 21:33:03 12 May 1988
IMPEDANCE PHASE

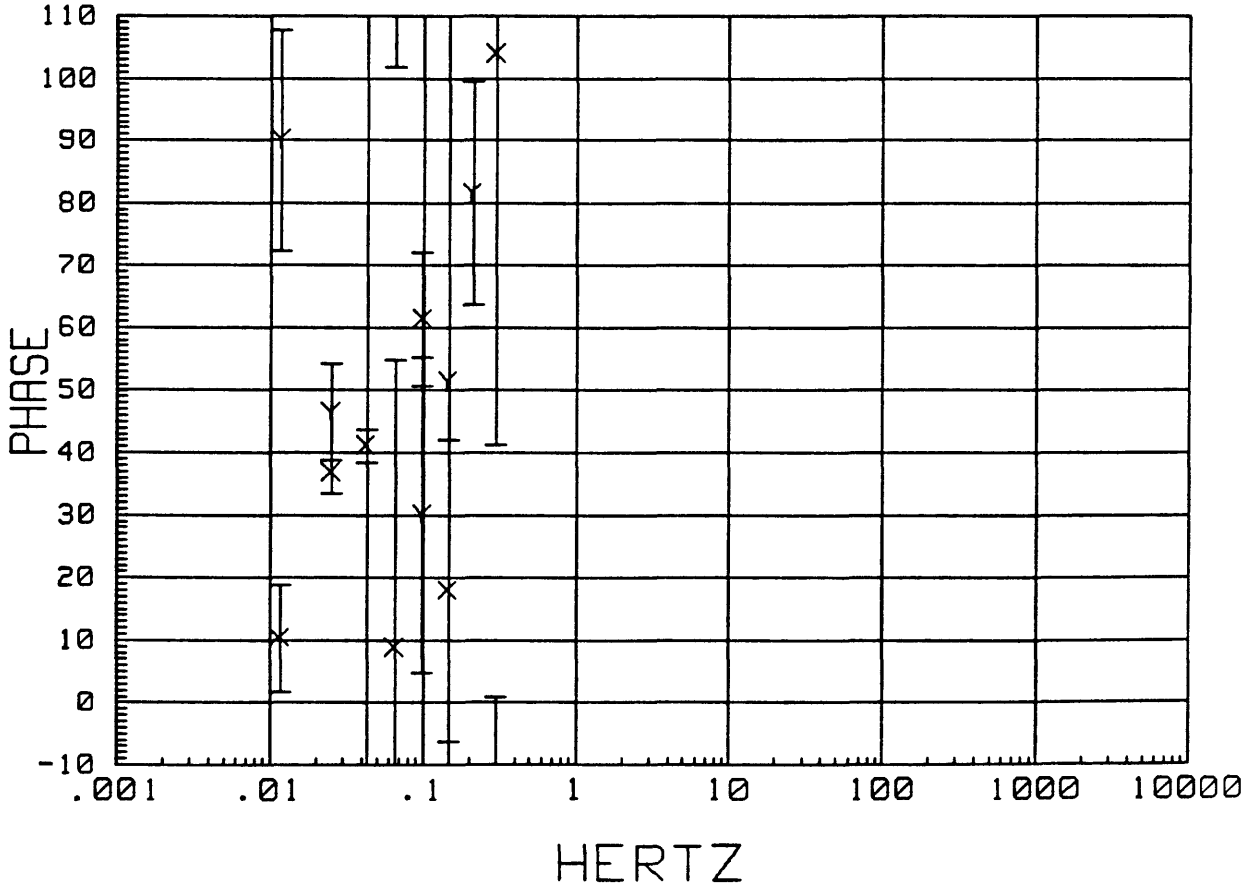

MTH001 LOCAL H-ref 21:33:03 12 May 1988
Z MAXIMUM DIRECTION

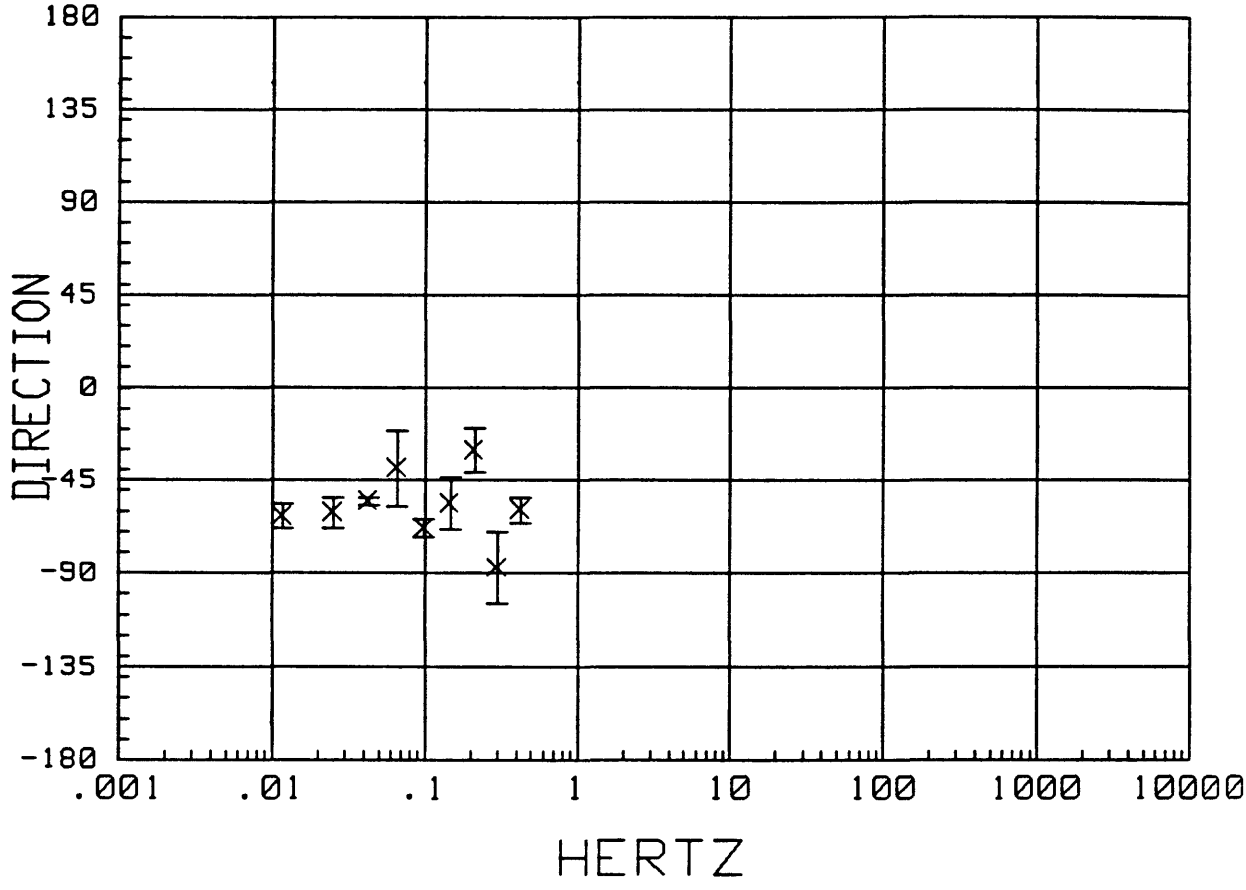

MTH001 LOCAL H-ref 21:33:03 12 May 1988
SKEW

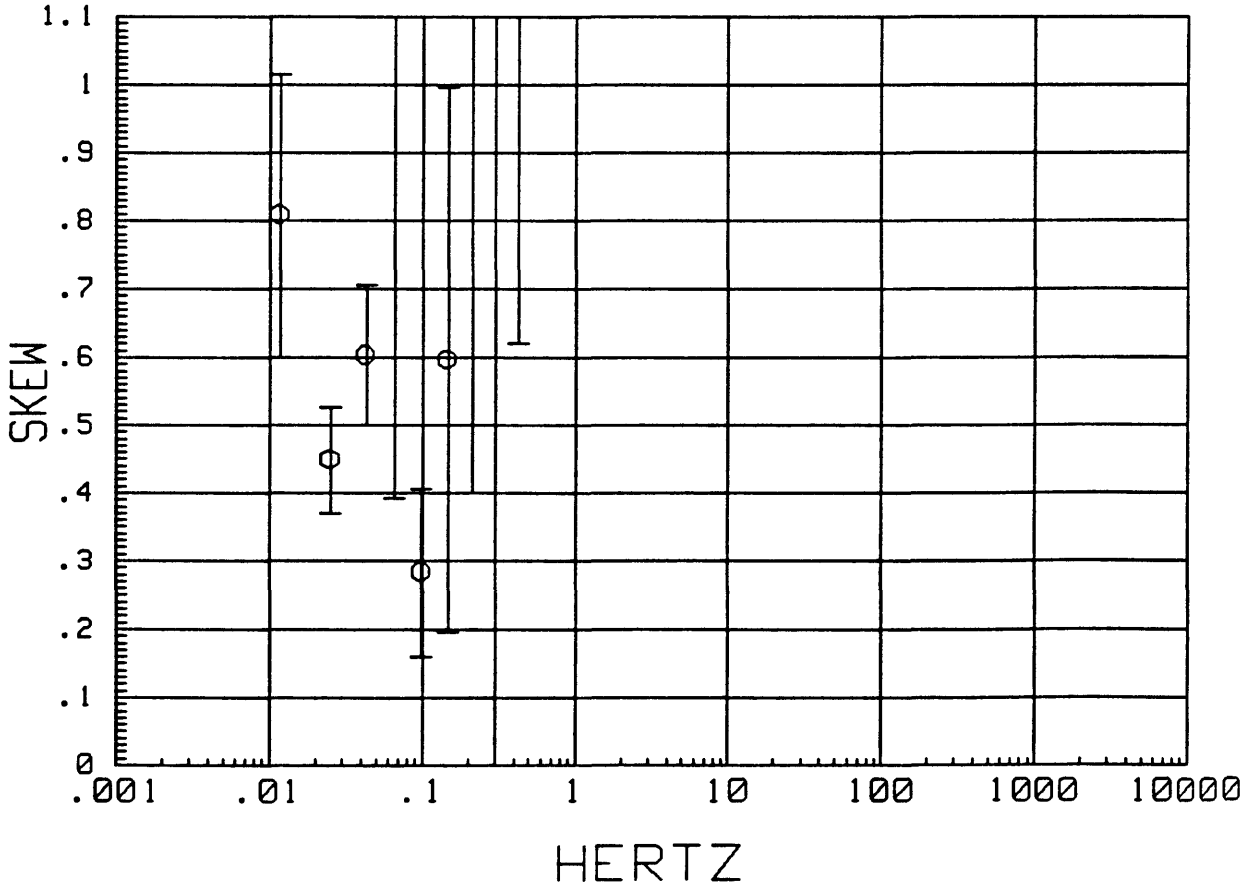

MTH002 LOCAL H-ref 21:10:24 12 May 1988
APPARENT RESISTIVITY

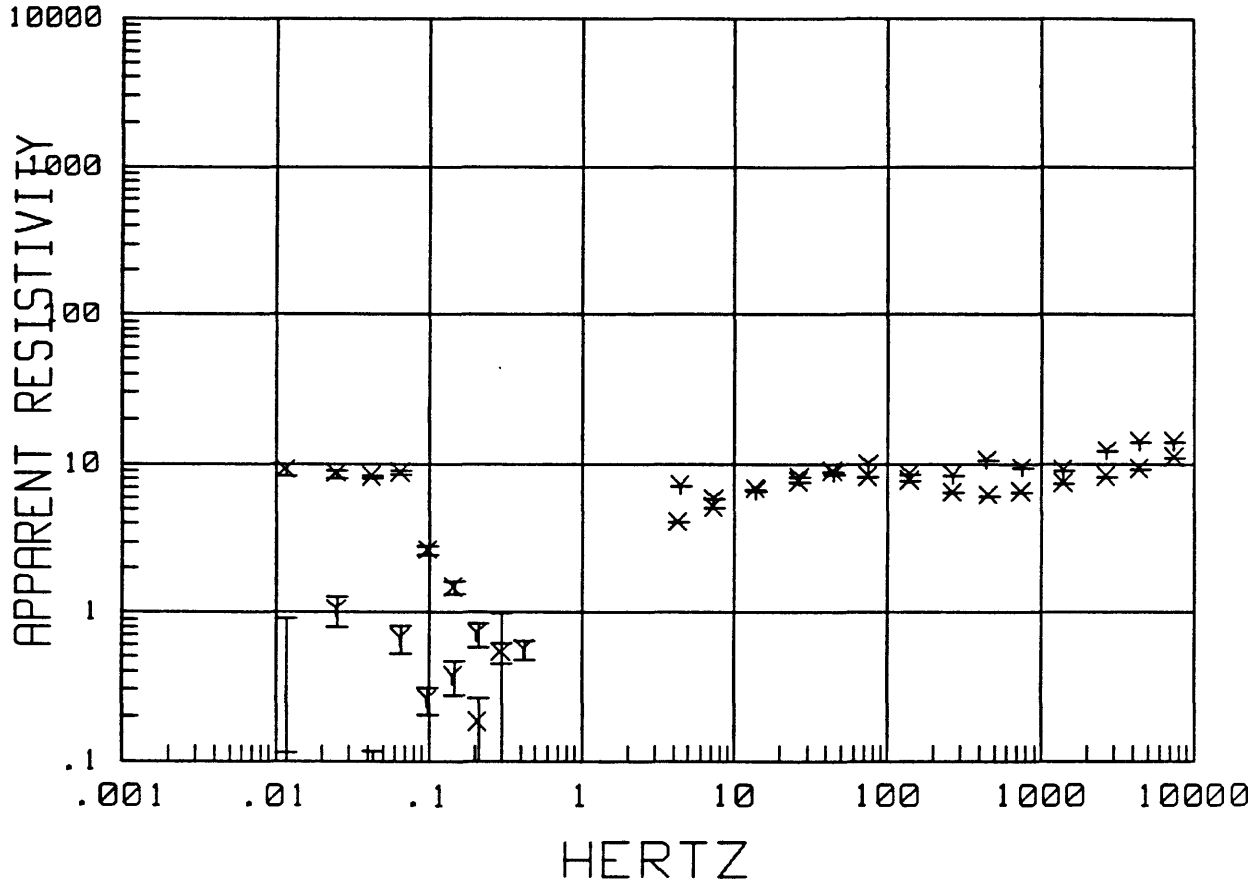

MTH002 LOCAL H-ref 21:10:24 12 May 1988
IMPEDANCE PHASE

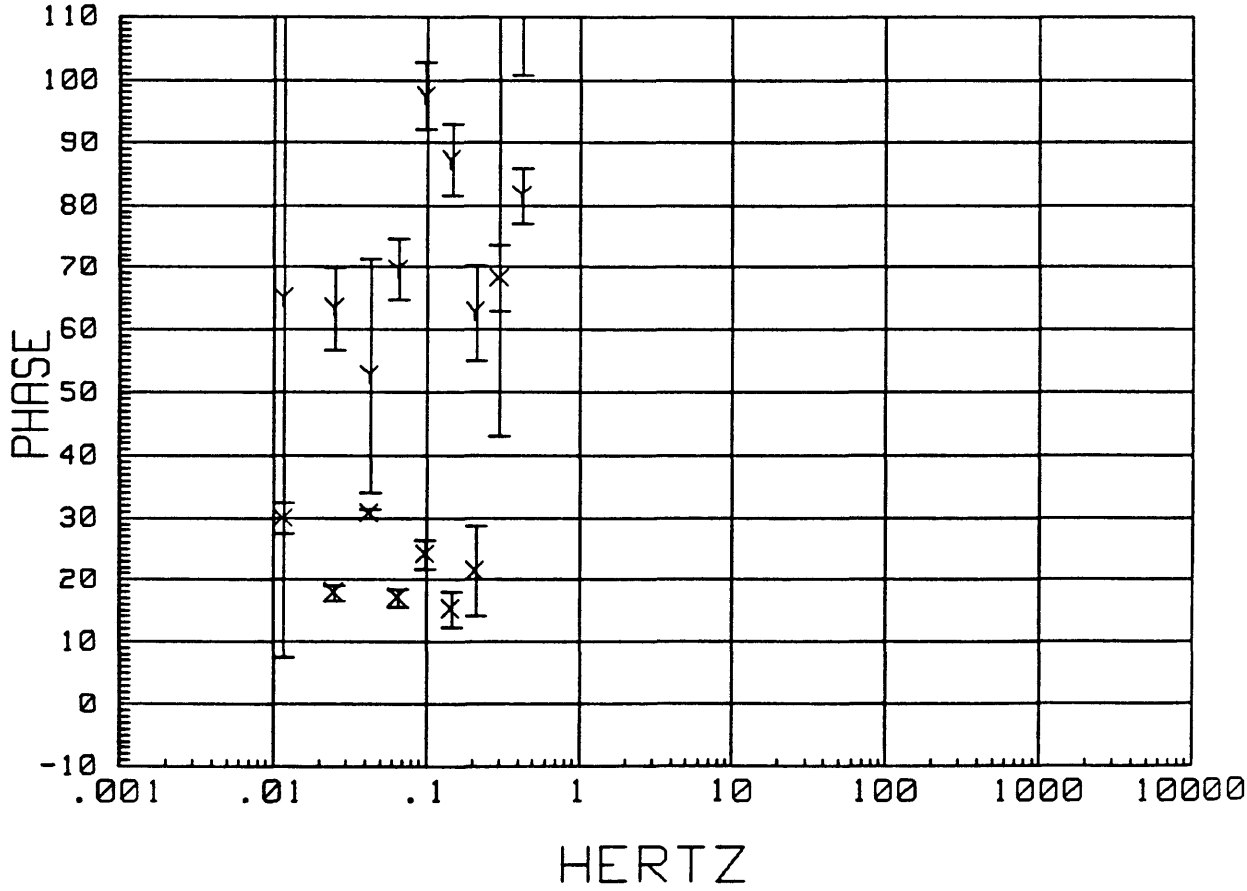

MTH002 LOCAL H-ref 21:10:24 12 May 1988
Z MAXIMUM DIRECTION

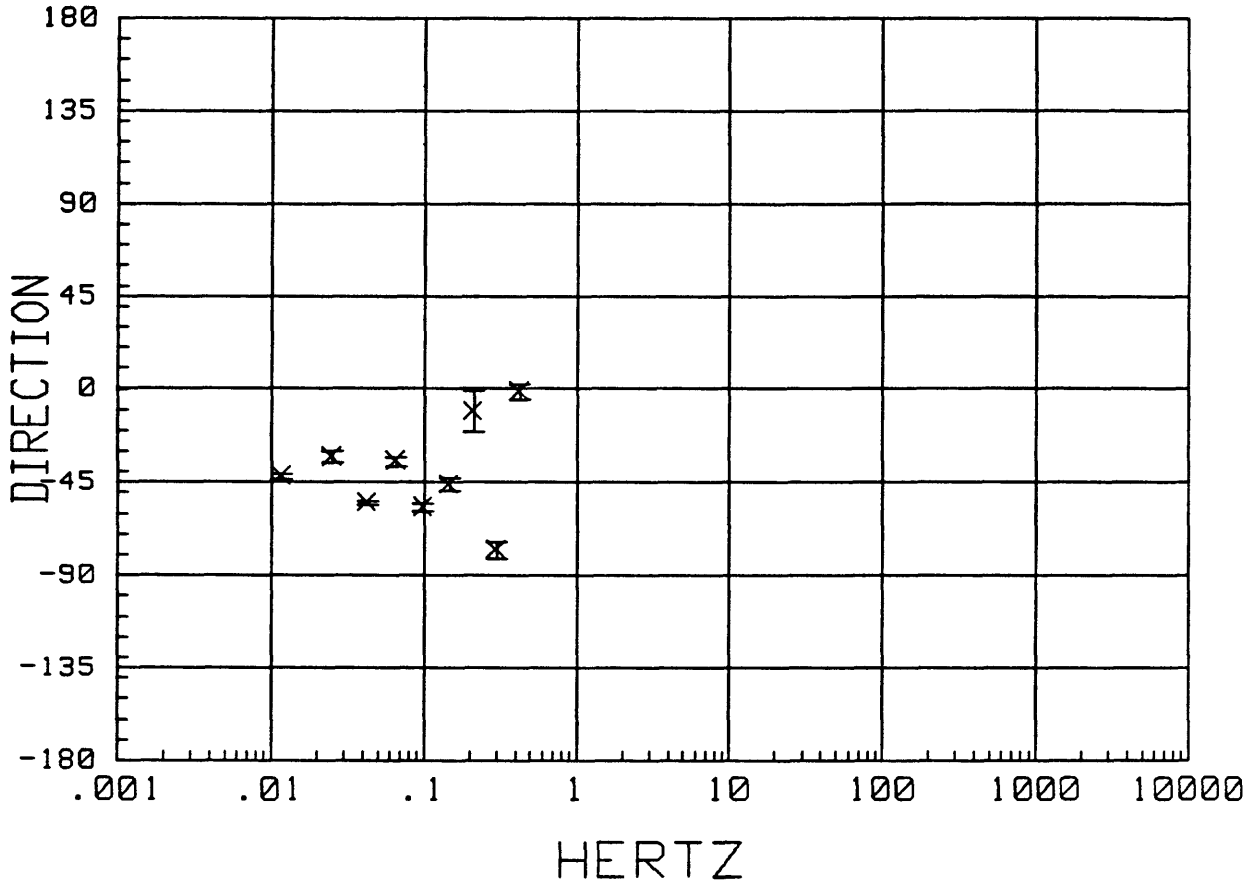

MTH002 LOCAL H-ref 21:10:24 12 May 1988
SKEW

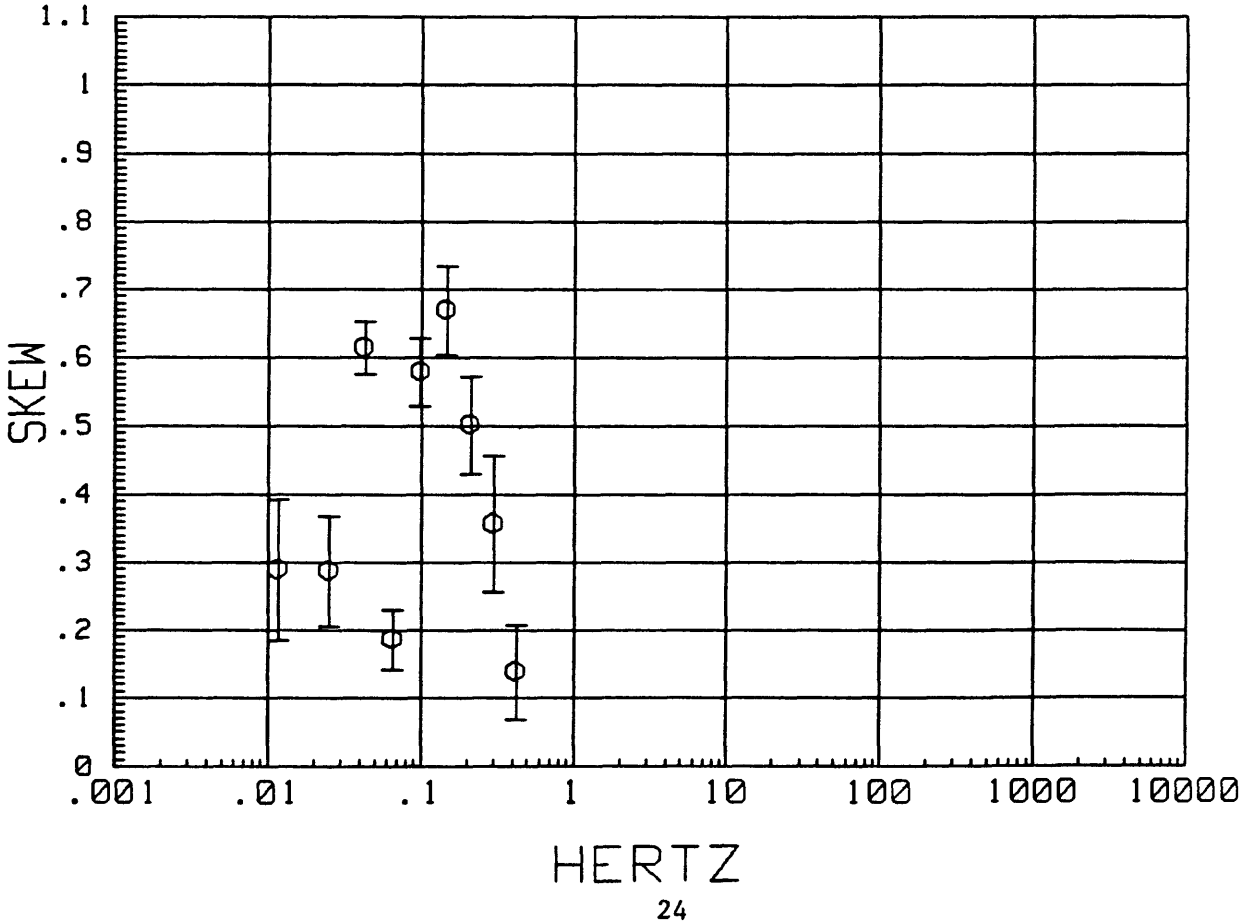

MTH003 LOCAL H-ref 21:52:47 12 May 1988
APPARENT RESISTIVITY

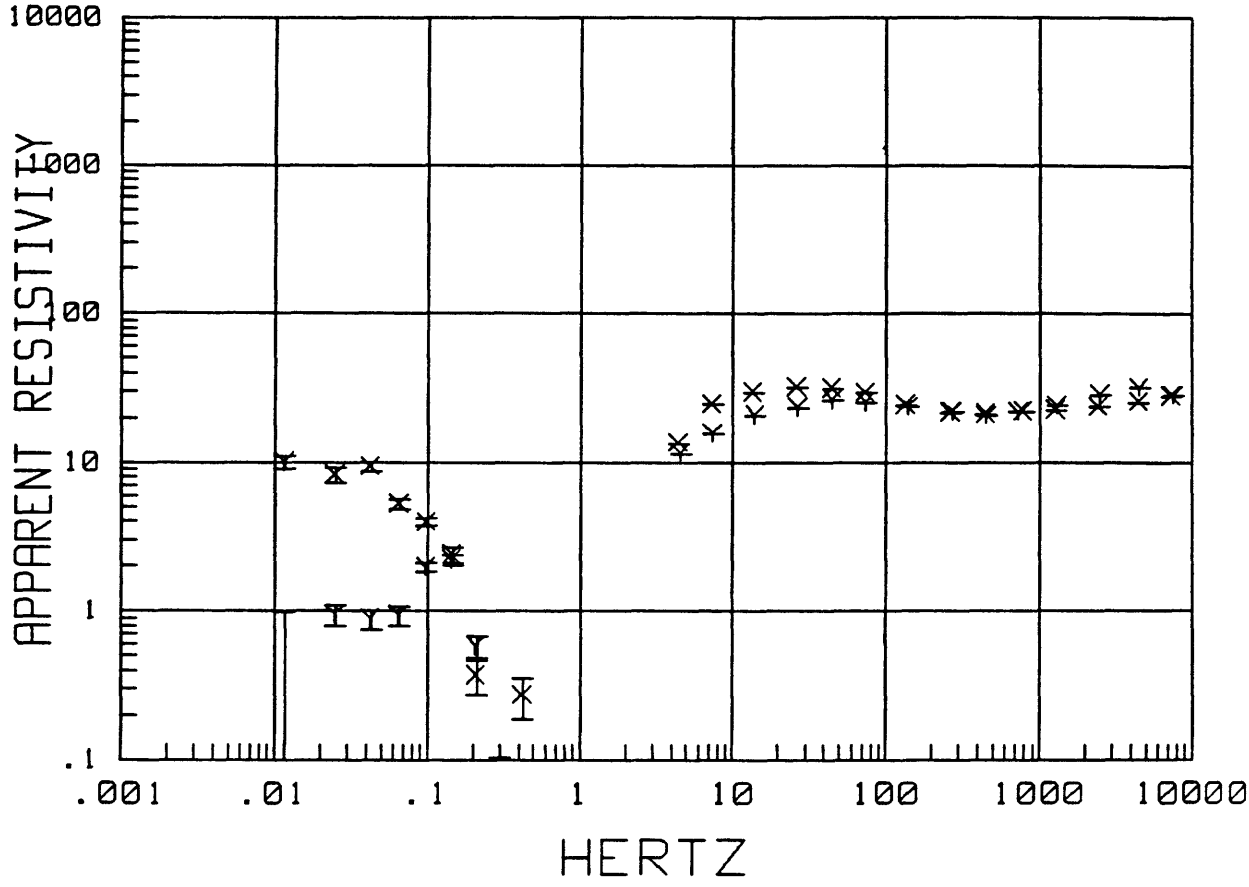

MTH003 LOCAL H-ref 21:52:47 12 May 1988
IMPEDANCE PHASE

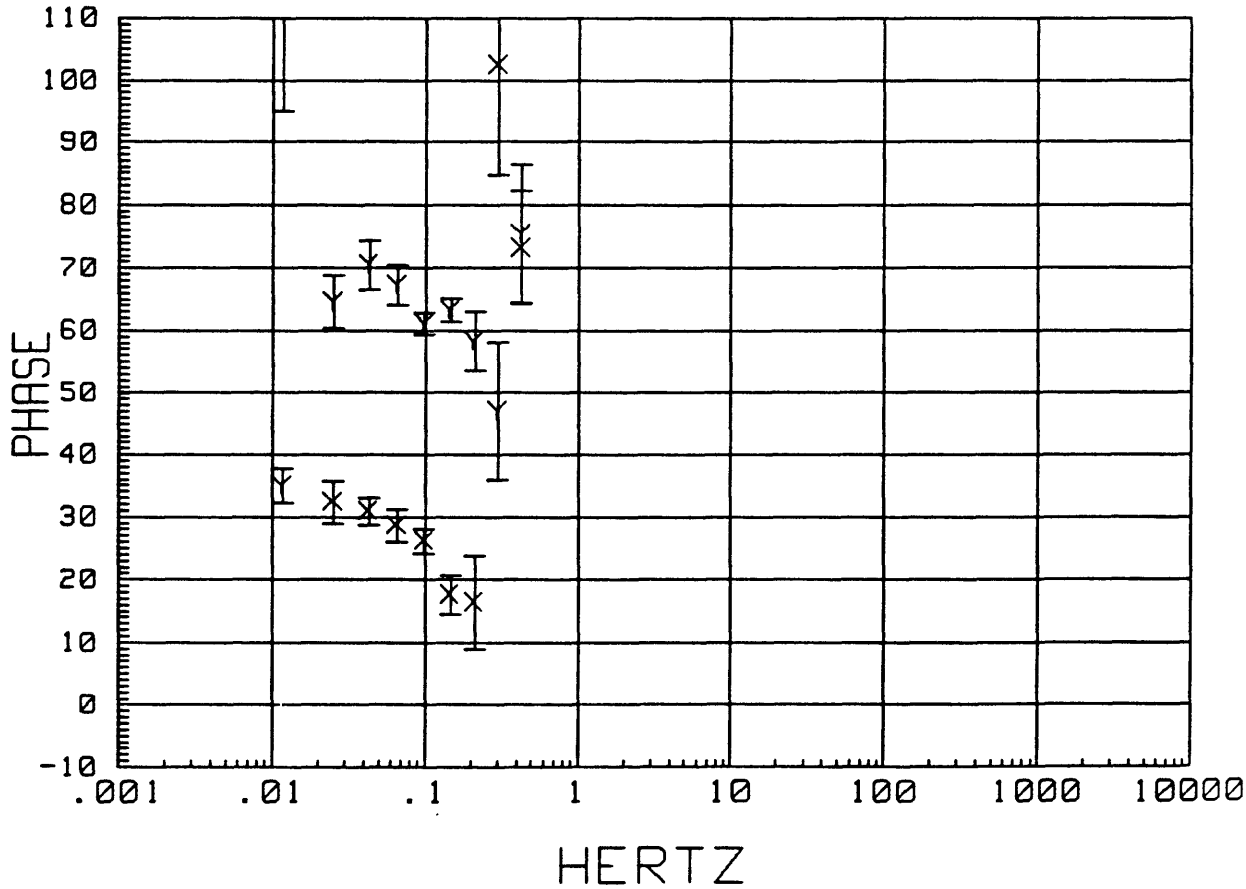

MTH003 LOCAL H-ref 21:52:47 12 May 1988
Z MAXIMUM DIRECTION

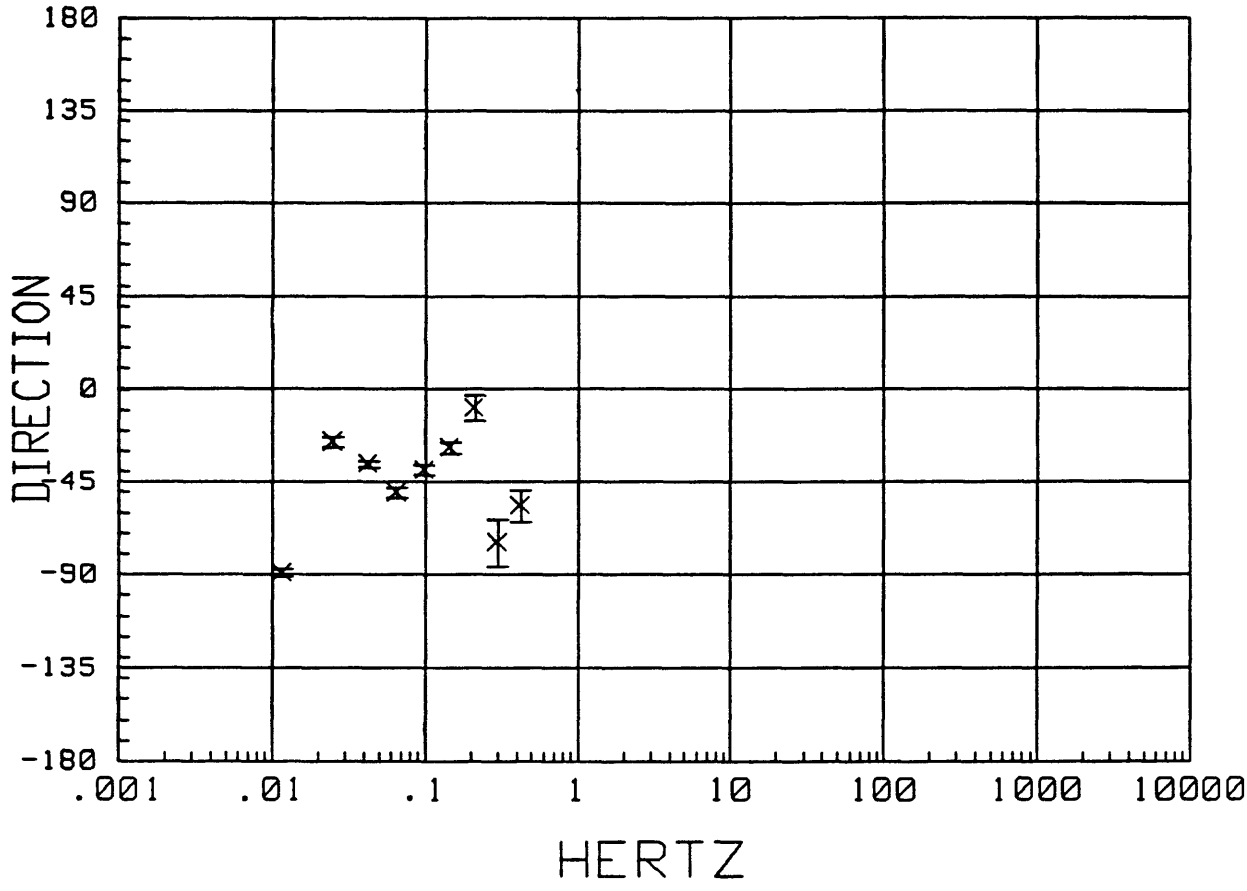

MTH003 LOCAL H-ref 21:52:47 12 May 1988
SKEW

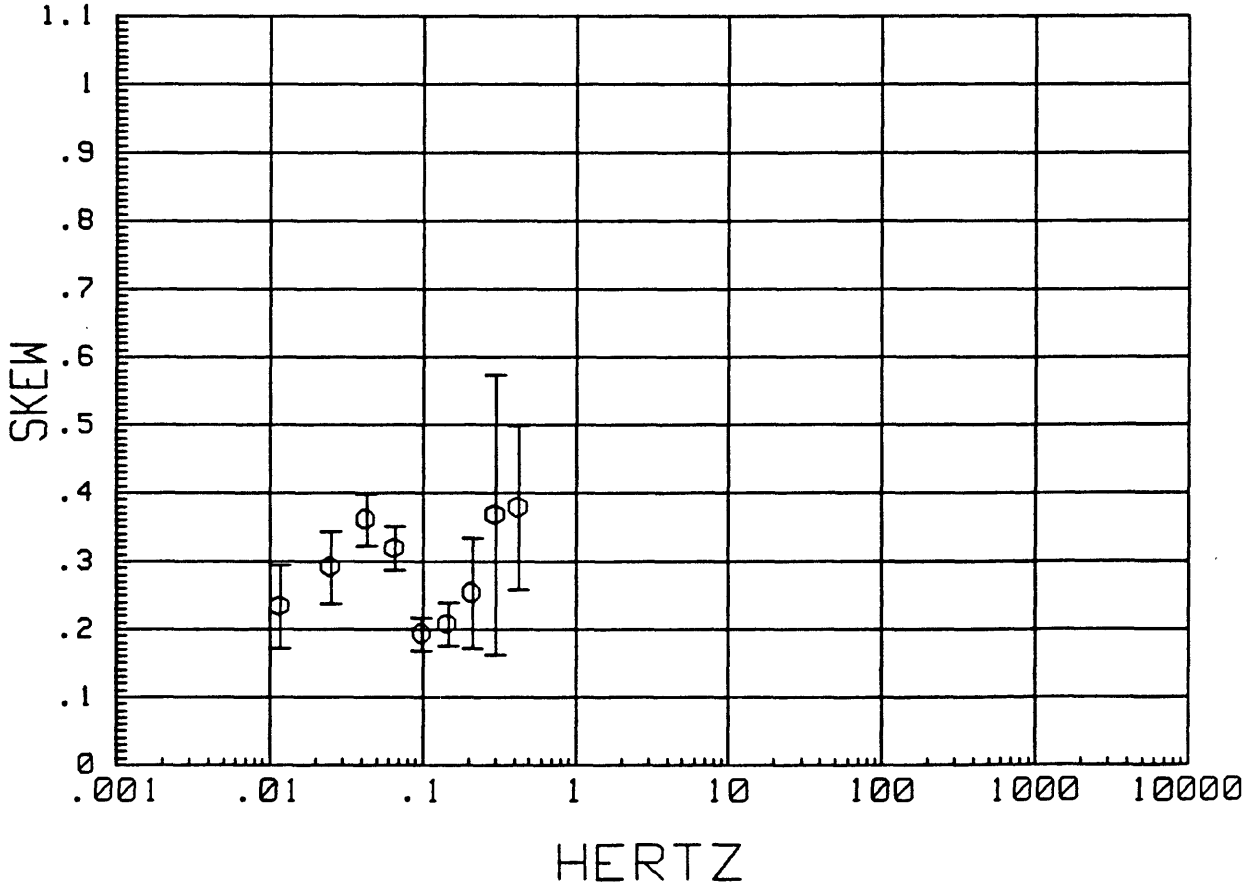

MTH004 LOCAL H-ref 15:23:01 13 May 1988
APPARENT RESISTIVITY

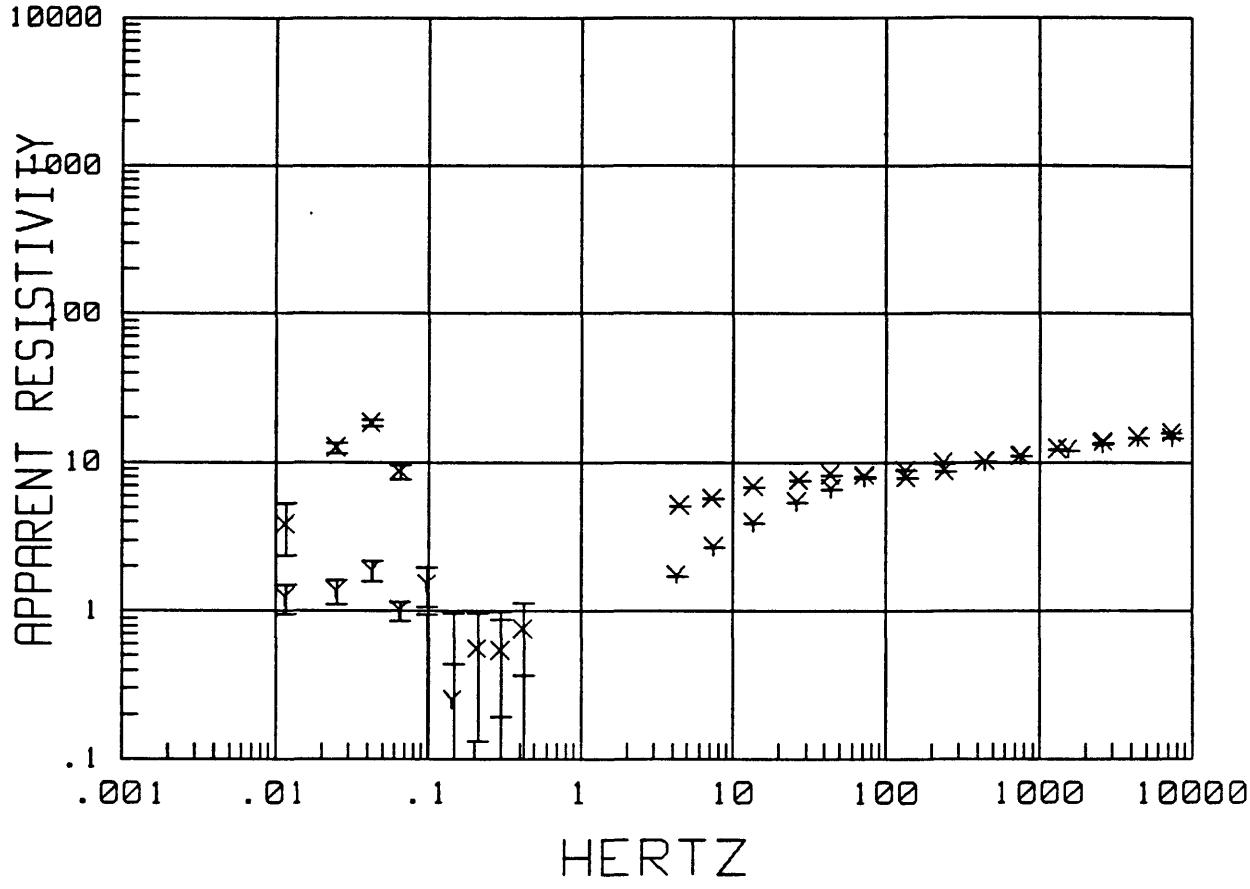

MTH004 LOCAL H-ref 15:23:01 13 May 1988
IMPEDANCE PHASE

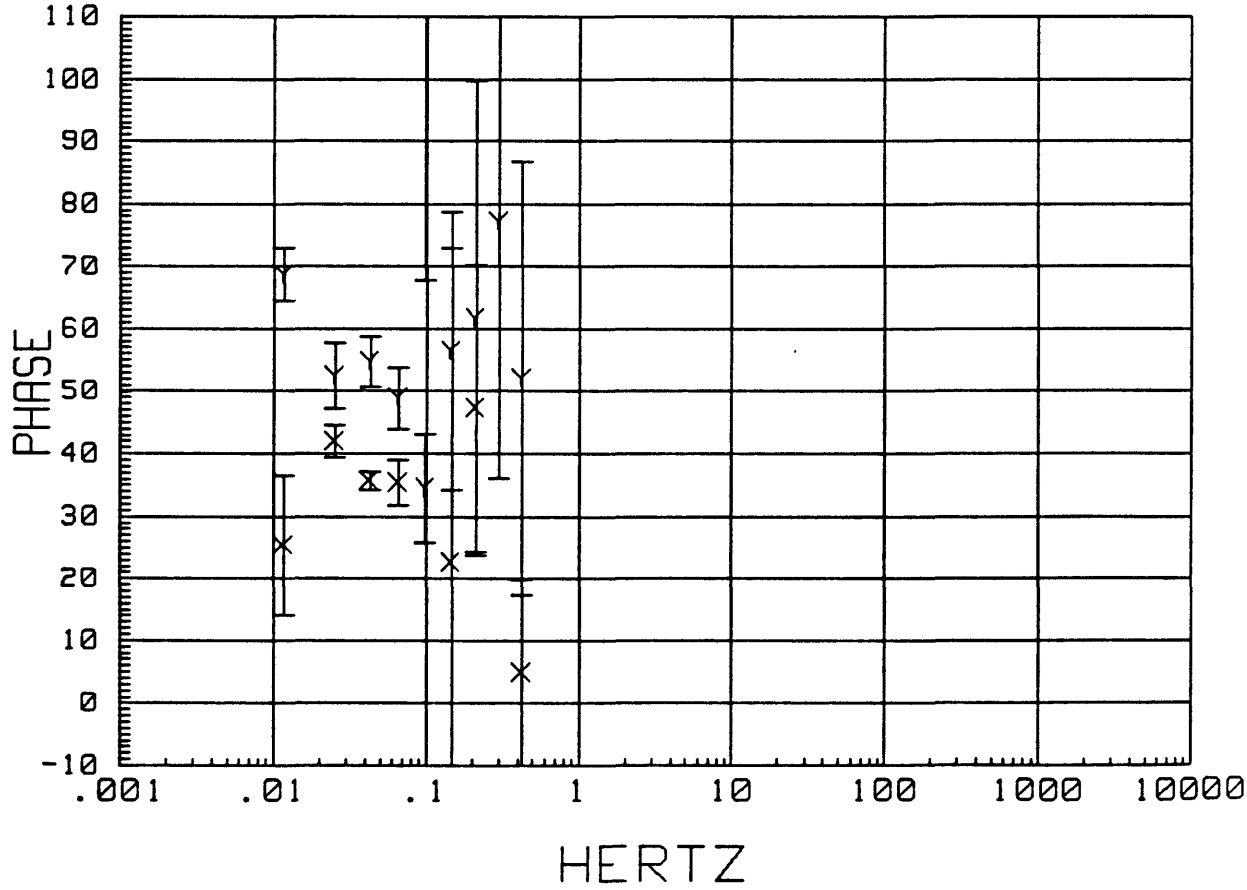

MTHO04 LOCAL H-ref 15:23:01 13 May 1988
Z MAXIMUM DIRECTION

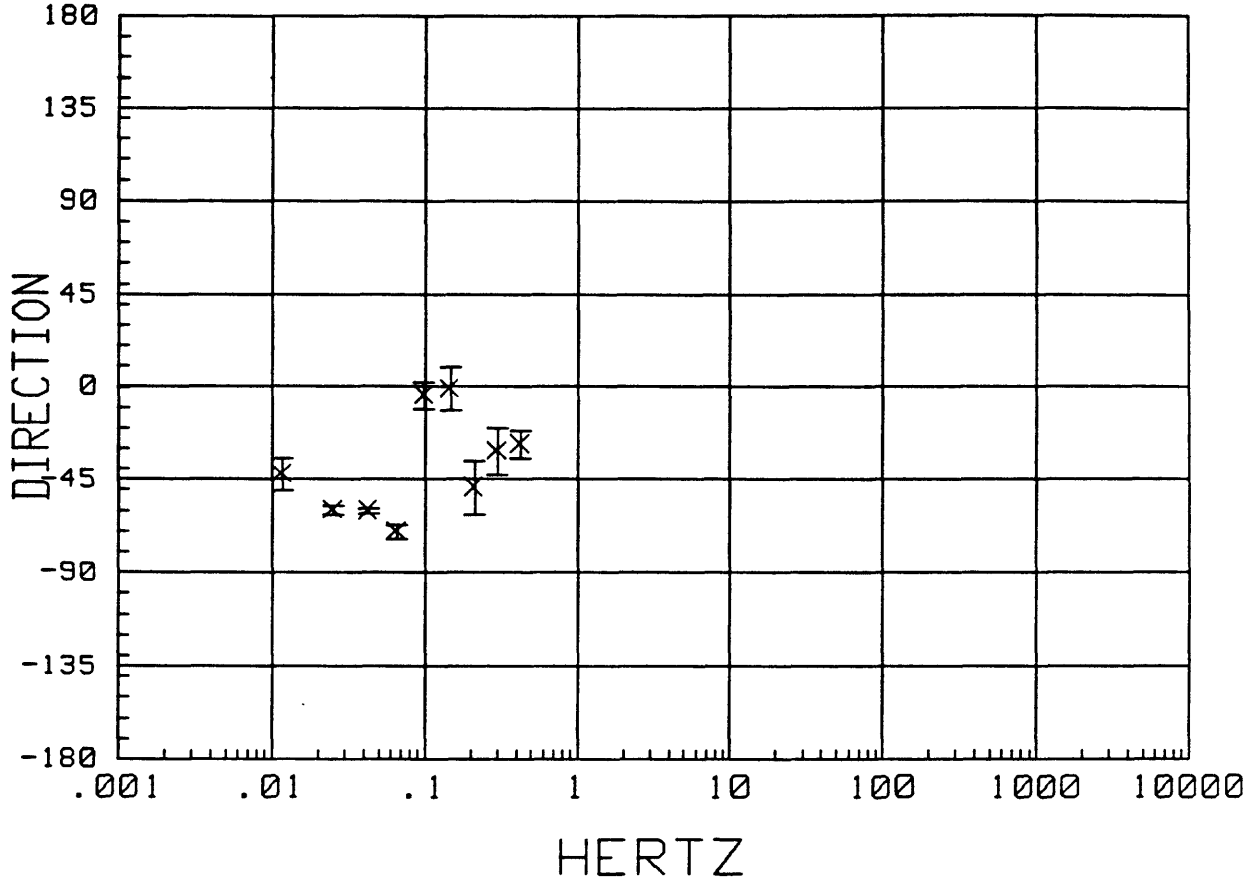

MTHO04 LOCAL H-ref 15:23:01 13 May 1988
SKEW

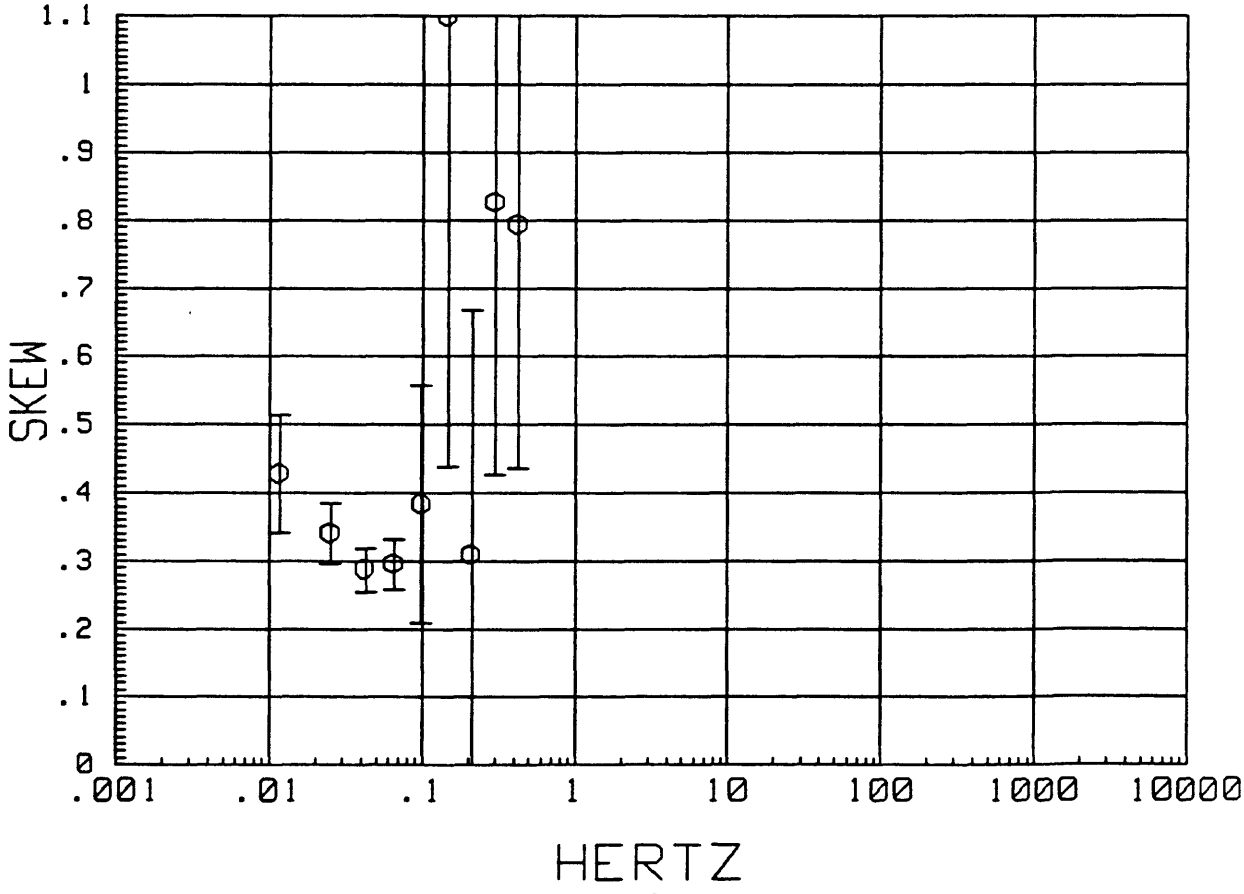

MTH005 LOCAL H-ref 15:45:24 13 May 1988
APPARENT RESISTIVITY

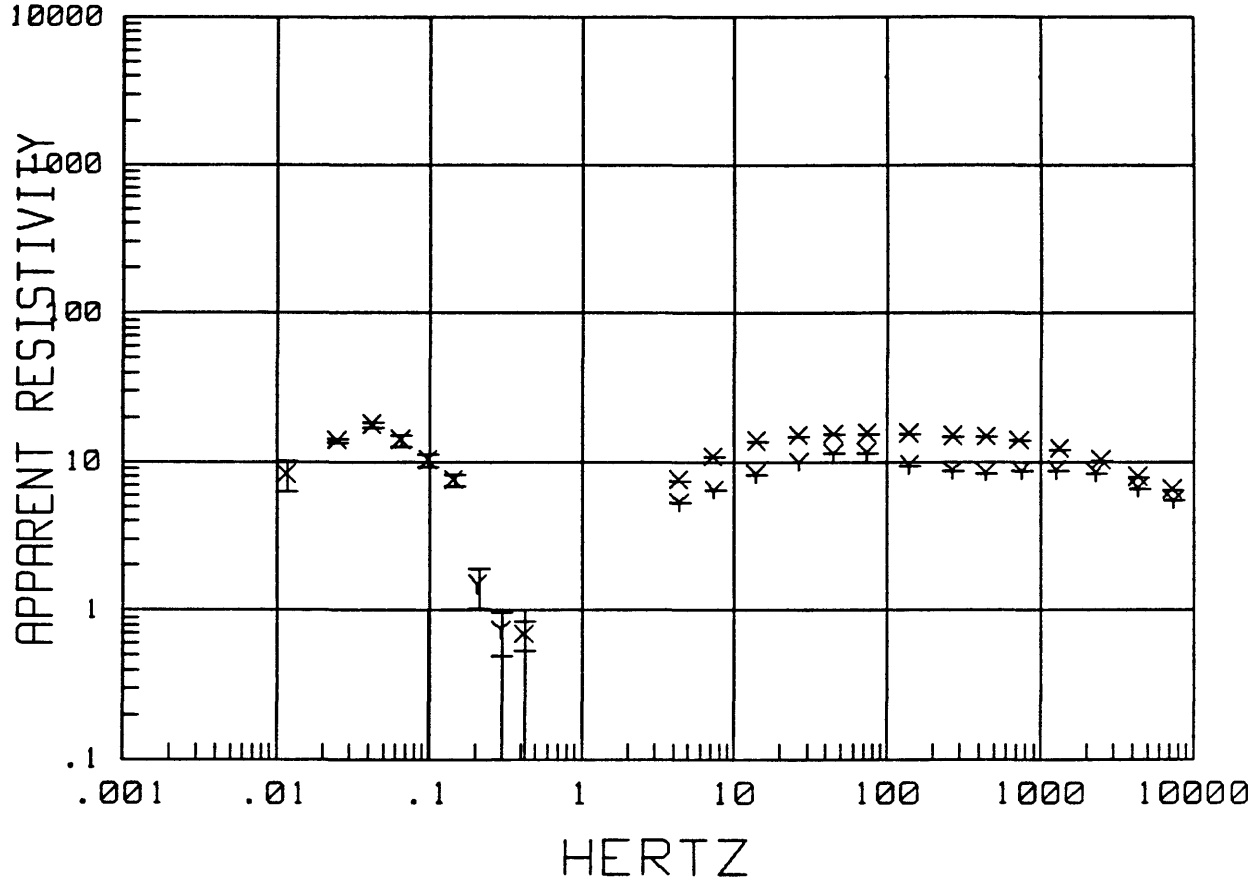

MTH005 LOCAL H-ref 15:45:24 13 May 1988
IMPEDANCE PHASE

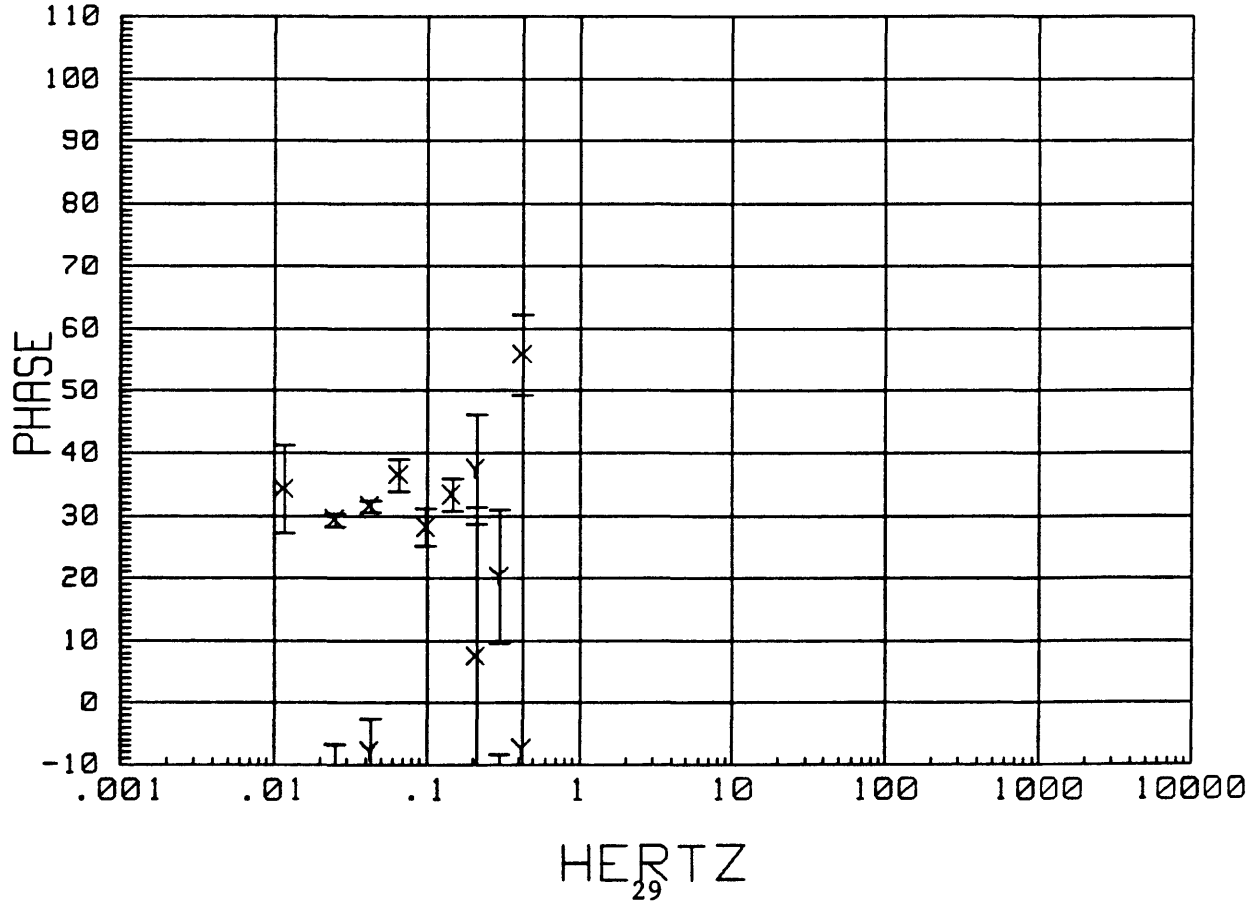

MTHO05 LOCAL H-ref 15:45:24 13 May 1988
Z MAXIMUM DIRECTION

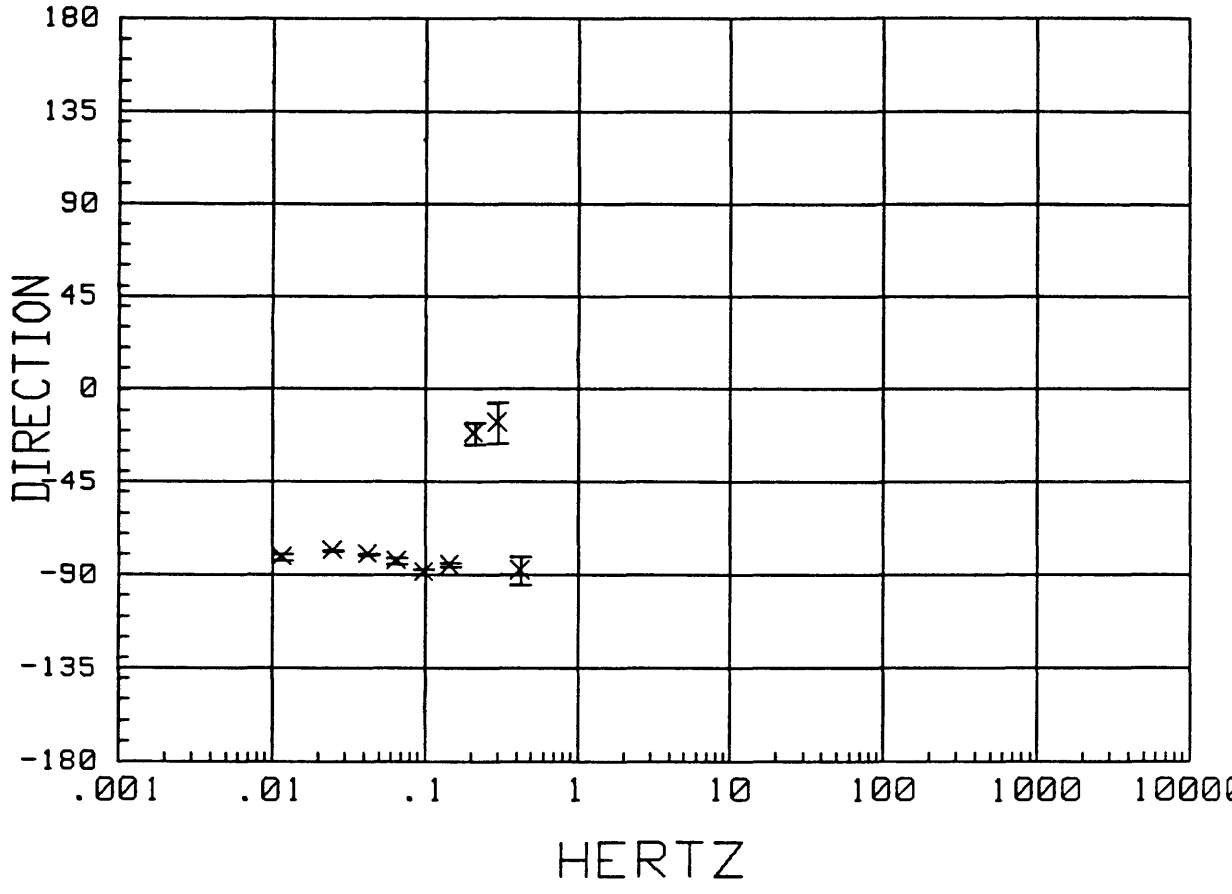

MTHO05 LOCAL H-ref 15:45:24 13 May 1988
SKEW

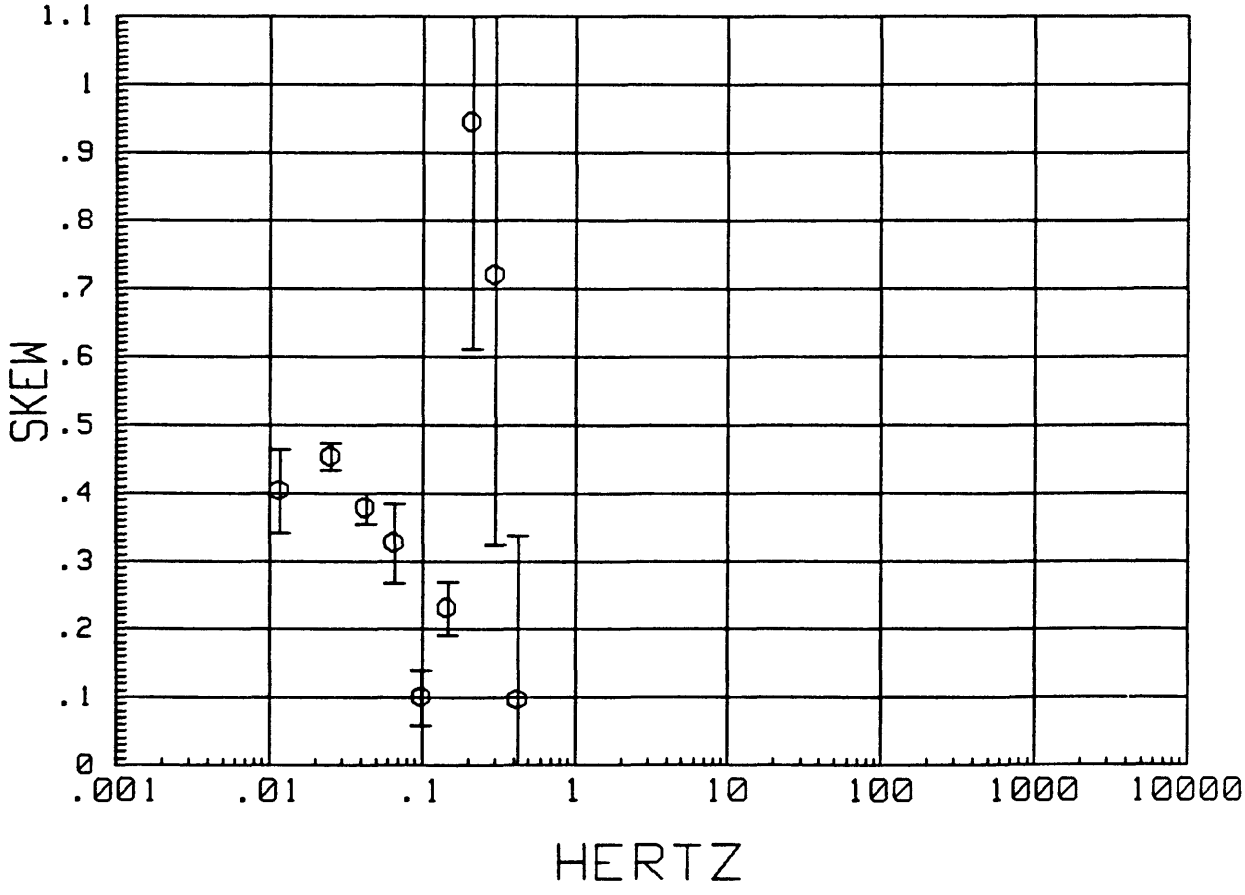

MTHO06 LOCAL H-ref 15:51:25 13 May 1988
APPARENT RESISTIVITY

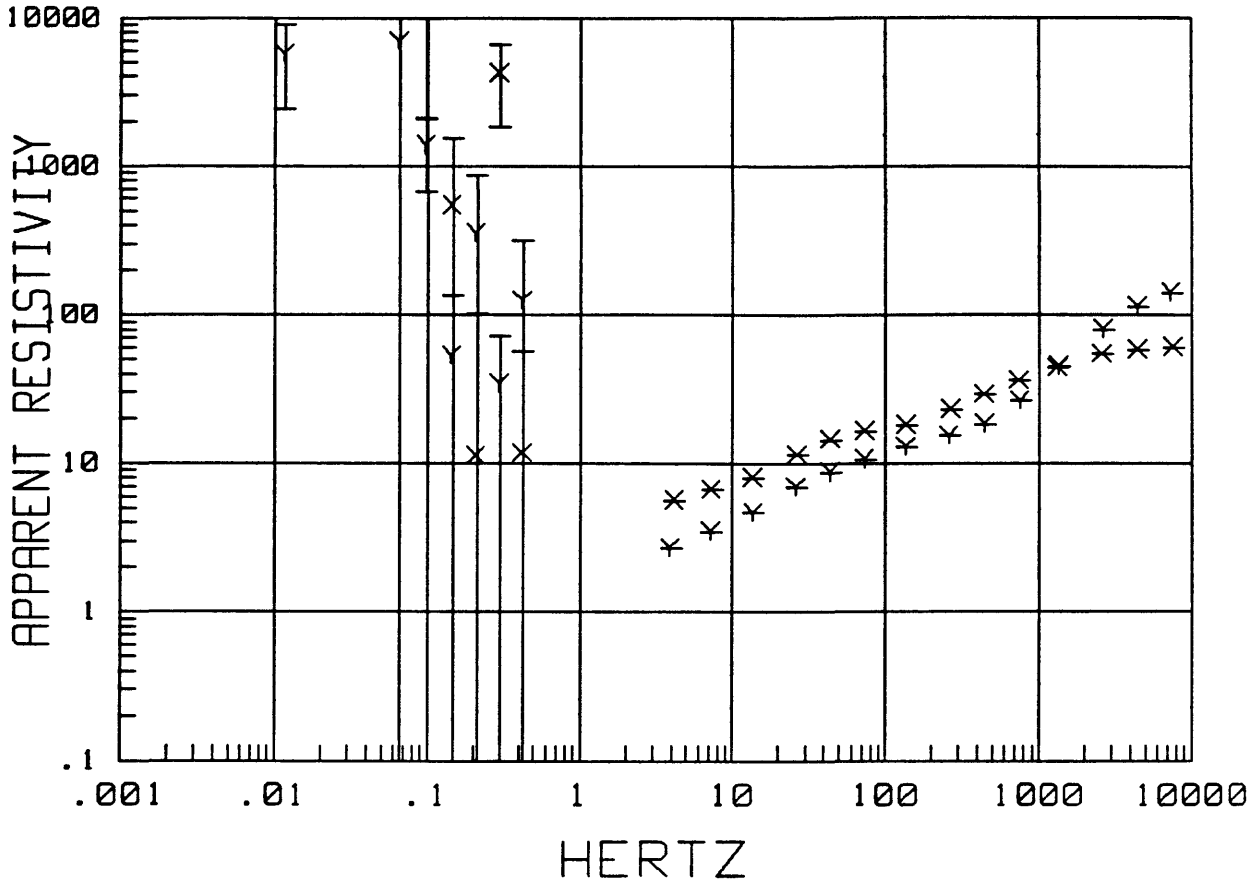

MTHO06 LOCAL H-ref 15:51:25 13 May 1988
IMPEDANCE PHASE

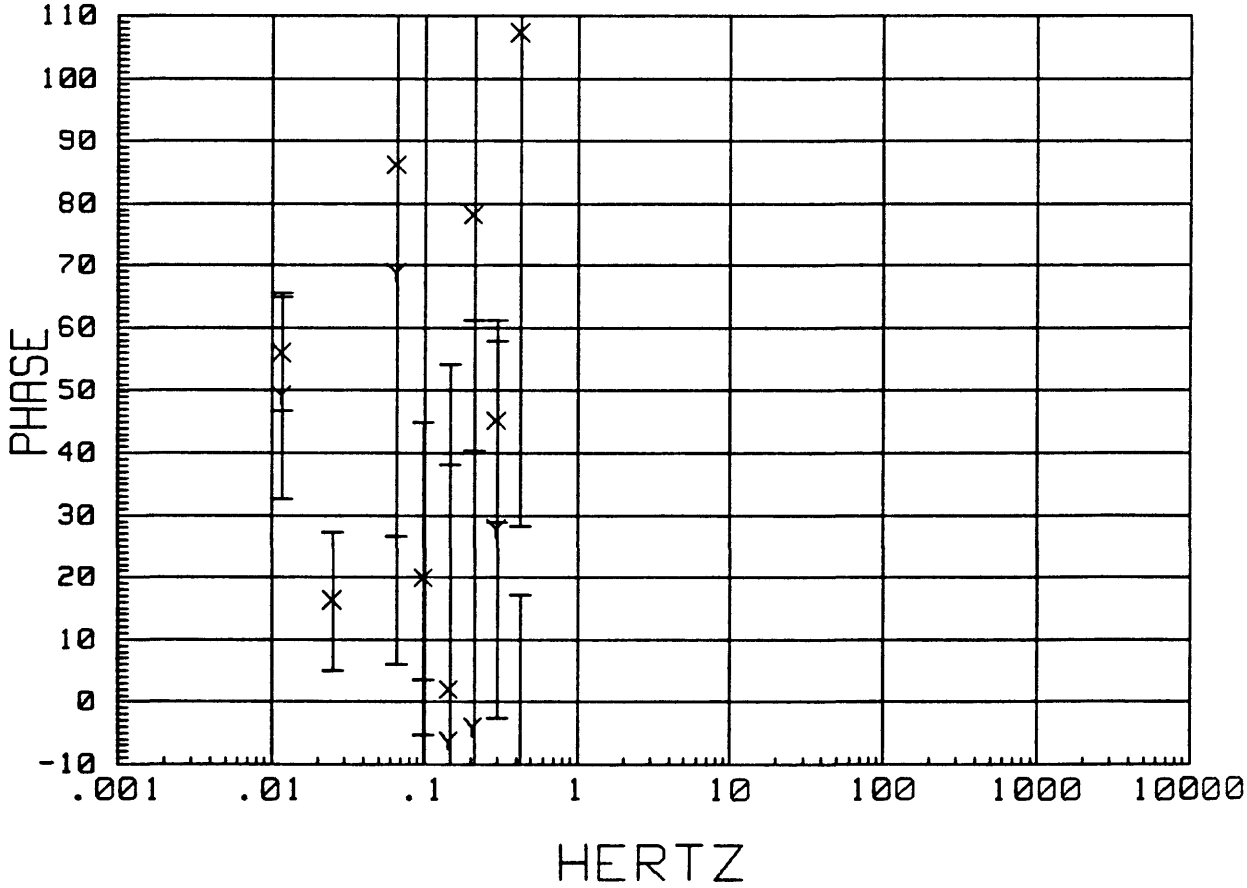

MTH006 LOCAL H-ref 15:51:25 13 May 1988
Z MAXIMUM DIRECTION

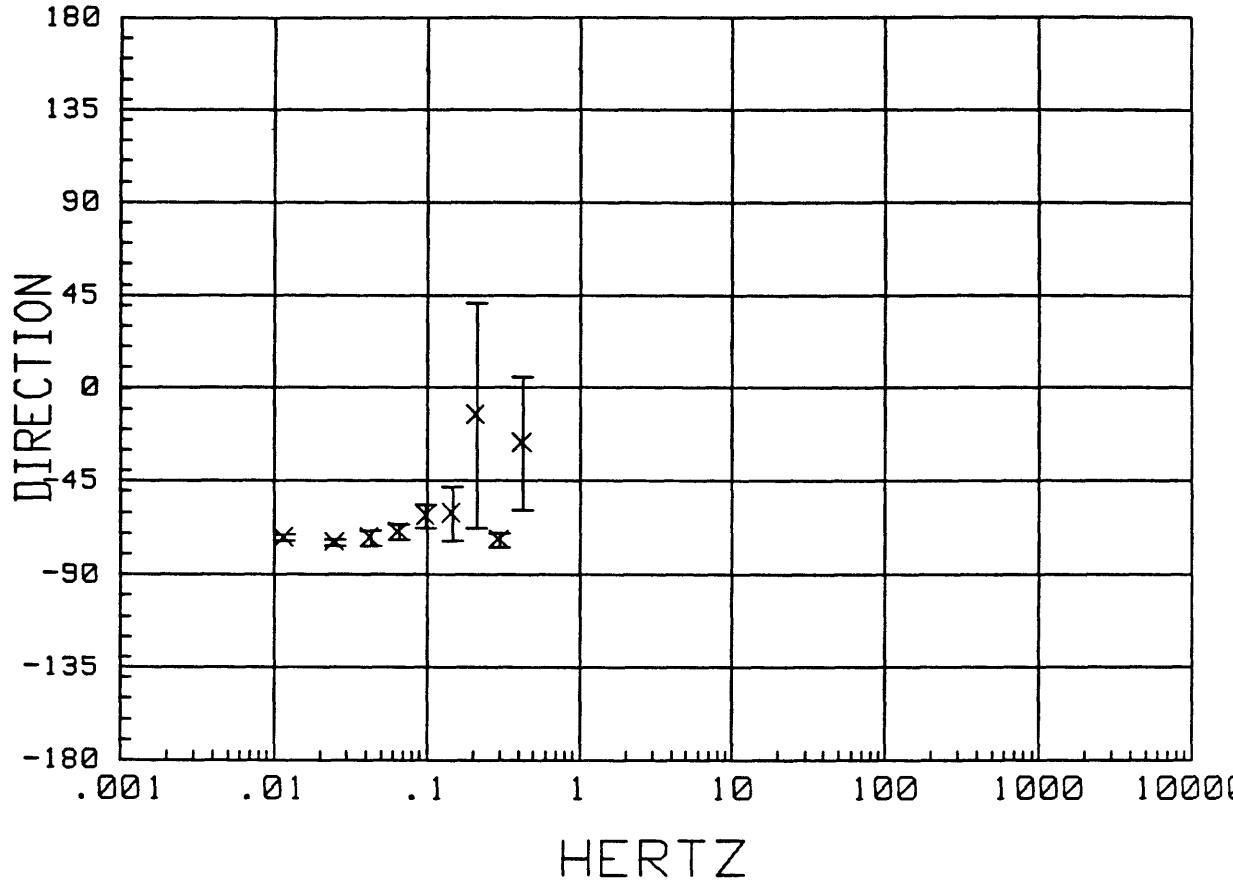

MTH006 LOCAL H-ref 15:51:25 13 May 1988
SKEW

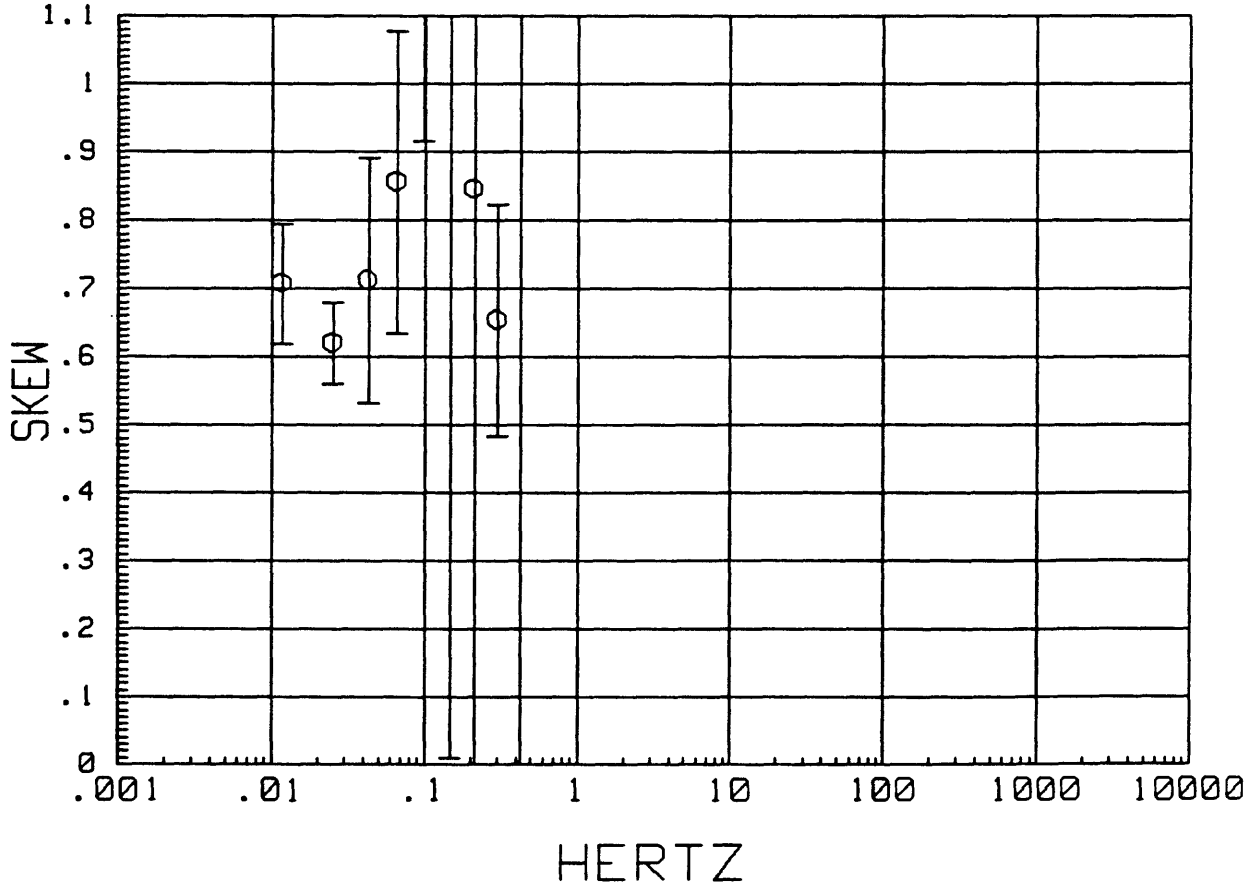

MTH007 LOCAL H-ref 16:12:00 13 May 1988
APPARENT RESISTIVITY

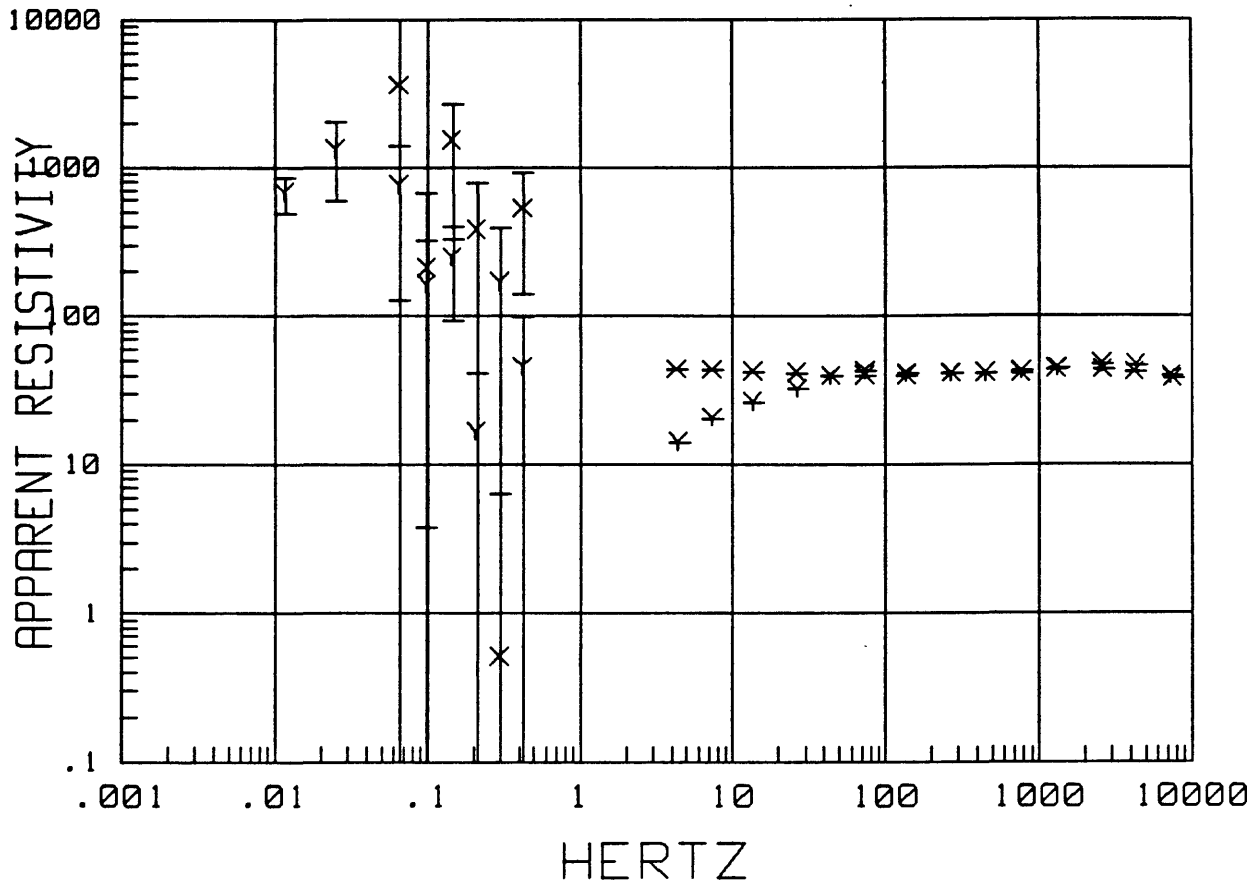

MTH007 LOCAL H-ref 16:12:00 13 May 1988
IMPEDANCE PHASE

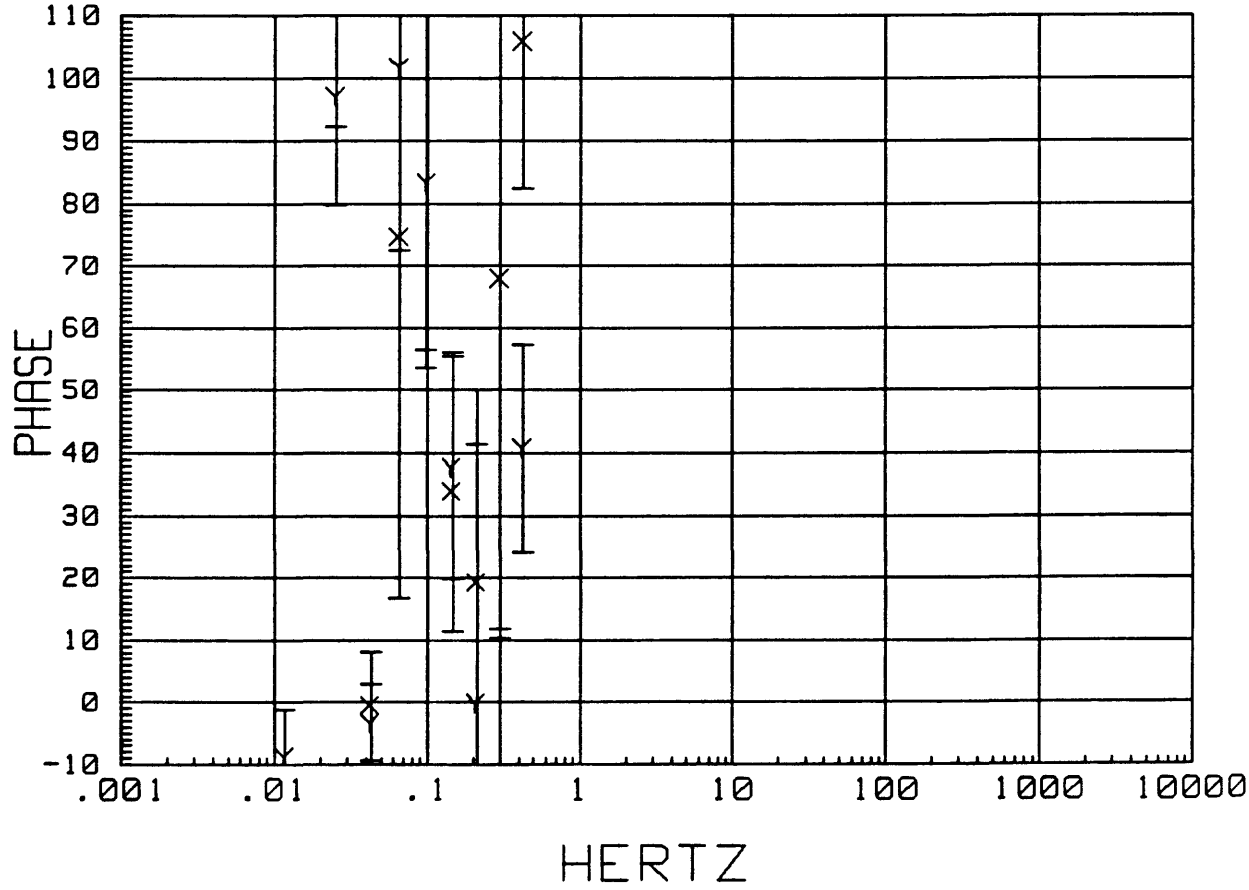

MTH007 LOCAL H-ref 16:12:00 13 May 1988
Z MAXIMUM DIRECTION

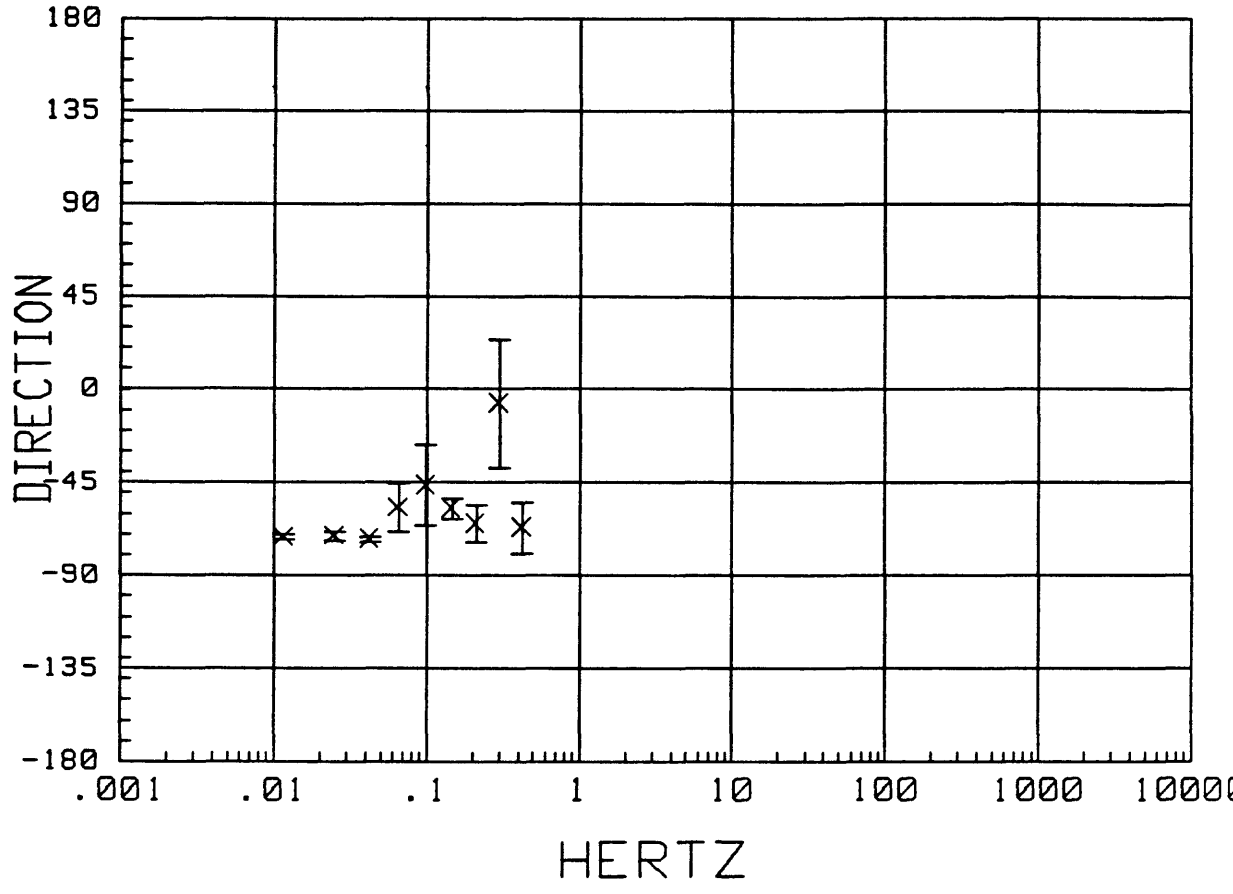

MTH007 LOCAL H-ref 16:12:00 13 May 1988
SKEW

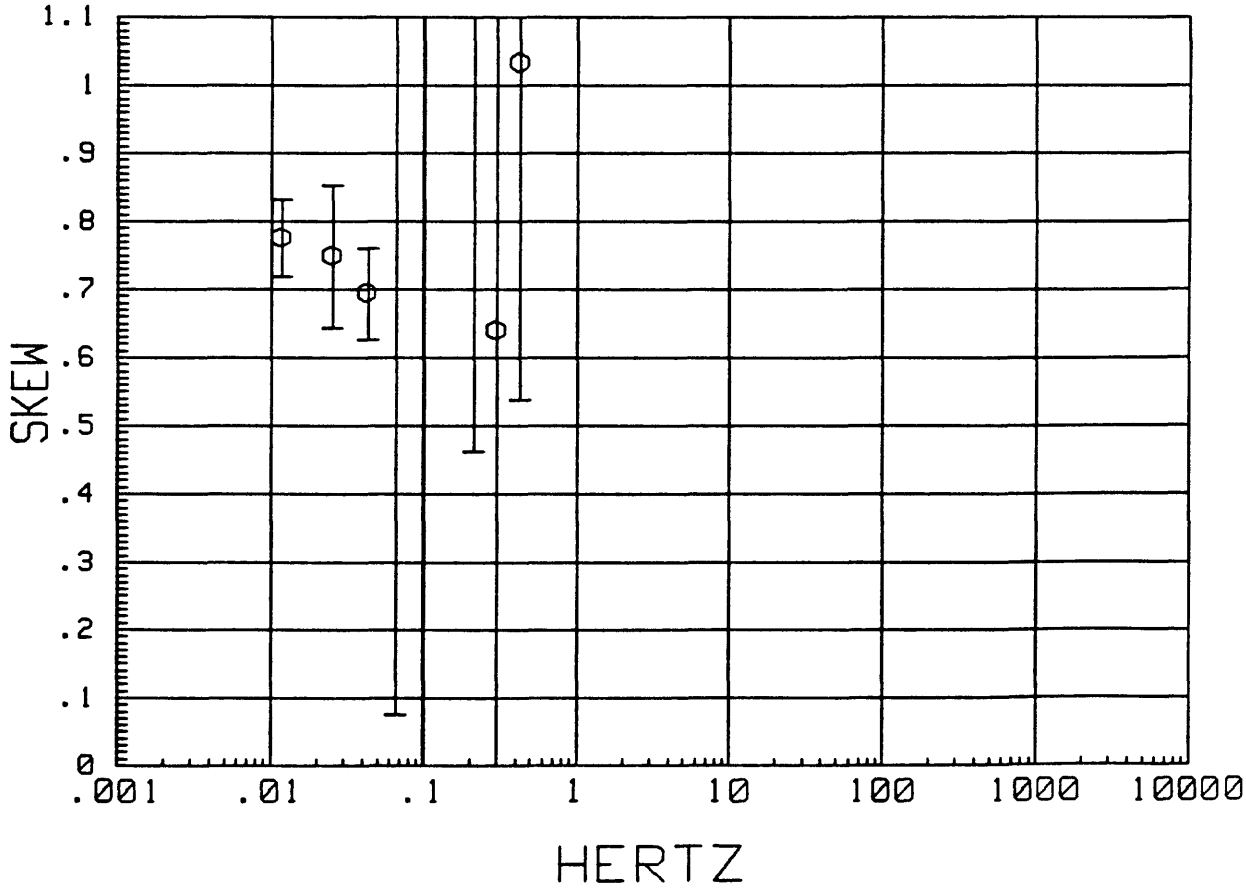

MTHO08 LOCAL H-ref 16:26:52 13 May 1988
APPARENT RESISTIVITY

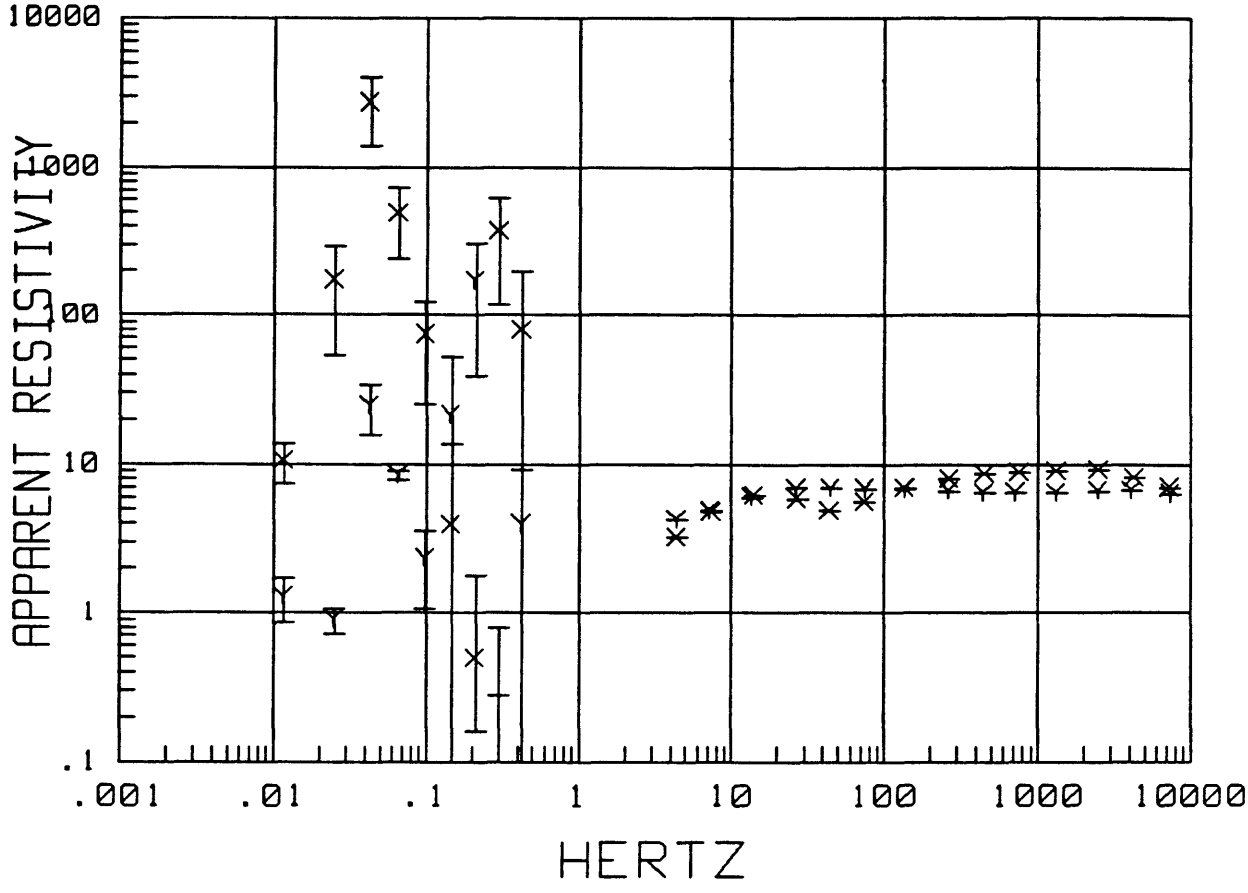

MTHO08 LOCAL H-ref 16:26:52 13 May 1988
IMPEDANCE PHASE

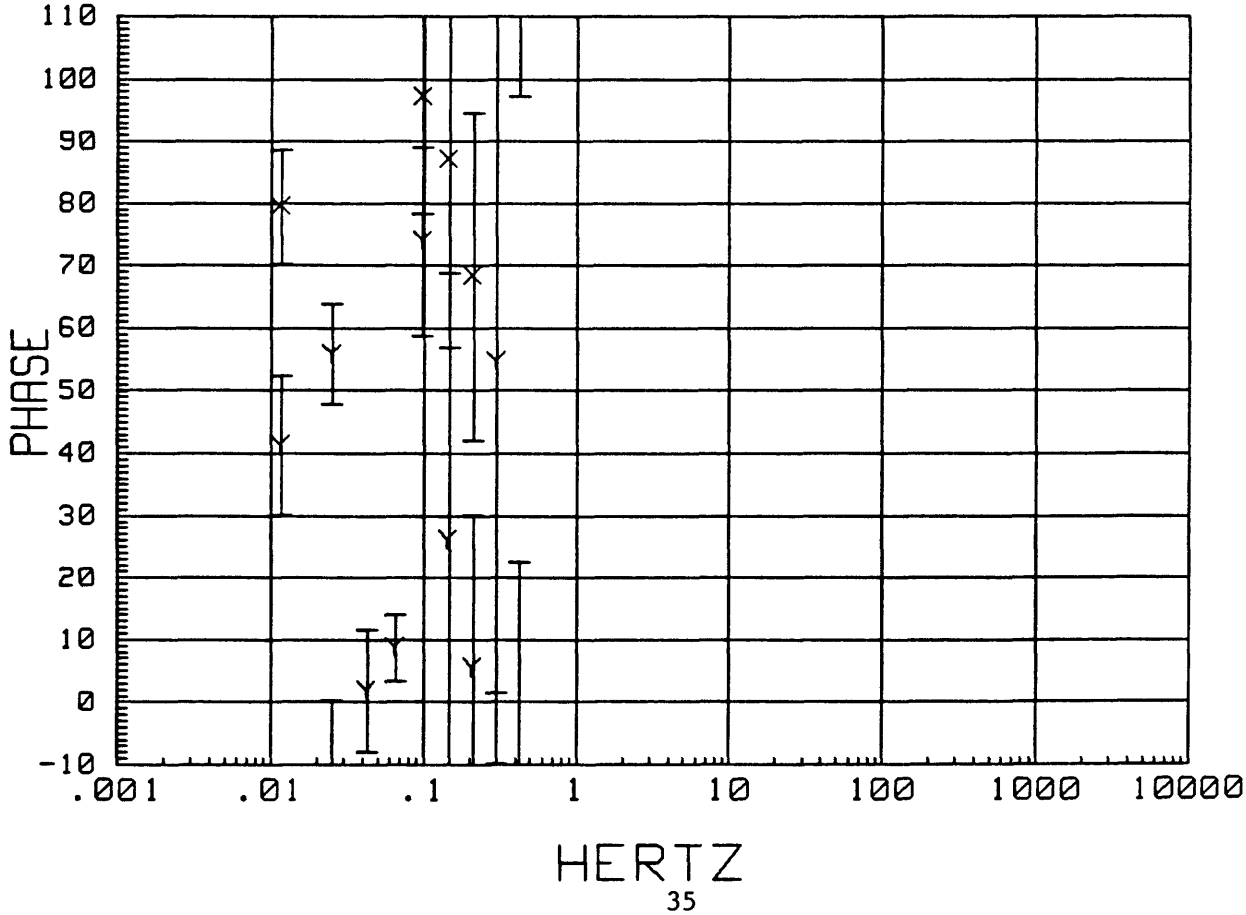

MTH008 LOCAL H-ref 16:26:52 13 May 1988
Z MAXIMUM DIRECTION

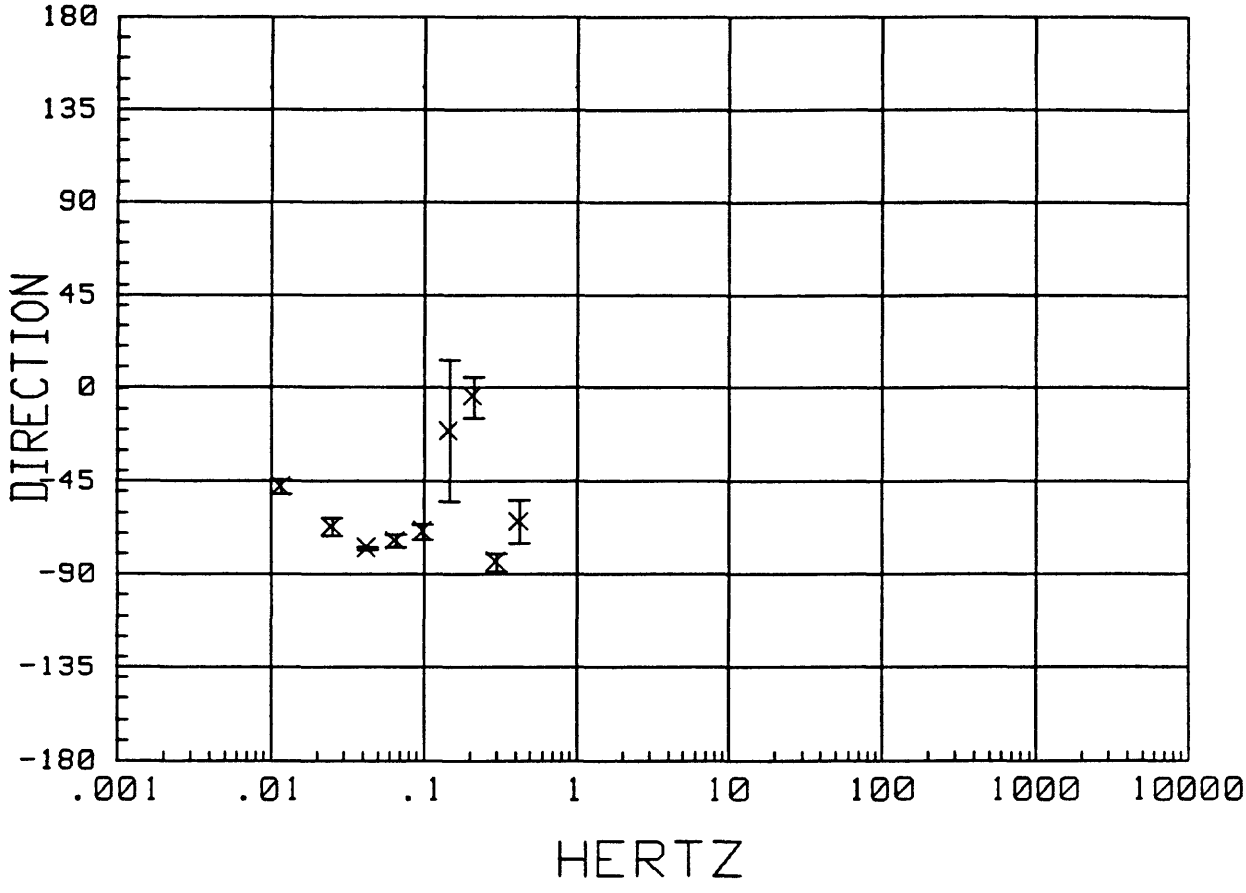

MTH008 LOCAL H-ref 16:26:52 13 May 1988
SKEW

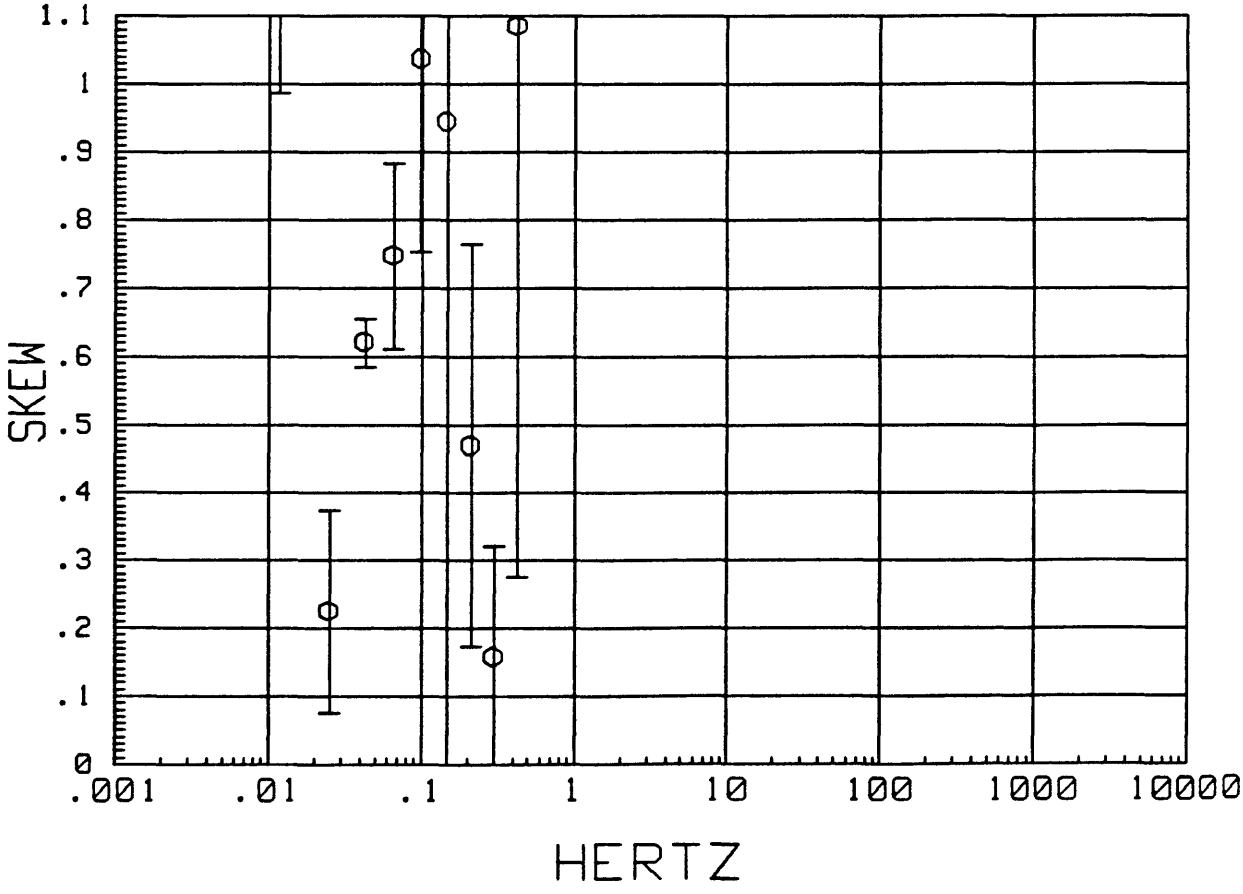

MTHO09 LOCAL H-ref 16:39:44 13 May 1988
APPARENT RESISTIVITY

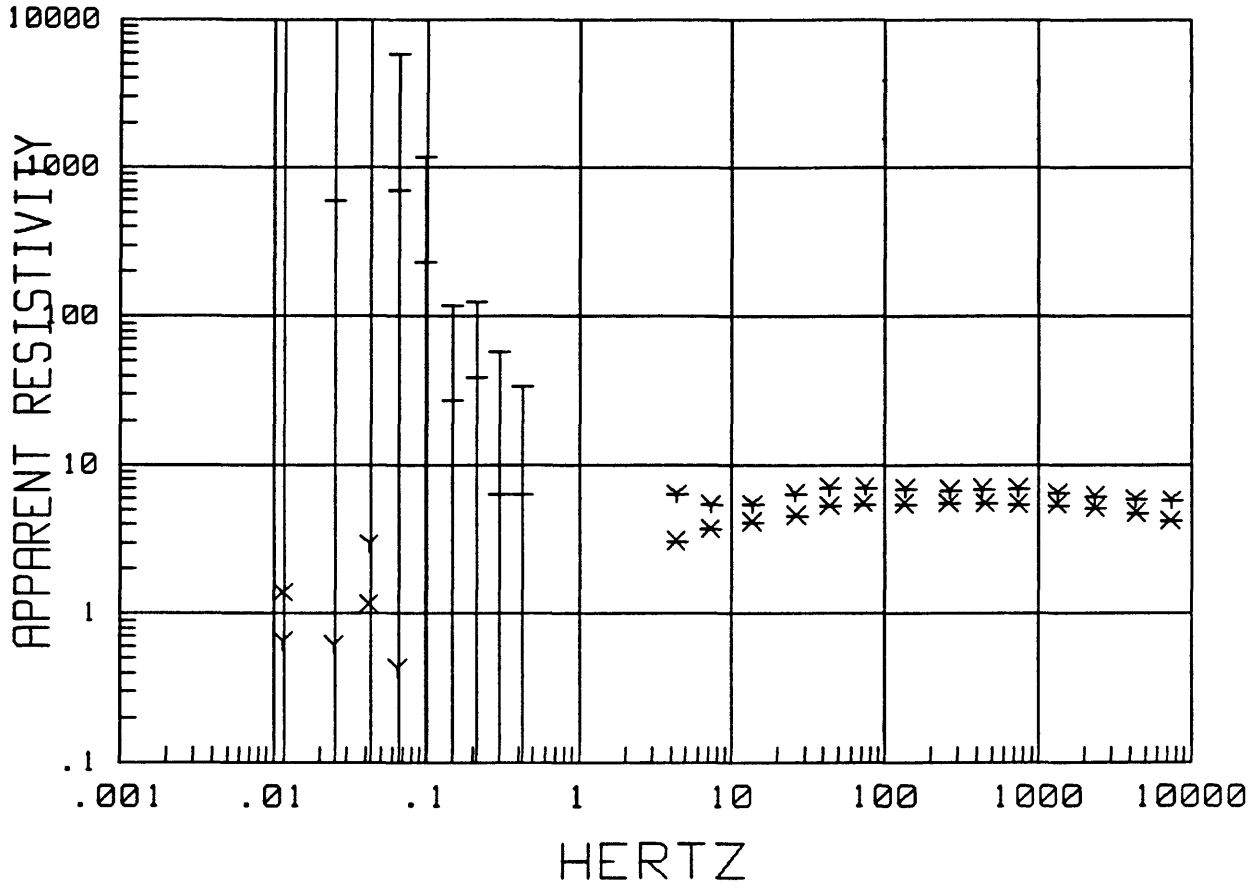

MTHO09 LOCAL H-ref 16:39:44 13 May 1988
IMPEDANCE PHASE

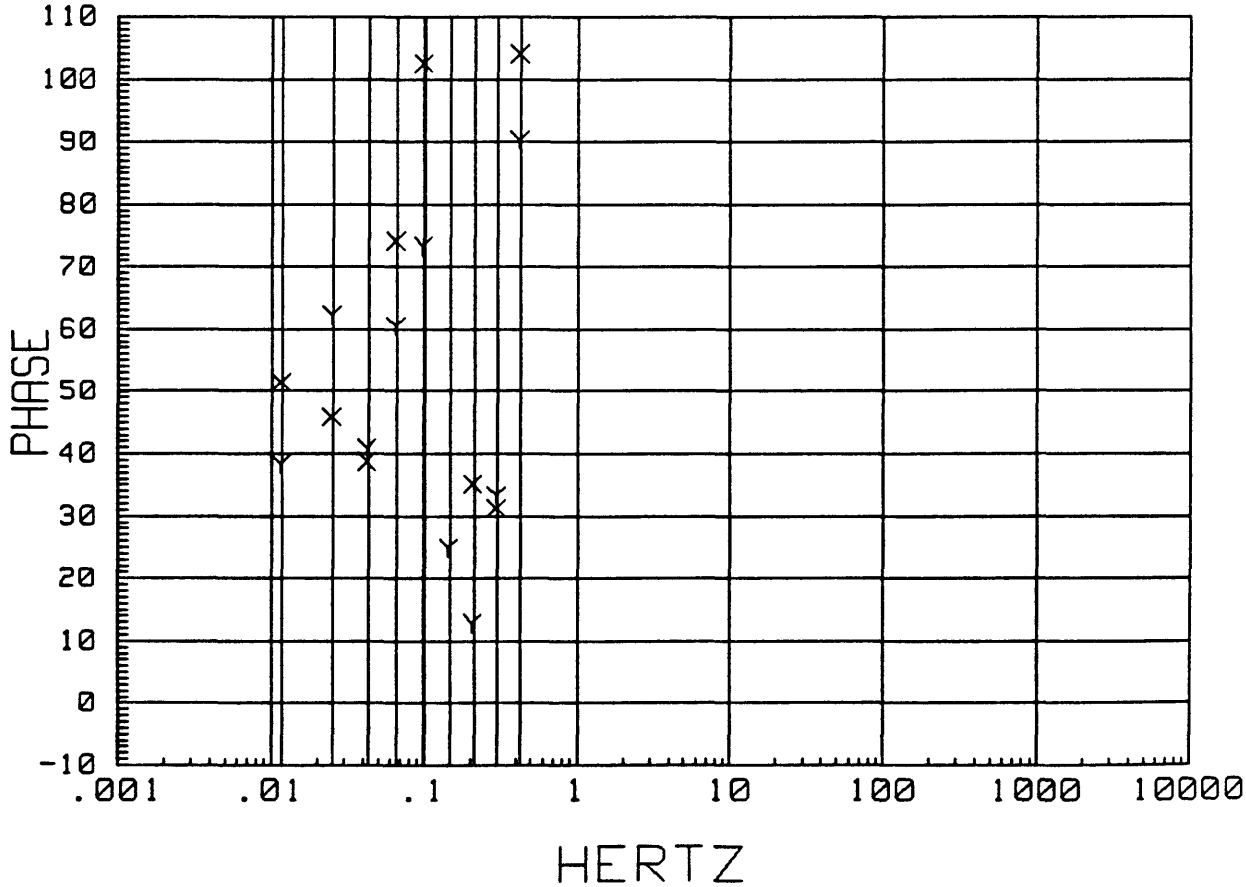

MTHO09 LOCAL H-ref 16:39:44 13 May 1988
Z MAXIMUM DIRECTION

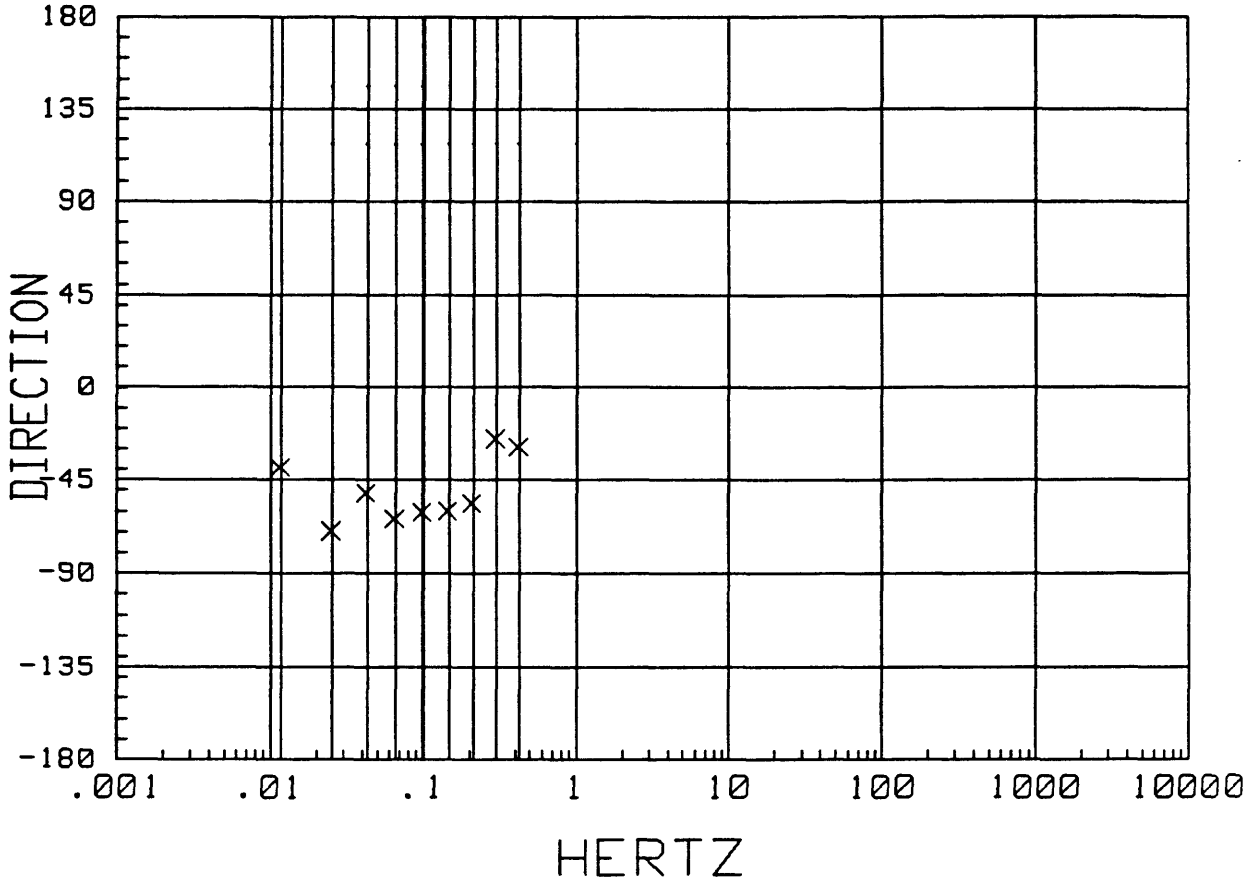

MTHO09 LOCAL H-ref 16:39:44 13 May 1988
SKEW

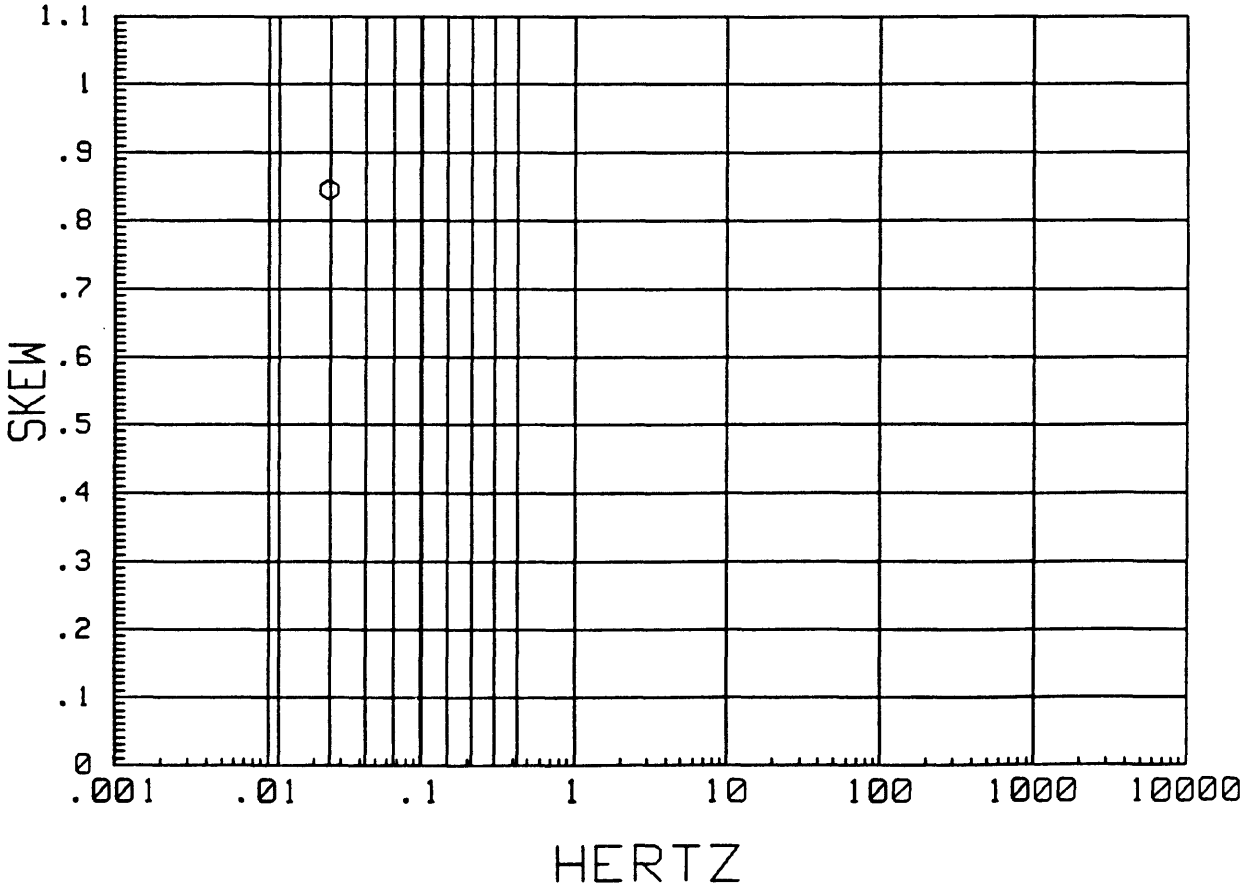

MTHO10 LOCAL H-ref 16:52:31 13 May 1988
APPARENT RESISTIVITY

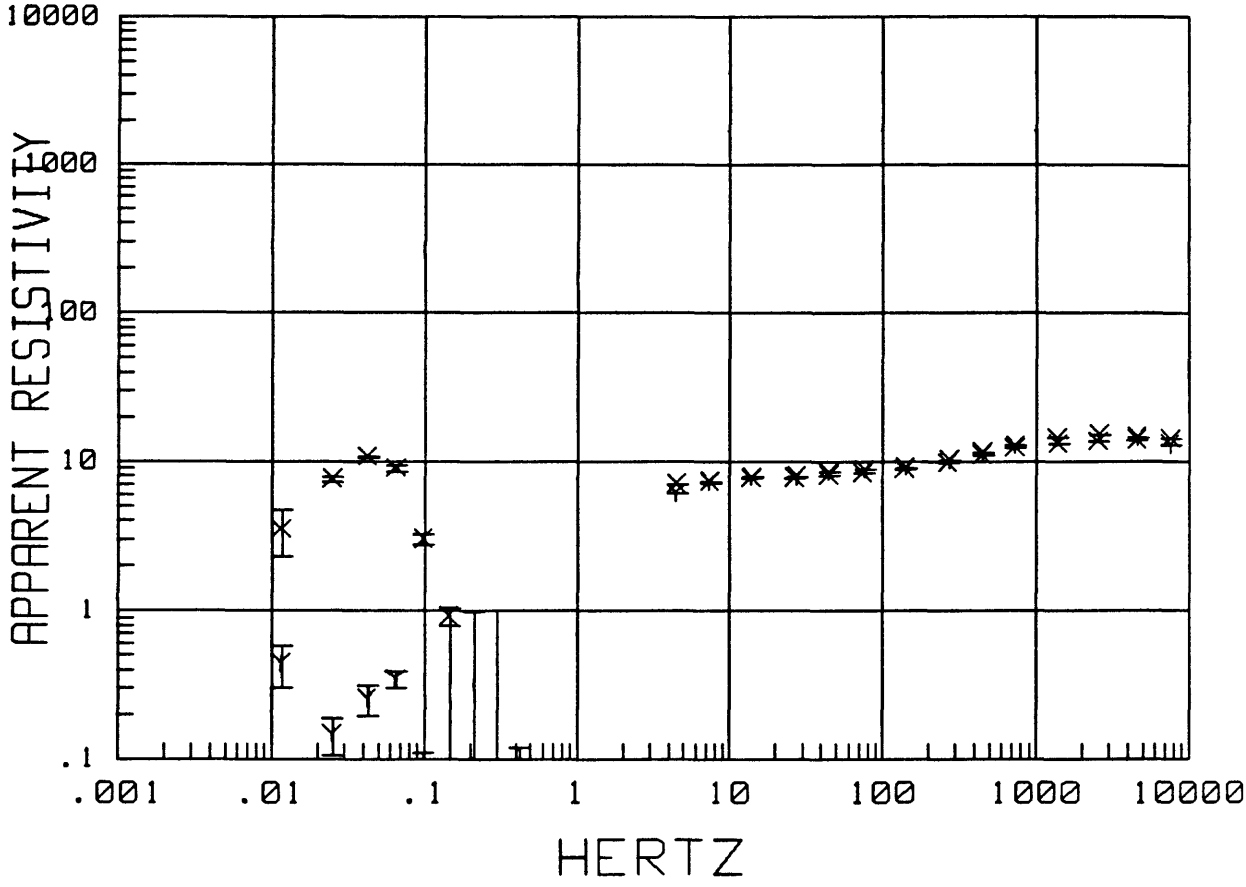

MTHO10 LOCAL H-ref 16:52:31 13 May 1988
IMPEDANCE PHASE

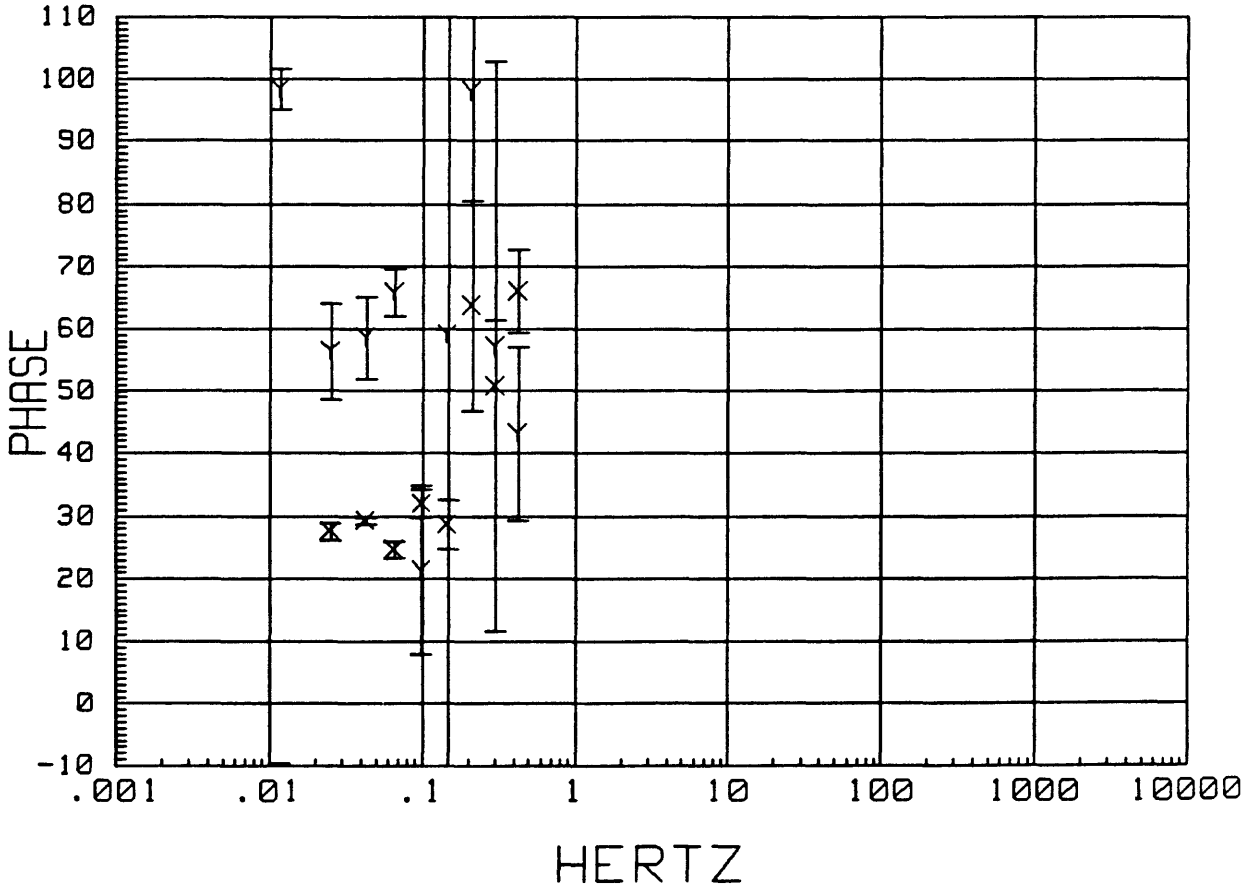

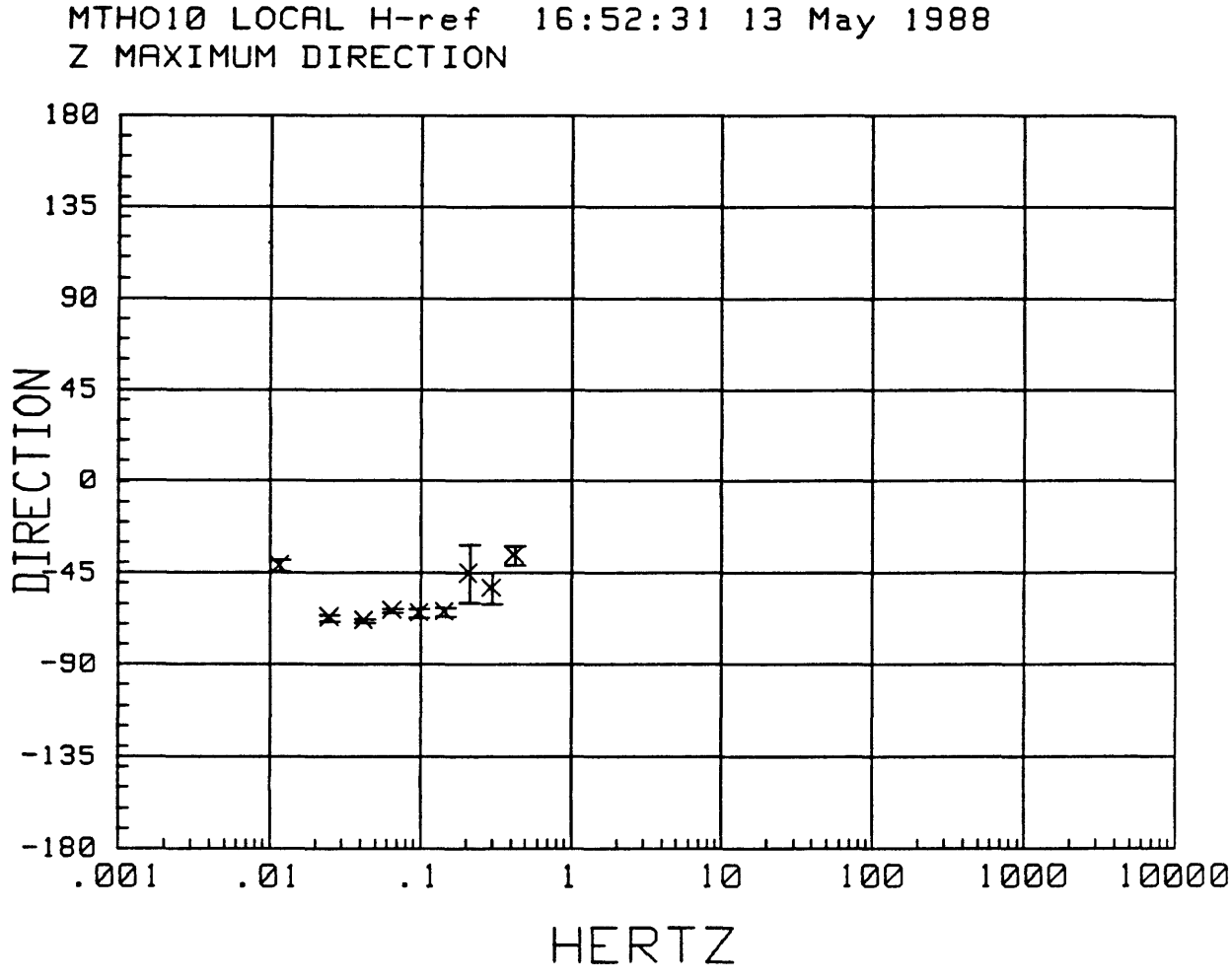
MTHO10 LOCAL H-ref 16:52:31 13 May 1988
Z MAXIMUM DIRECTION
180
135
90
45
0
-45
-90
-135
-180
DIRECTION
.001
.01
.1
1
10
100
1000
10000
HERTZ

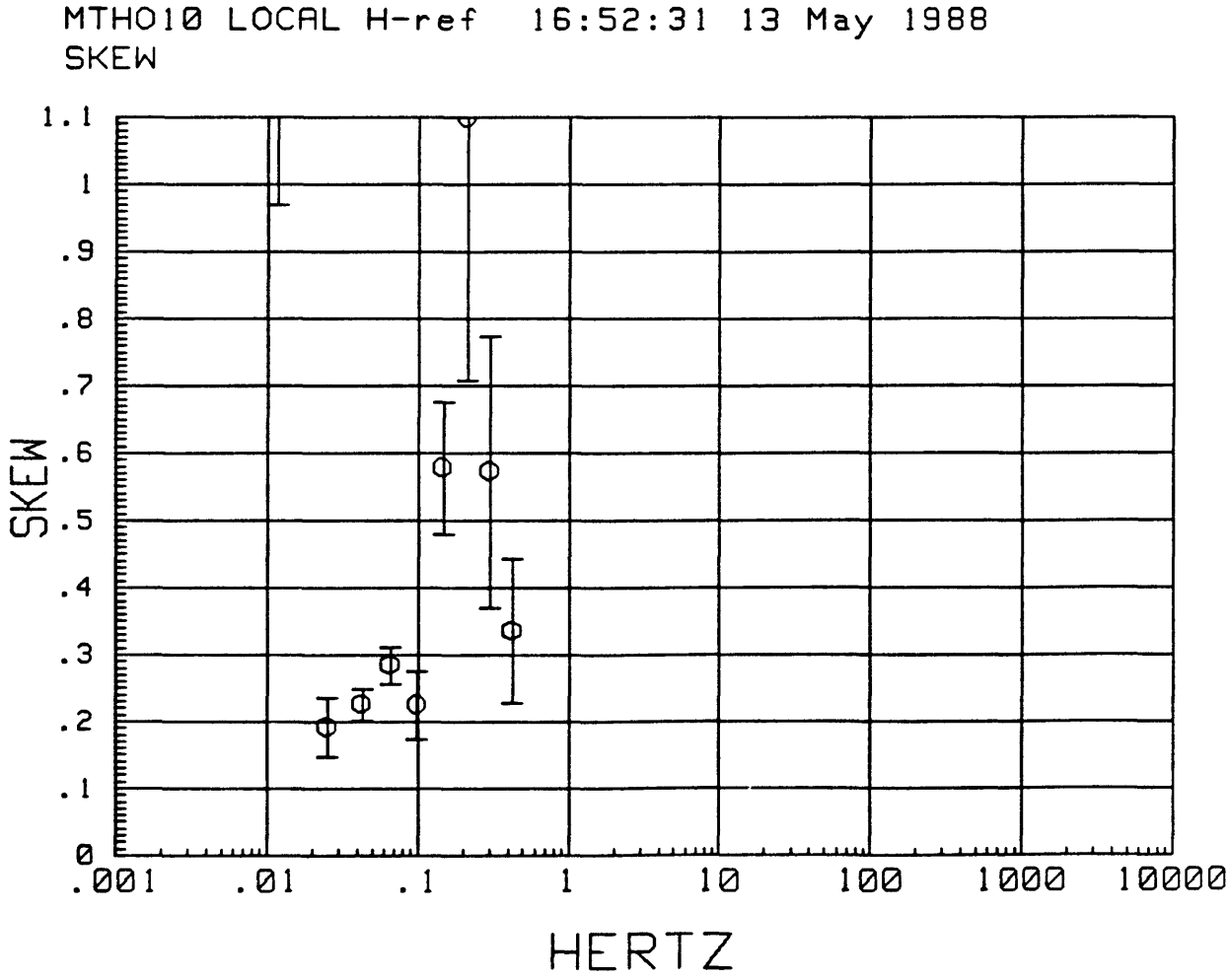
MTHO10 LOCAL H-ref 16:52:31 13 May 1988
SKEW
1.1
1
.9
.8
.7
.6
.5
.4
.3
.2
.1
0
SKEW
.001
.01
.1
1
10
100
1000
10000
HERTZ

MTHO11 LOCAL H-ref 17:05:51 13 May 1988
APPARENT RESISTIVITY

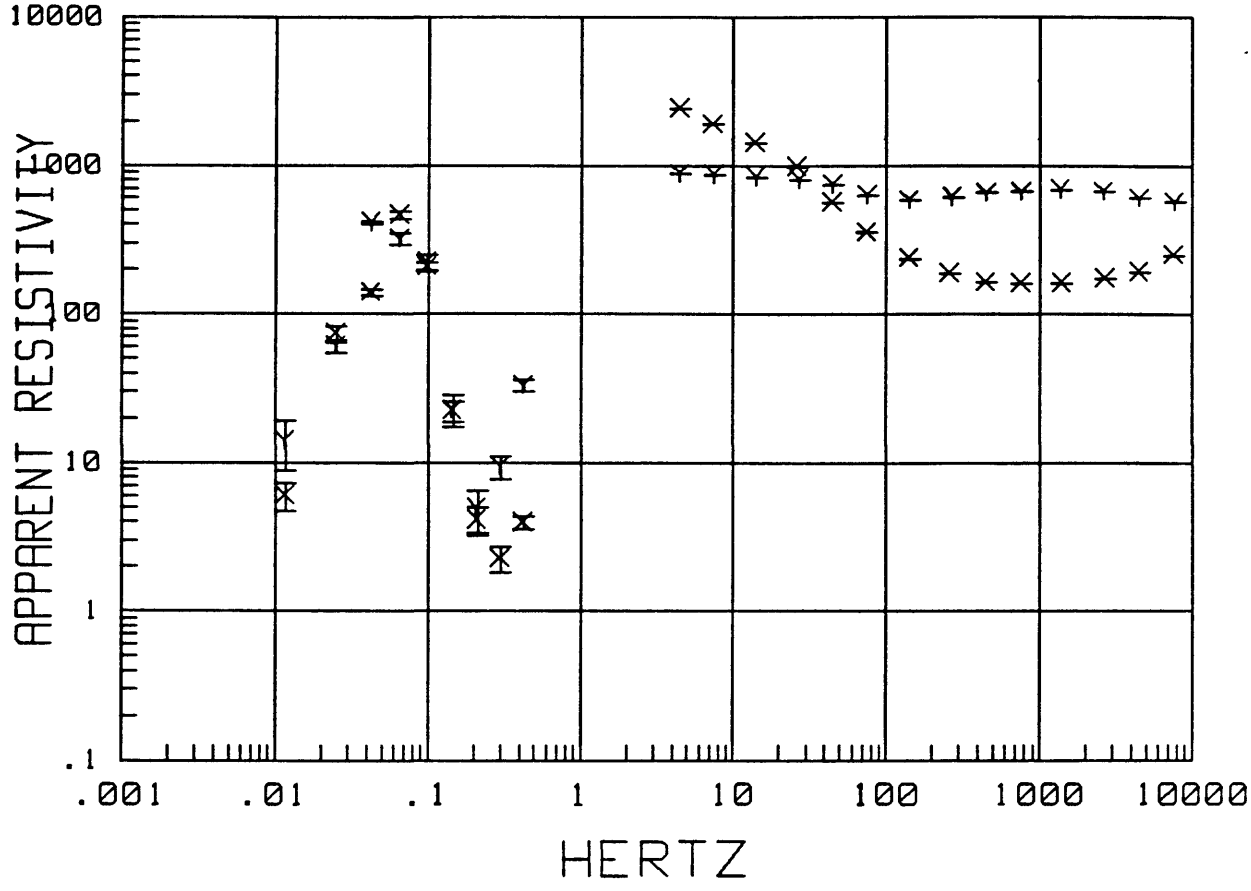

MTHO11 LOCAL H-ref 17:05:51 13 May 1988
IMPEDANCE PHASE

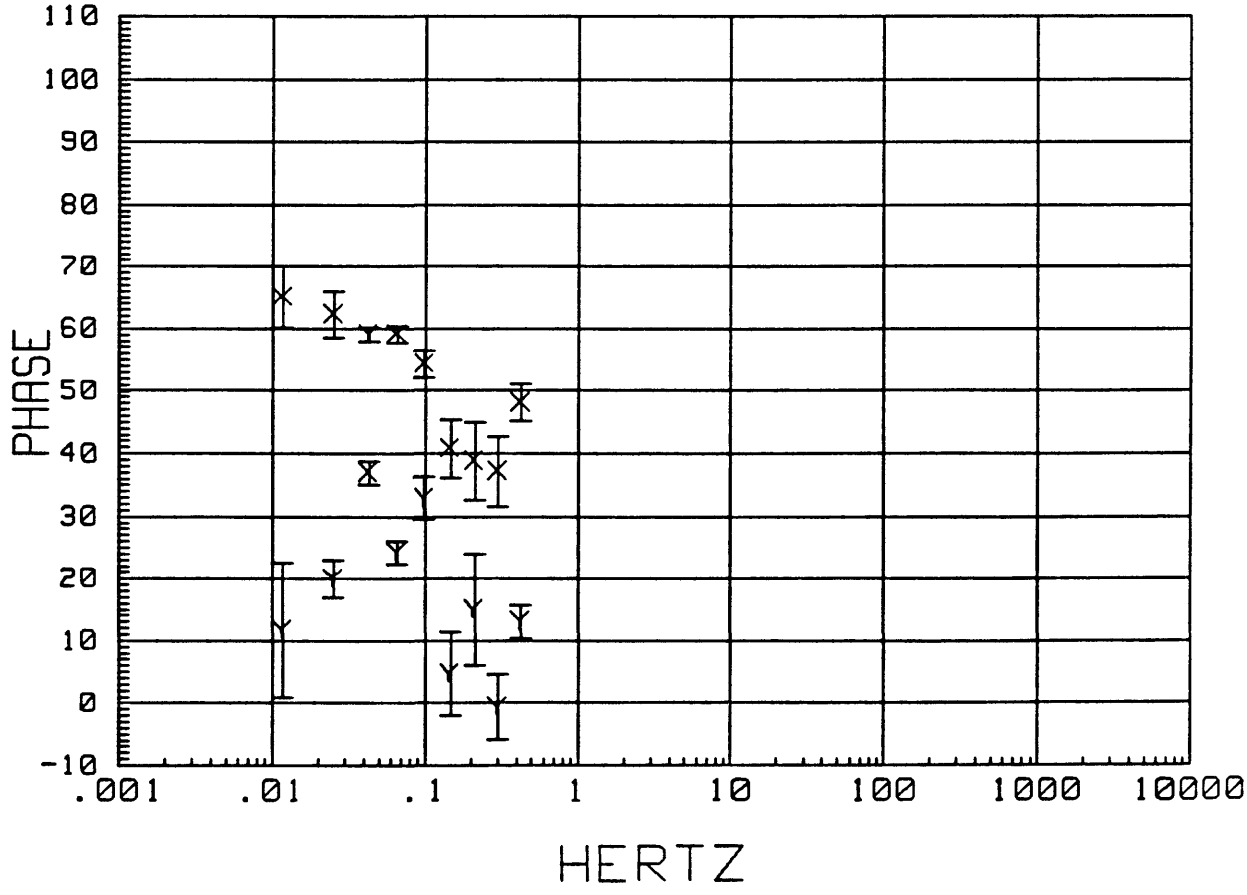

MTHO11 LOCAL H-ref 17:05:51 13 May 1988
Z MAXIMUM DIRECTION

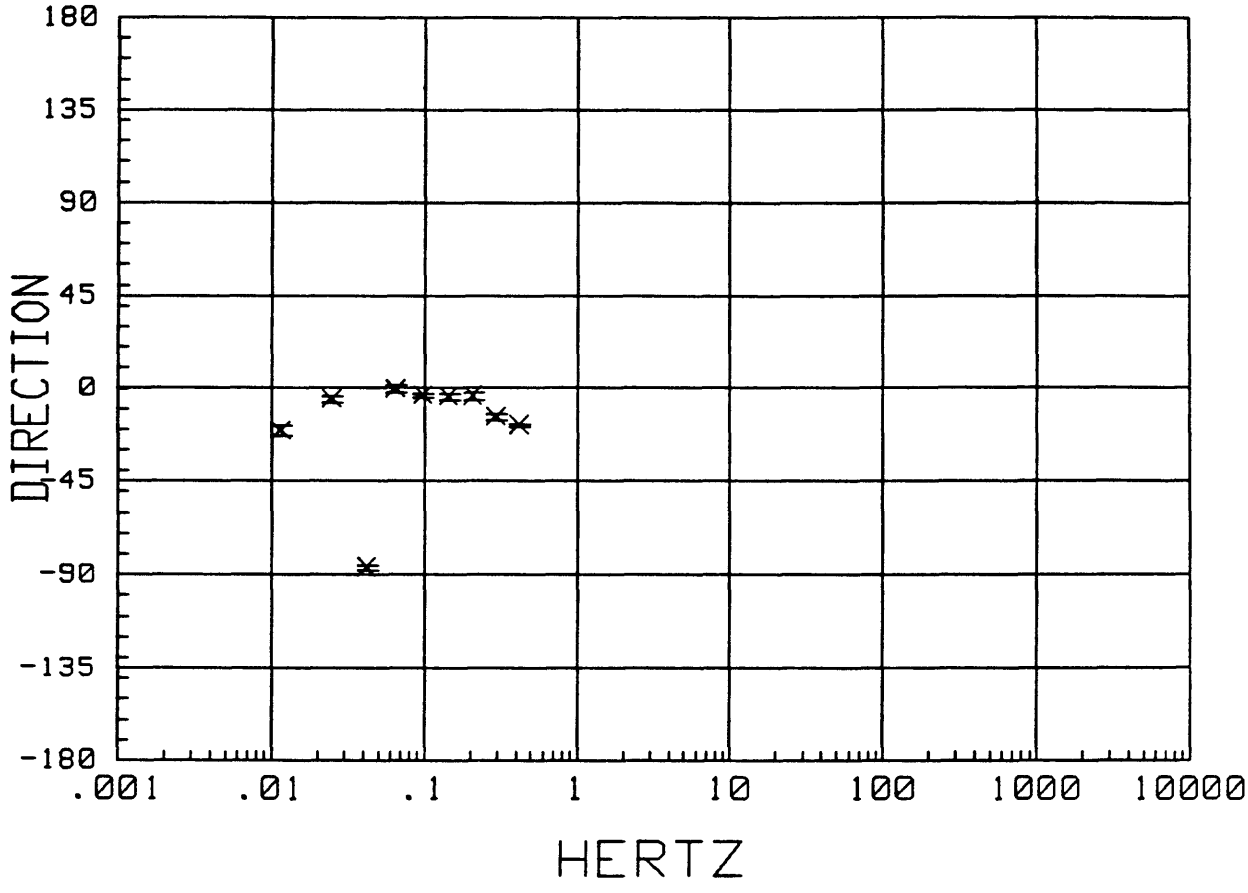

MTHO11 LOCAL H-ref 17:05:51 13 May 1988
SKEW

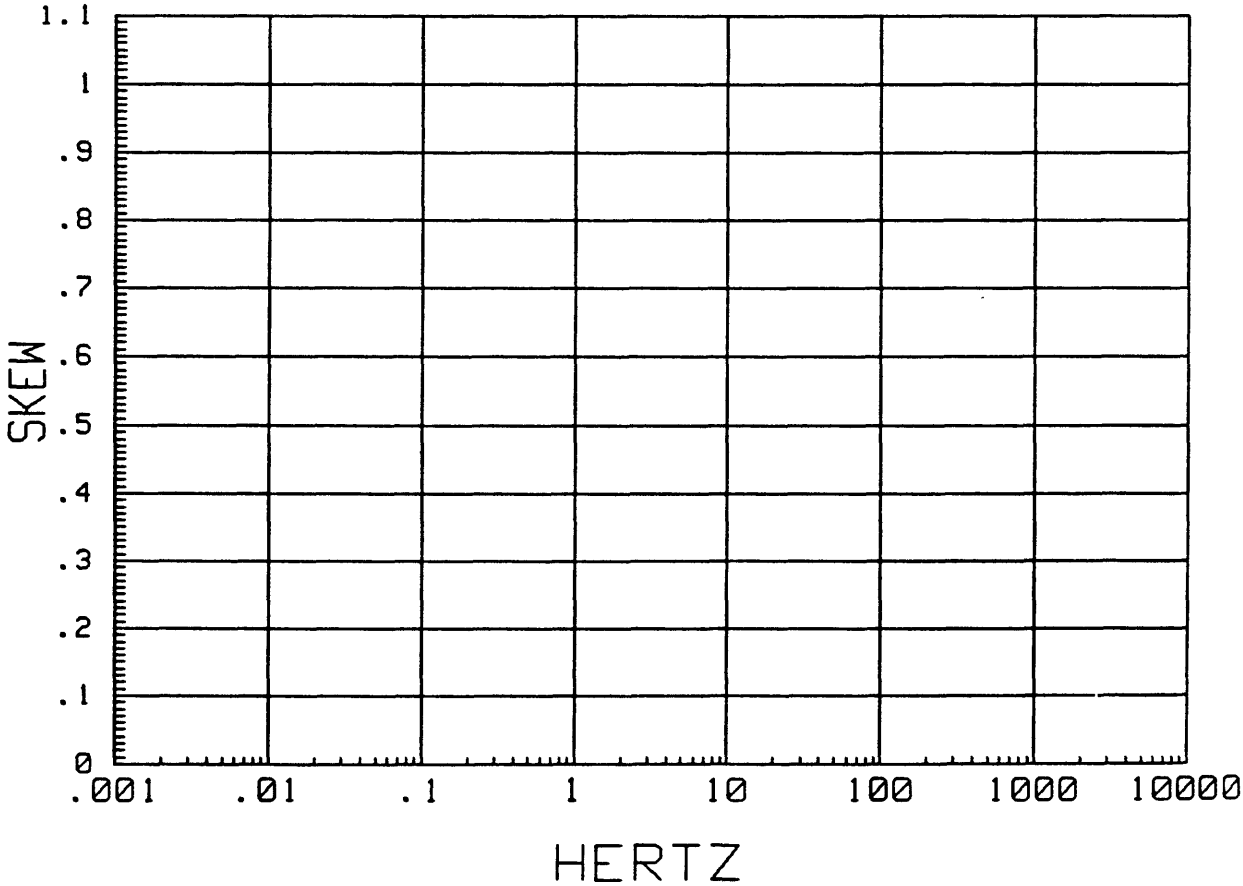

MTHO12 LOCAL H-ref 17:14:24 13 May 1988
APPARENT RESISTIVITY

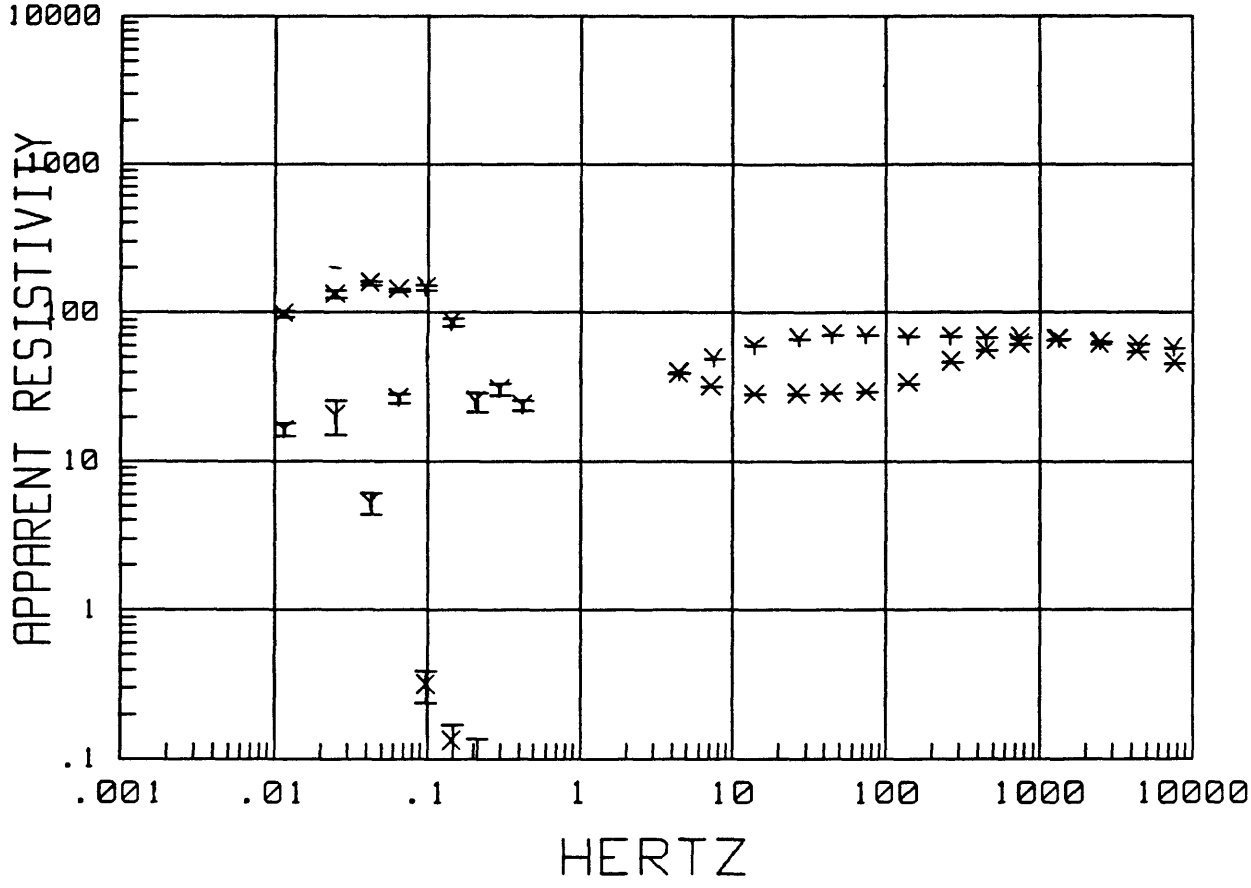

MTHO12 LOCAL H-ref 17:14:24 13 May 1988
IMPEDANCE PHASE

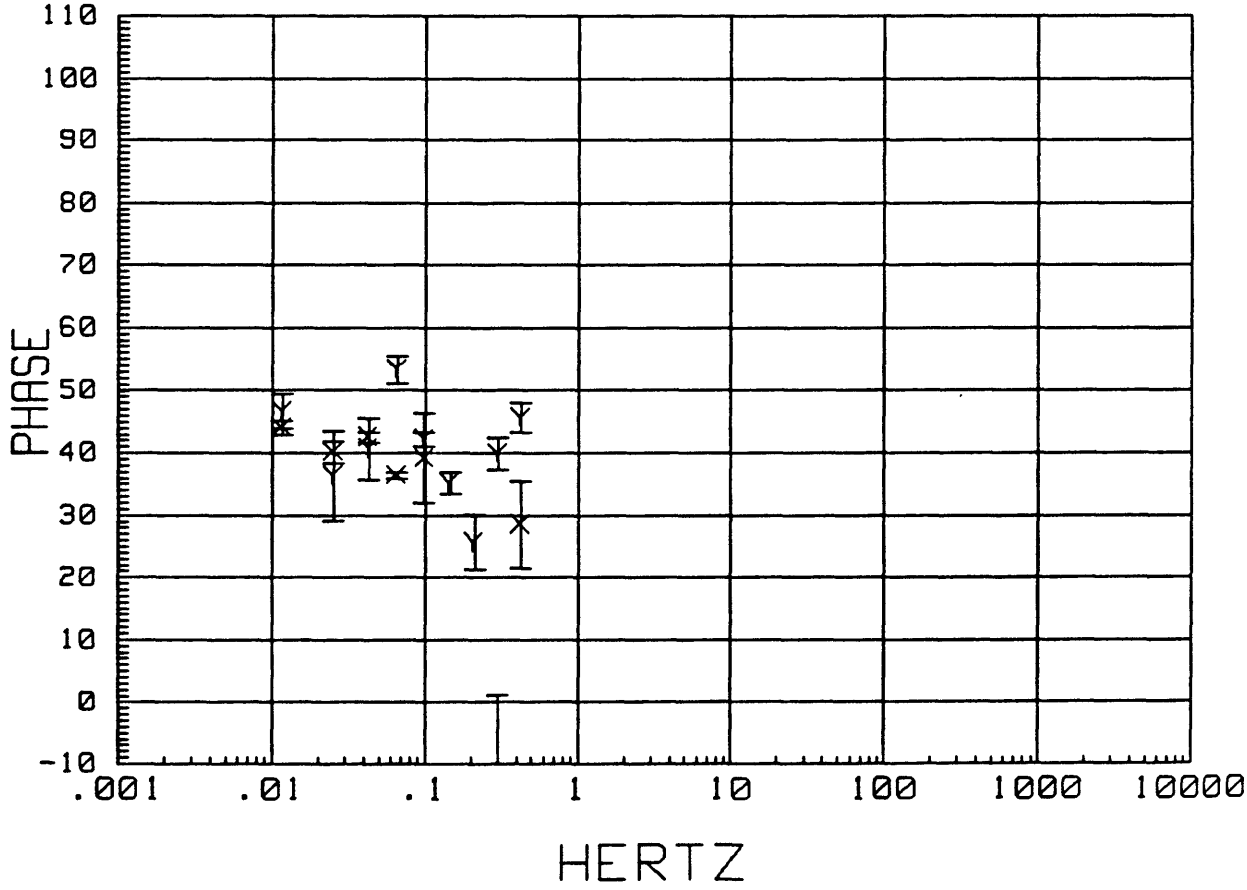

MTHO12 LOCAL H-ref 17:14:24 13 May 1988
Z MAXIMUM DIRECTION

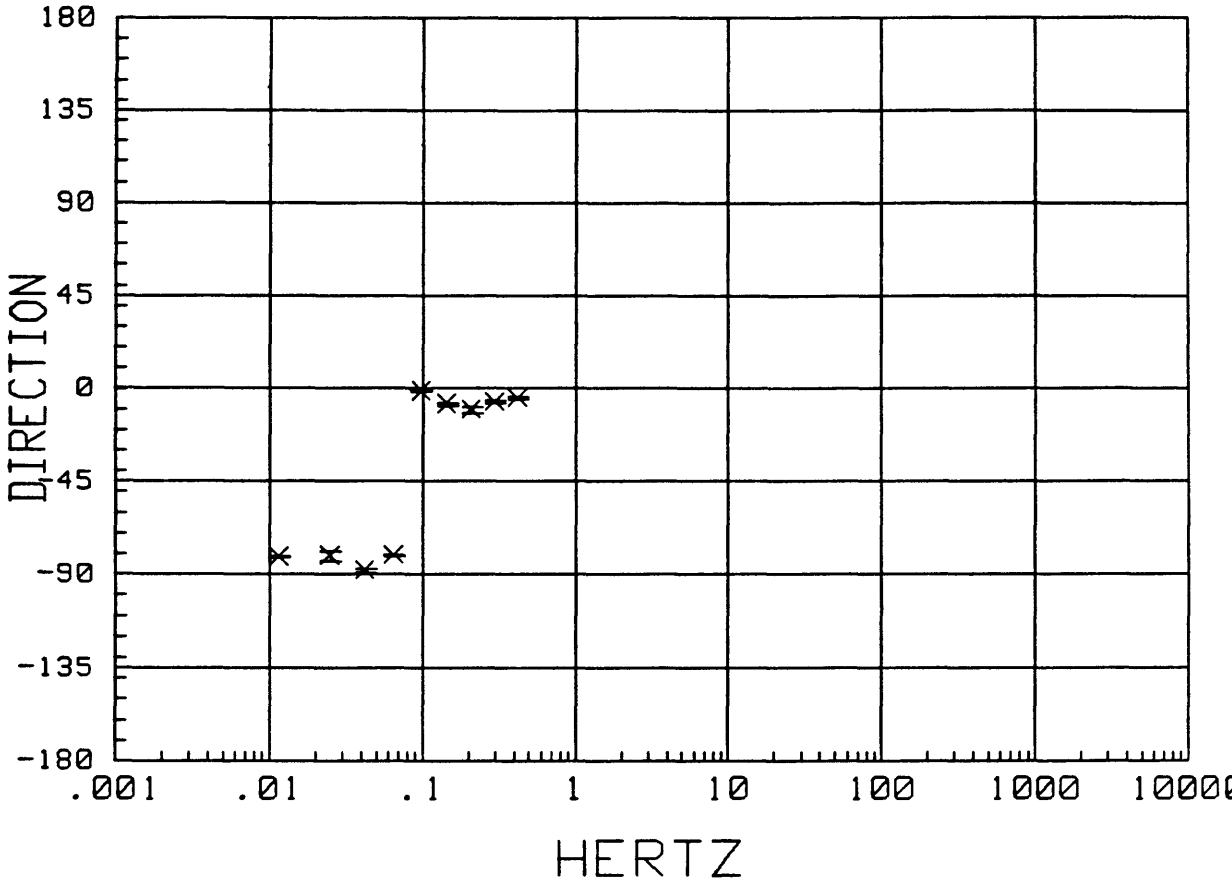

MTHO12 LOCAL H-ref 17:14:24 13 May 1988
SKEW

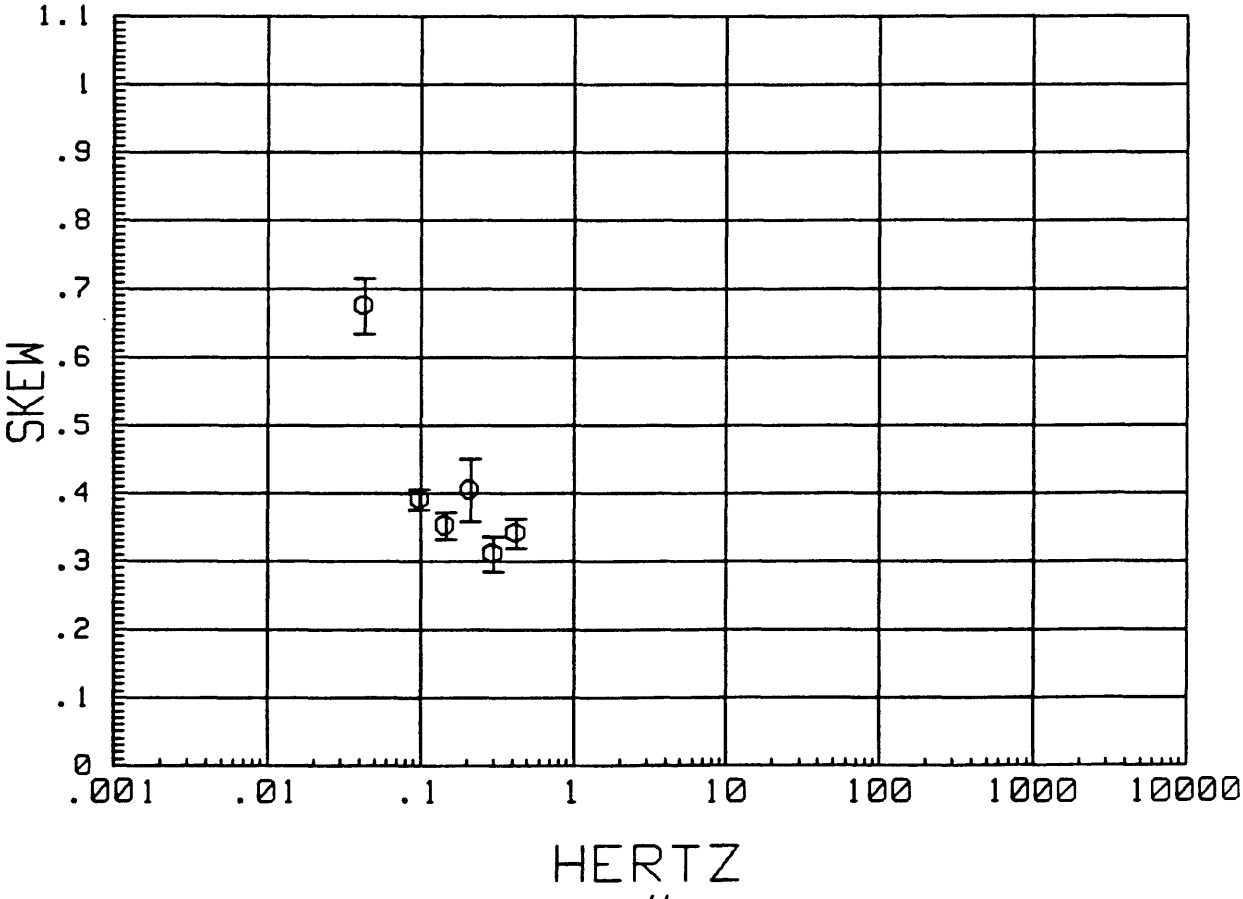

MTHO13 LOCAL H-ref 18:53:57 13 May 1988
APPARENT RESISTIVITY

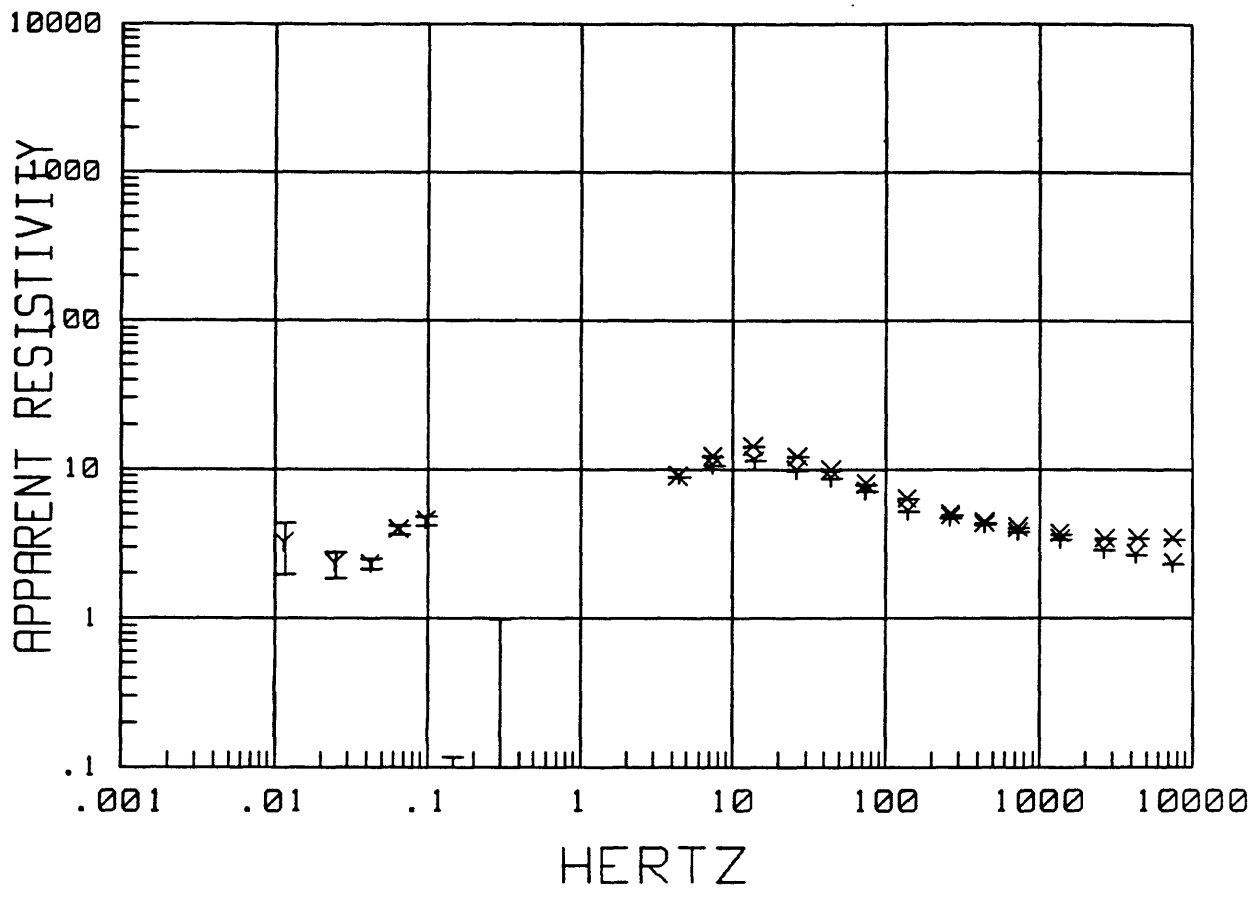

MTHO13 LOCAL H-ref 18:53:57 13 May 1988
IMPEDANCE PHASE

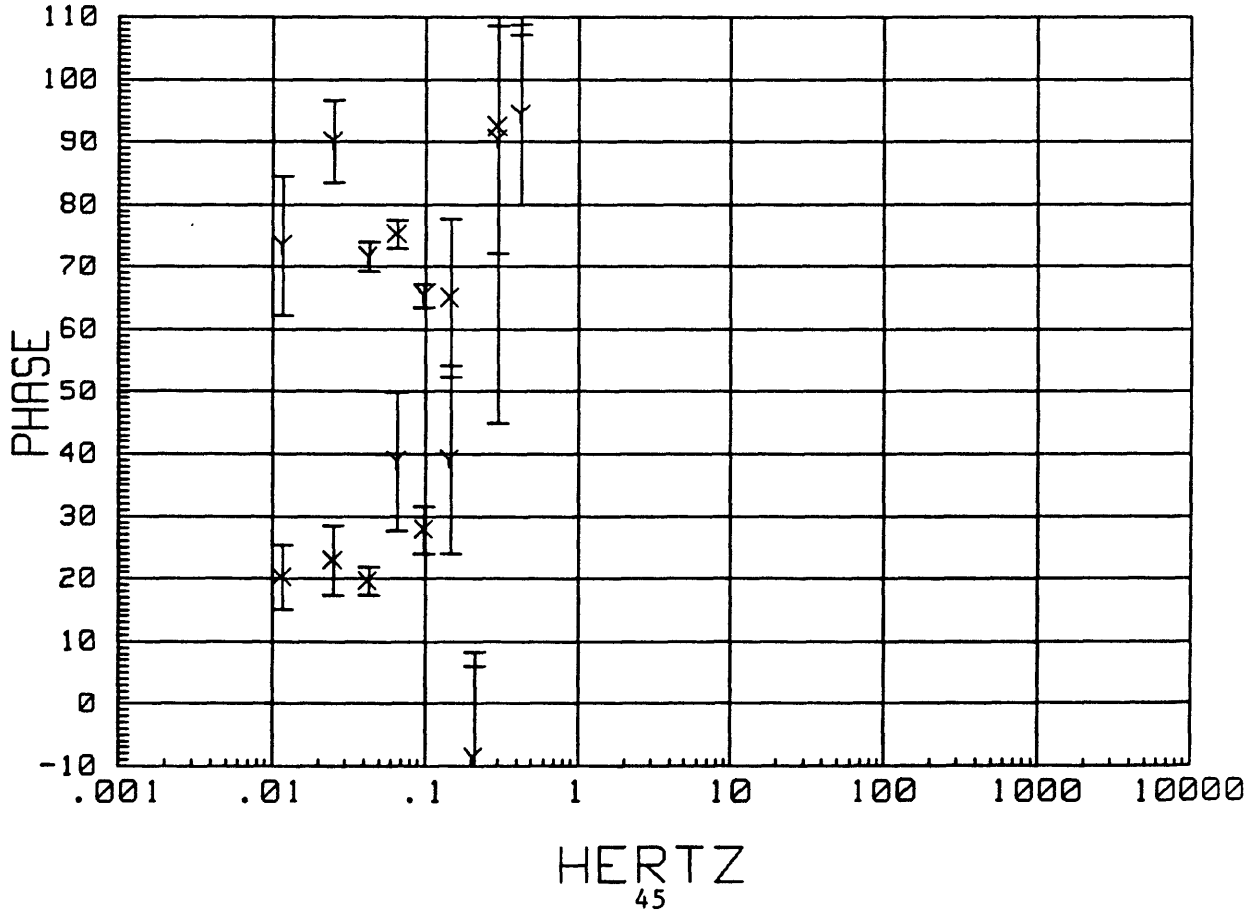

MTHO13 LOCAL H-ref 18:53:57 13 May 1988
Z MAXIMUM DIRECTION

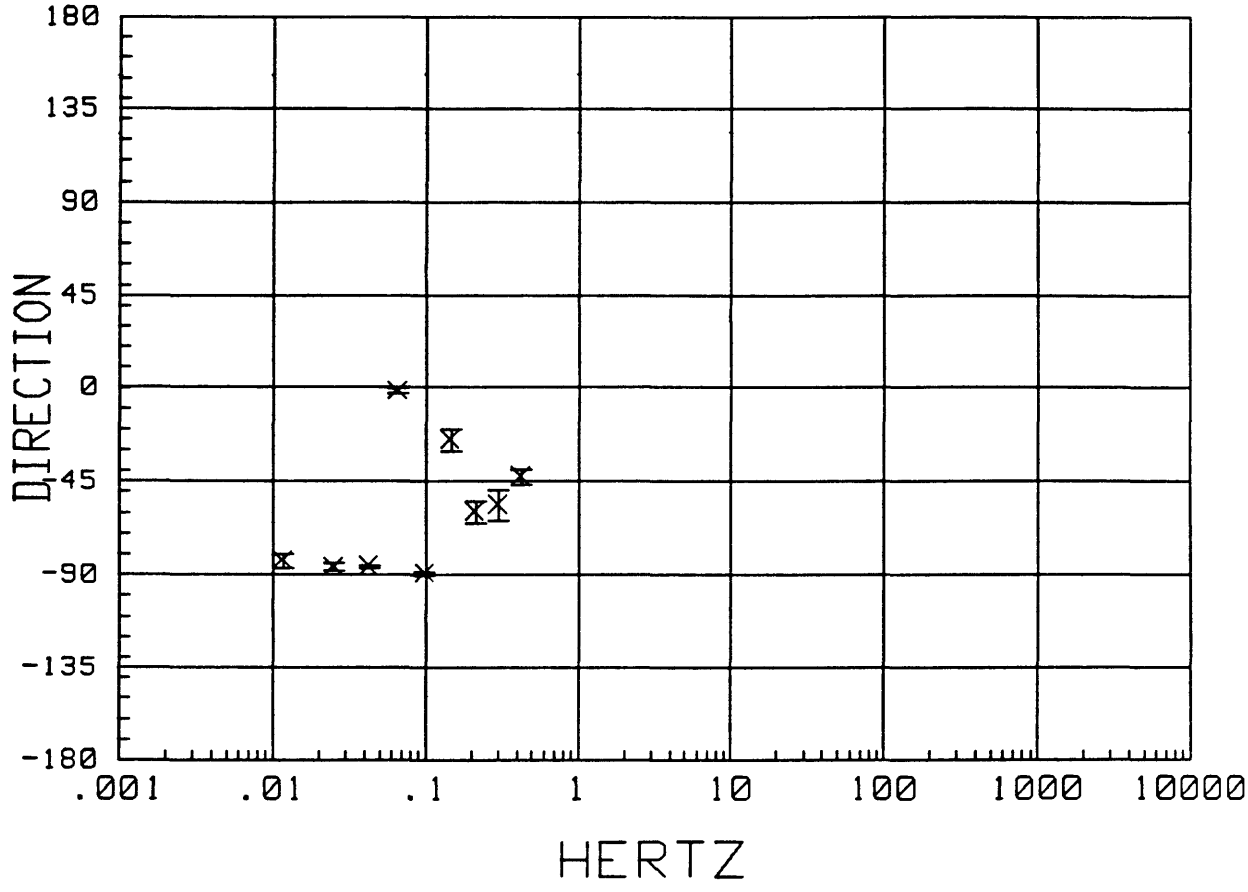

MTHO13 LOCAL H-ref 18:53:57 13 May 1988
SKEW

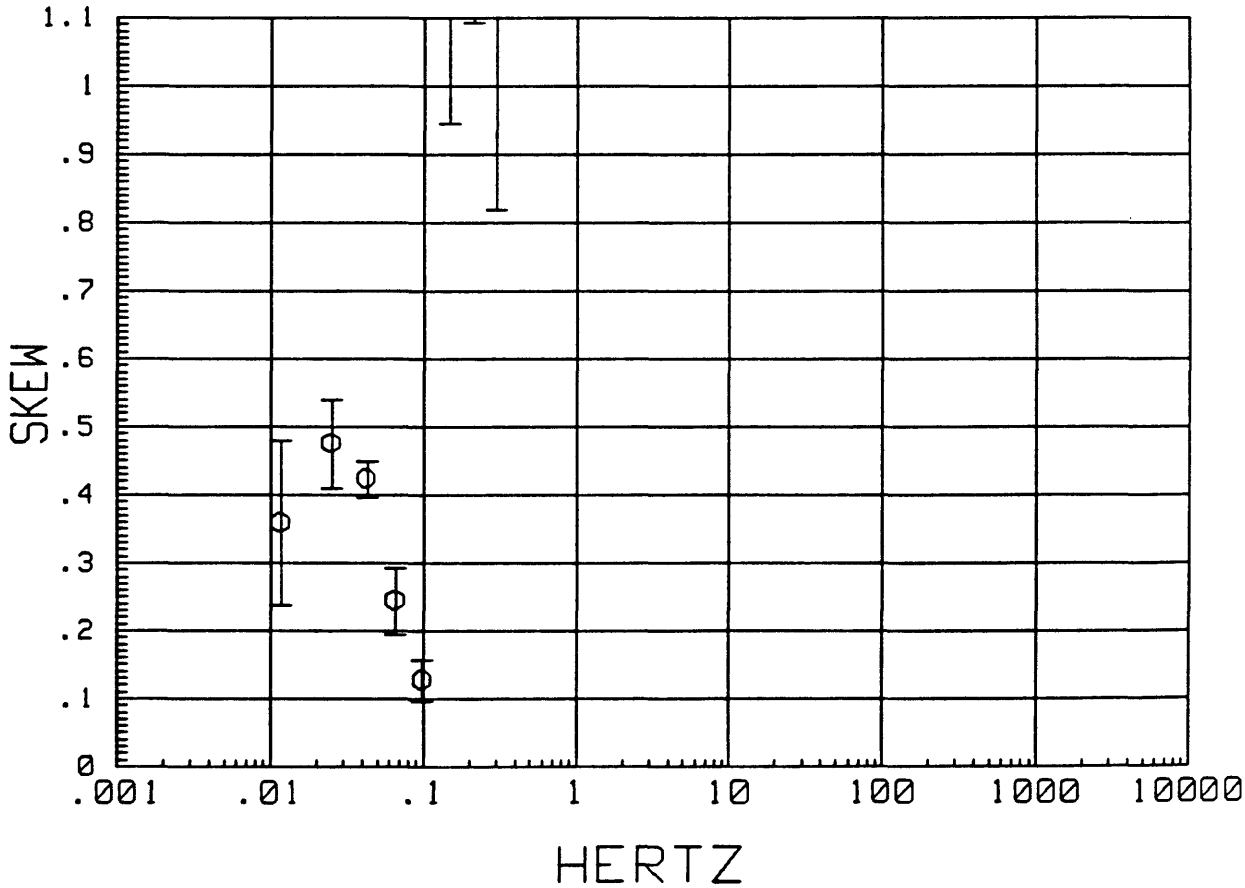

MTHO14 LOCAL H-ref 19:09:03 13 May 1988
APPARENT RESISTIVITY

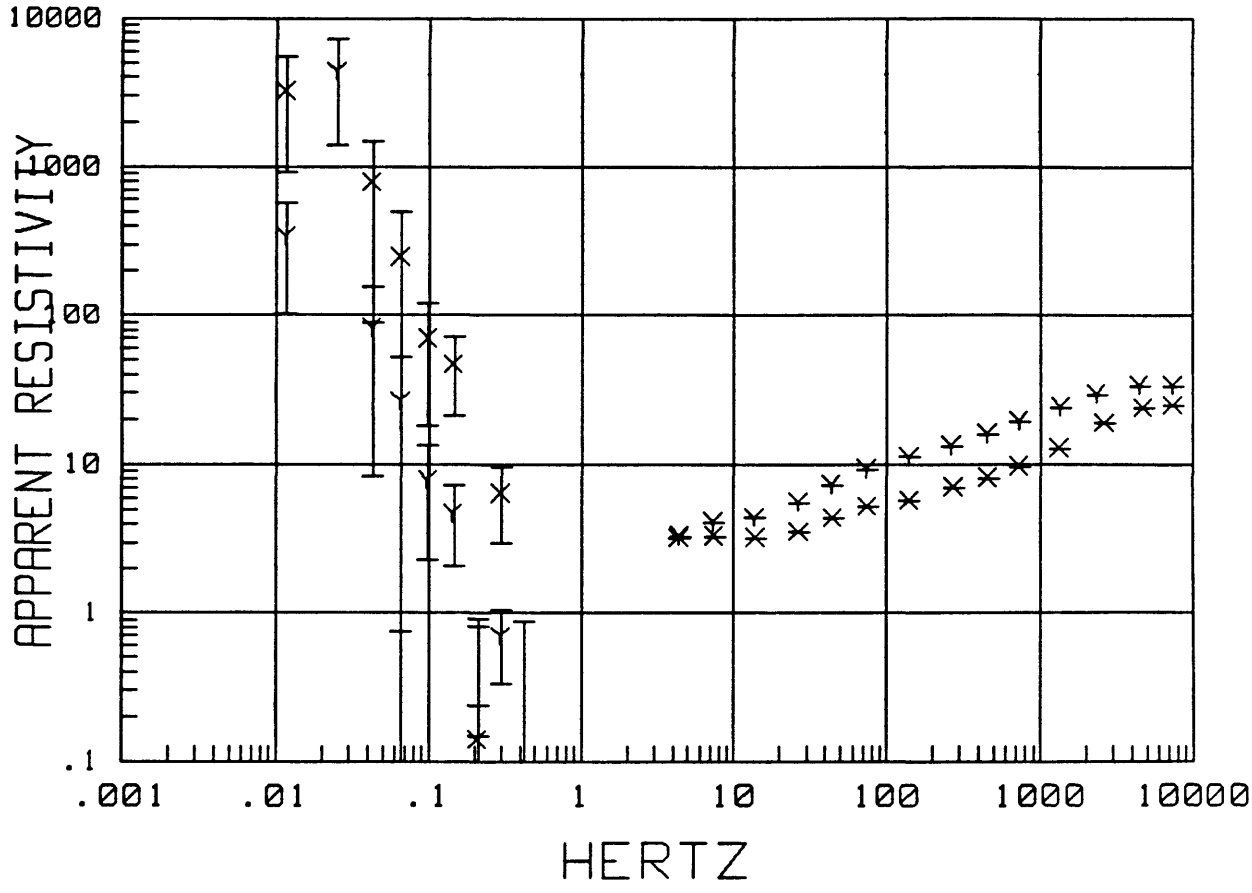

MTHO14 LOCAL H-ref 19:09:03 13 May 1988
IMPEDANCE PHASE

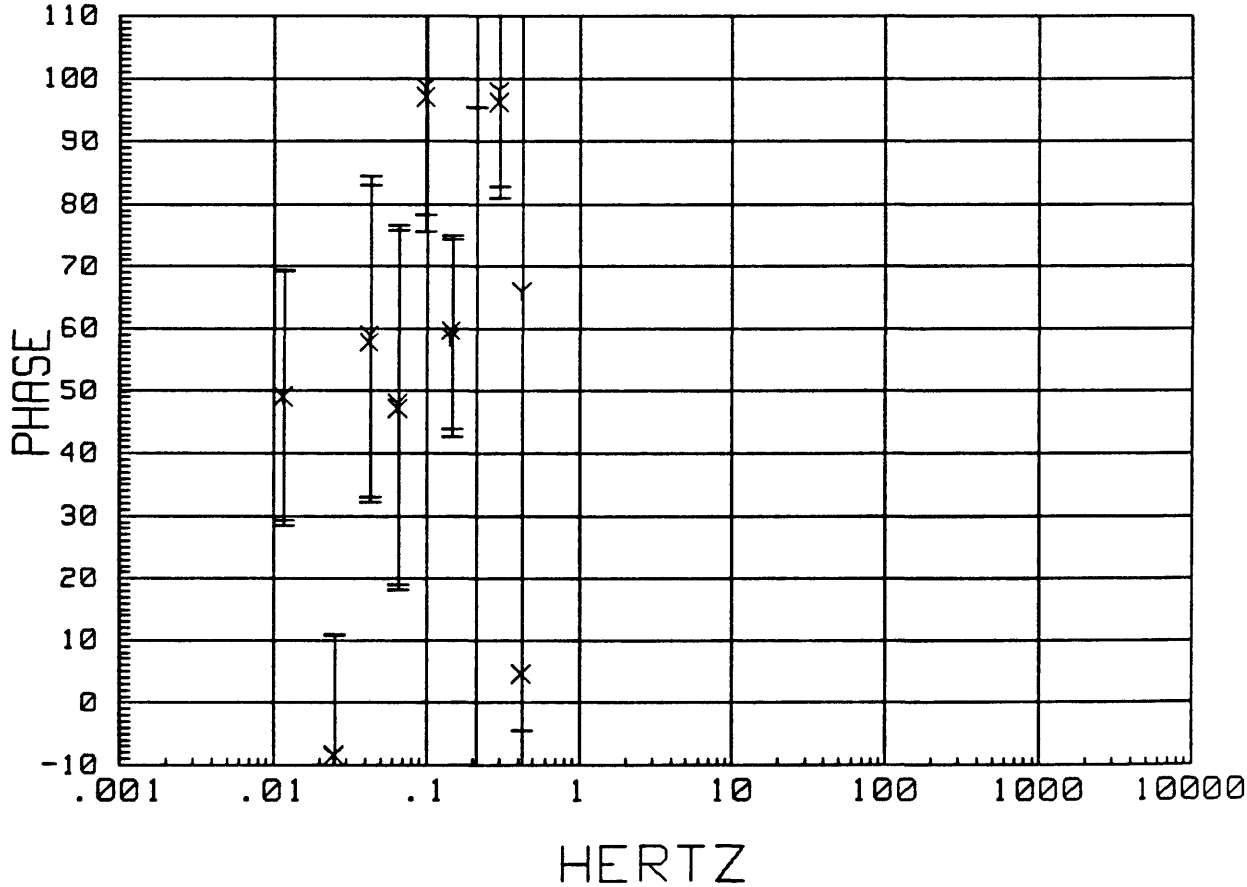

MTHO14 LOCAL H-ref 19:09:03 13 May 1988
Z MAXIMUM DIRECTION

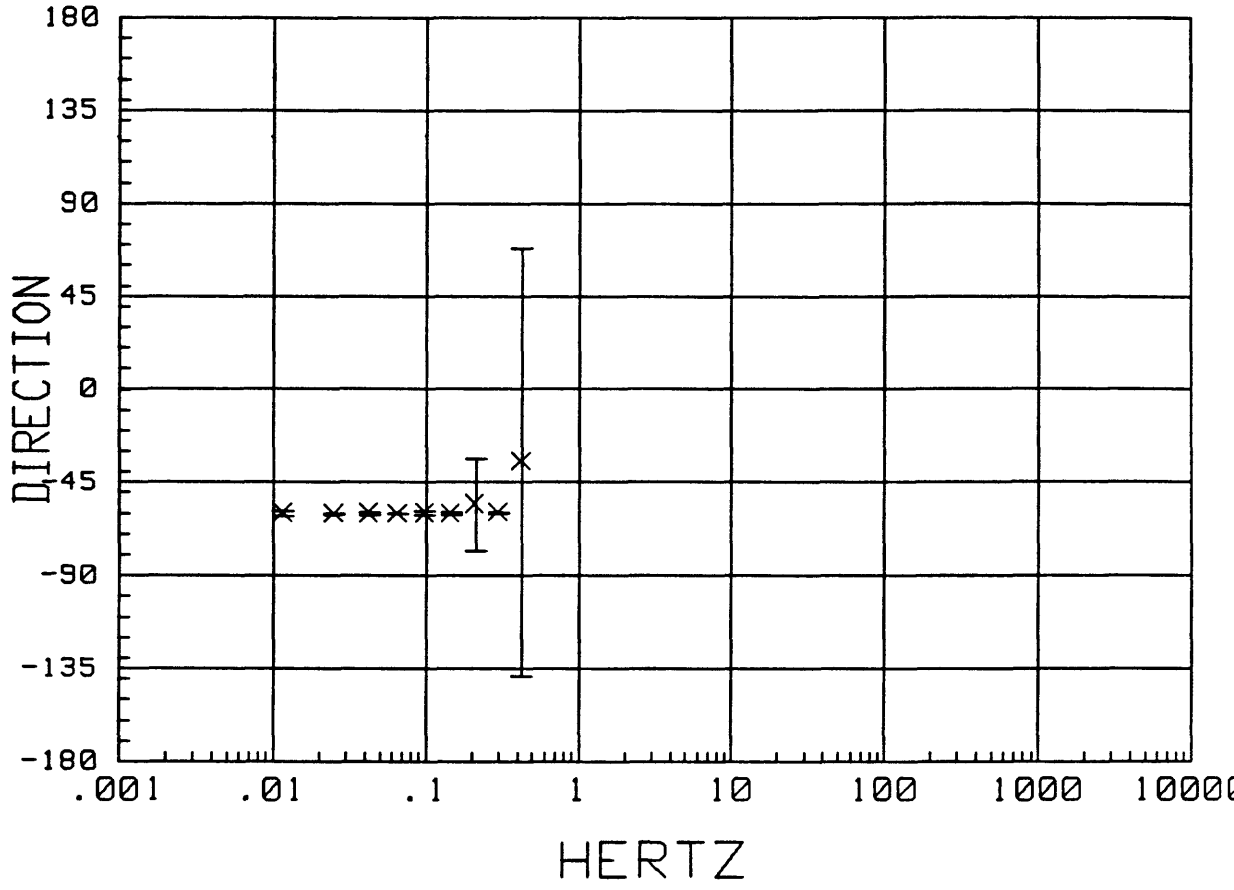

MTHO14 LOCAL H-ref 19:09:03 13 May 1988
SKEW

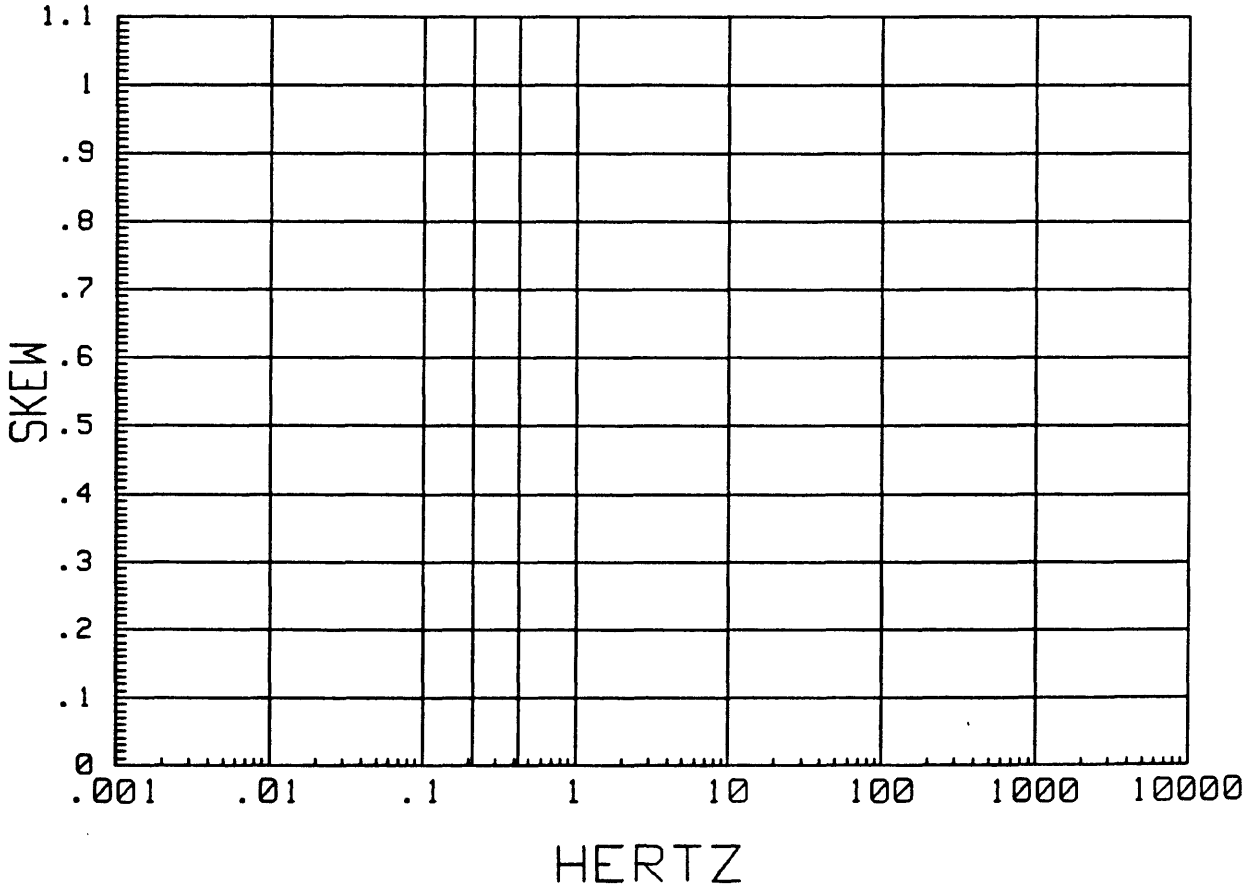

MTHO15 LOCAL H-ref 21:21:41 13 May 1988
APPARENT RESISTIVITY

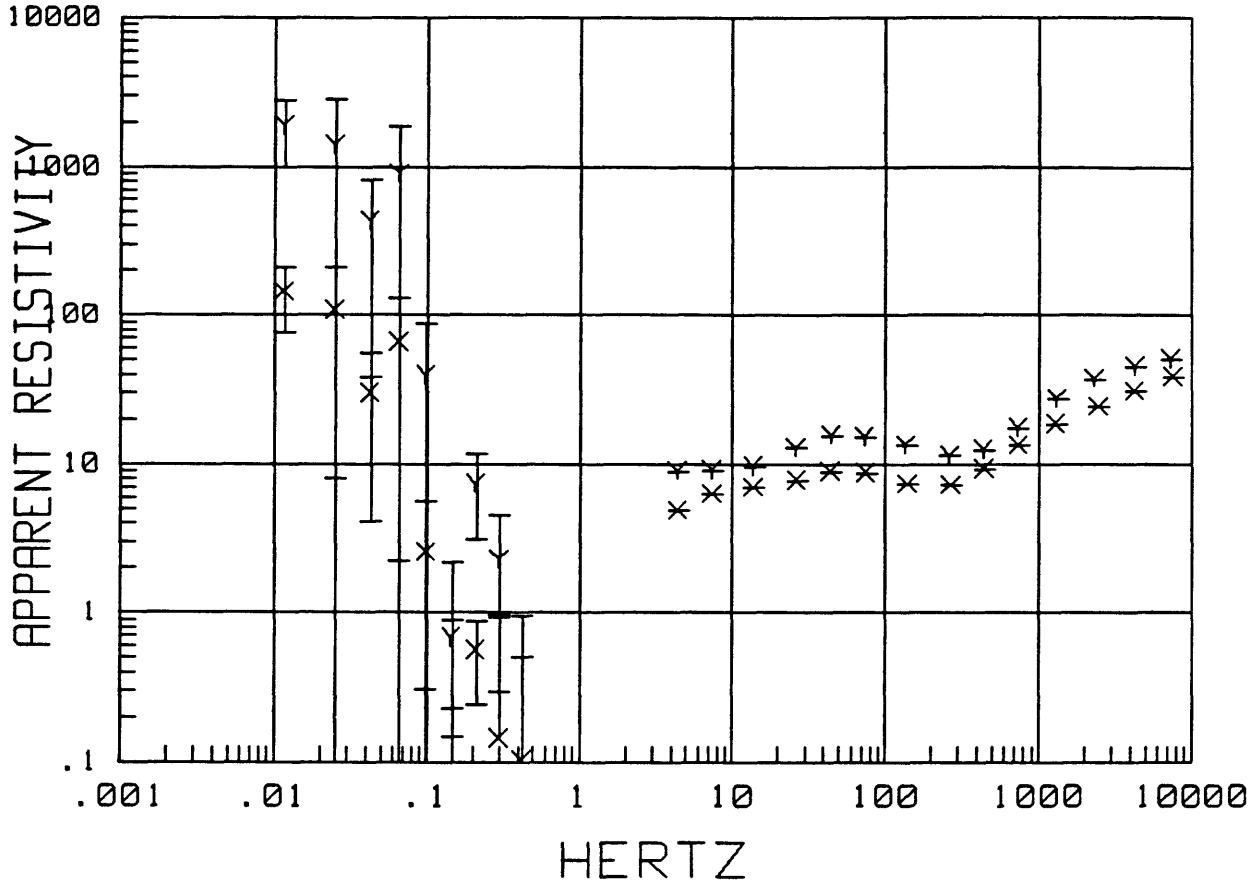

MTHO15 LOCAL H-ref 21:21:41 13 May 1988
IMPEDANCE PHASE

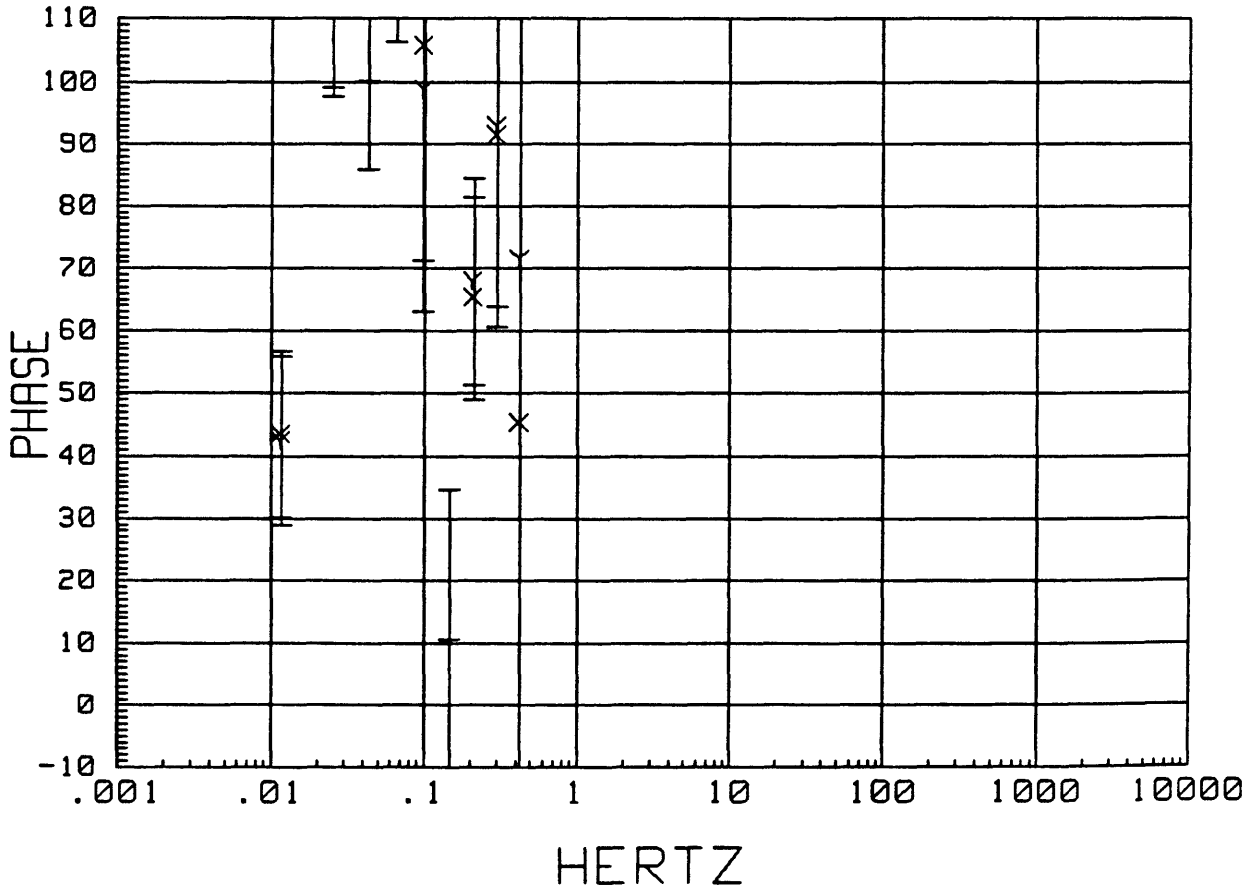

MTHO15 LOCAL H-ref 21:21:41 13 May 1988
Z MAXIMUM DIRECTION

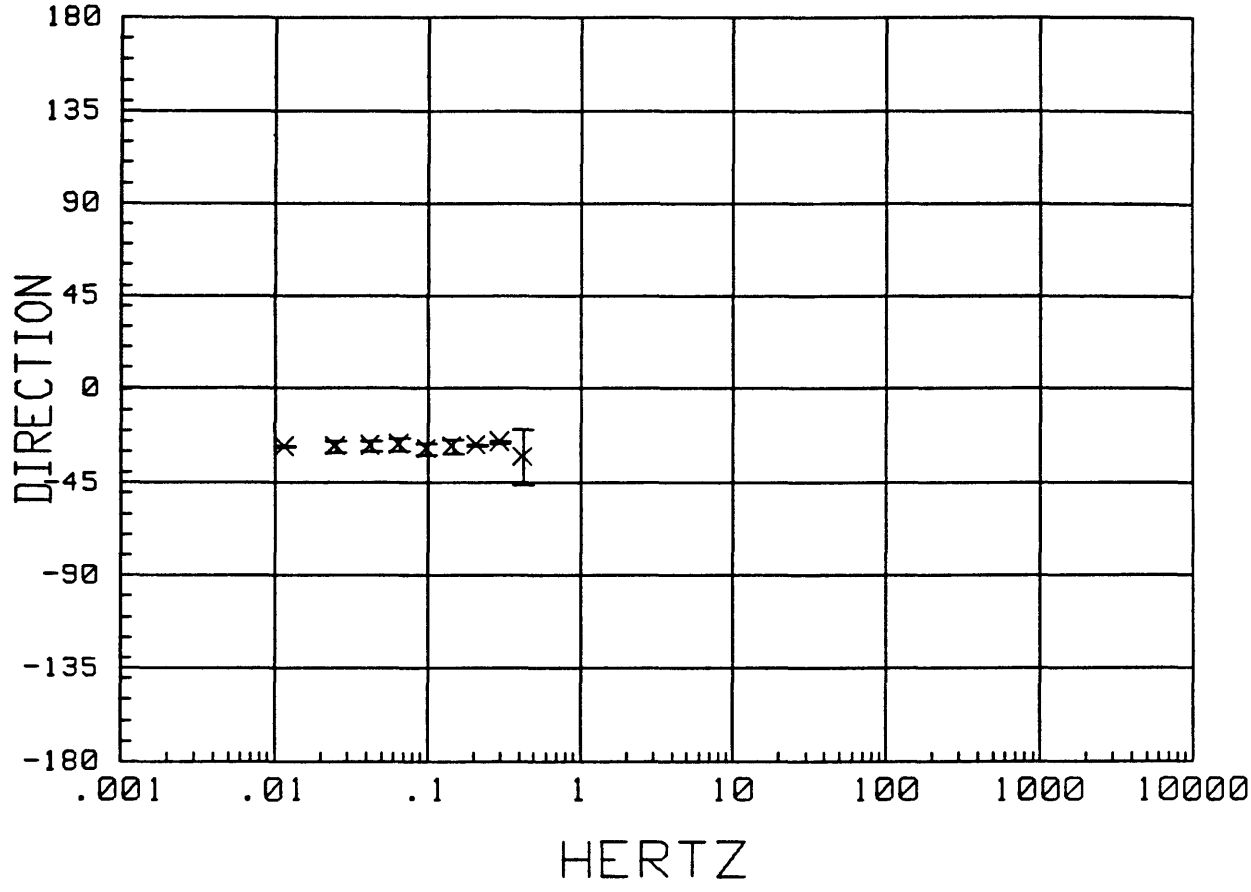

MTHO15 LOCAL H-ref 21:21:41 13 May 1988
SKEW

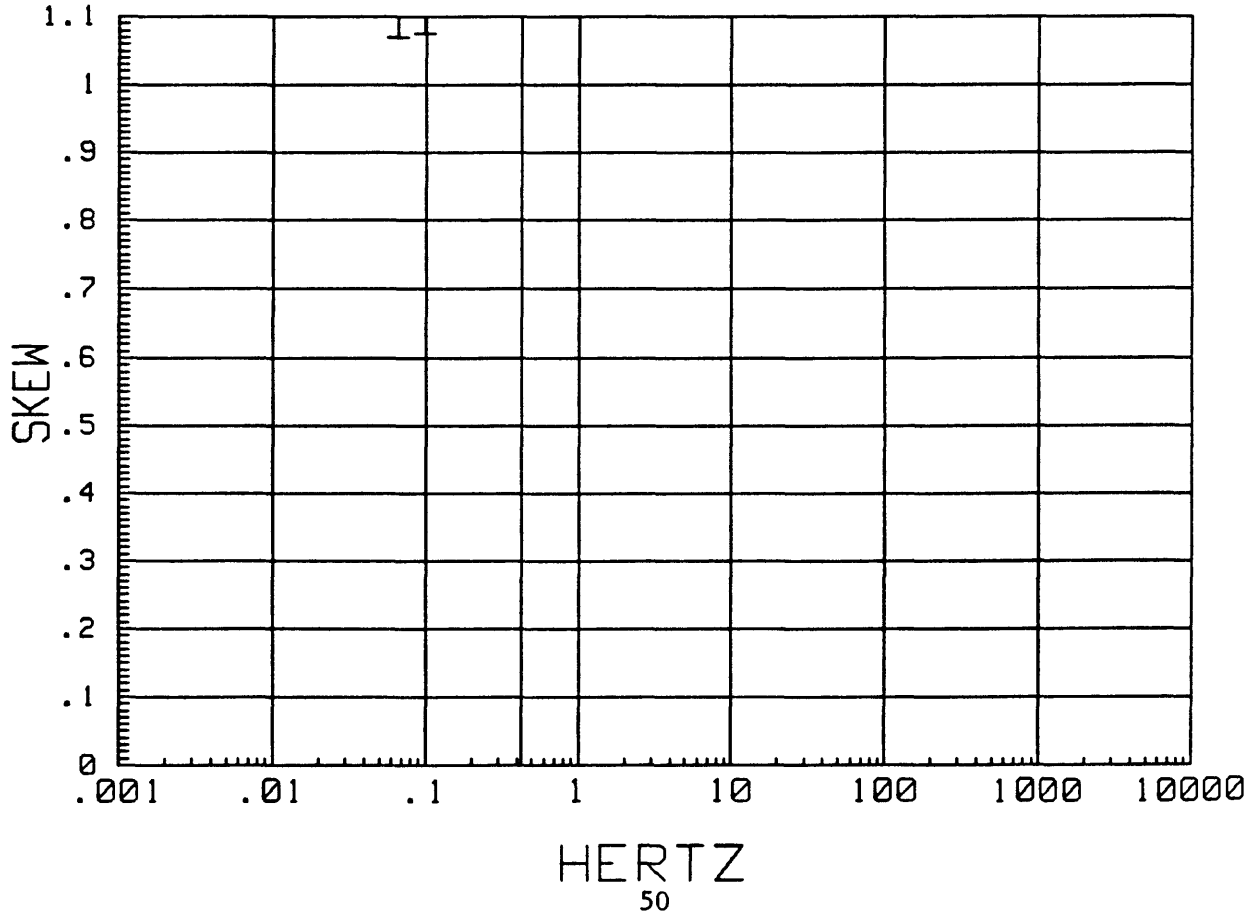

MTH016 LOCAL H-ref 21:32:41 13 May 1988
APPARENT RESISTIVITY

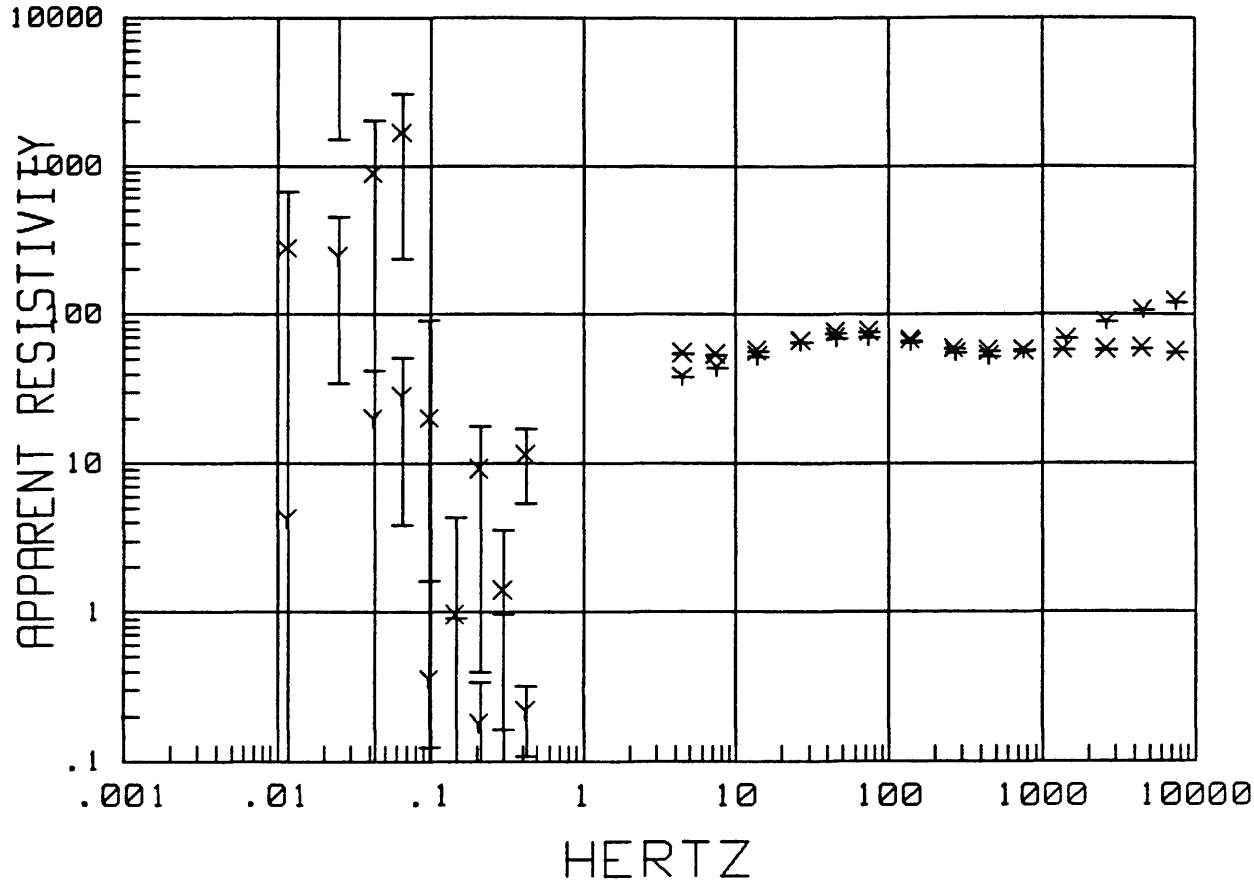

MTH016 LOCAL H-ref 21:32:41 13 May 1988
IMPEDANCE PHASE

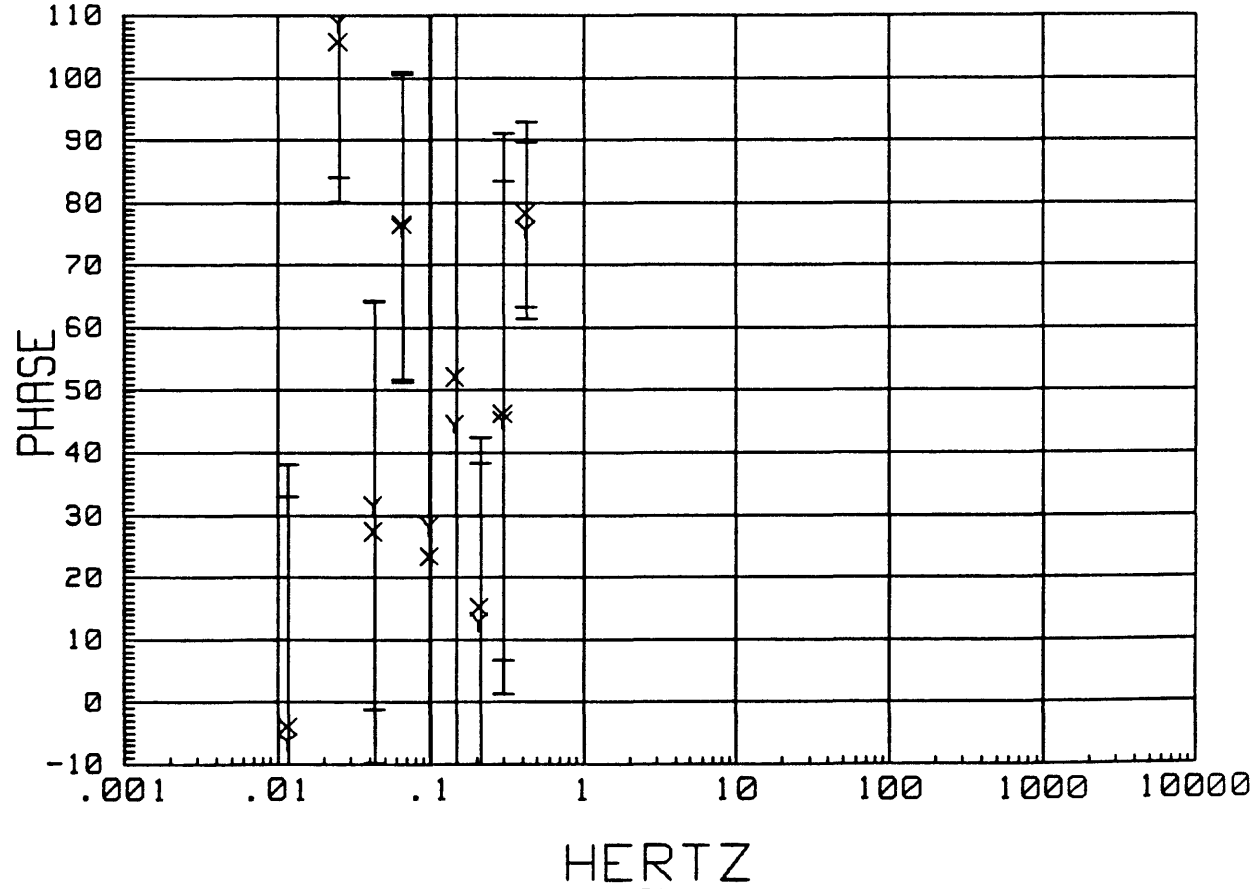

MTH016 LOCAL H-ref 21:32:41 13 May 1988
Z MAXIMUM DIRECTION

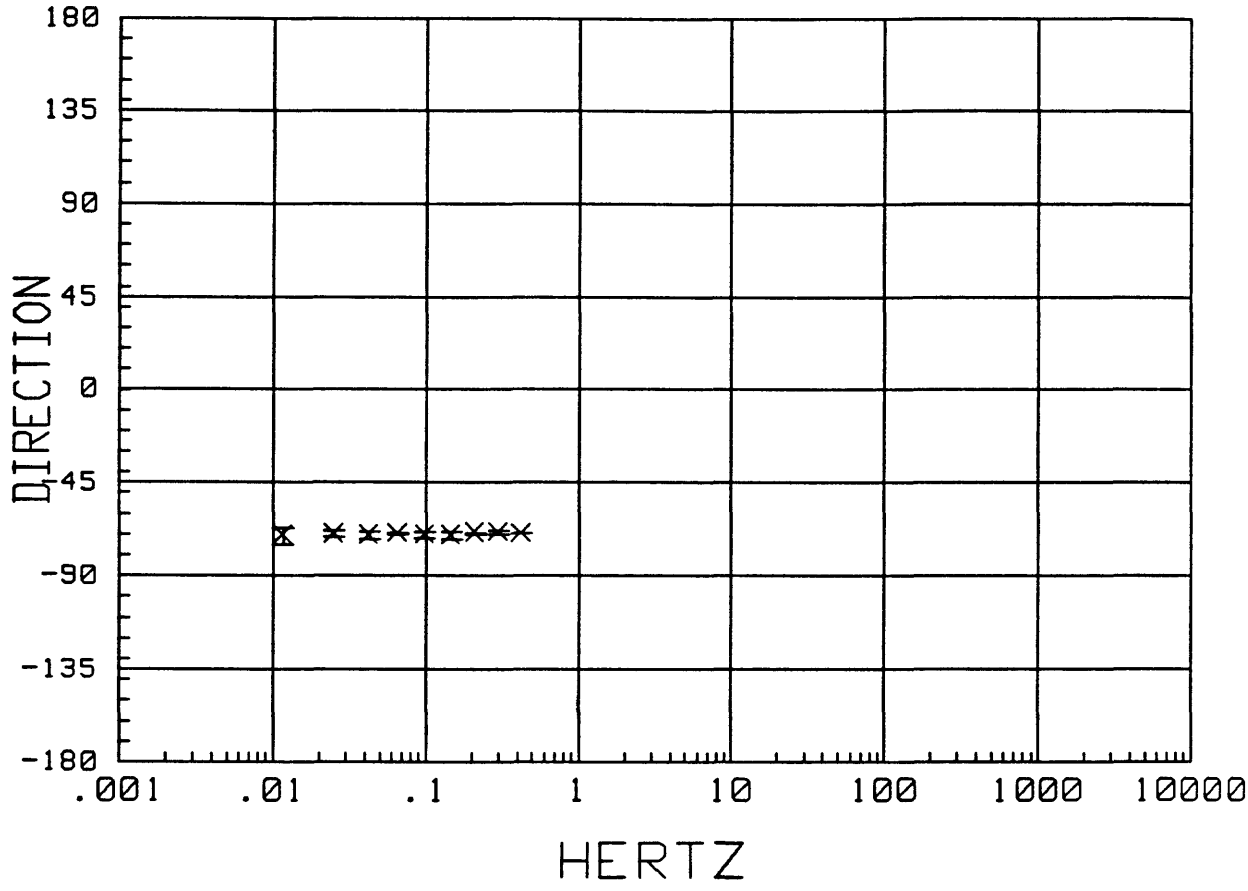

MTH016 LOCAL H-ref 21:32:41 13 May 1988
SKEW

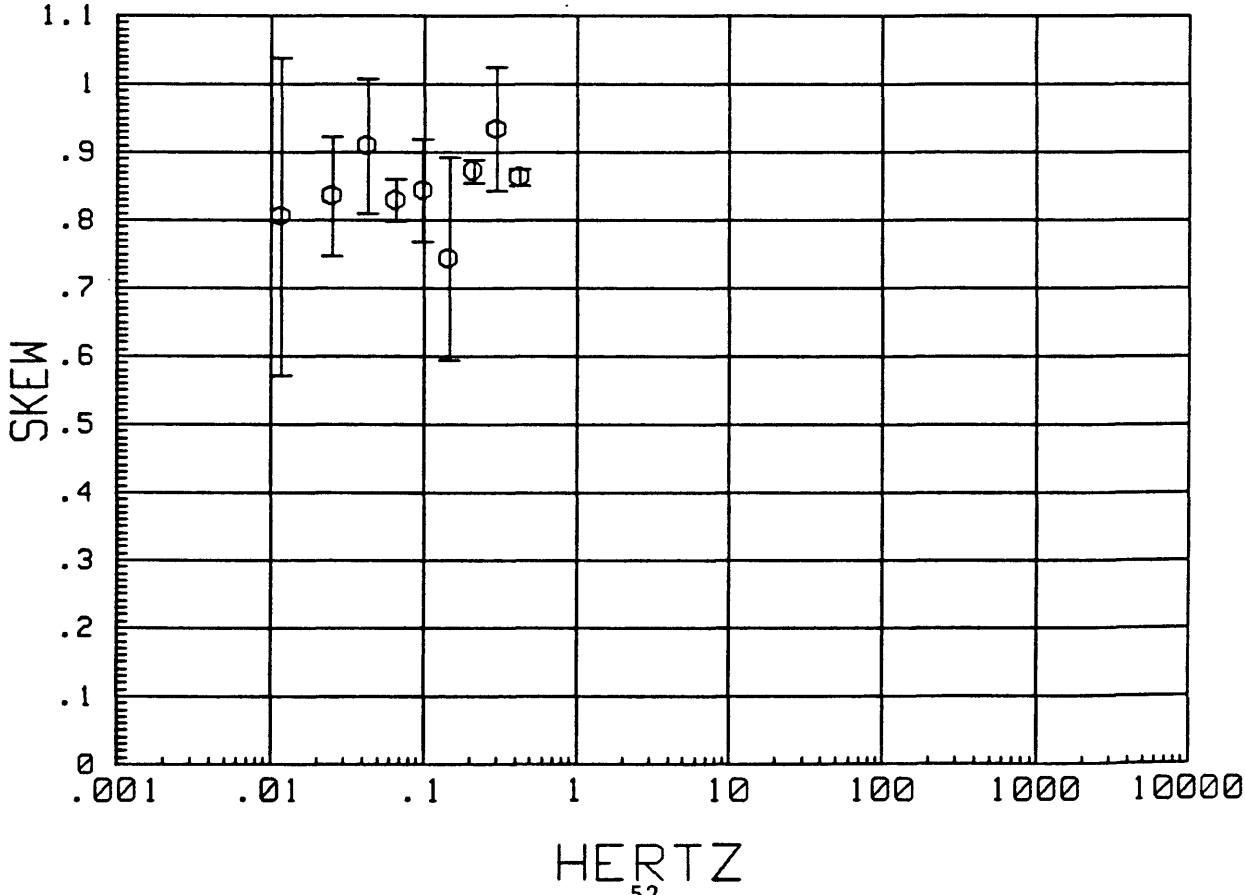

MTH017 LOCAL H-ref 21:40:48 13 May 1988
APPARENT RESISTIVITY

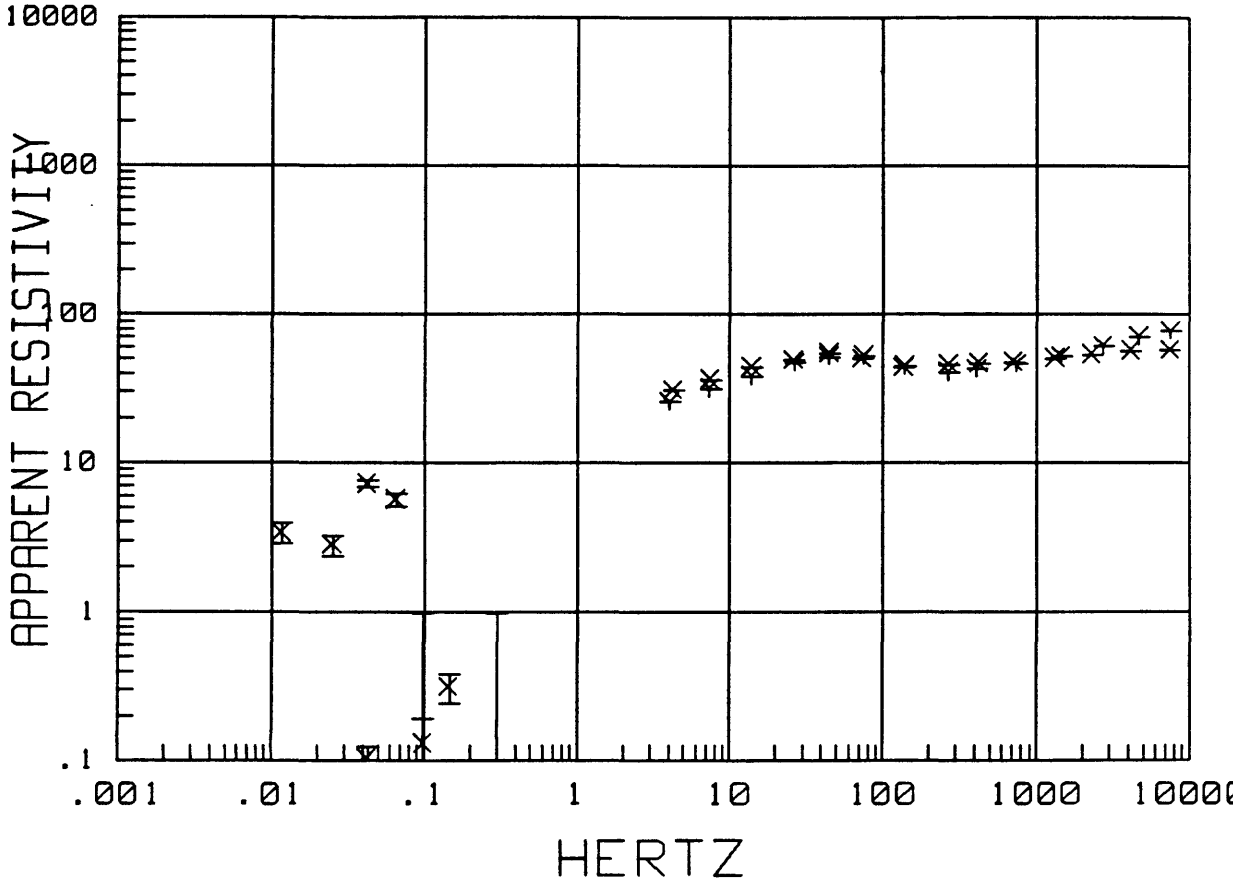

MTH017 LOCAL H-ref 21:40:48 13 May 1988
IMPEDANCE PHASE

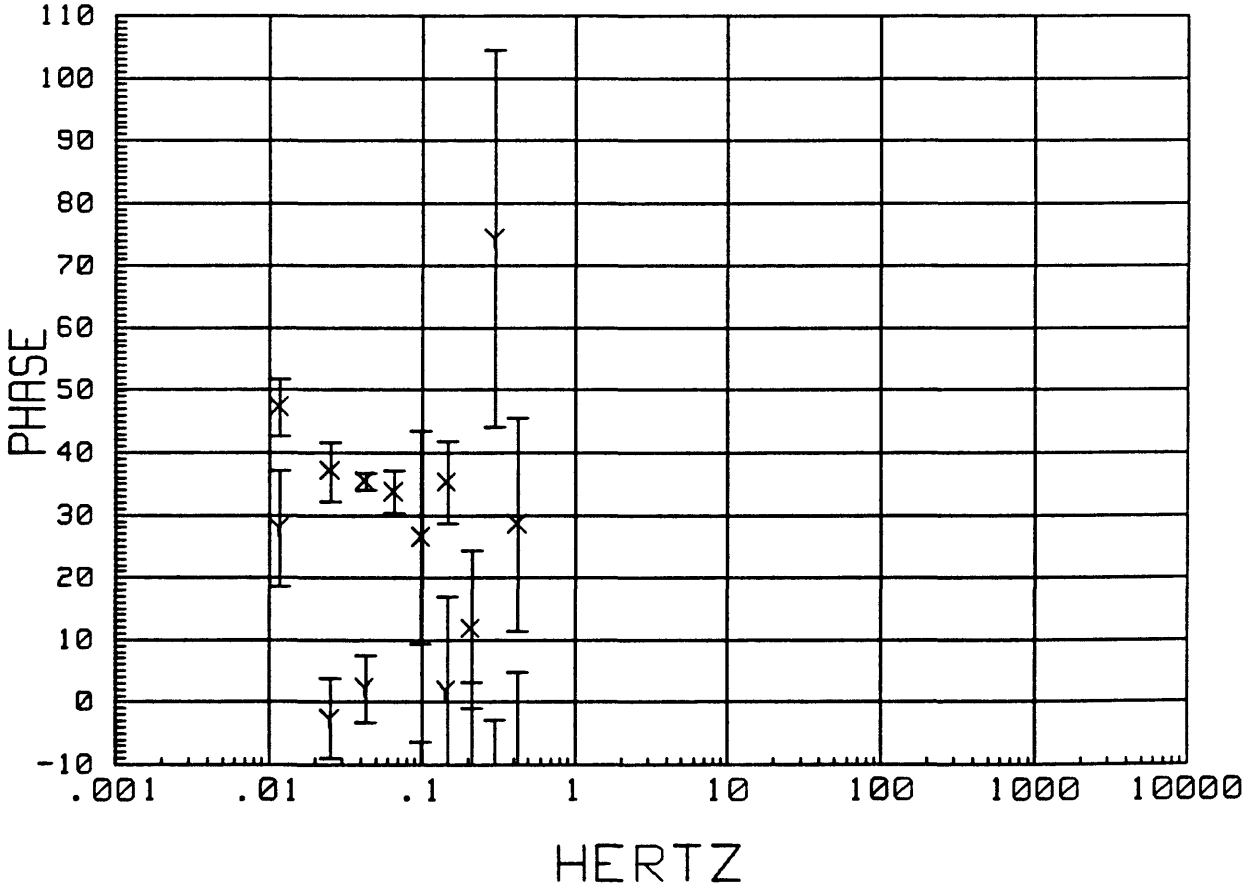

MTHO17 LOCAL H-ref 21:40:48 13 May 1988
Z MAXIMUM DIRECTION

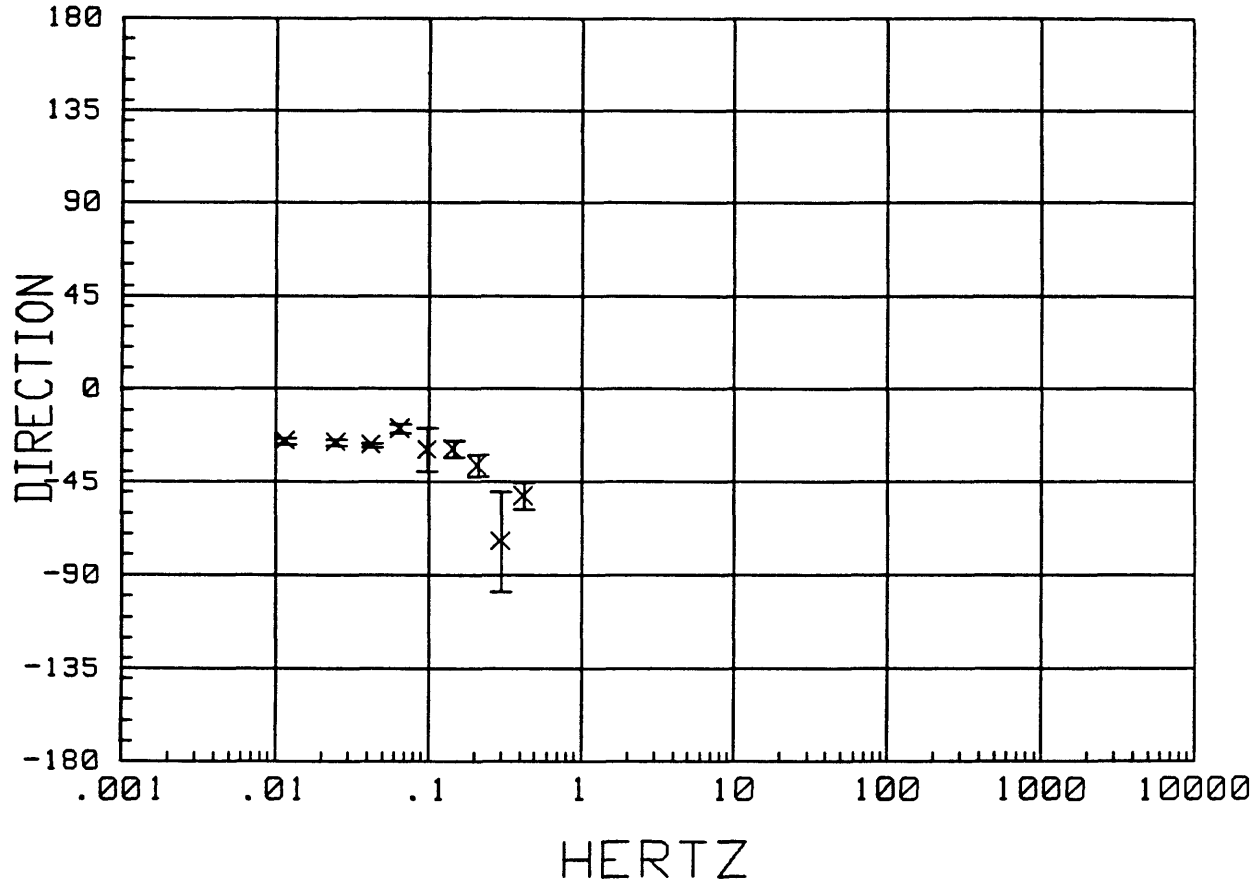

MTHO17 LOCAL H-ref 21:40:48 13 May 1988
SKEW

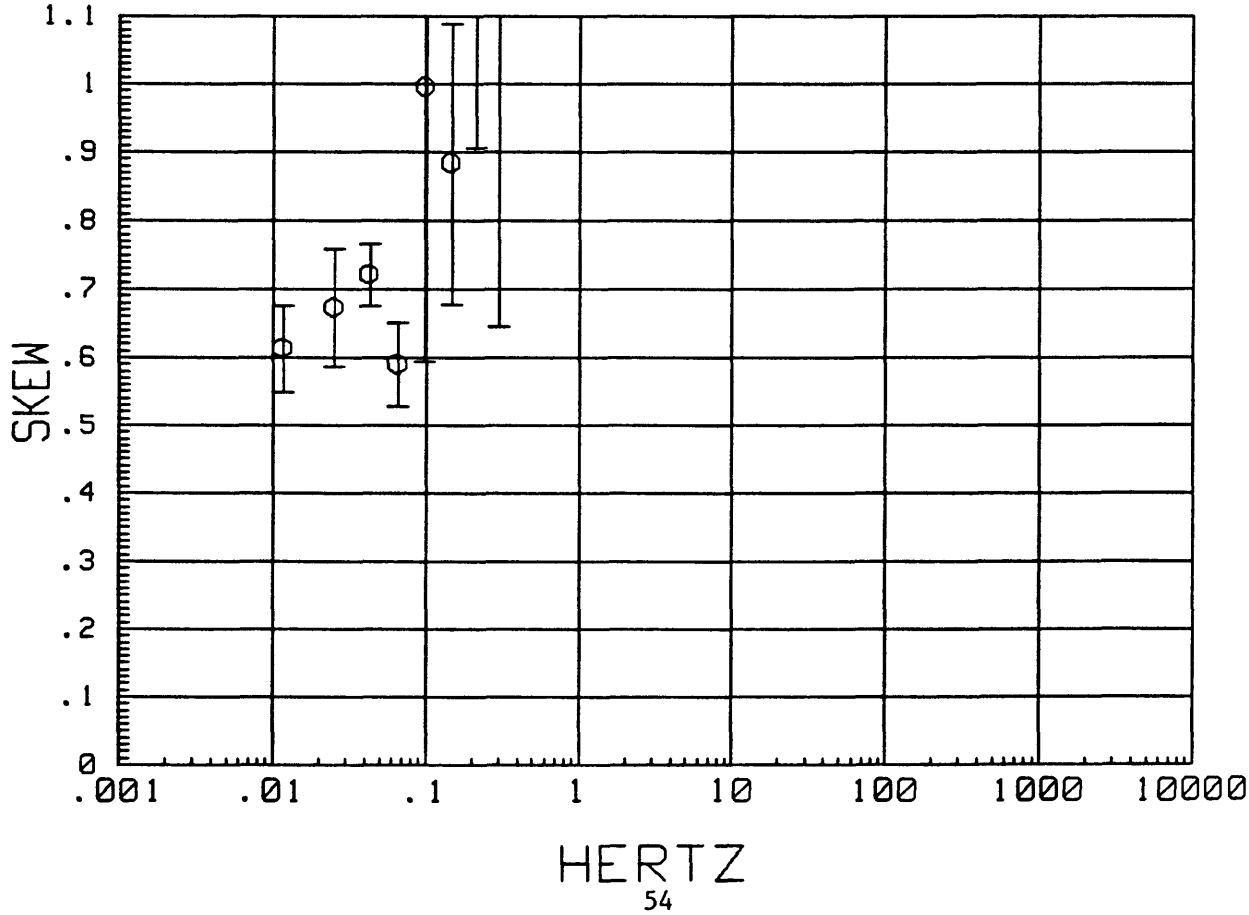

Appendix 2

MTH001 LOCAL H-ref 14:58:33 20 May 1988
APPARENT RESISTIVITY

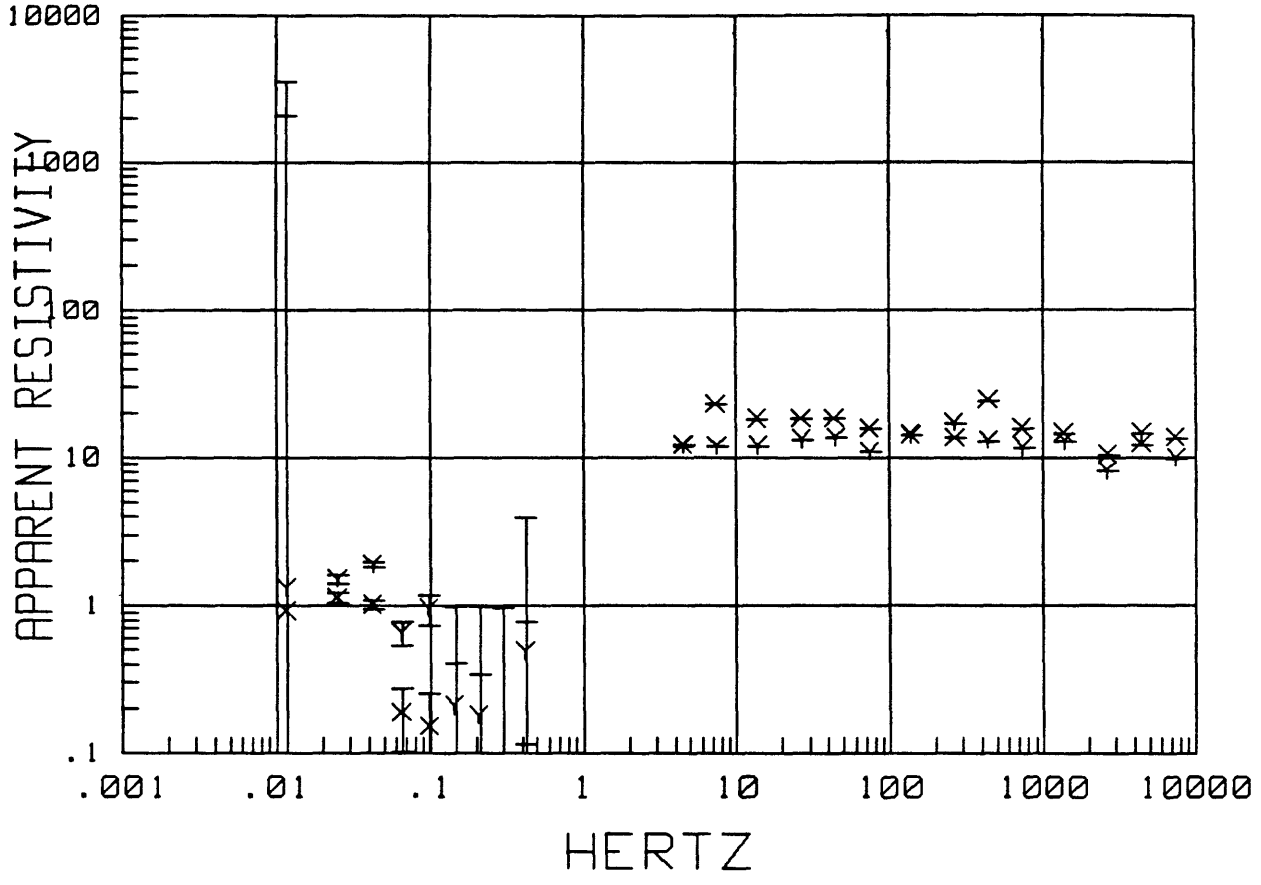

MTH001 LOCAL H-ref 14:58:33 20 May 1988
IMPEDANCE PHASE

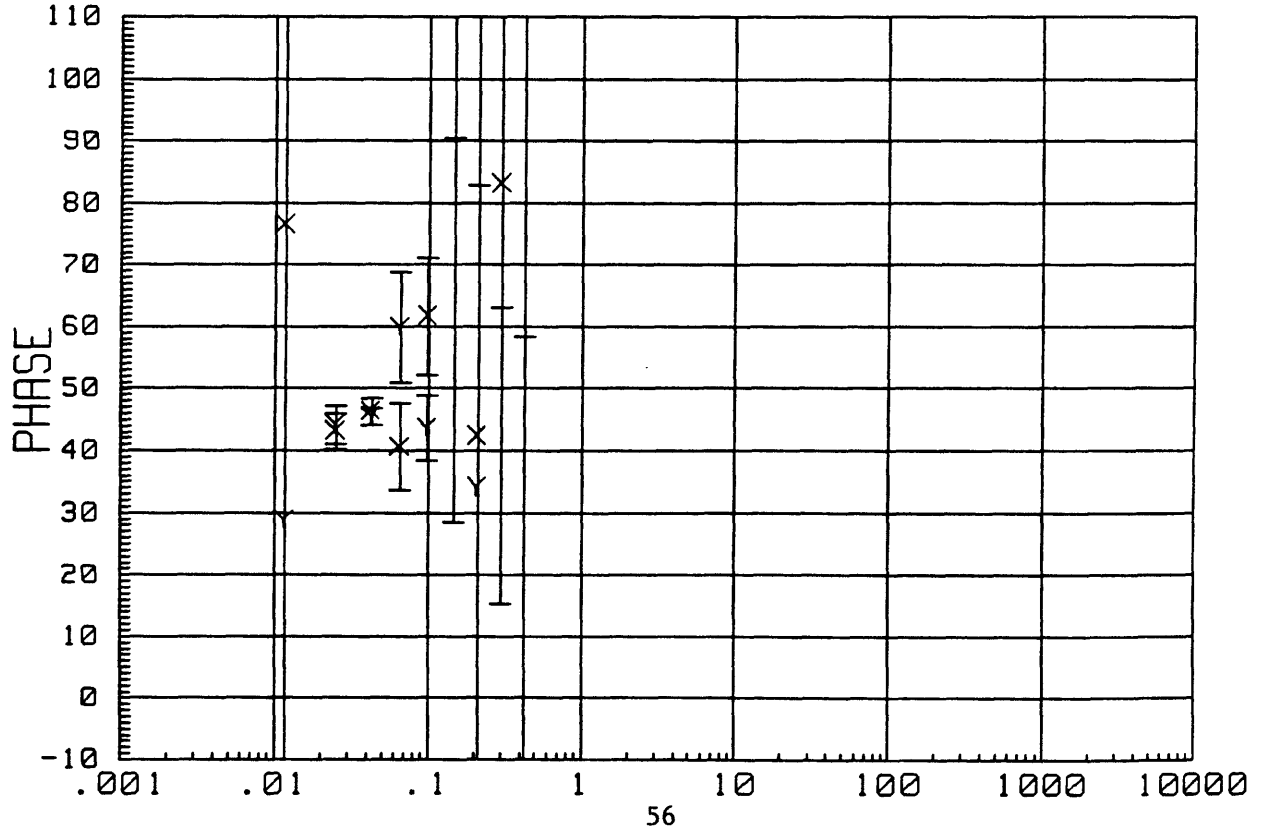

MTH001 LOCAL H-ref 14:58:33 20 May 1988
Z MAXIMUM DIRECTION

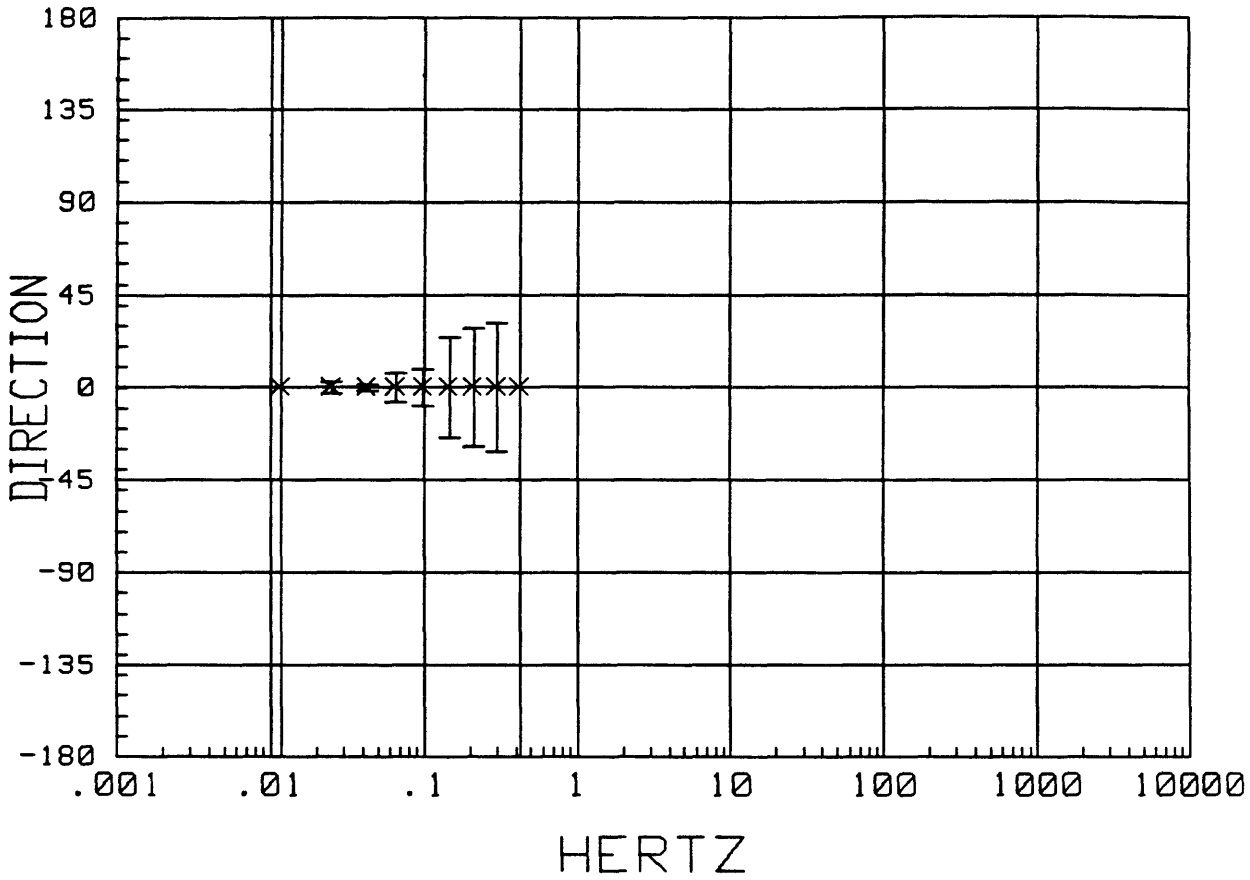

MTH001 LOCAL H-ref 14:58:33 20 May 1988
SKEW

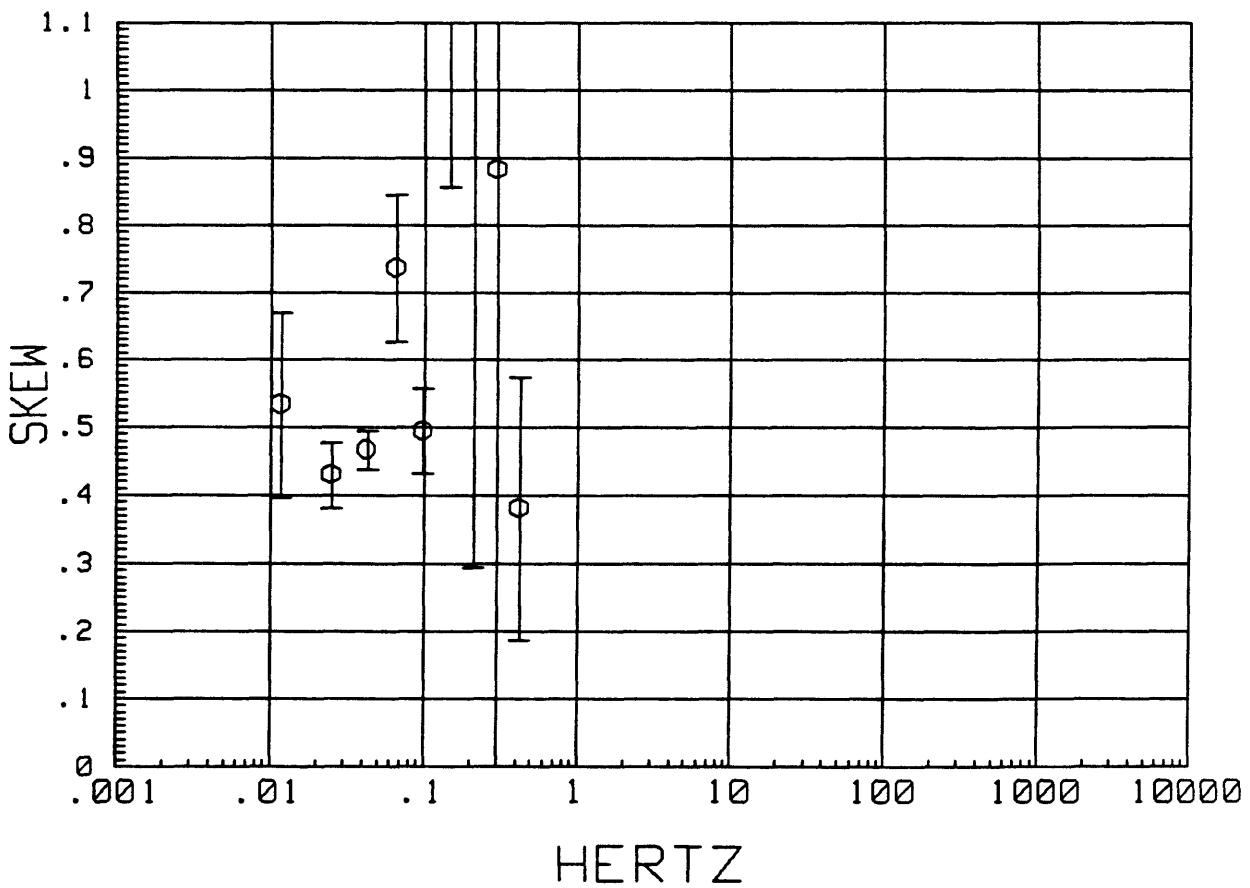

MTH002 LOCAL H-ref 15:20:08 20 May 1988
APPARENT RESISTIVITY

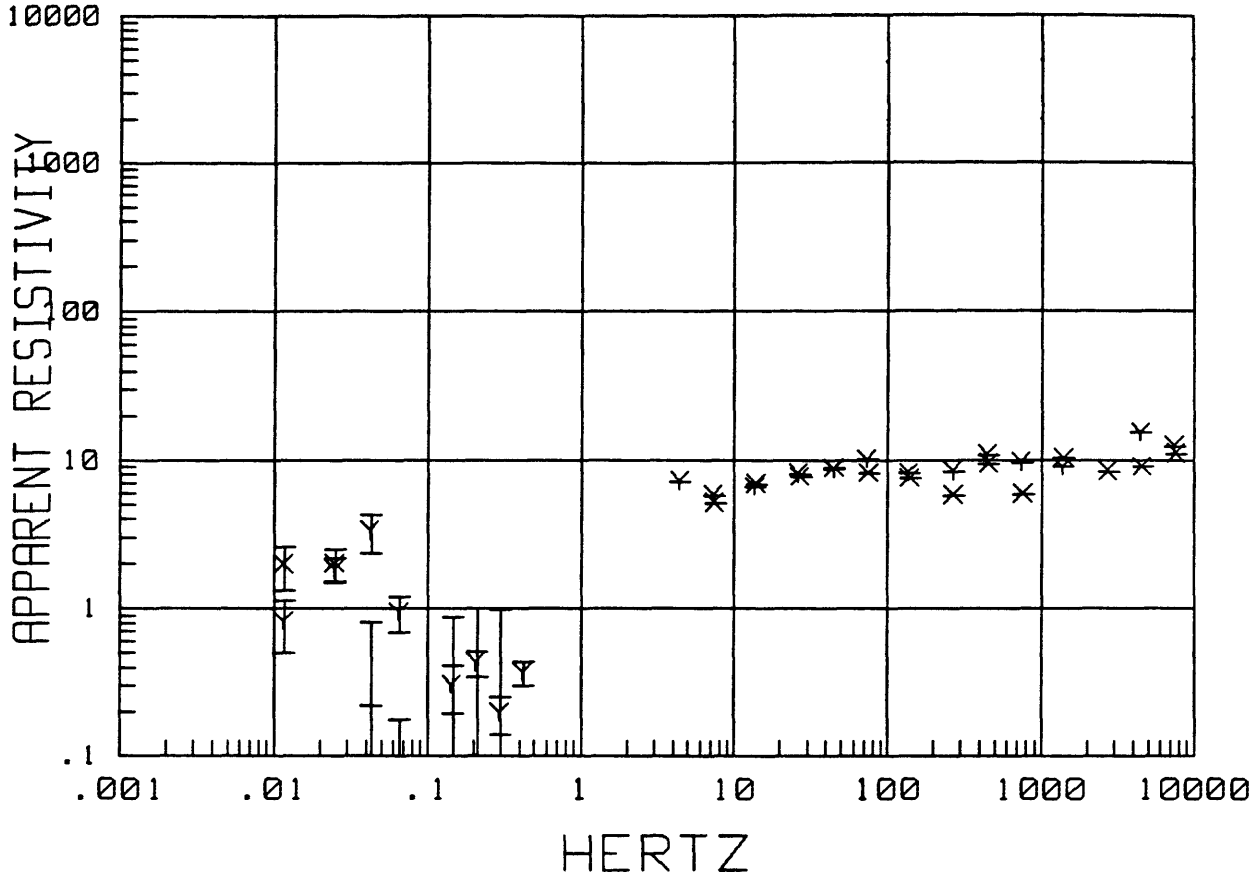

MTH002 LOCAL H-ref 15:20:08 20 May 1988
IMPEDANCE PHASE

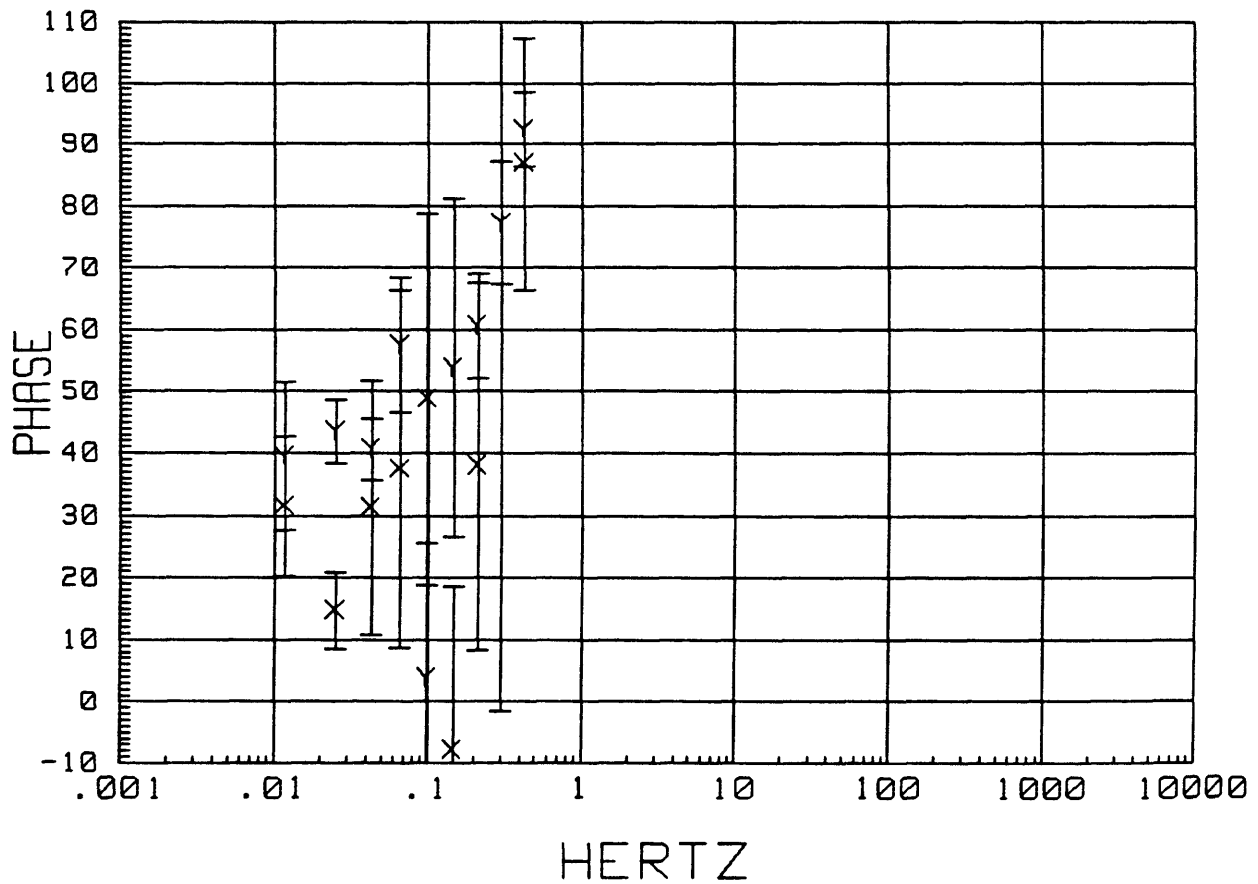

MTHO02 LOCAL H-ref 15:20:08 20 May 1988
Z MAXIMUM DIRECTION

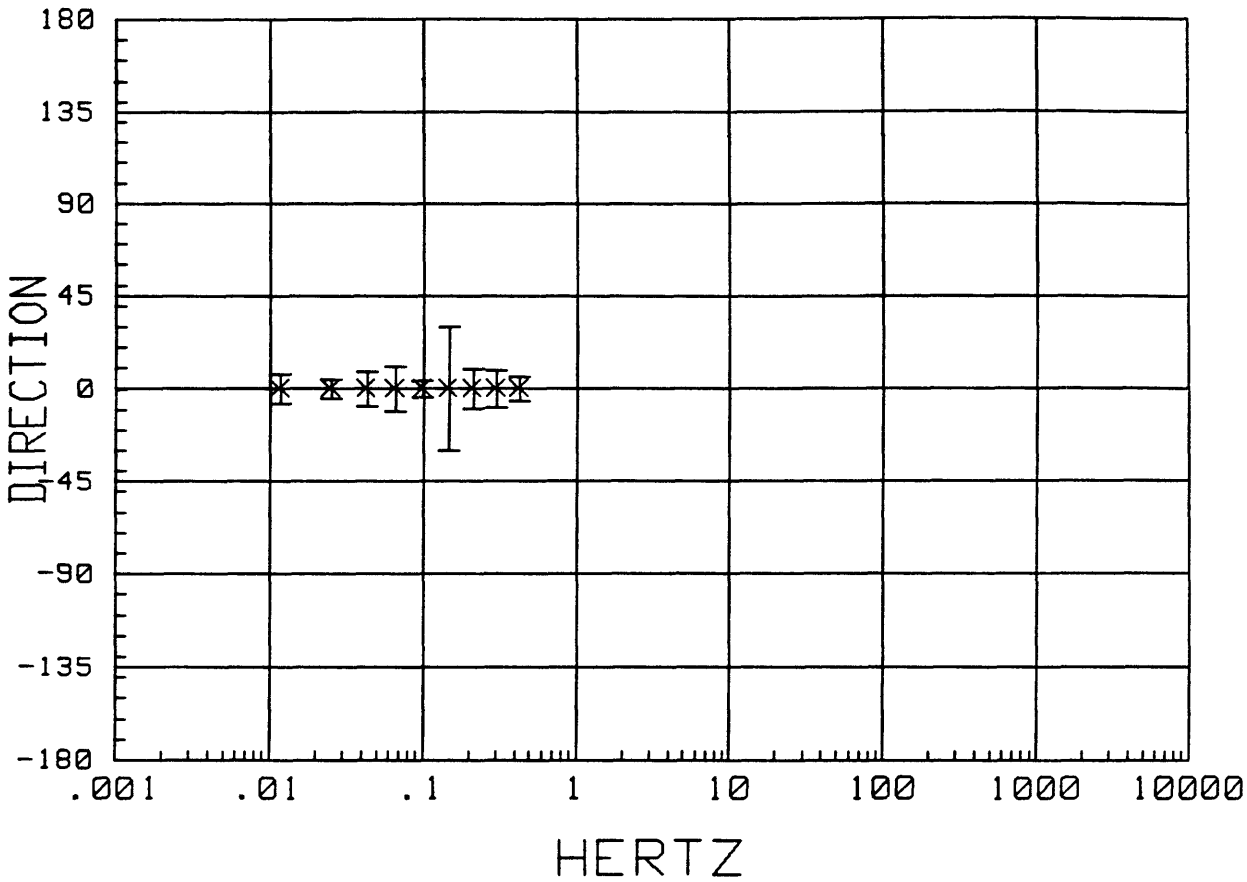

MTHO02 LOCAL H-ref 15:20:08 20 May 1988
SKEW

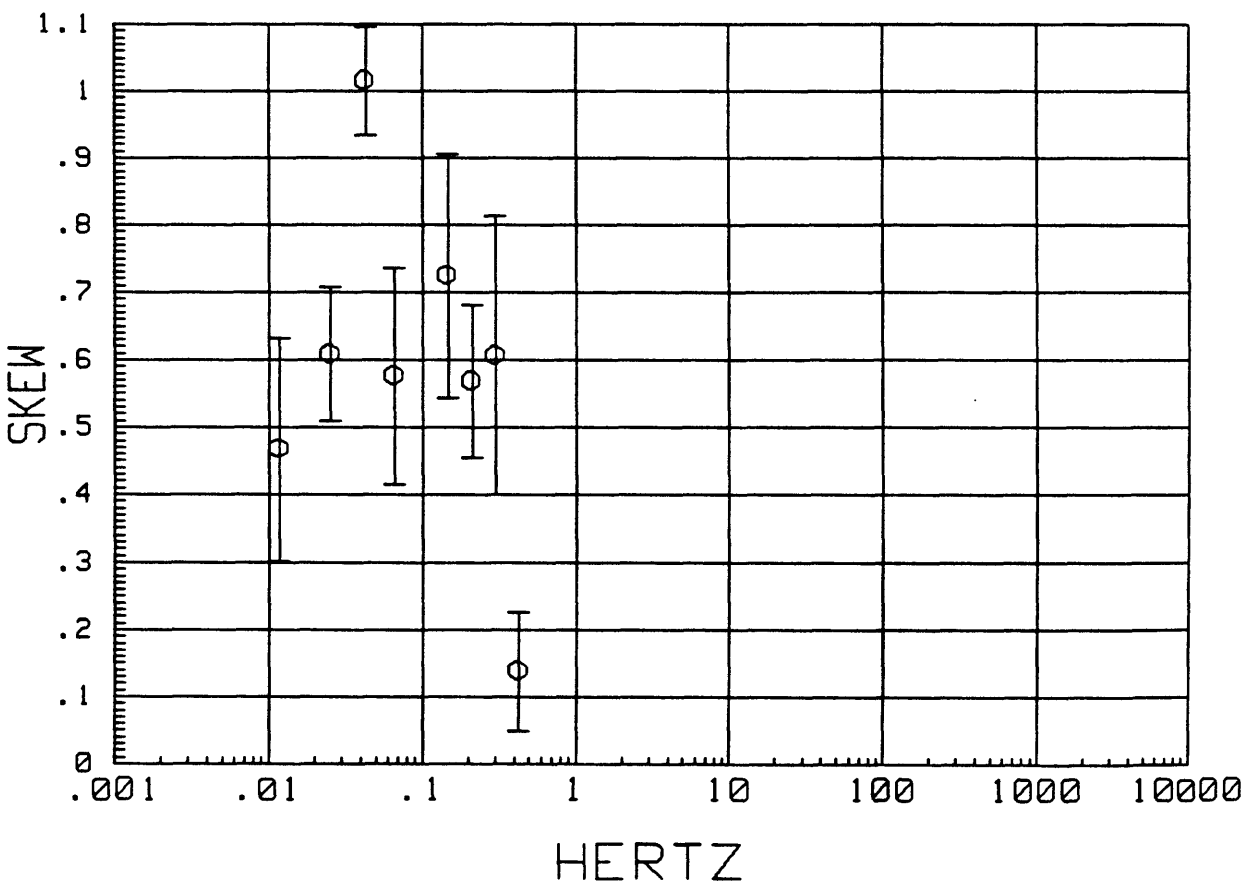

MTH003 LOCAL H-ref 15:28:58 20 May 1988
APPARENT RESISTIVITY

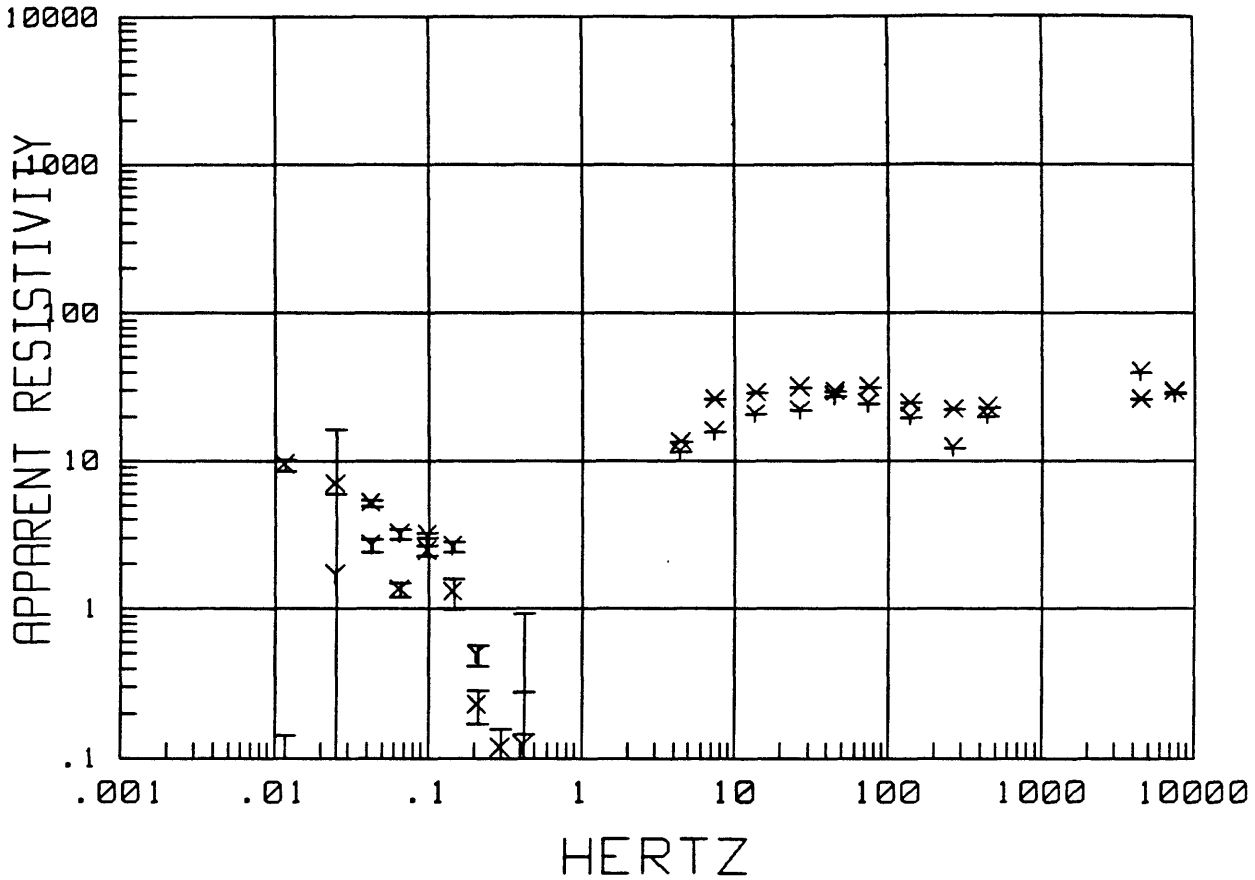

MTH003 LOCAL H-ref 15:28:58 20 May 1988
IMPEDANCE PHASE

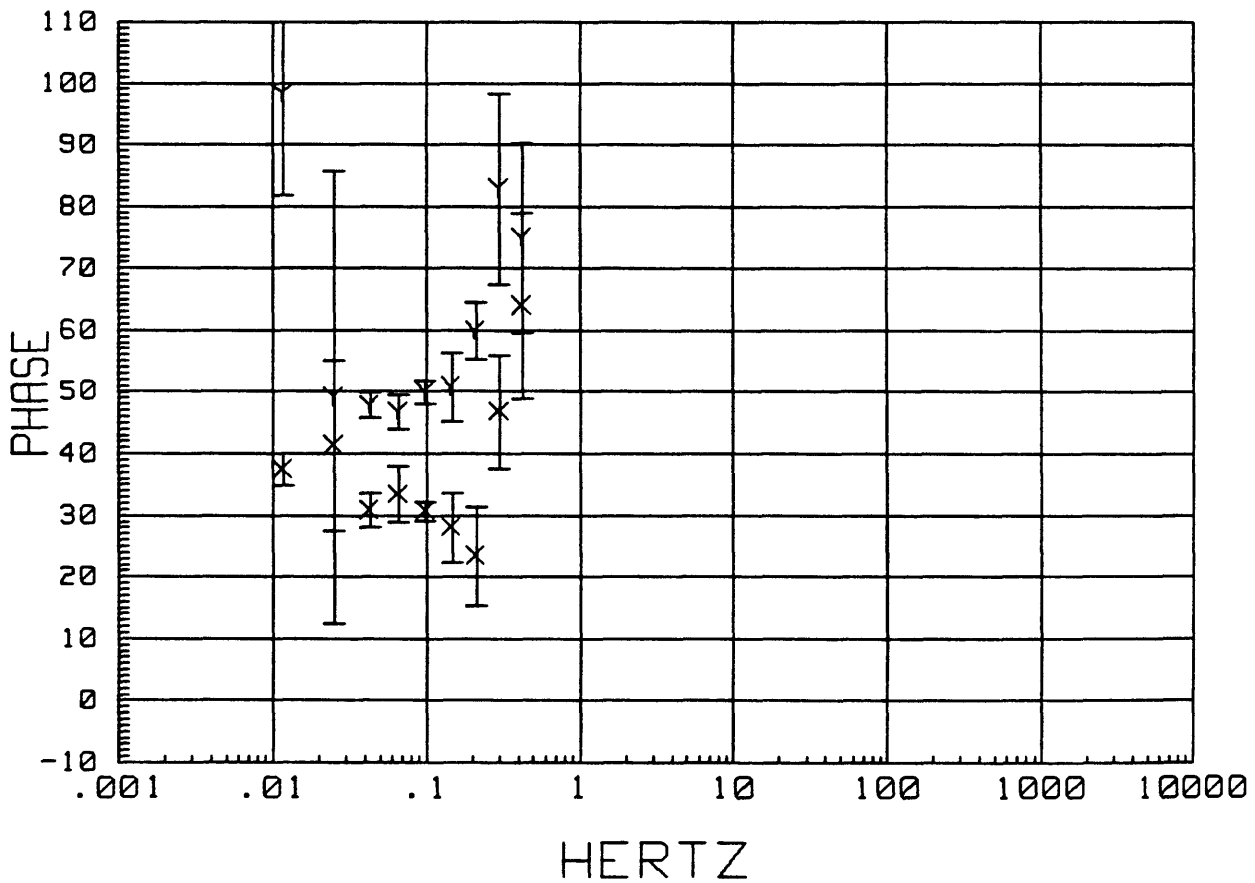

MTH003 LOCAL H-ref 15:28:58 20 May 1988
Z MAXIMUM DIRECTION

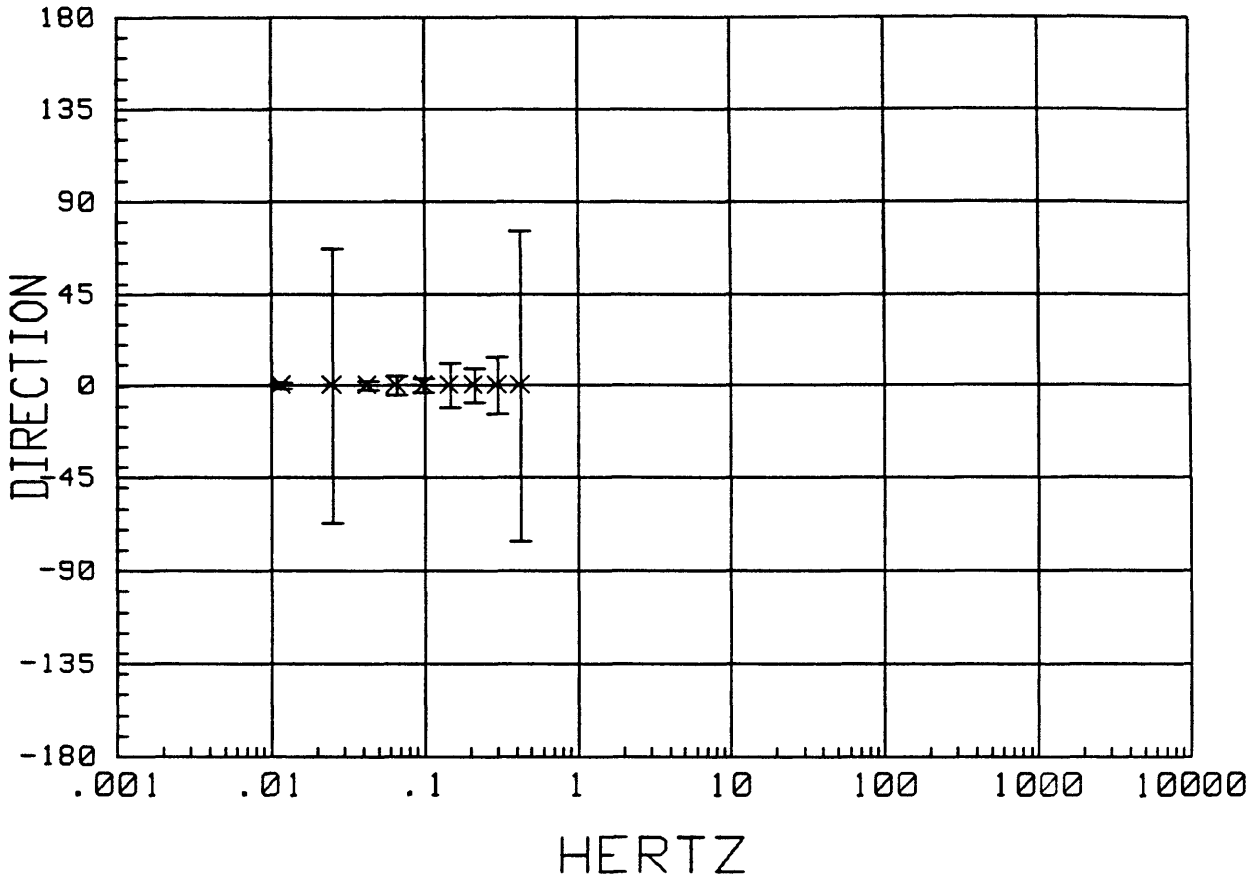

MTH003 LOCAL H-ref 15:28:58 20 May 1988
SKEW

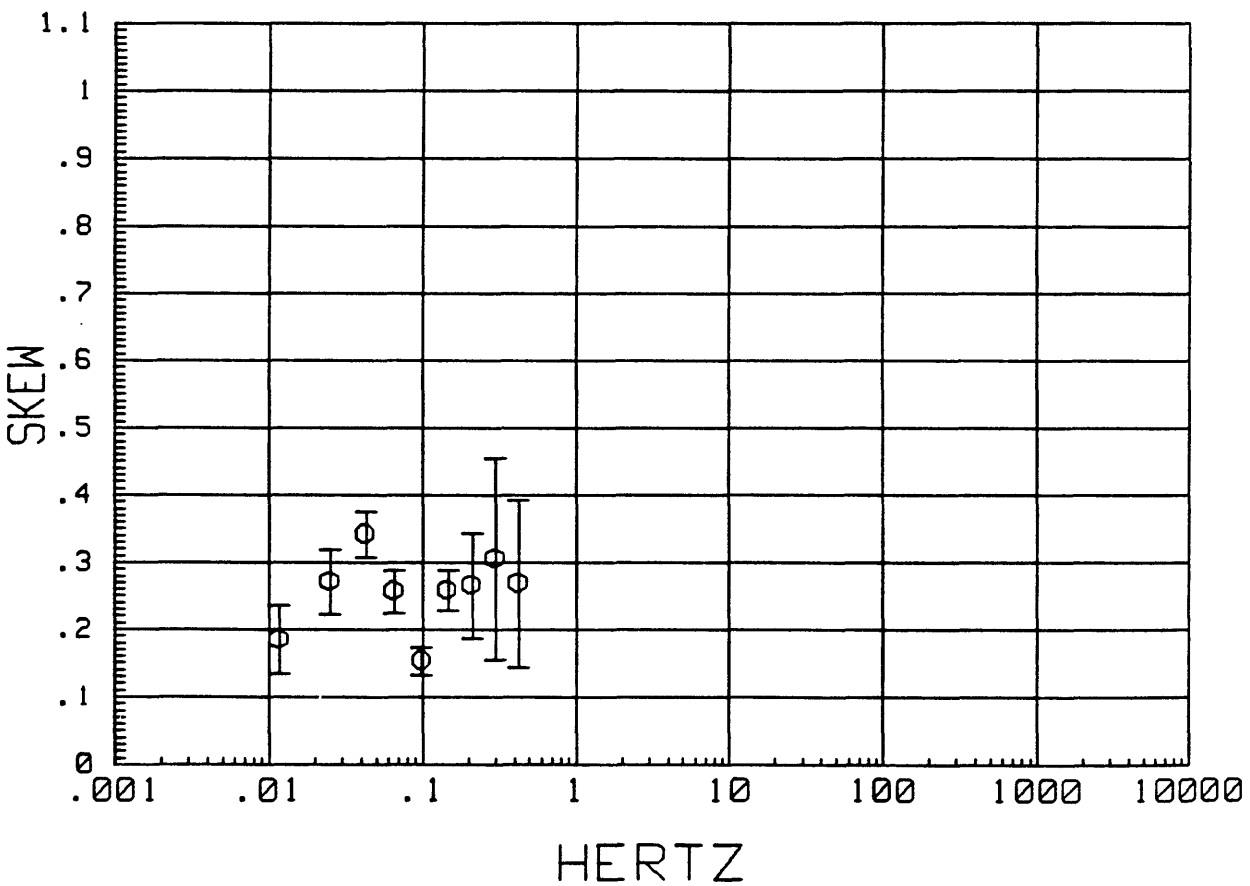

MTH004 LOCAL H-ref 15:39:25 20 May 1988
APPARENT RESISTIVITY

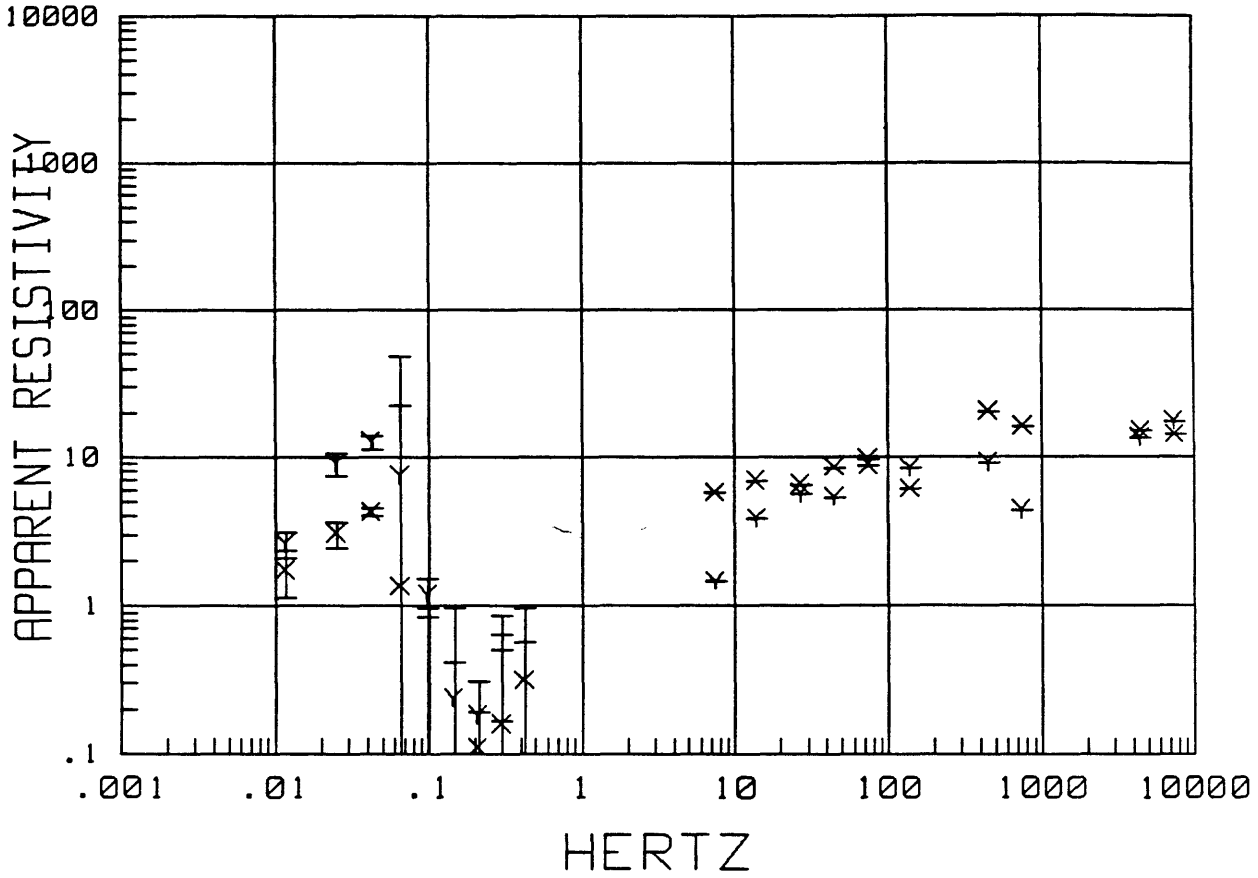

MTH004 LOCAL H-ref 15:39:25 20 May 1988
IMPEDANCE PHASE

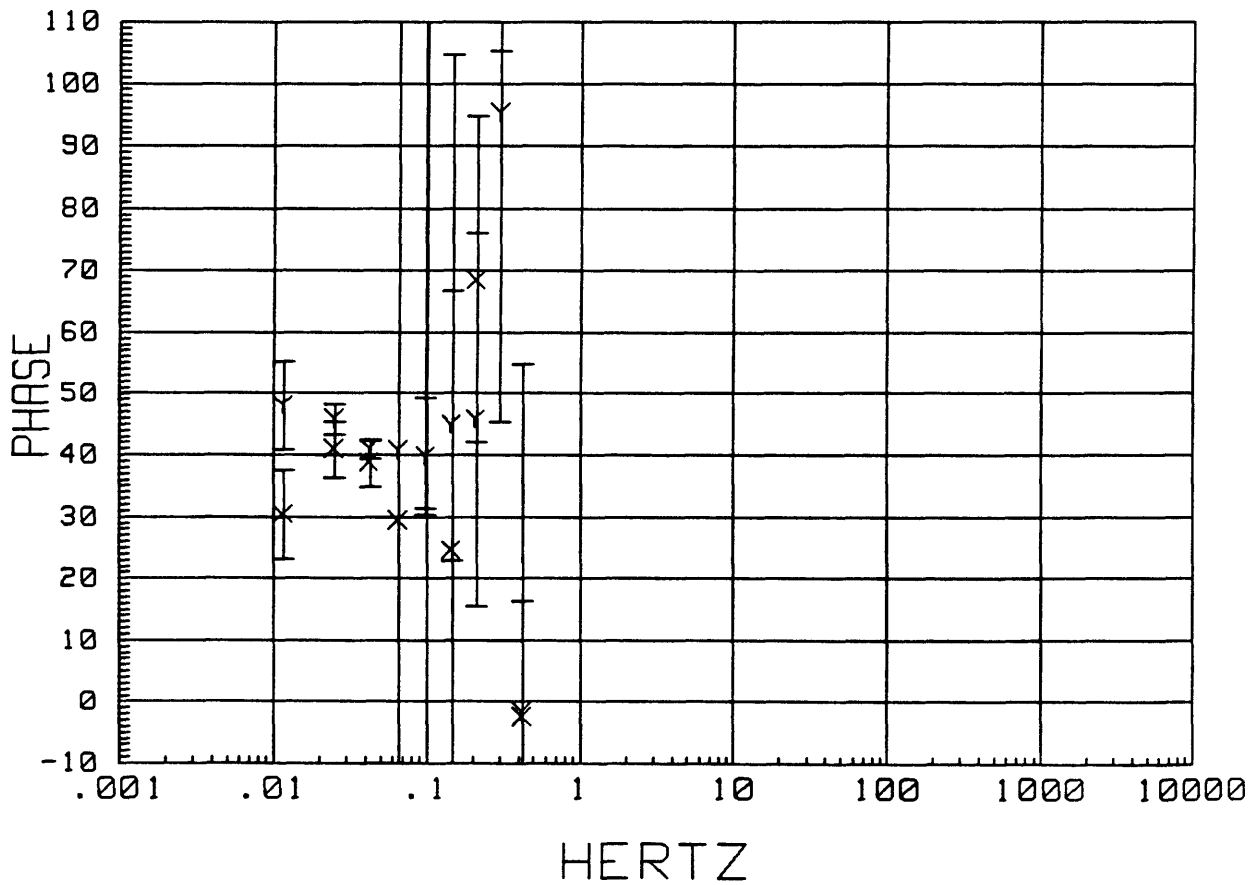

MTH004 LOCAL H-ref 15:39:25 20 May 1988
Z MAXIMUM DIRECTION

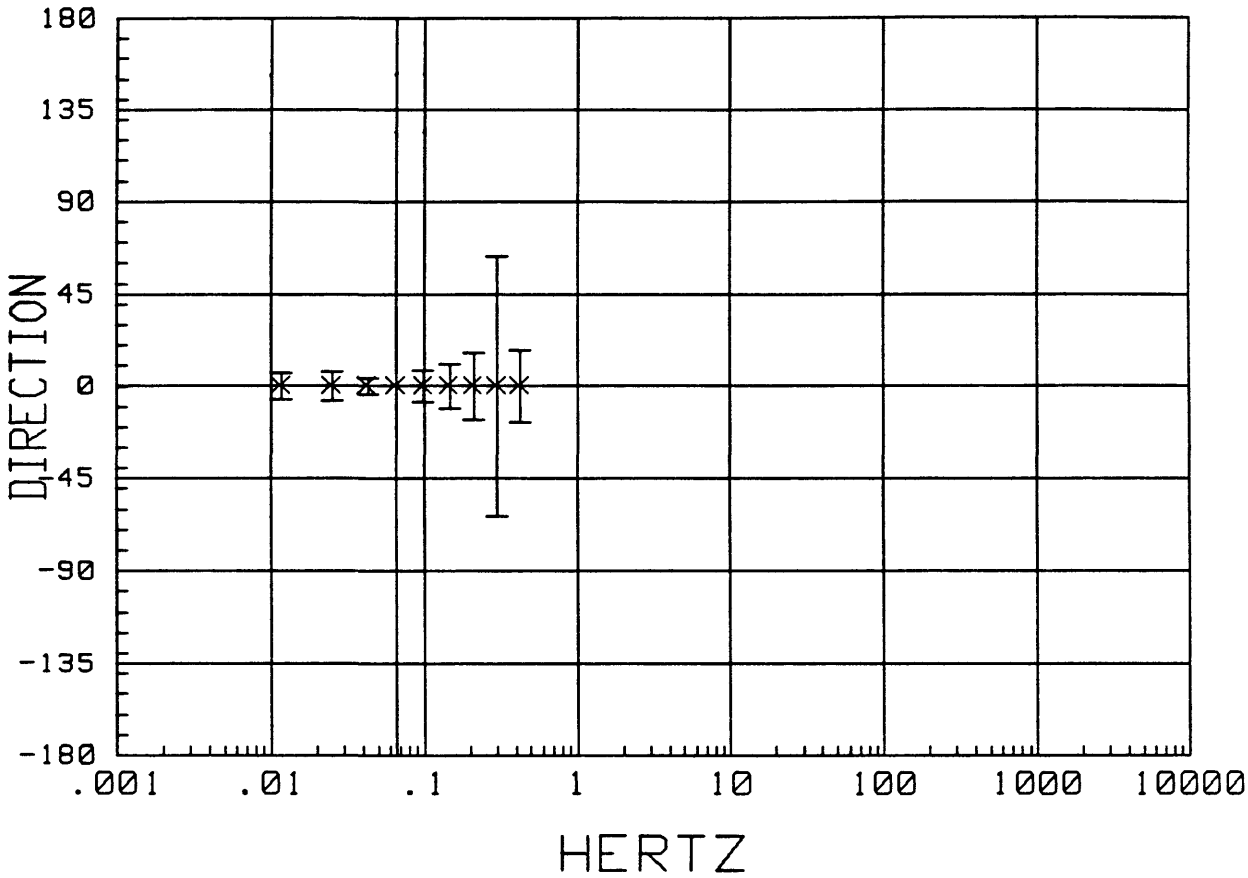

MTH004 LOCAL H-ref 15:39:25 20 May 1988
SKEW

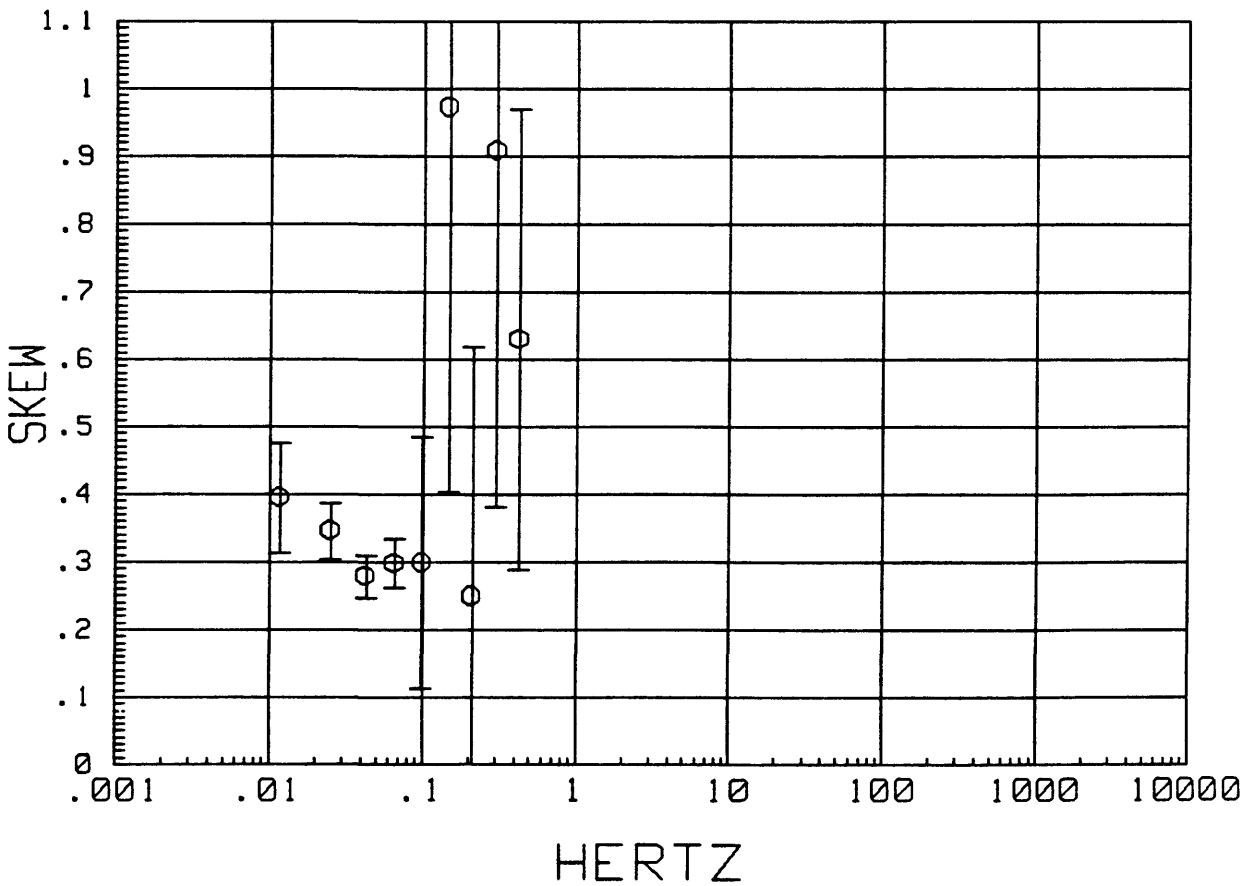

MTH005 LOCAL H-ref 15:56:12 20 May 1988
APPARENT RESISTIVITY

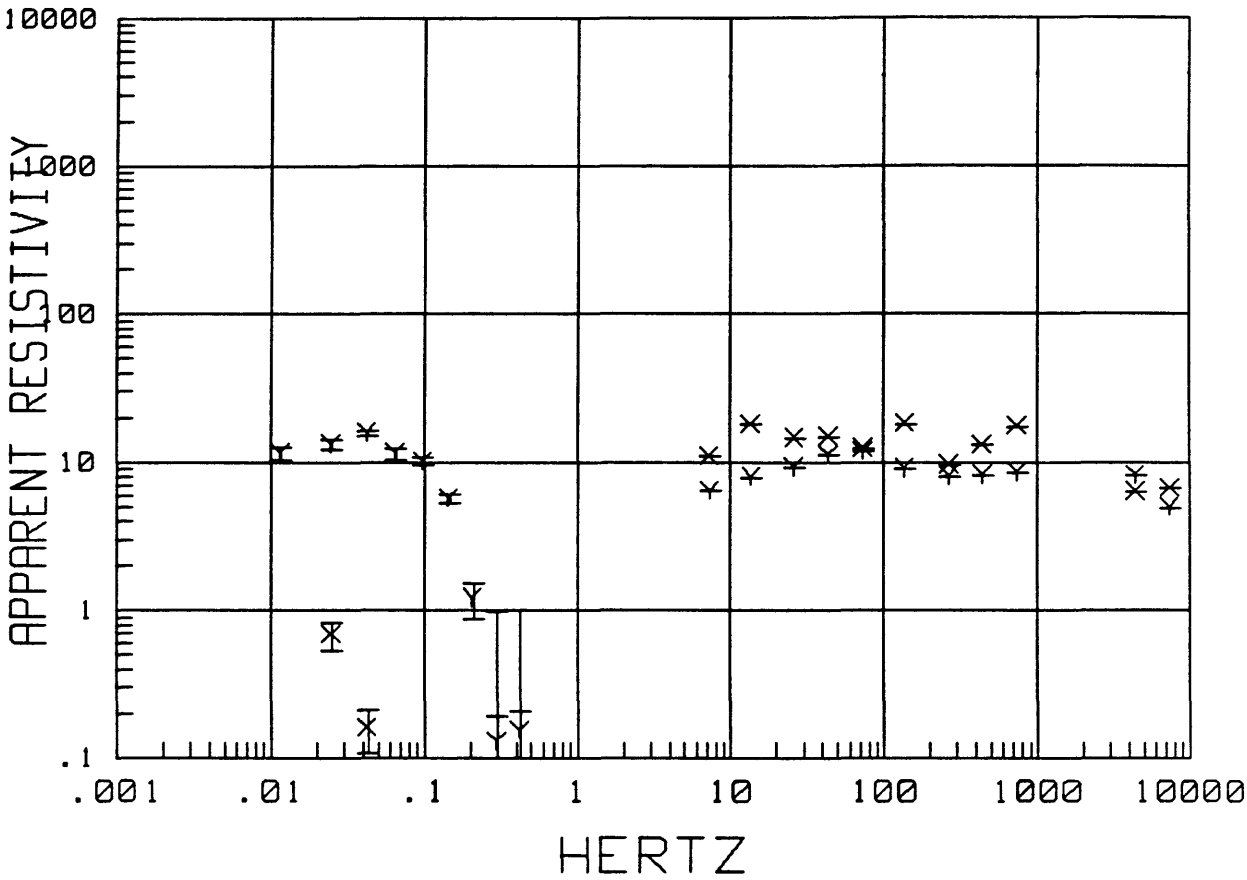

MTH005 LOCAL H-ref 15:56:12 20 May 1988
IMPEDANCE PHASE

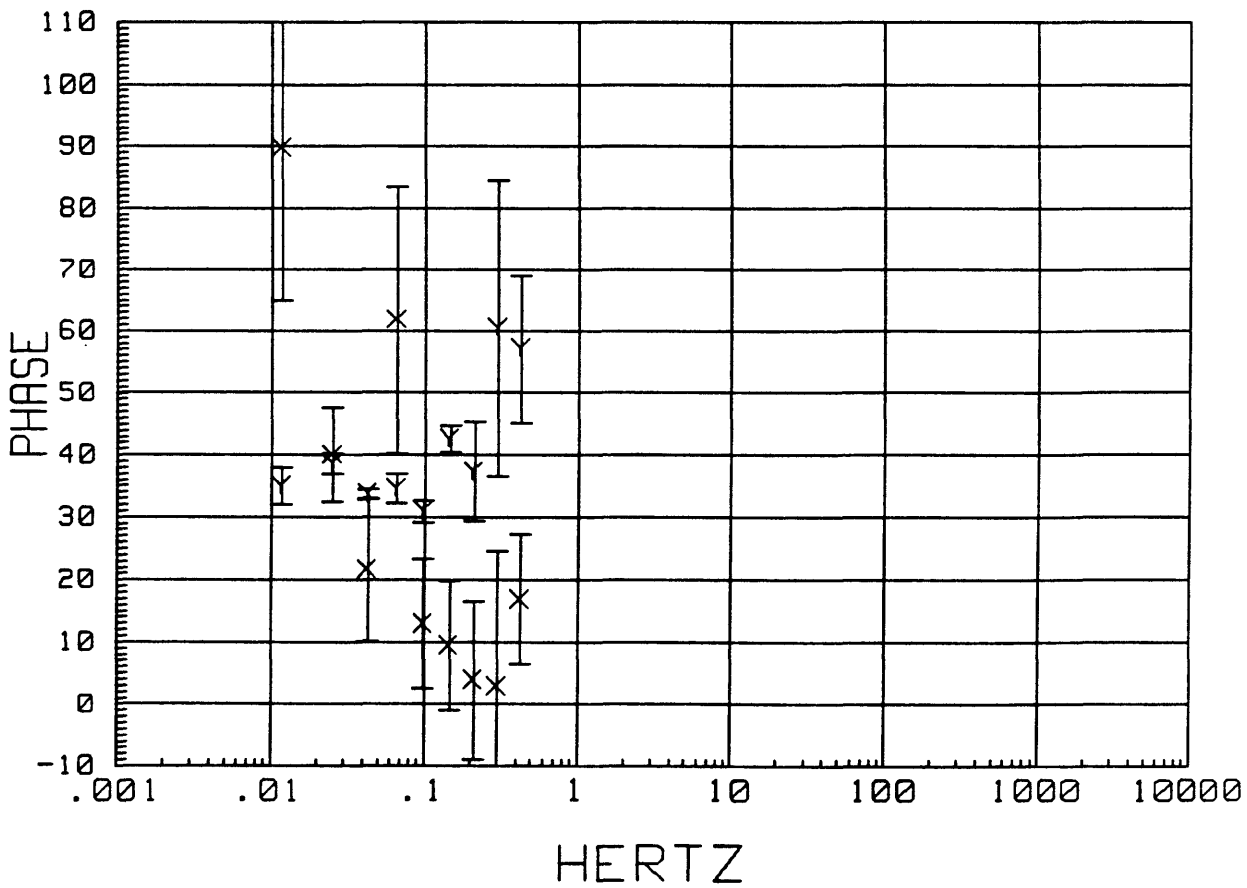

MTH005 LOCAL H-ref 15:56:12 20 May 1988
Z MAXIMUM DIRECTION

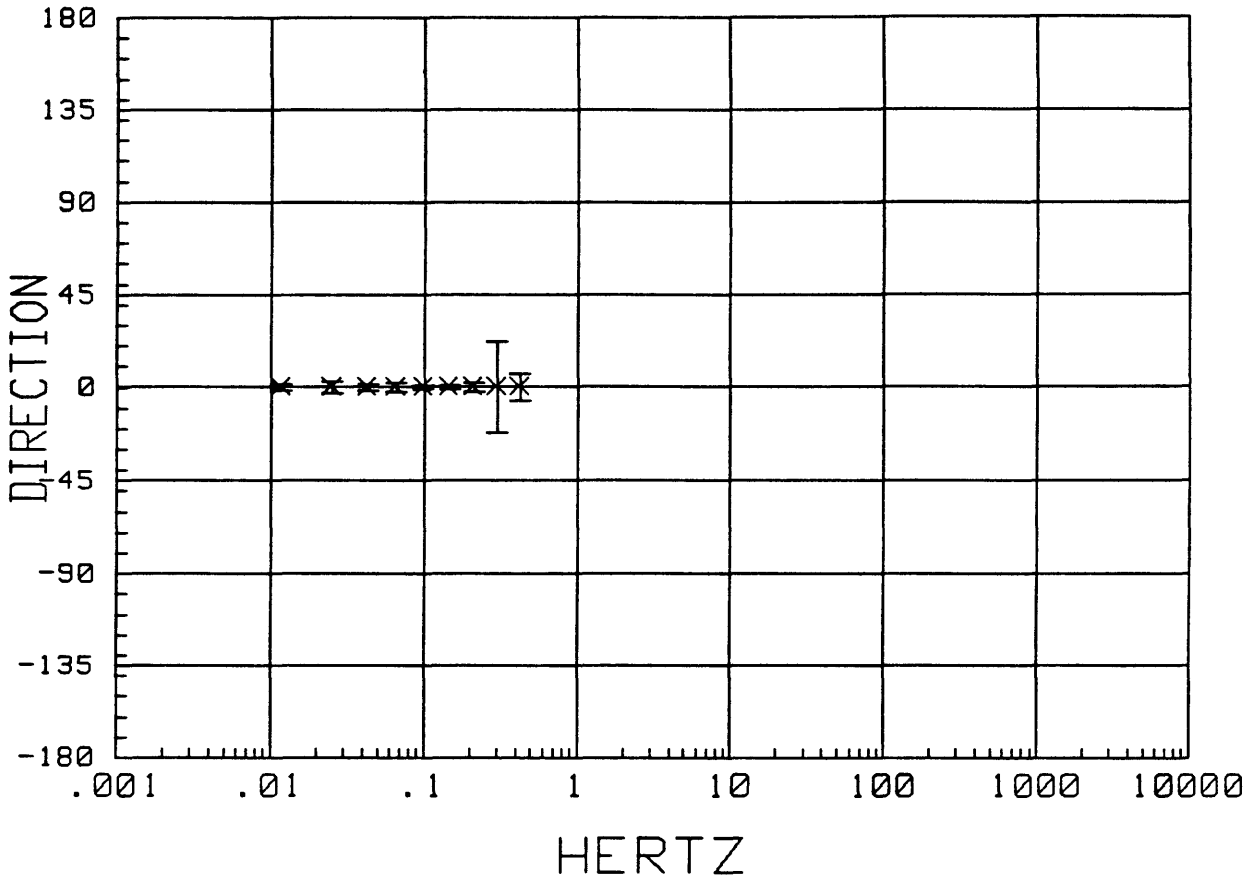

MTH005 LOCAL H-ref 15:56:12 20 May 1988
SKEW

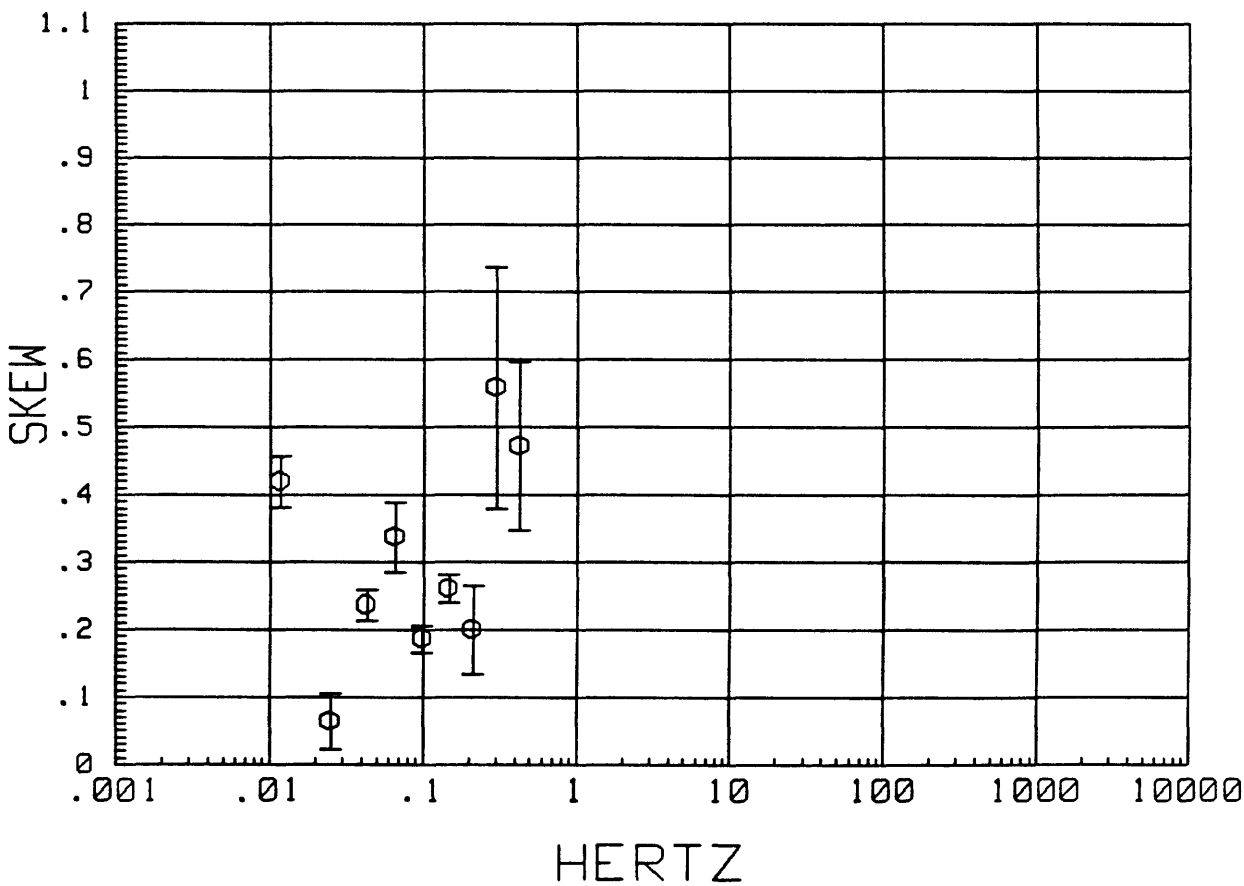

MTH006 LOCAL H-ref 16:06:37 20 May 1988
APPARENT RESISTIVITY

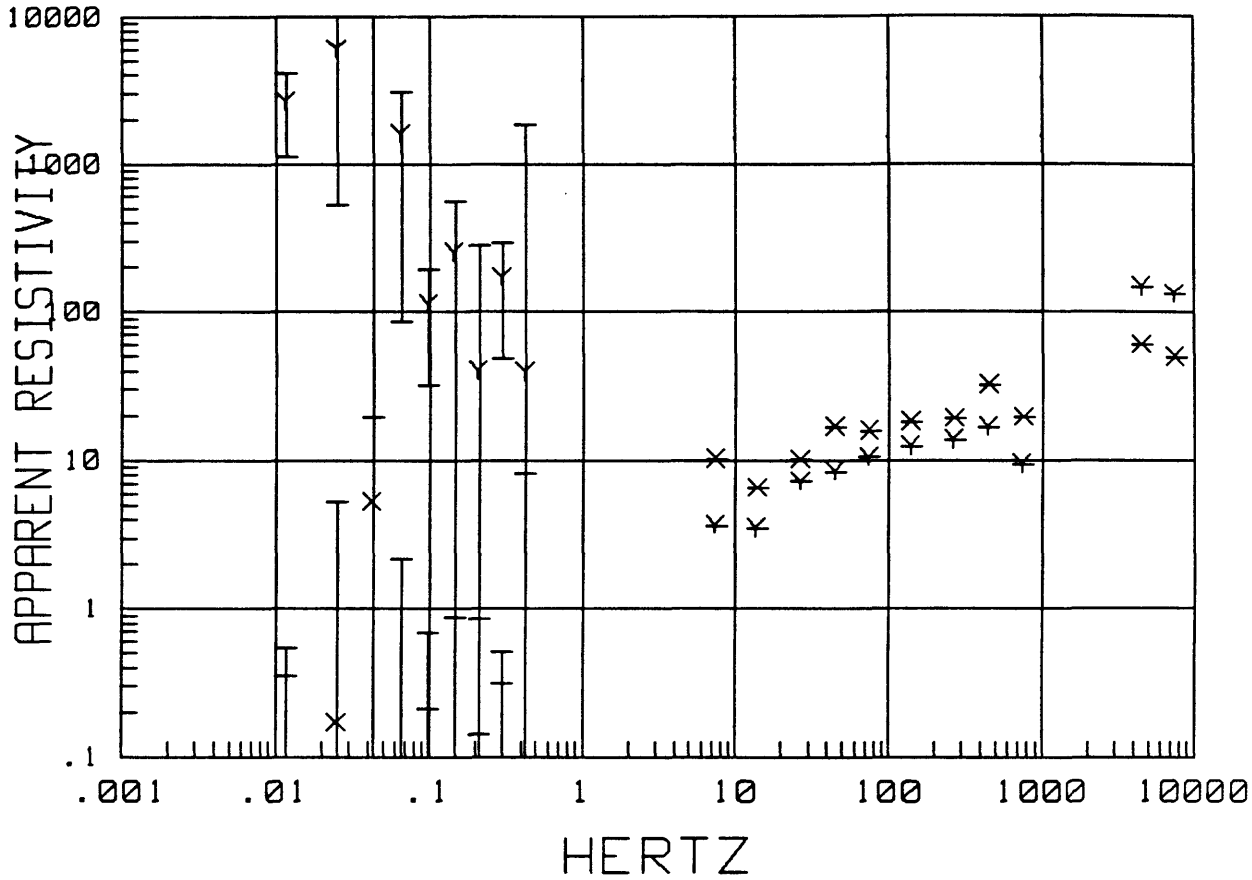

MTH006 LOCAL H-ref 16:06:37 20 May 1988
IMPEDANCE PHASE

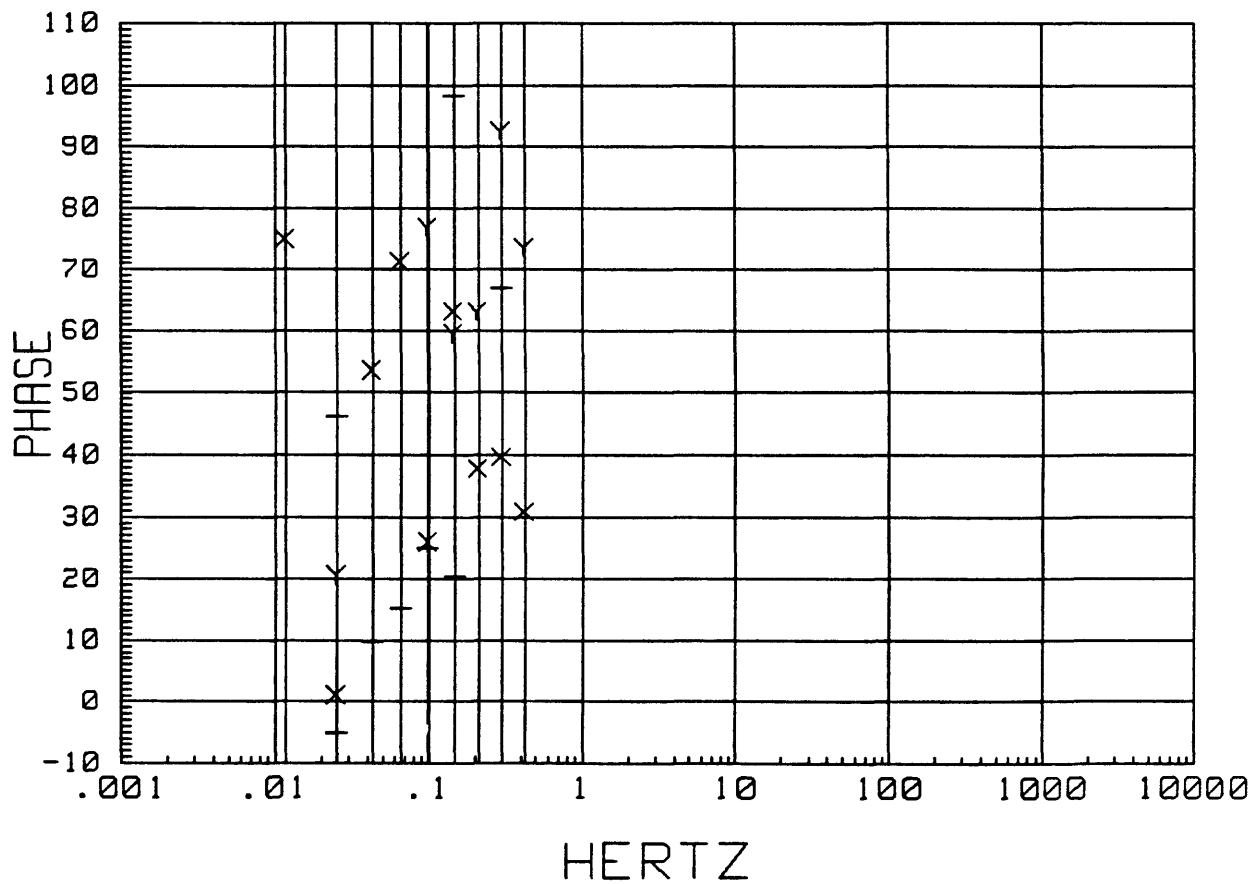

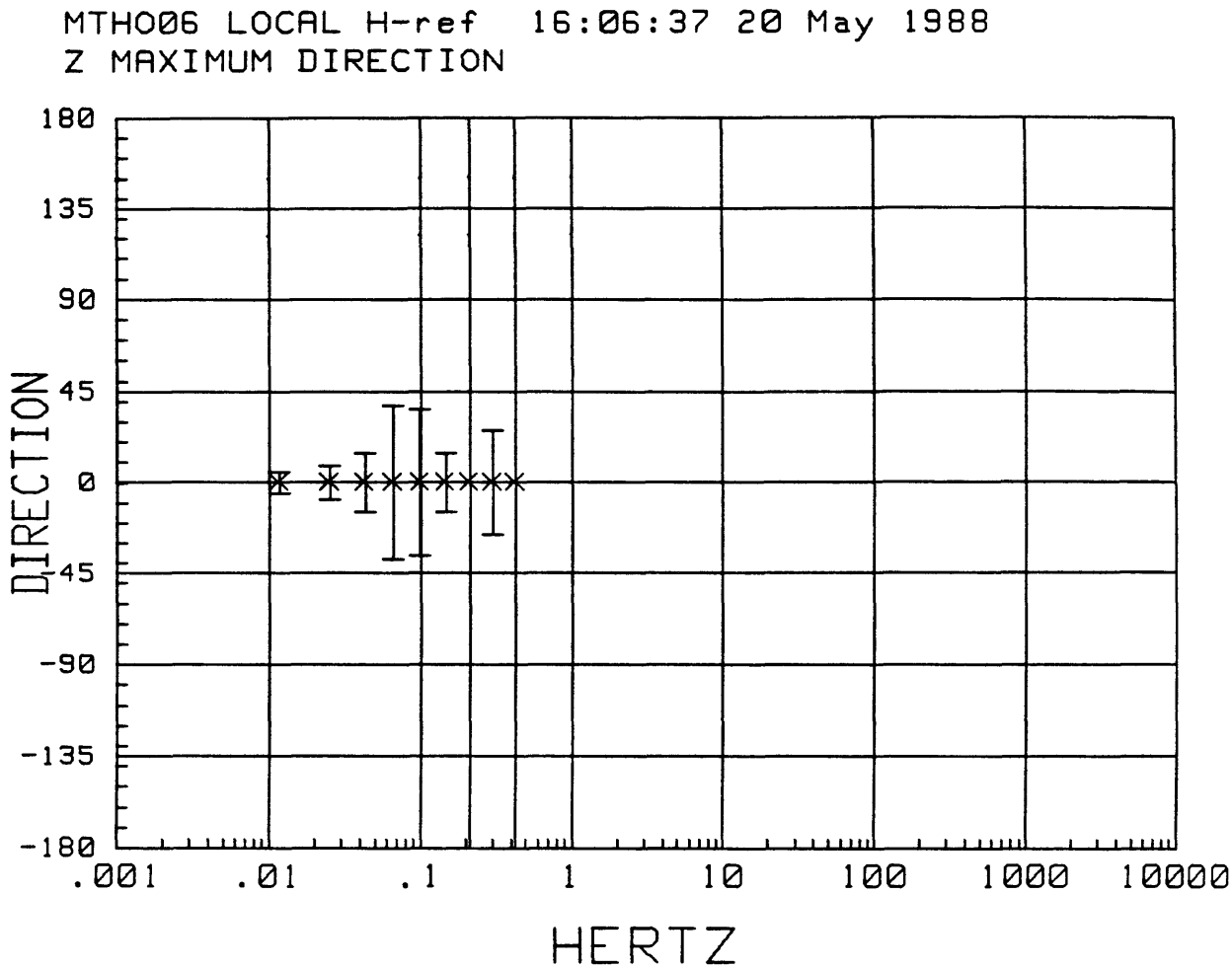
MTH006 LOCAL H-ref 16:06:37 20 May 1988
Z MAXIMUM DIRECTION
180
135
90
45
0
-45
-90
-135
-180
DIRECTION
.001
.01
.1
1
10
100
1000
10000
HERTZ

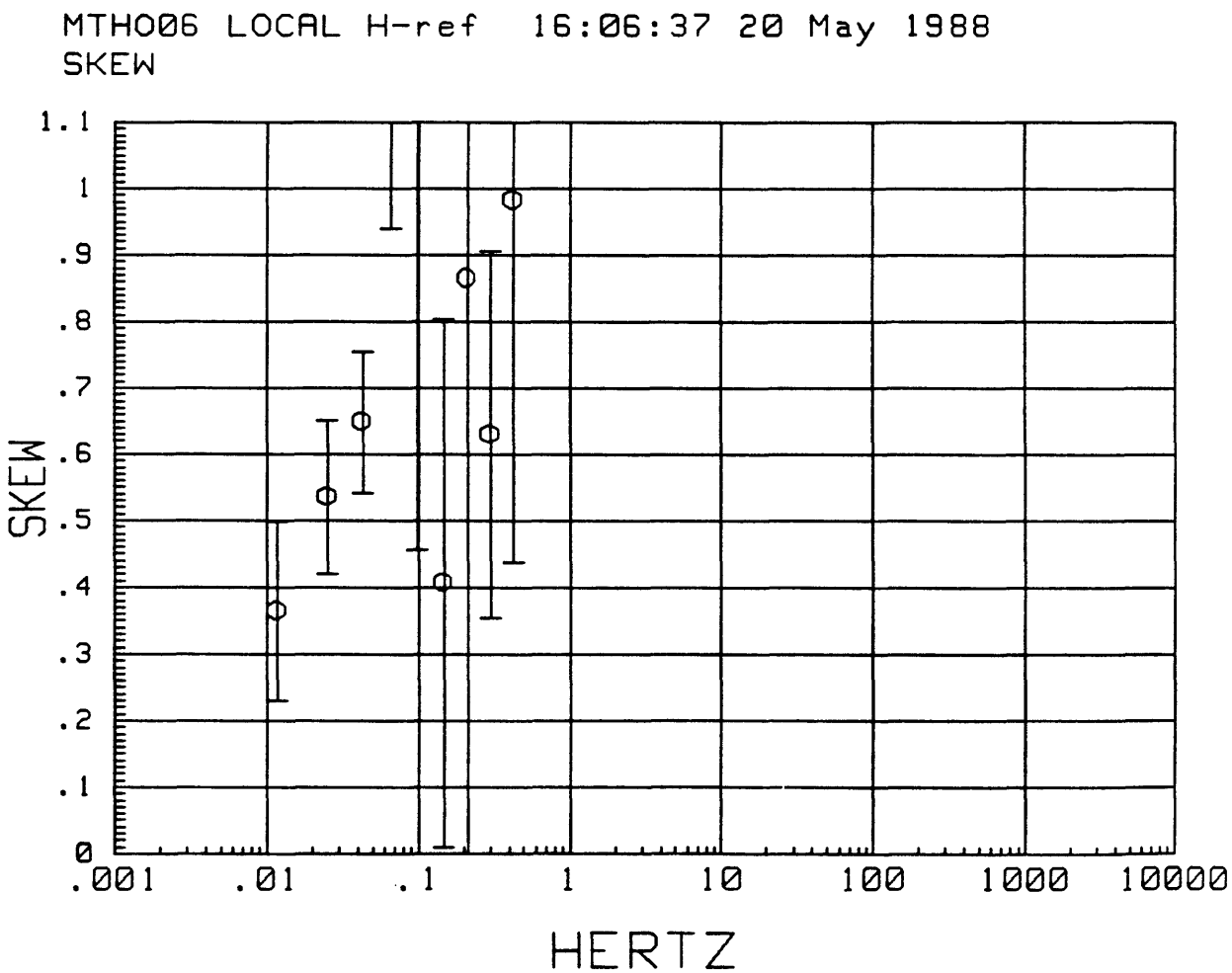
MTH006 LOCAL H-ref 16:06:37 20 May 1988
SKEW
1.1
1
.9
.8
.7
.6
.5
.4
.3
.2
.1
0
SKEW
.001
.01
.1
1
10
100
1000
10000
HERTZ

MTH007 LOCAL H-ref 16:16:17 20 May 1988
APPARENT RESISTIVITY

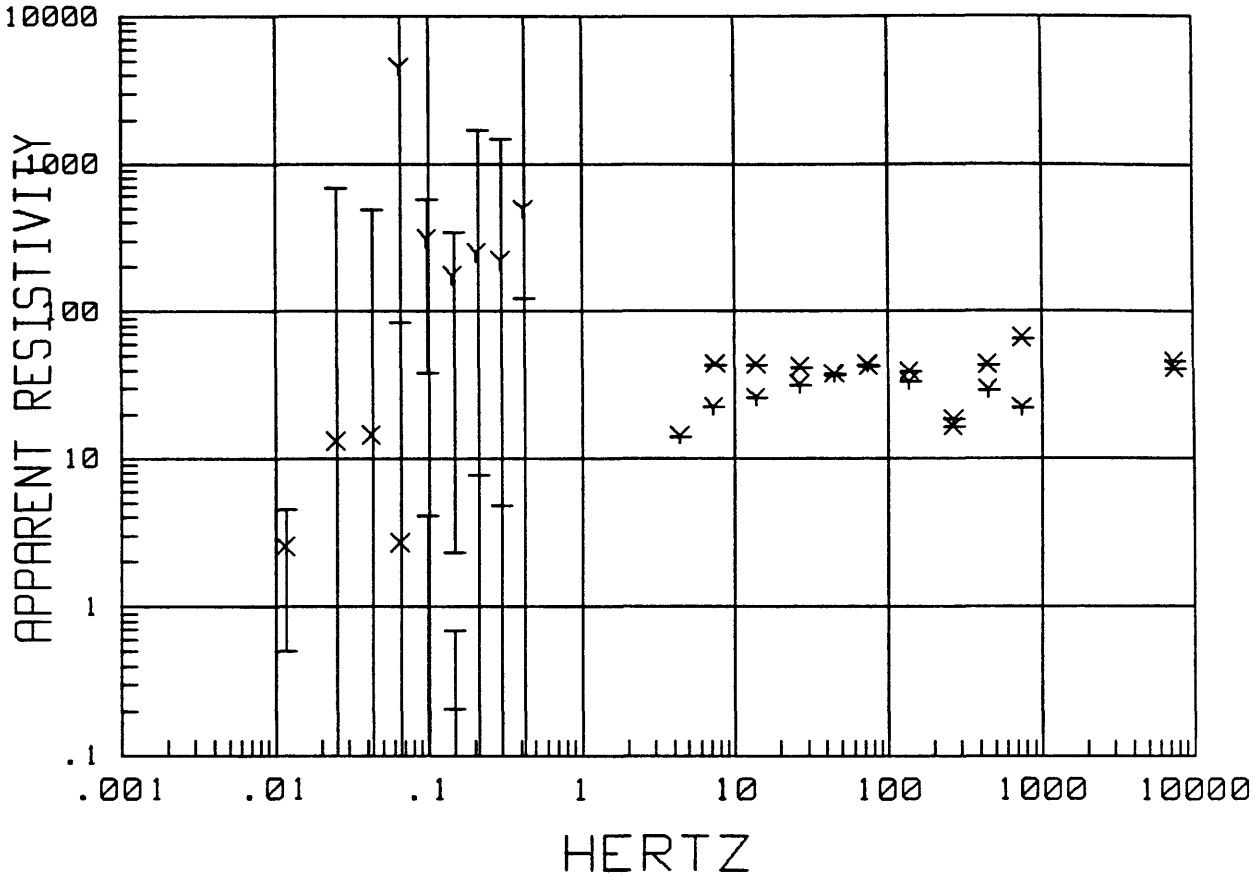

MTH007 LOCAL H-ref 16:16:17 20 May 1988
IMPEDANCE PHASE

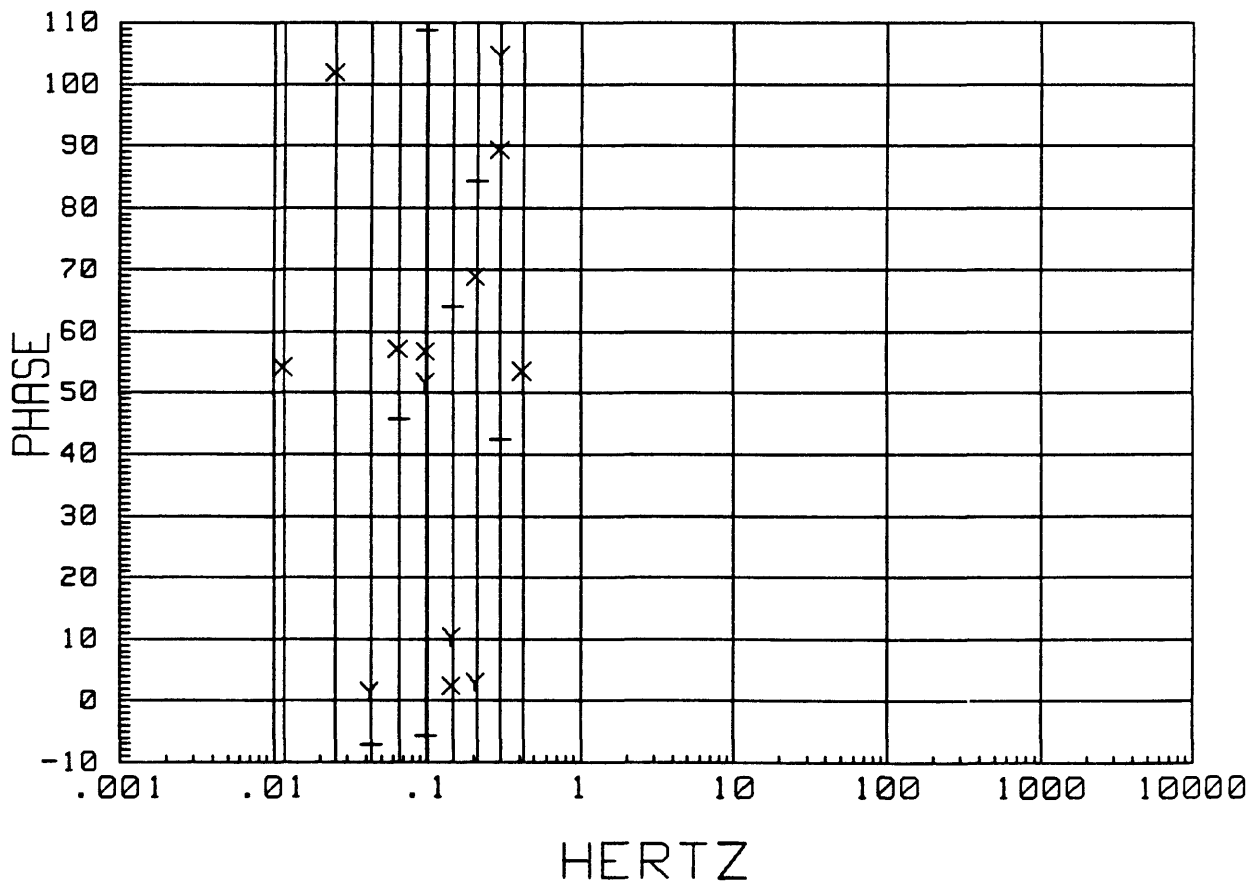

MTH007 LOCAL H-ref 16:16:17 20 May 1988
Z MAXIMUM DIRECTION

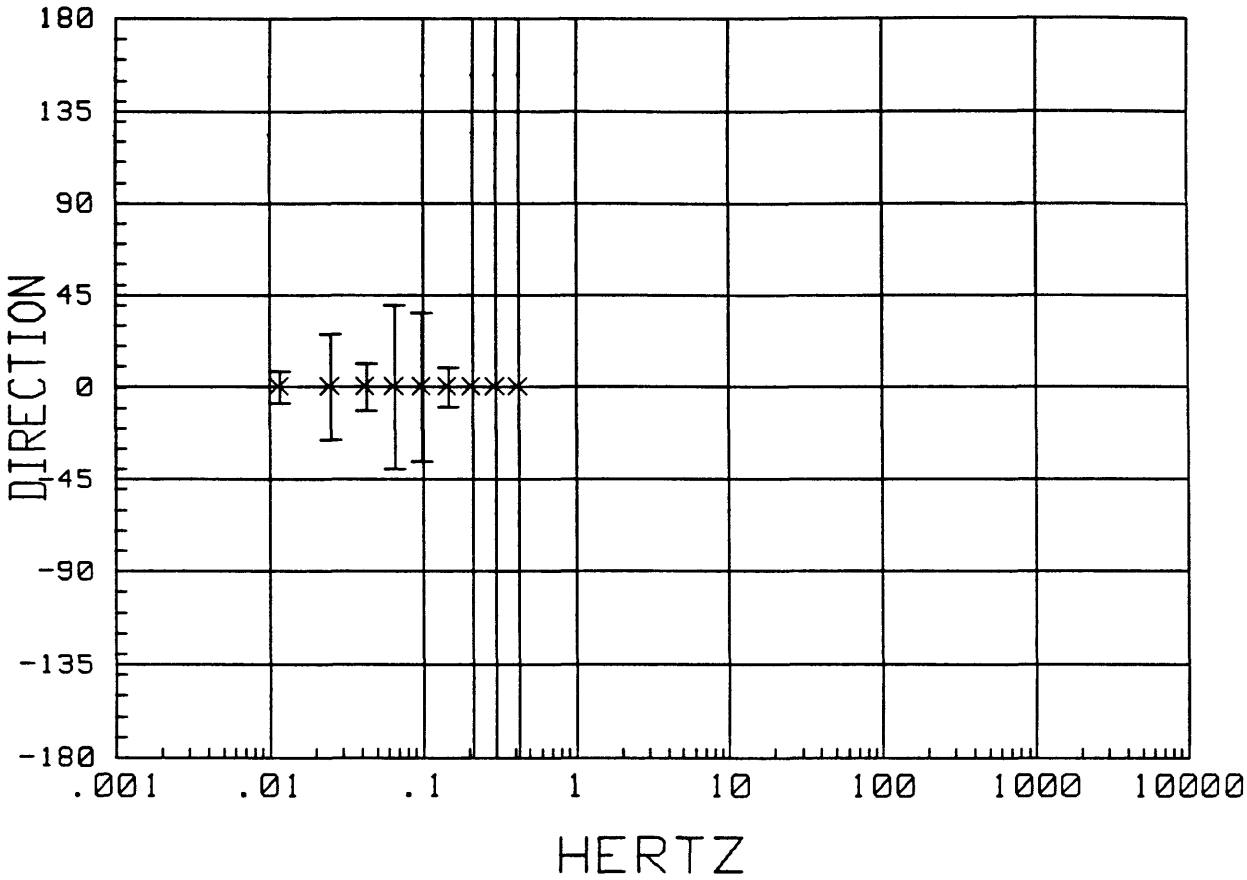

MTH007 LOCAL H-ref 16:16:17 20 May 1988
SKEW

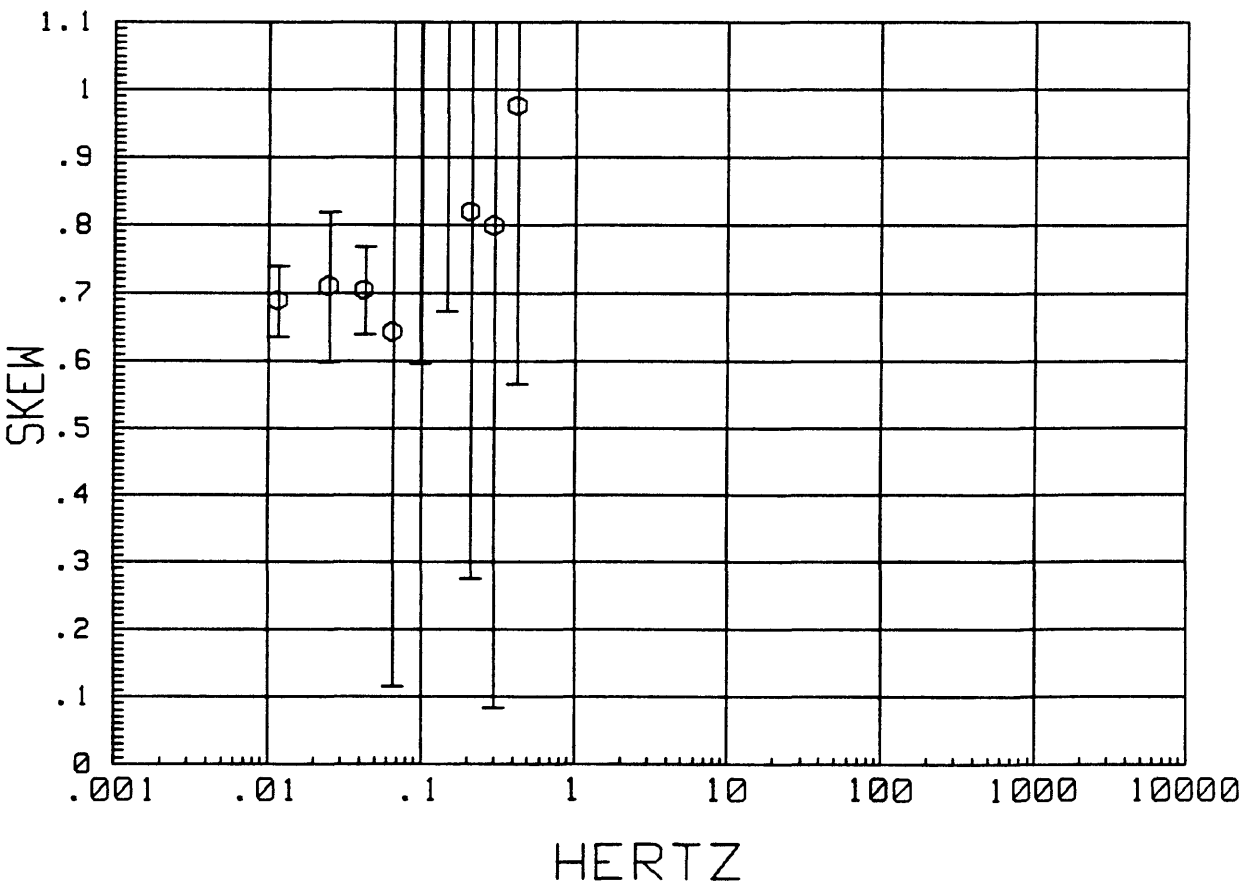

MTHO08 LOCAL H-ref 16:25:04 20 May 1988
APPARENT RESISTIVITY

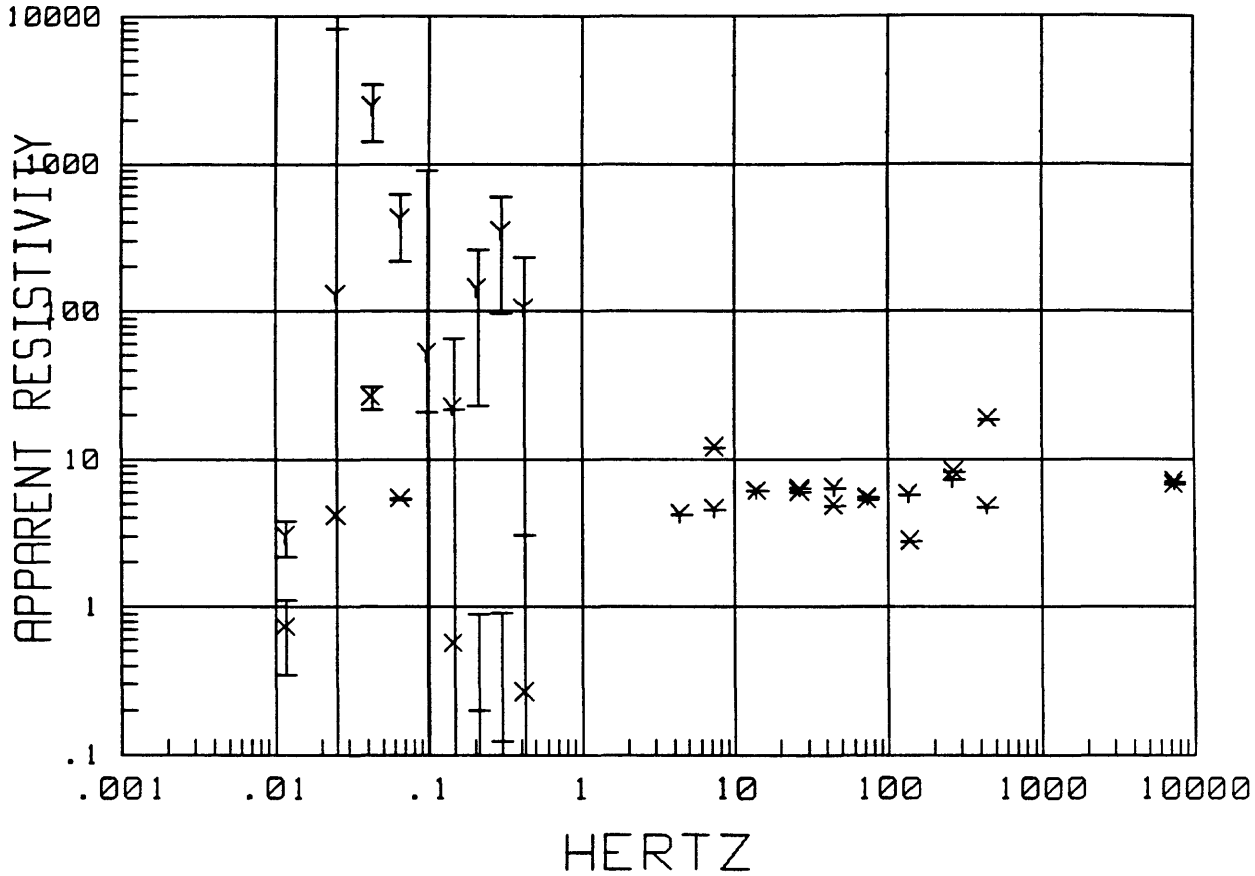

MTHO08 LOCAL H-ref 16:25:04 20 May 1988
IMPEDANCE PHASE

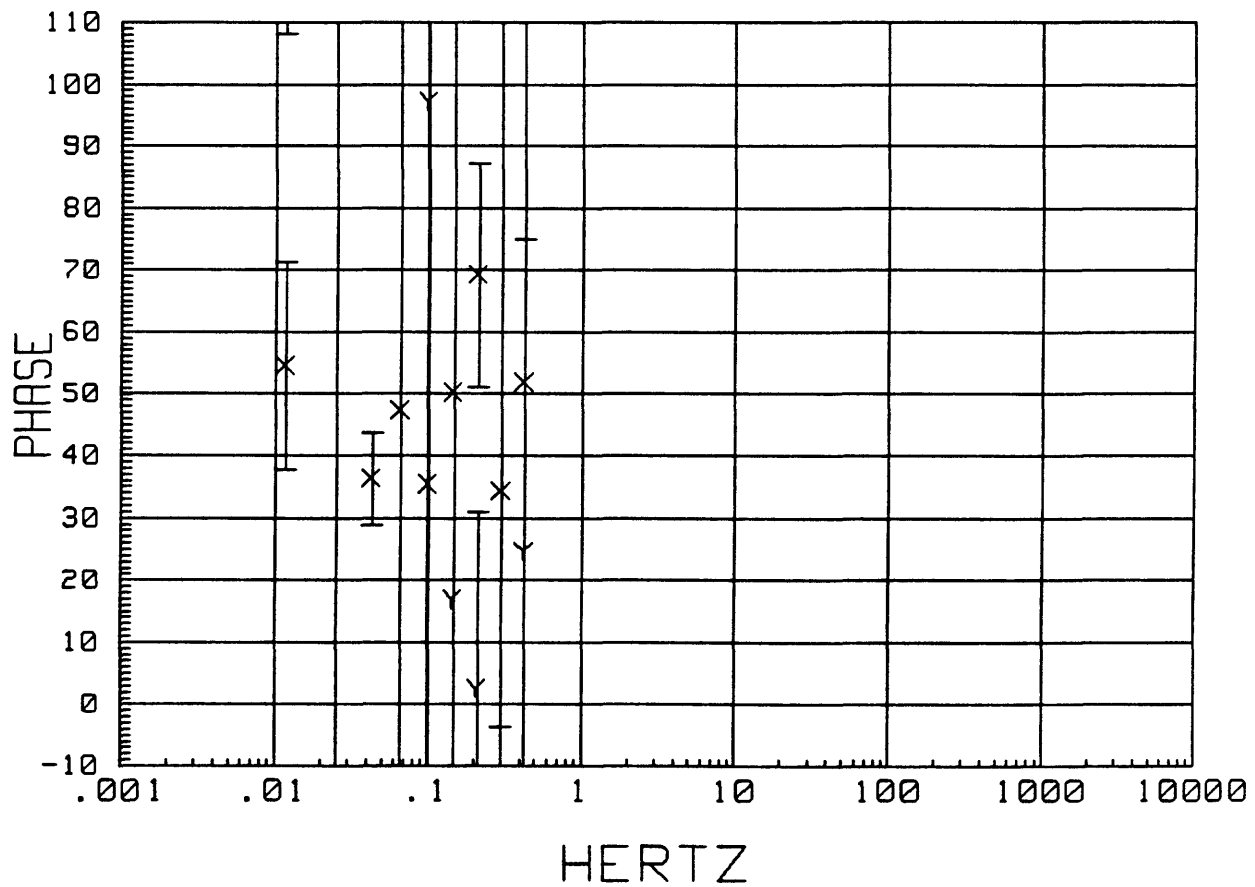

MTH008 LOCAL H-ref 16:25:04 20 May 1988
Z MAXIMUM DIRECTION

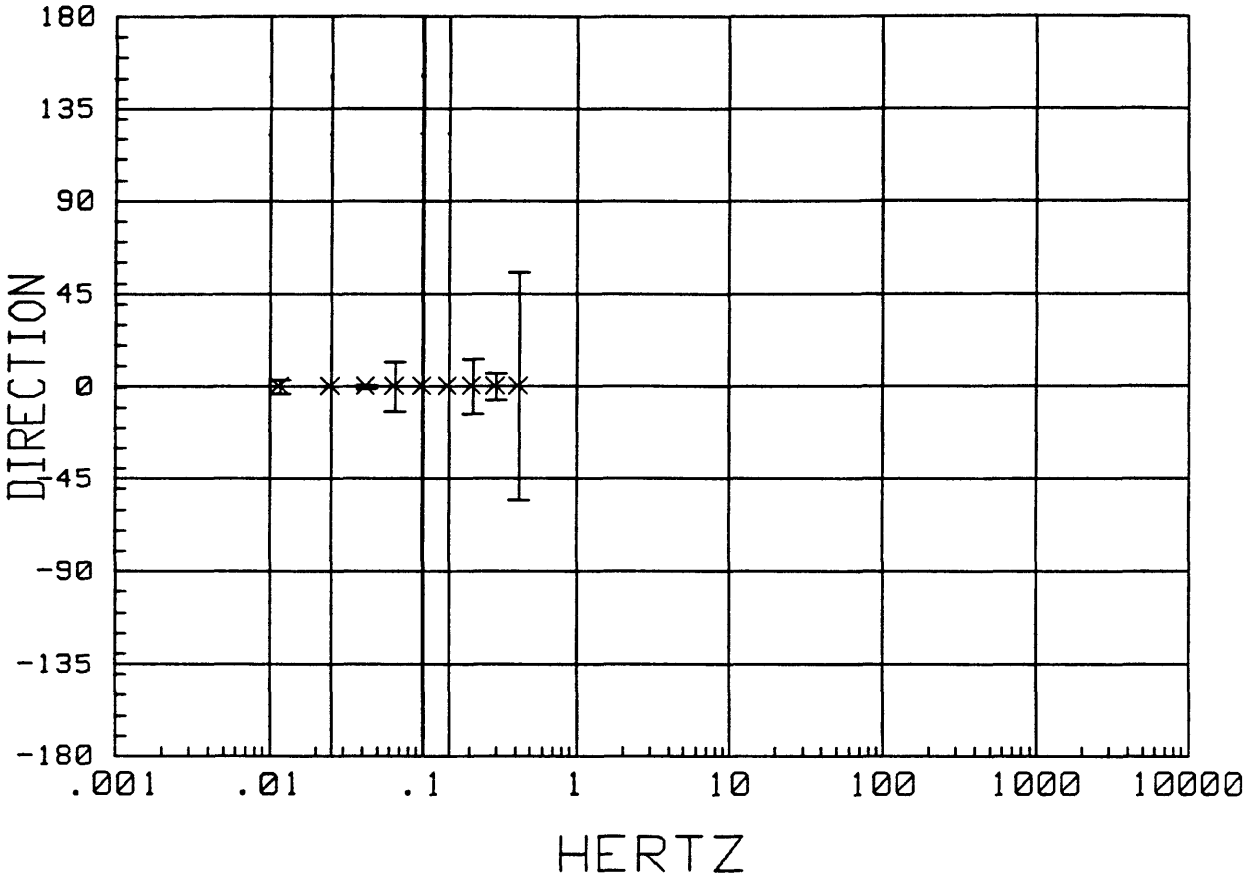

MTH008 LOCAL H-ref 16:25:04 20 May 1988
SKEW

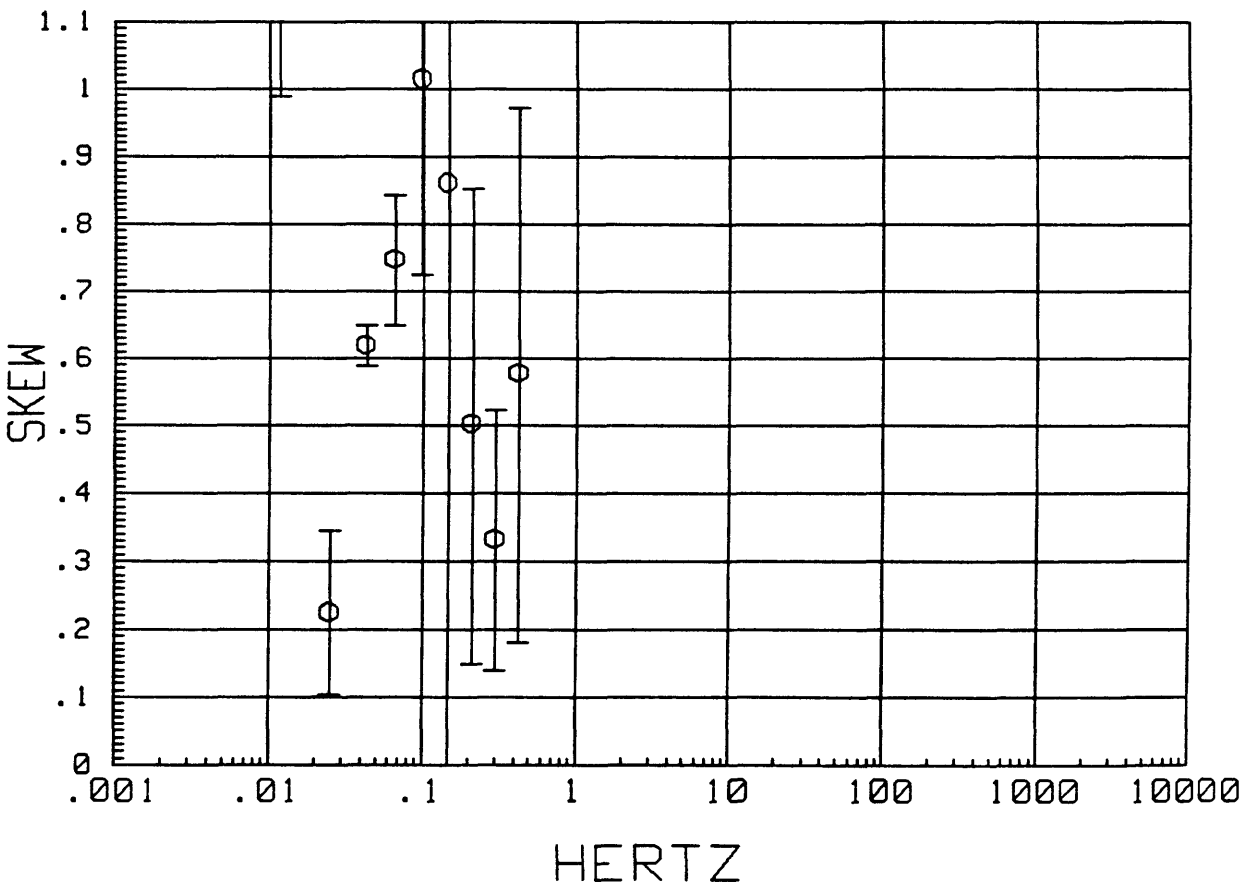

MTH009 LOCAL H-ref 16:33:23 20 May 1988
APPARENT RESISTIVITY

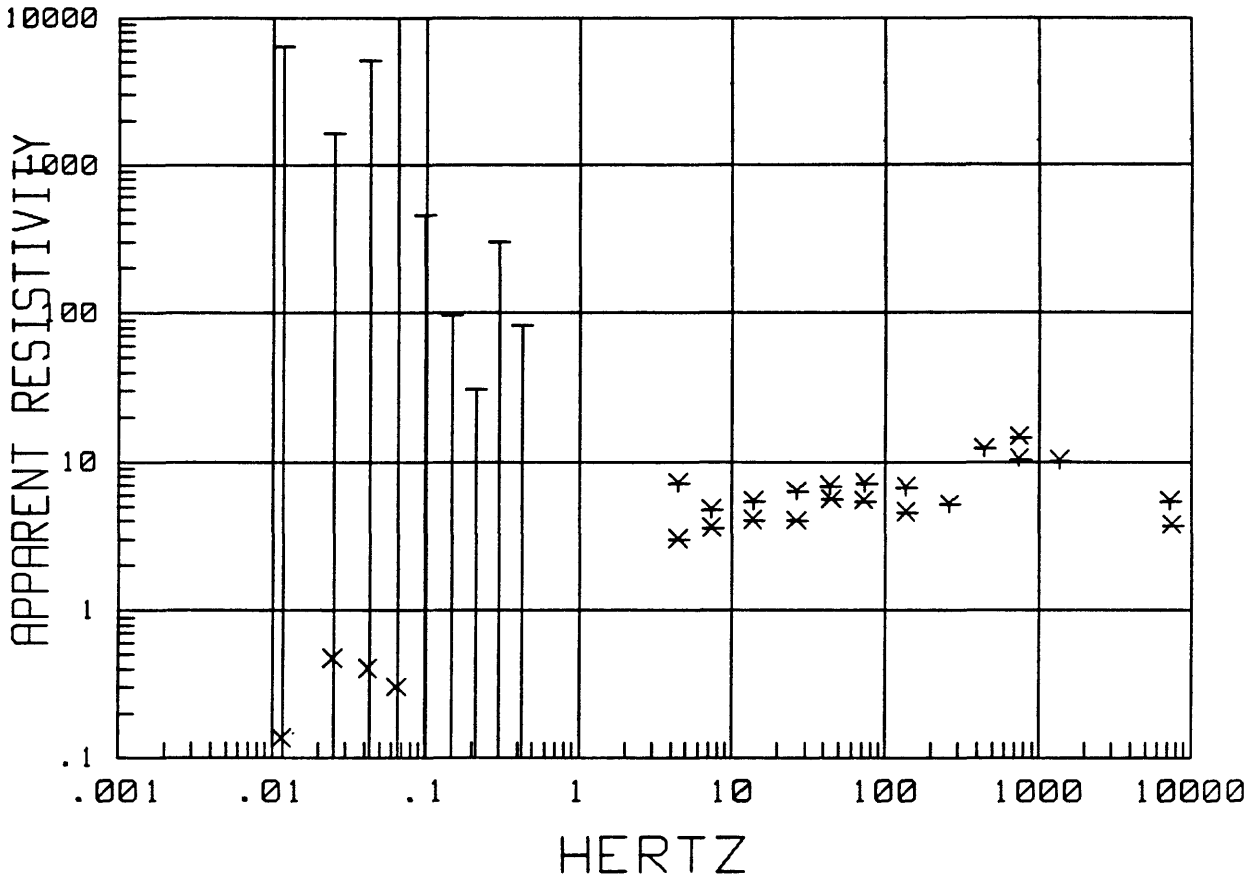

MTH009 LOCAL H-ref 16:46:50 20 May 1988
APPARENT RESISTIVITY

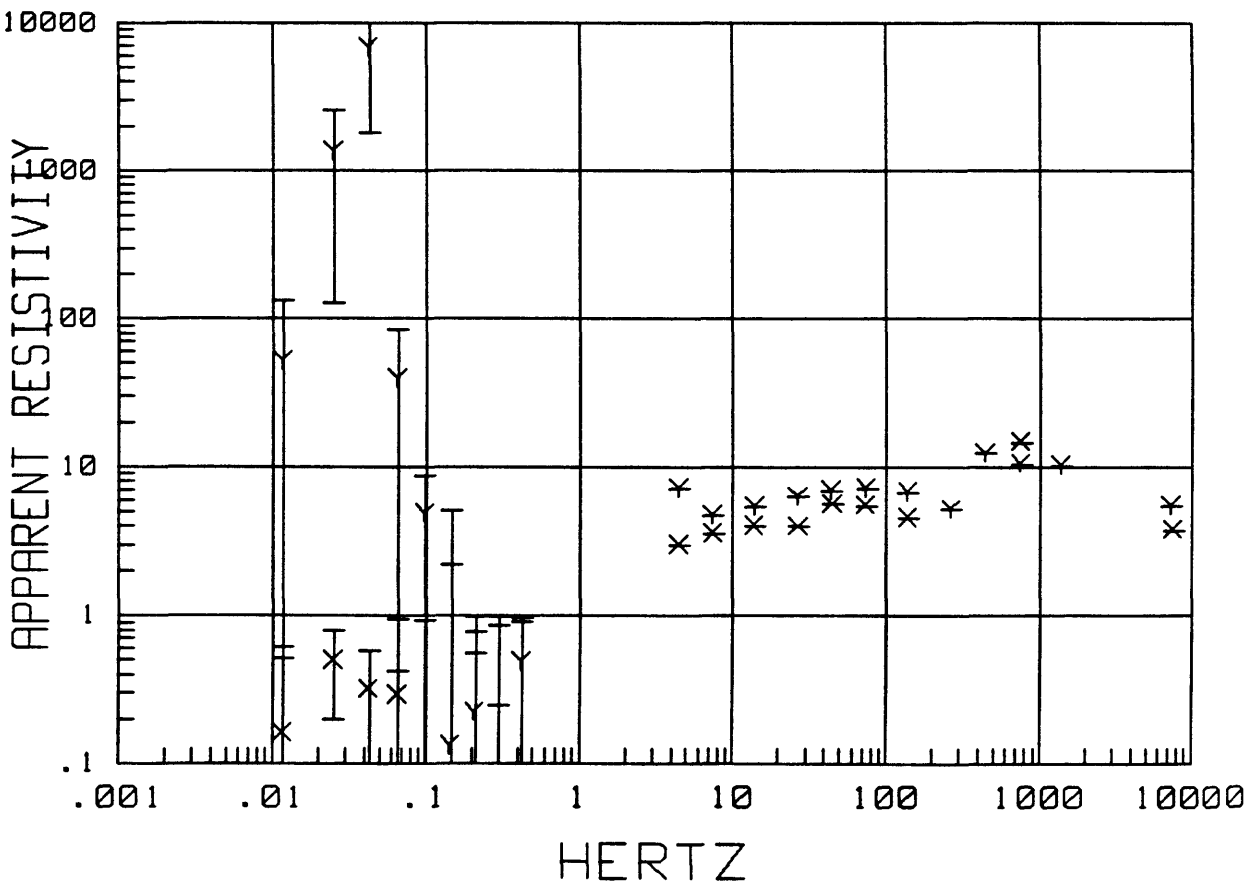

MTHO09 LOCAL H-ref 16:46:50 20 May 1988
Z MAXIMUM DIRECTION

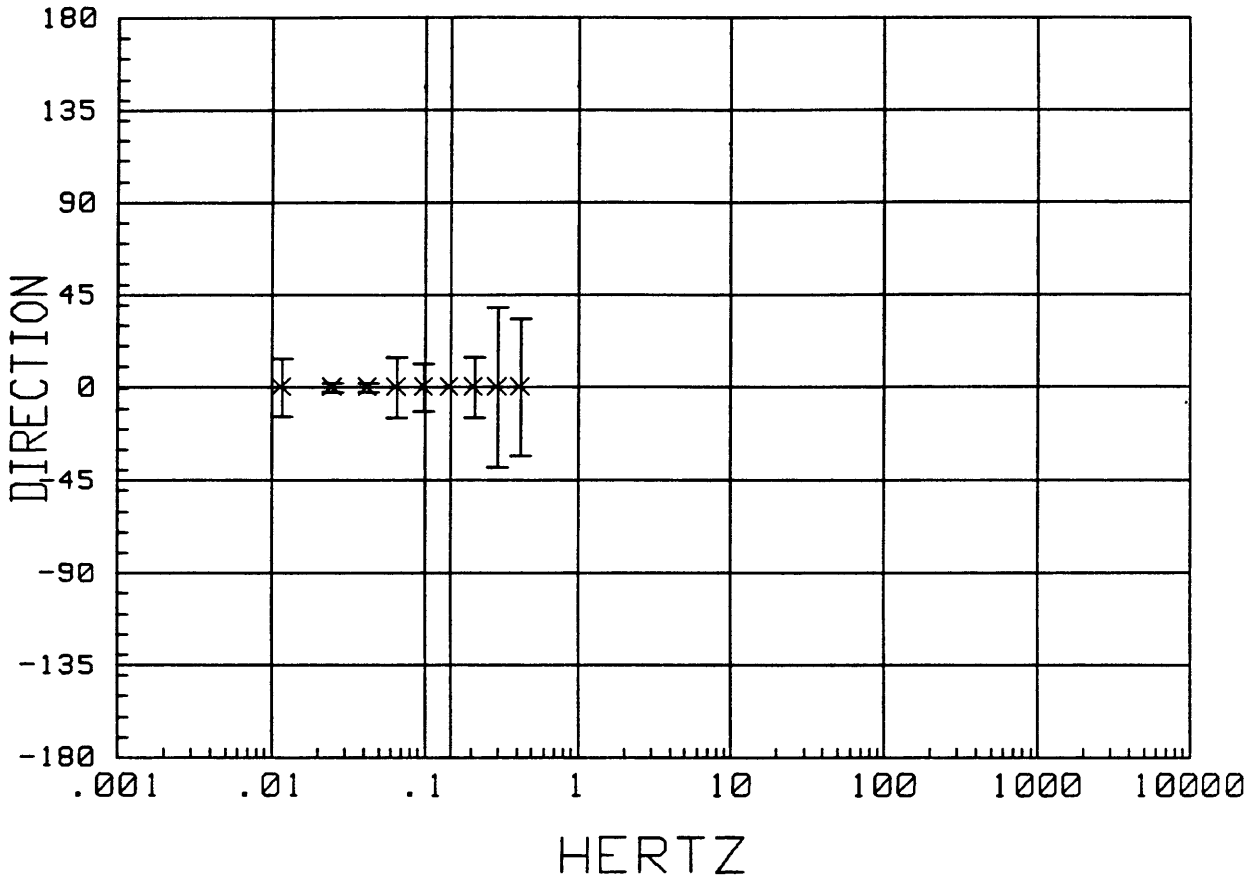

MTHO09 LOCAL H-ref 16:46:50 20 May 1988
SKEW

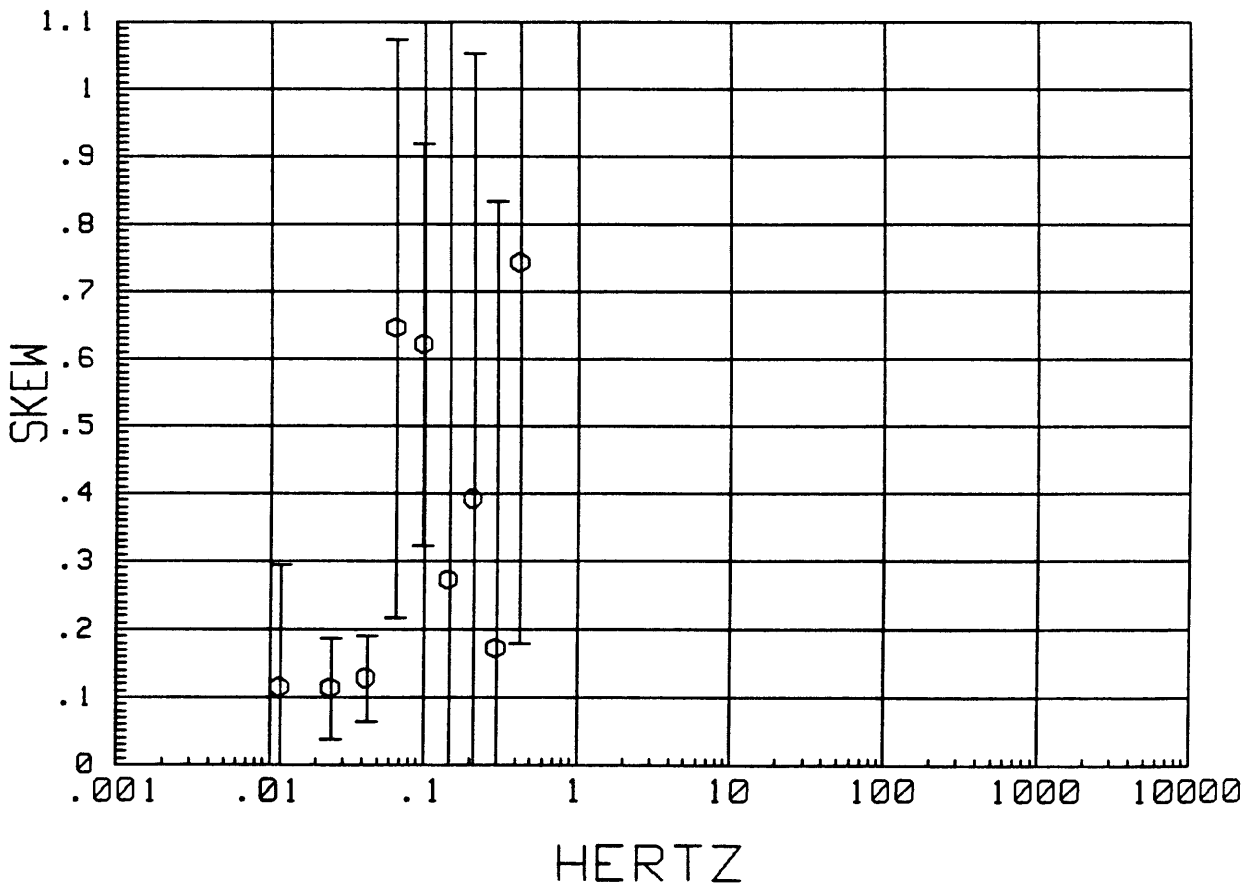

MTHO10 LOCAL H-ref 17:01:39 20 May 1988
APPARENT RESISTIVITY

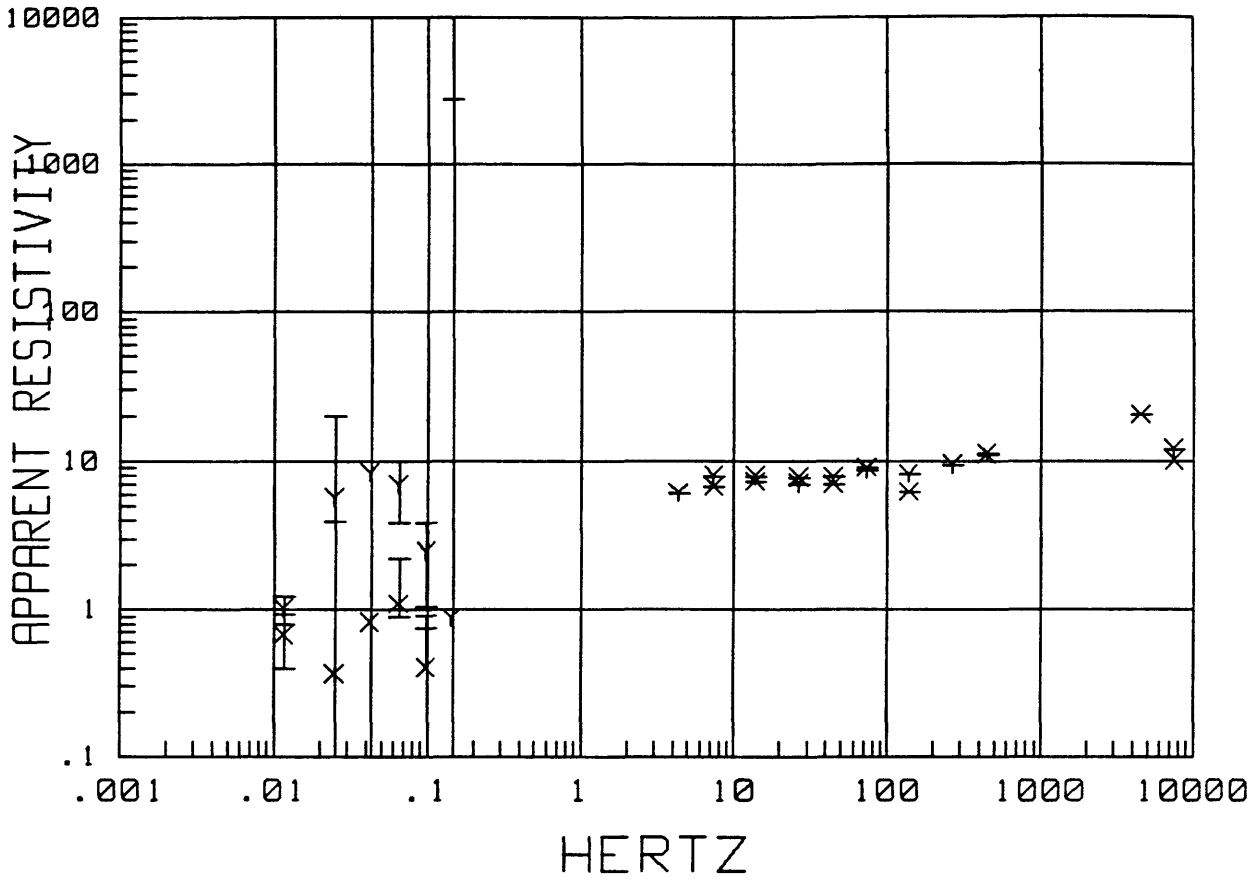

MTHO10 LOCAL H-ref 17:01:39 20 May 1988
IMPEDANCE PHASE

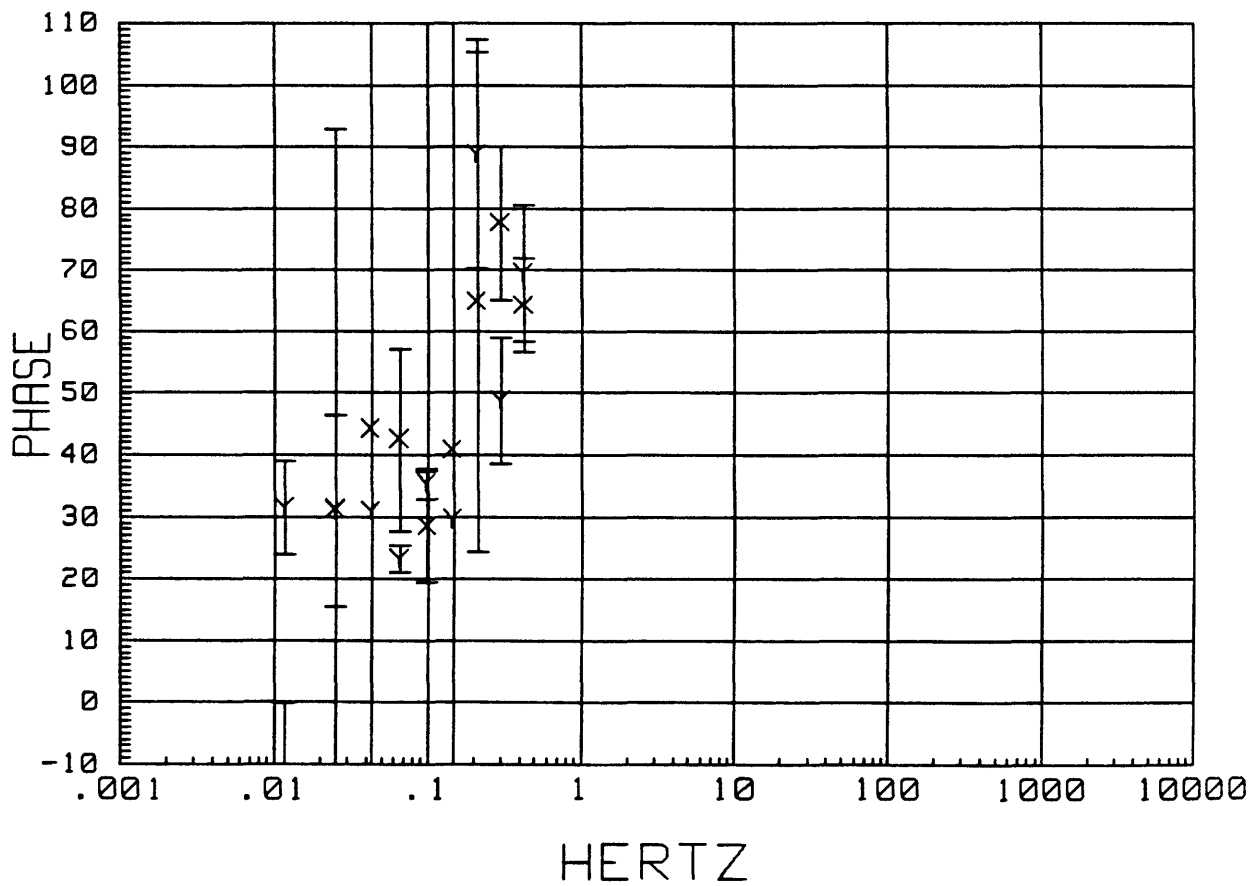

MTHO10 LOCAL H-ref 17:01:39 20 May 1988
Z MAXIMUM DIRECTION

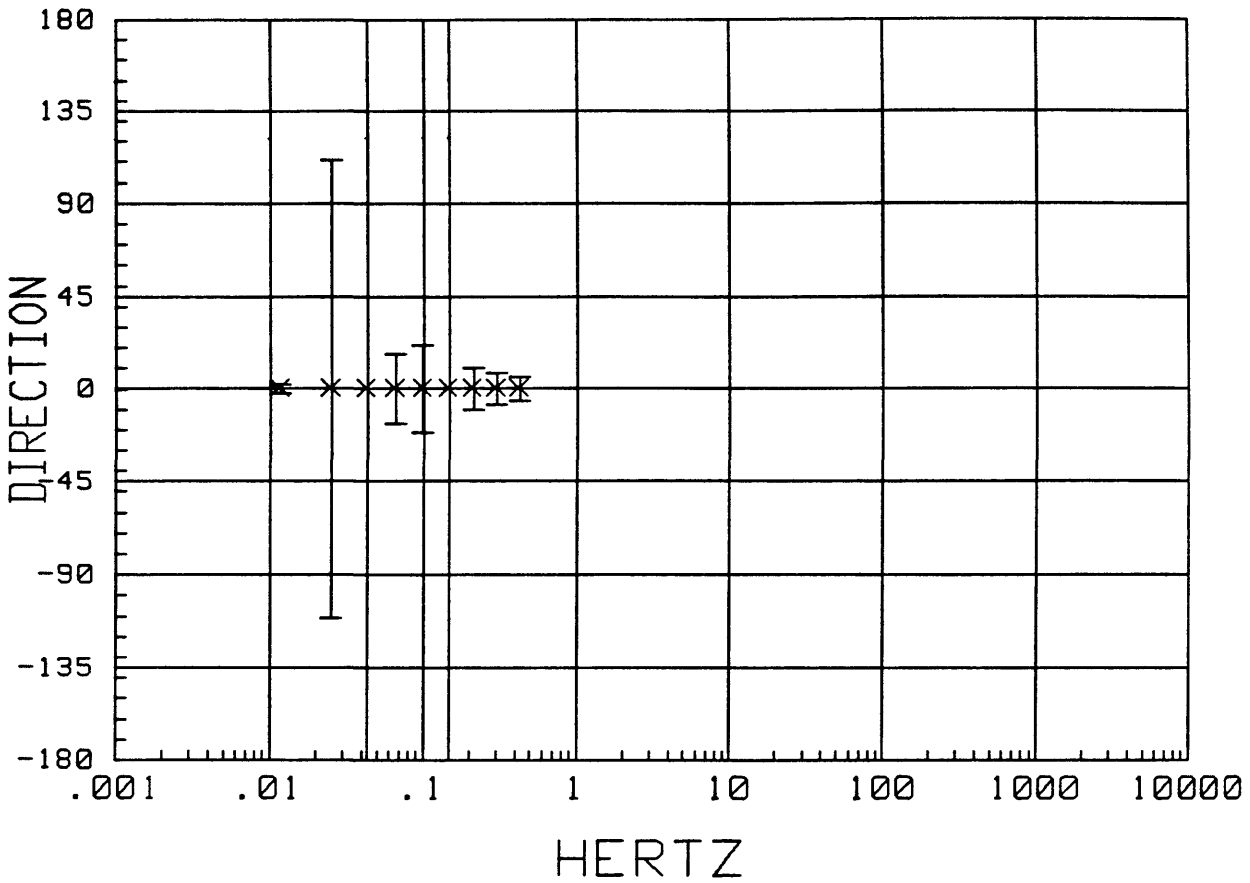

MTHO10 LOCAL H-ref 17:01:39 20 May 1988
SKEW

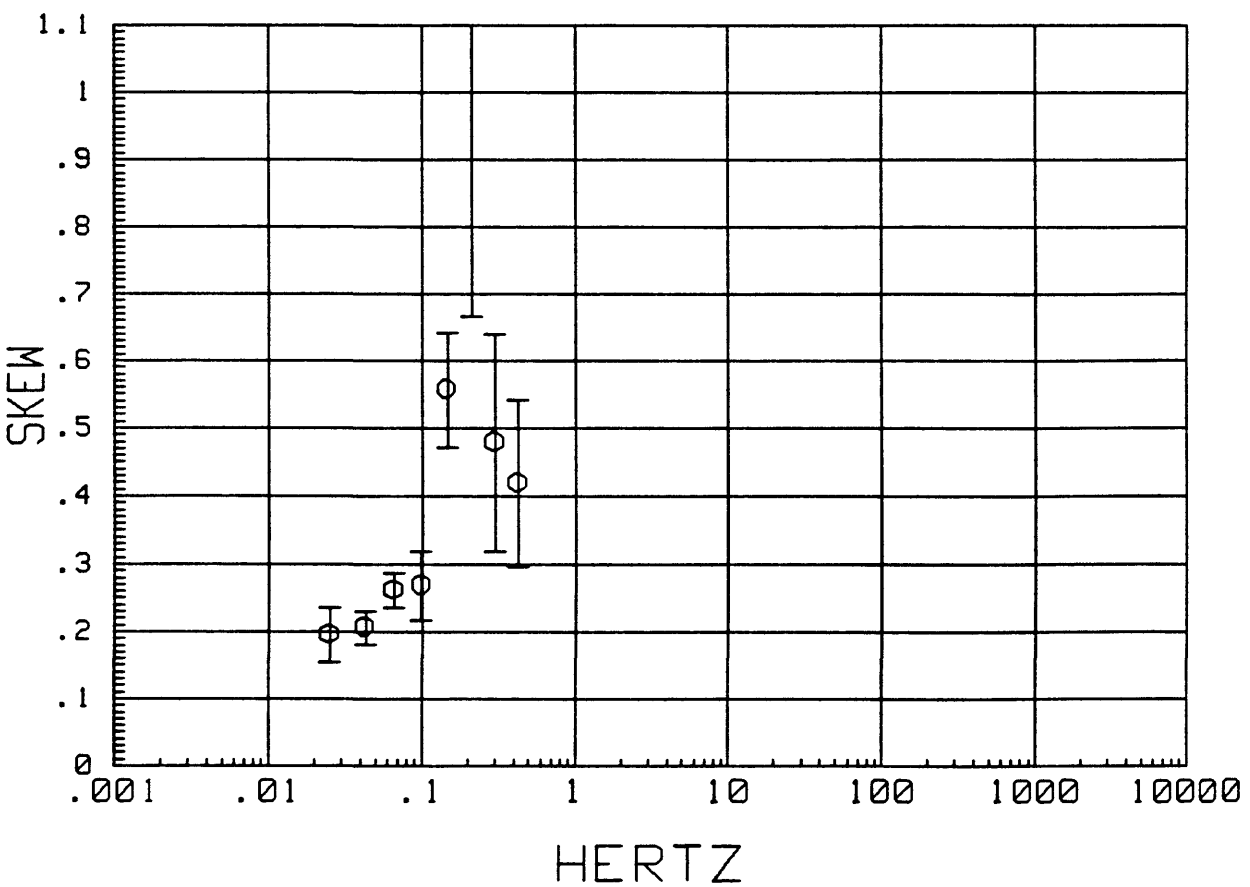

MTH011 LOCAL H-ref 17:11:57 20 May 1988
APPARENT RESISTIVITY

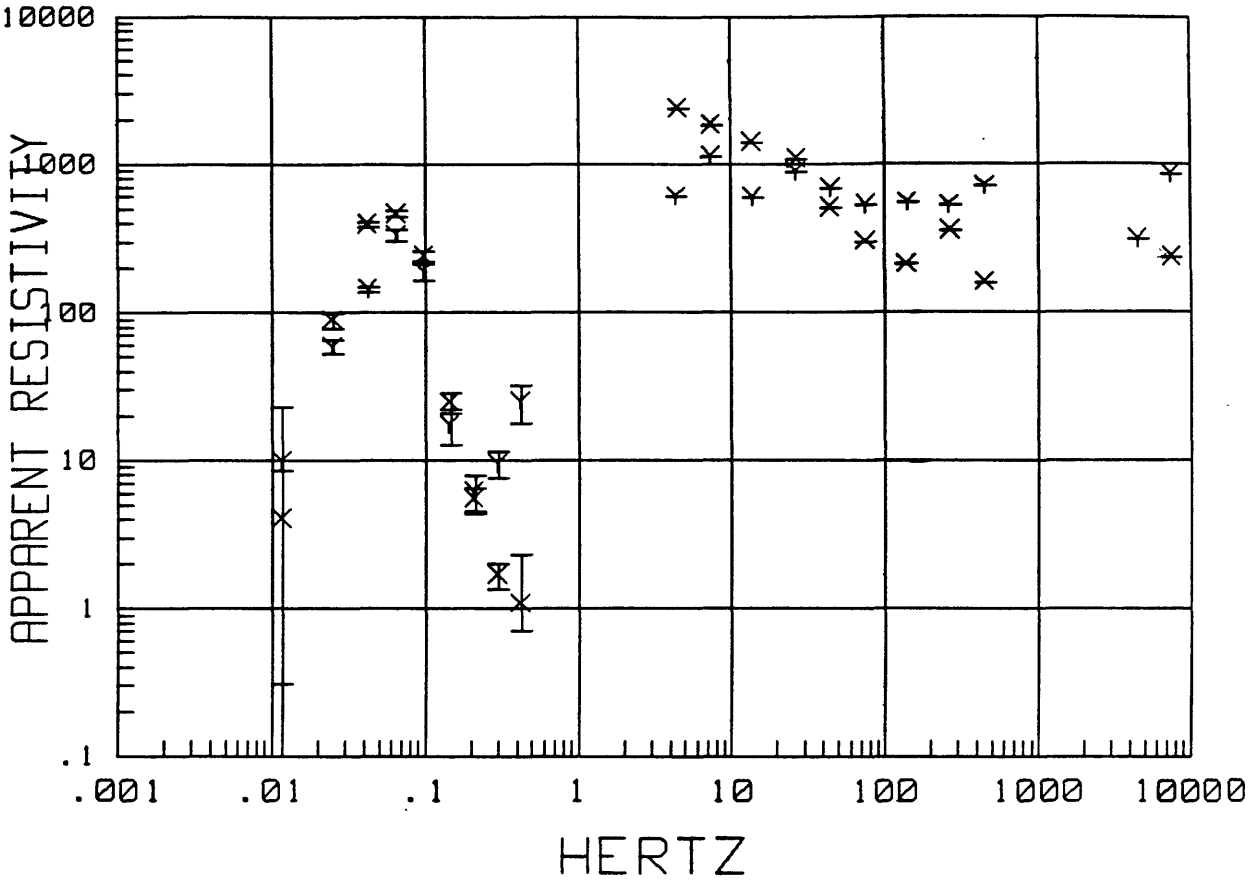

MTH011 LOCAL H-ref 17:11:57 20 May 1988
IMPEDANCE PHASE

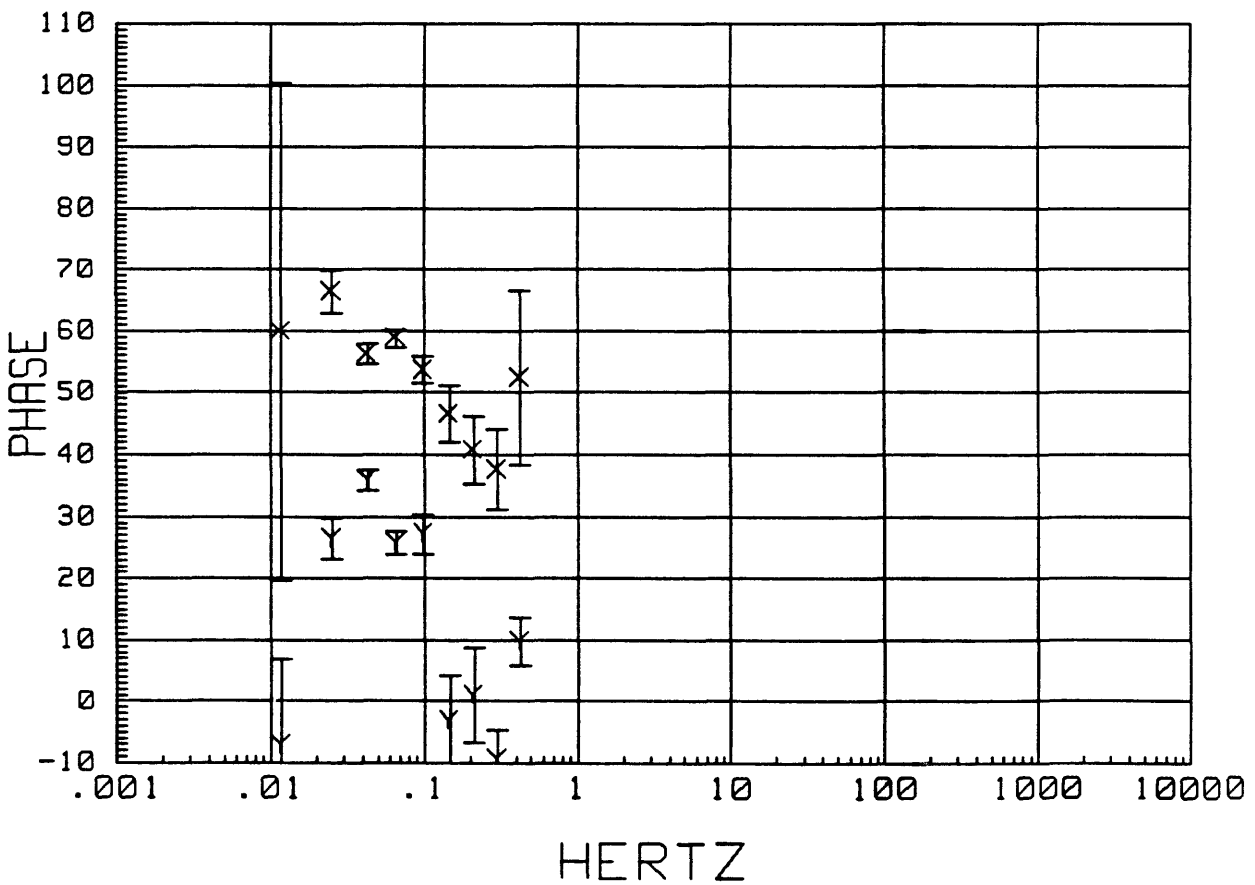

MTHO11 LOCAL H-ref 17:11:57 20 May 1988
Z MAXIMUM DIRECTION

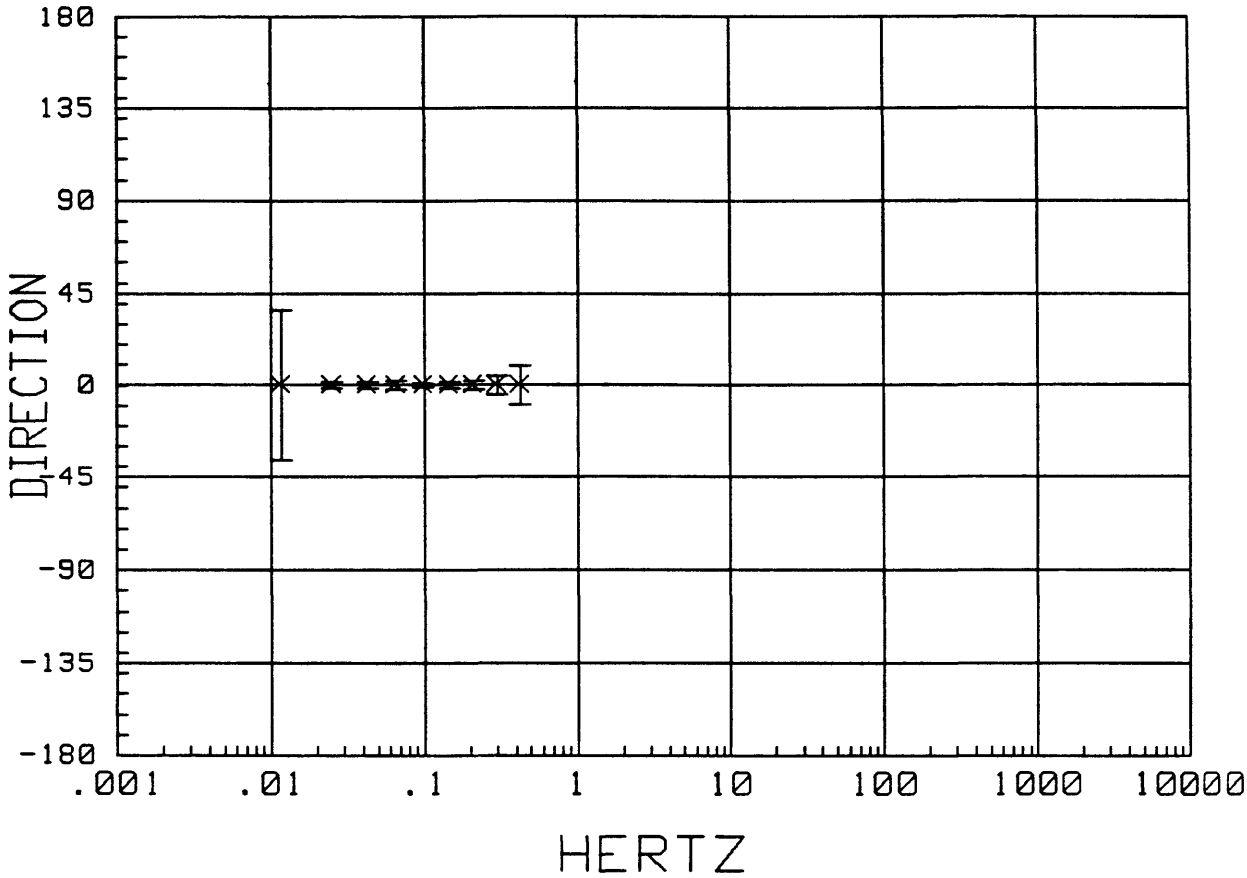

MTHO11 LOCAL H-ref 17:11:57 20 May 1988
SKEW

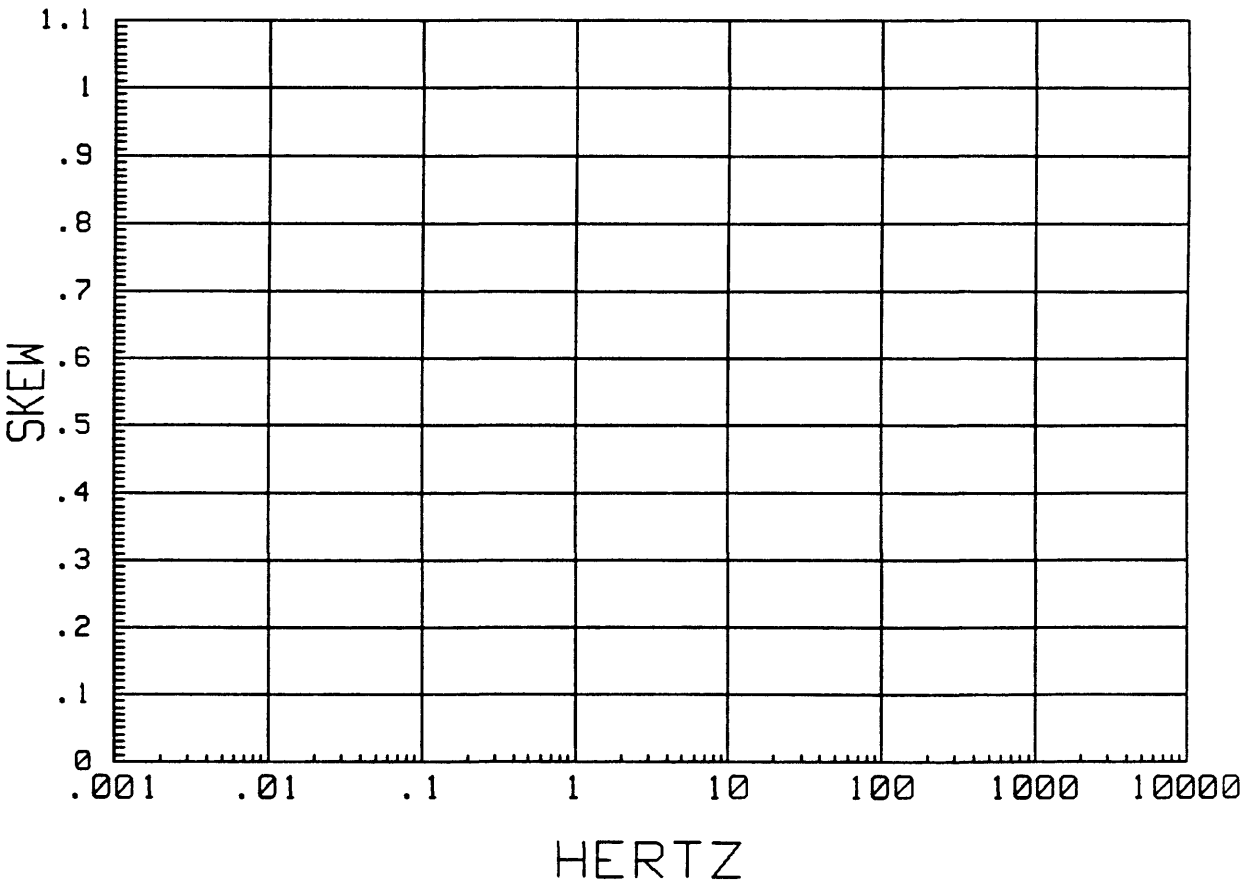

MTH012 LOCAL H-ref 20:15:50 7 Jul 1988
APPARENT RESISTIVITY

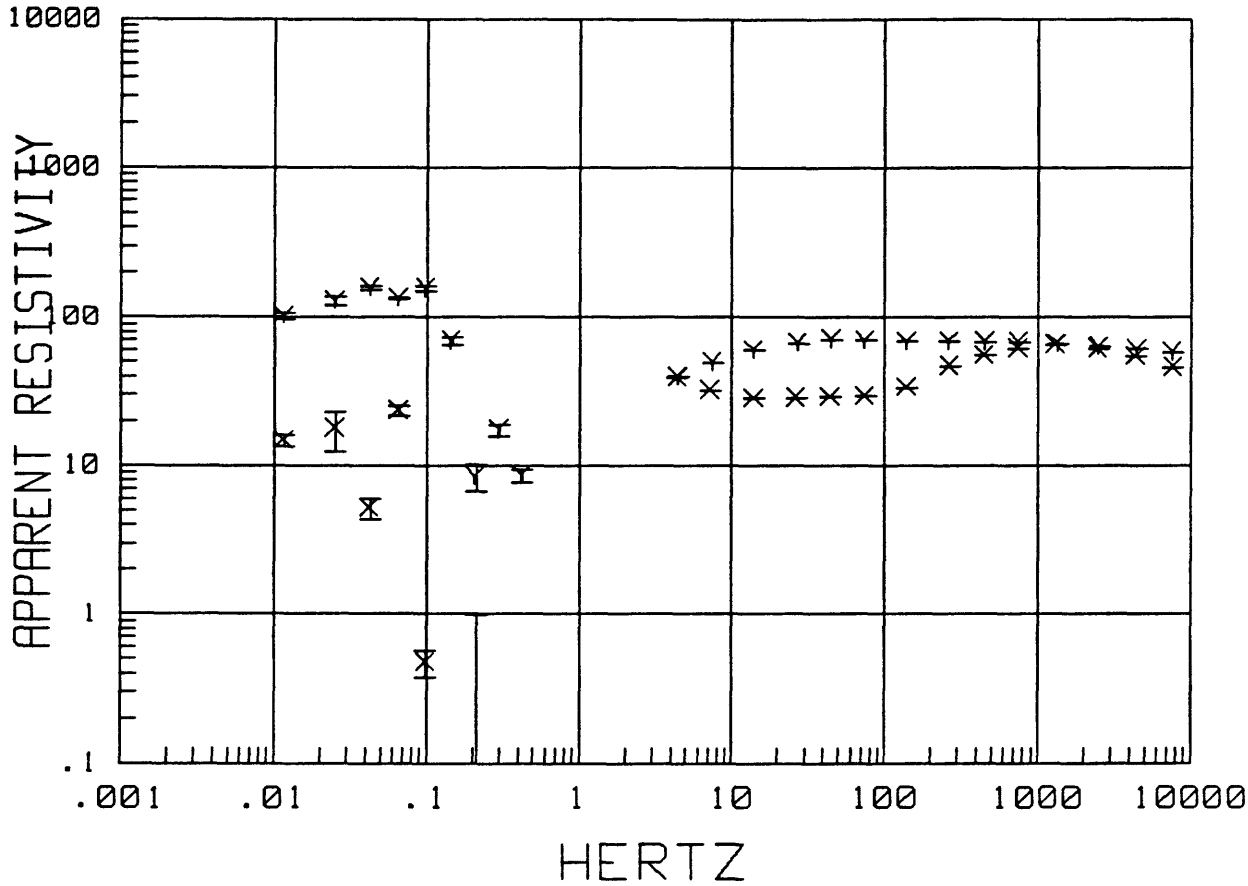

MTH012 LOCAL H-ref 20:15:50 7 Jul 1988
IMPEDANCE PHASE

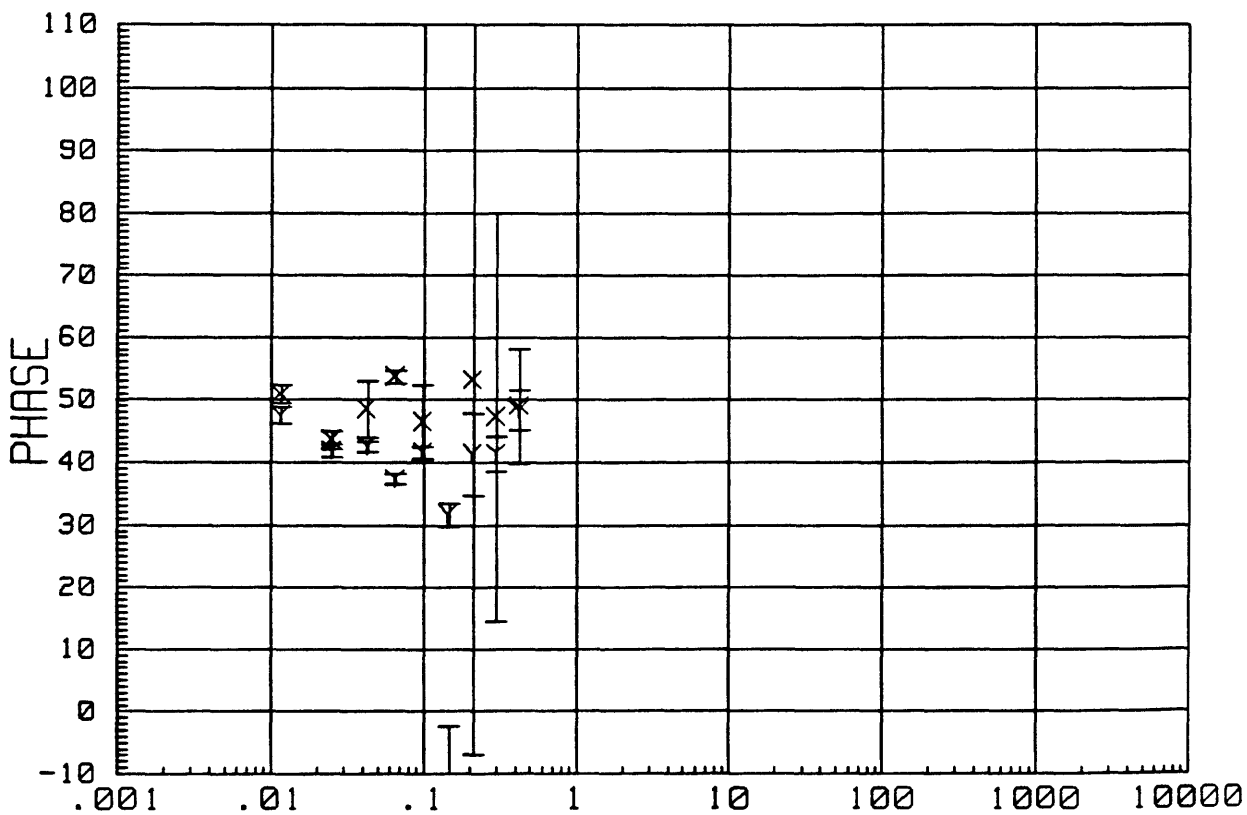

MTHO12 LOCAL H-ref 20:15:50 7 Jul 1988
Z MAXIMUM DIRECTION

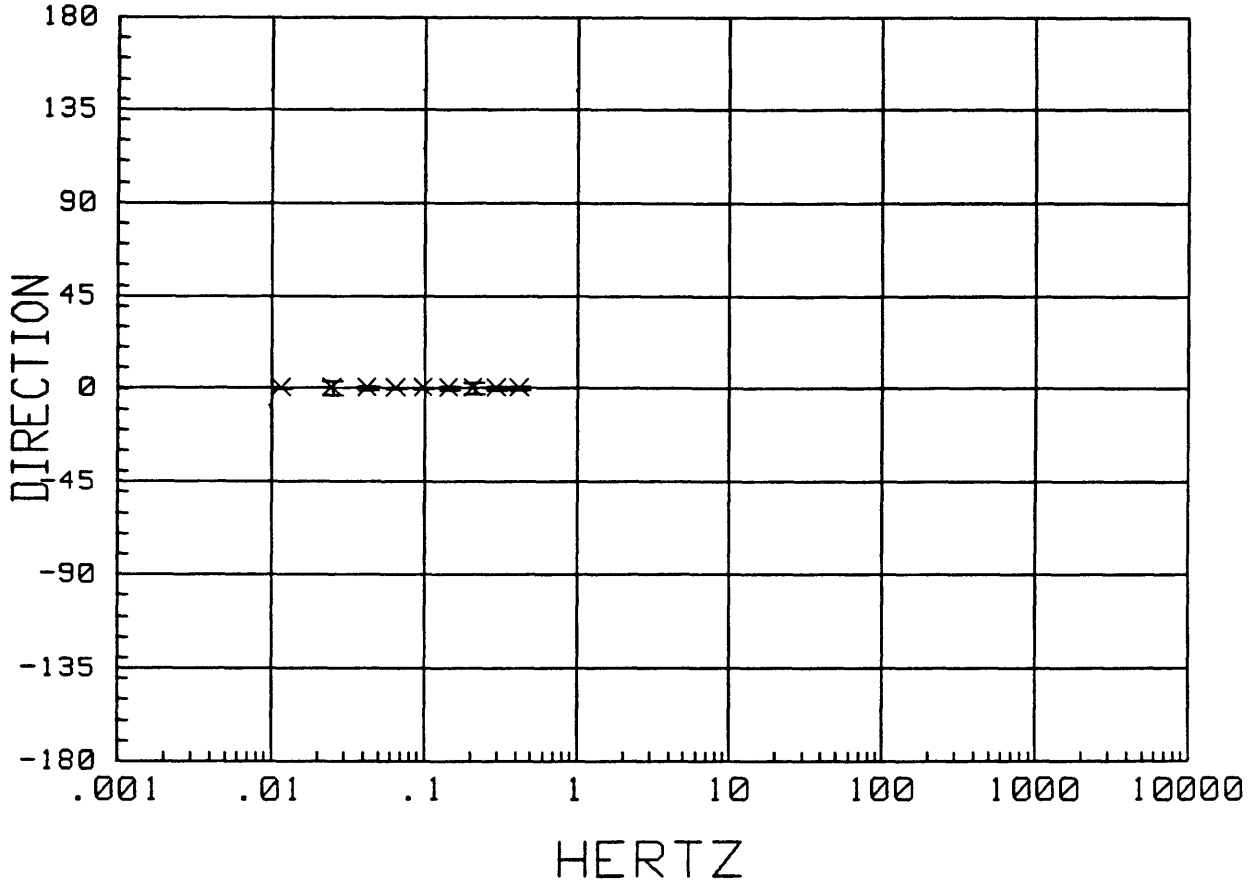

MTHO12 LOCAL H-ref 20:15:50 7 Jul 1988
SKEW

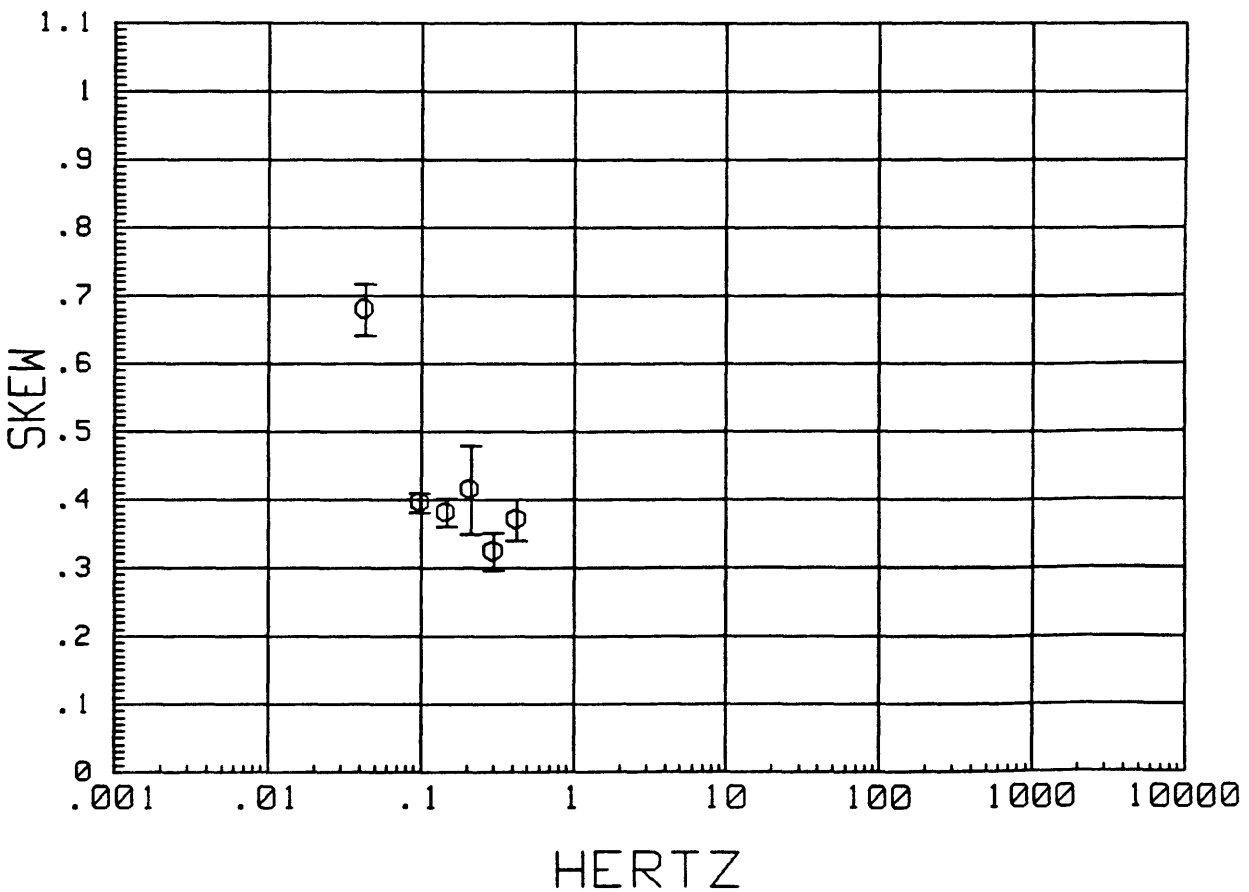

MTH013 LOCAL H-ref 15:53:47 25 Jul 1988
APPARENT RESISTIVITY

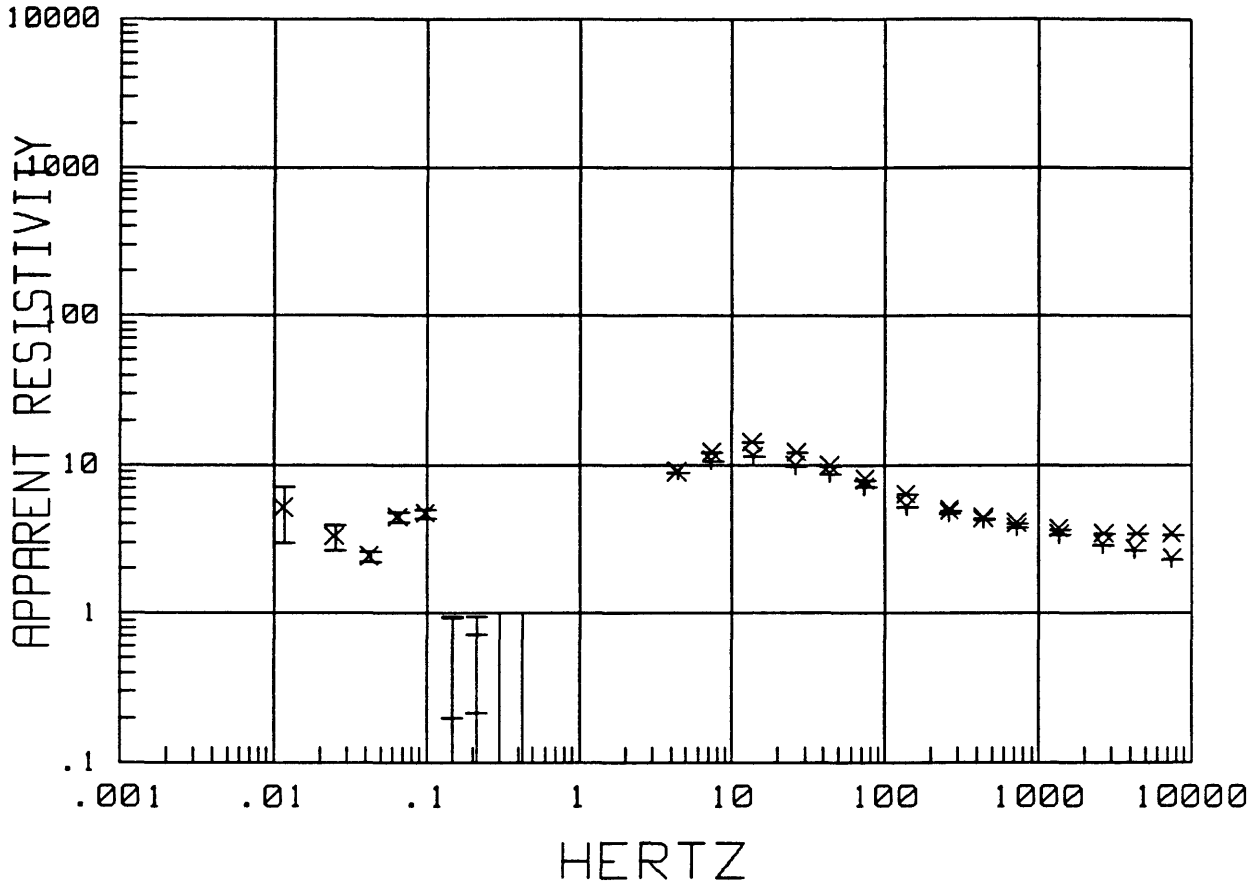

MTH013 LOCAL H-ref 15:53:47 25 Jul 1988
IMPEDANCE PHASE

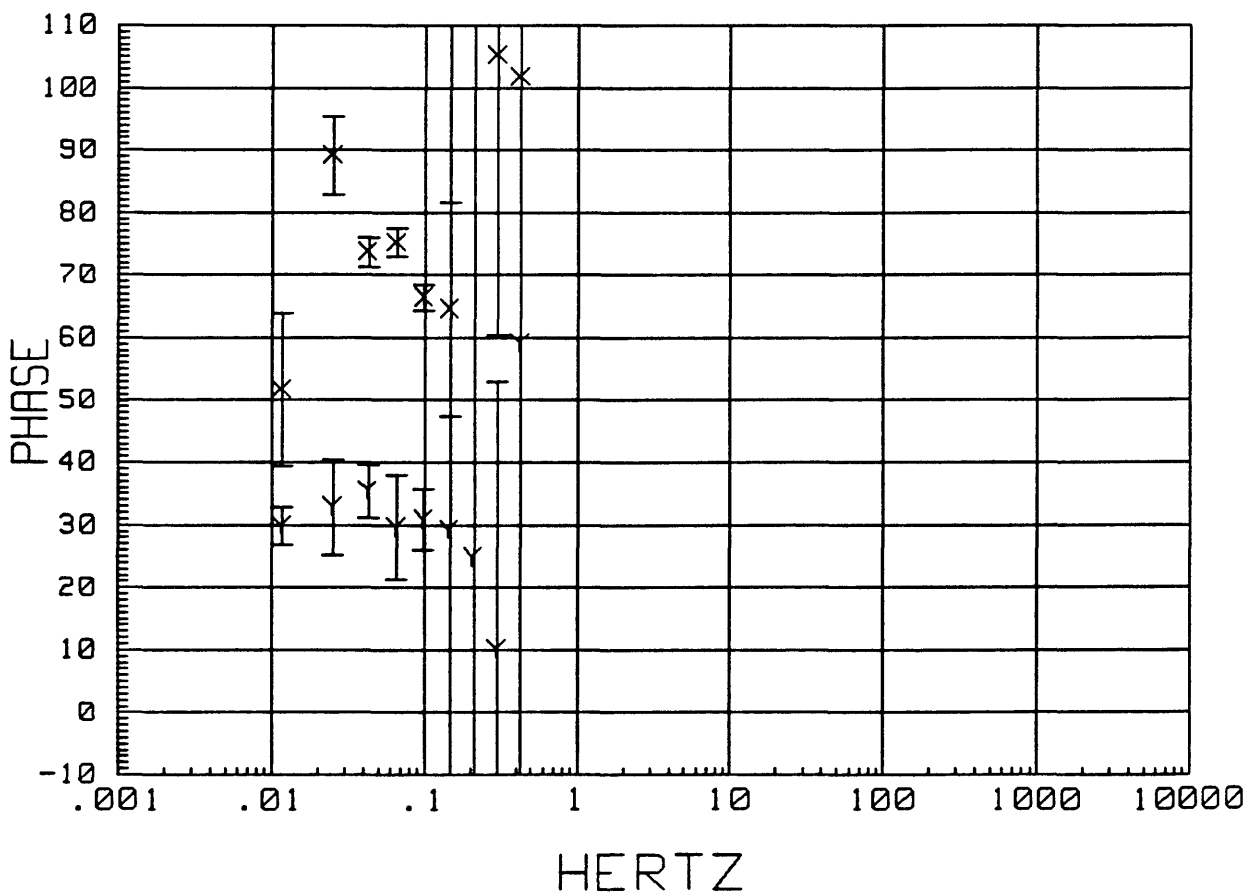

MTHO13 LOCAL H-ref 15:53:47 25 Jul 1988
Z MAXIMUM DIRECTION

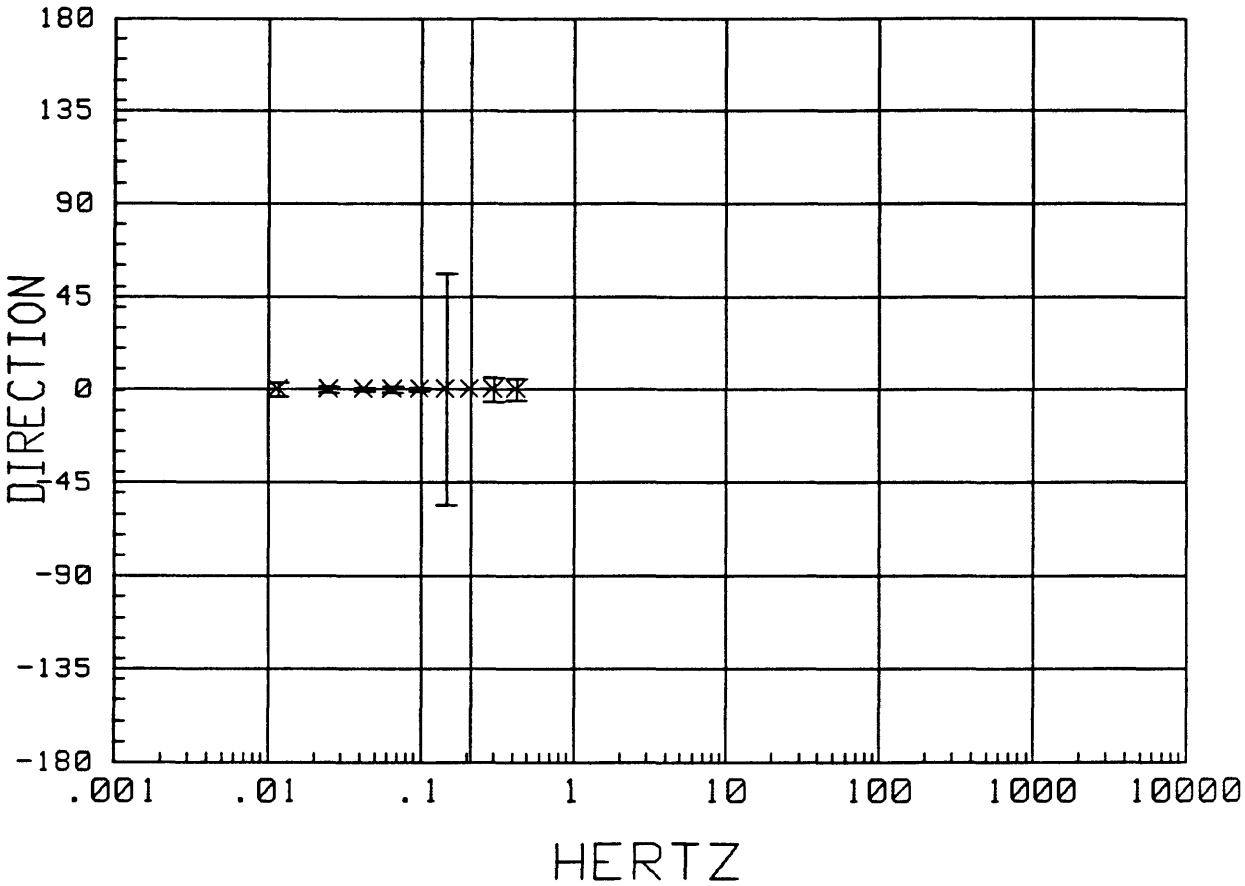

MTHO13 LOCAL H-ref 15:53:47 25 Jul 1988
SKEW

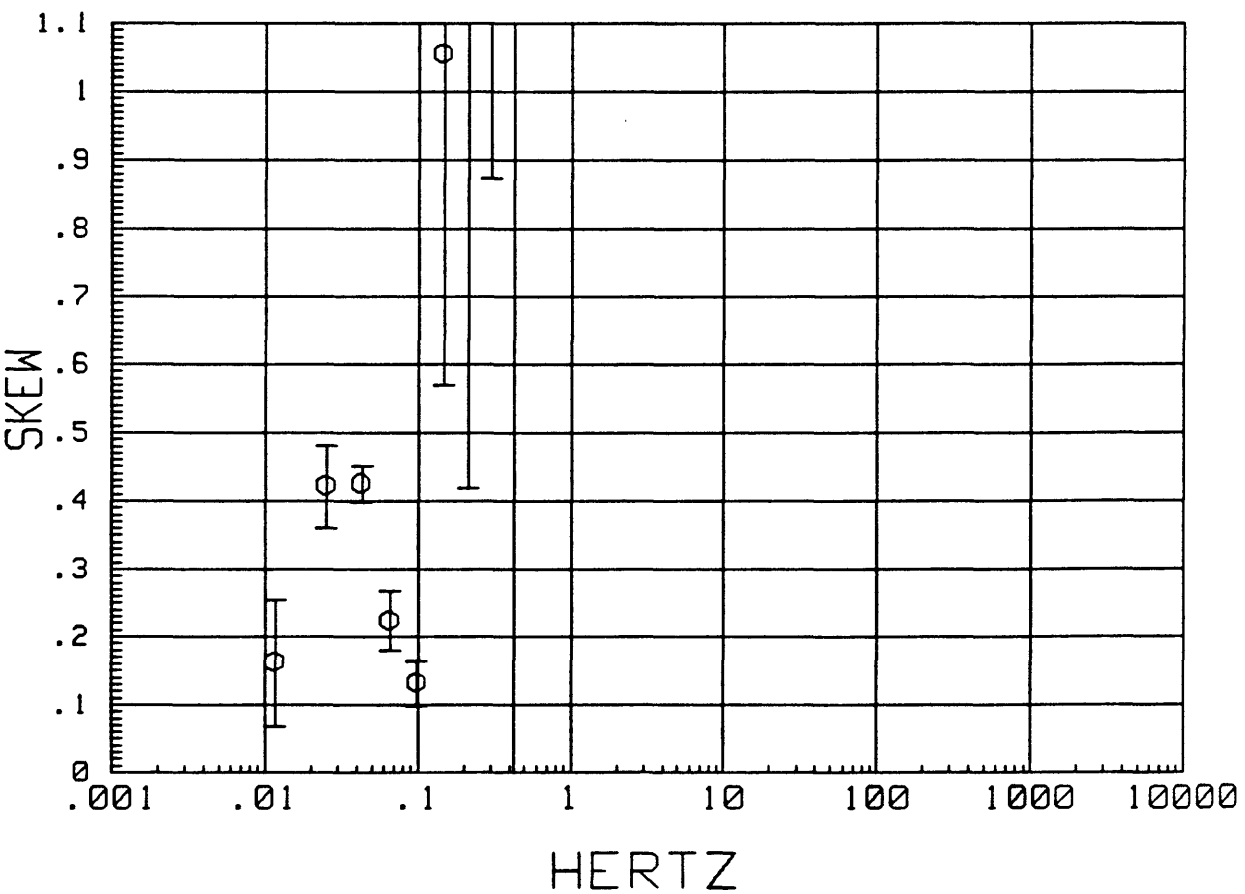

MTHO14 LOCAL H-ref 20:52:57 7 Jul 1988
APPARENT RESISTIVITY

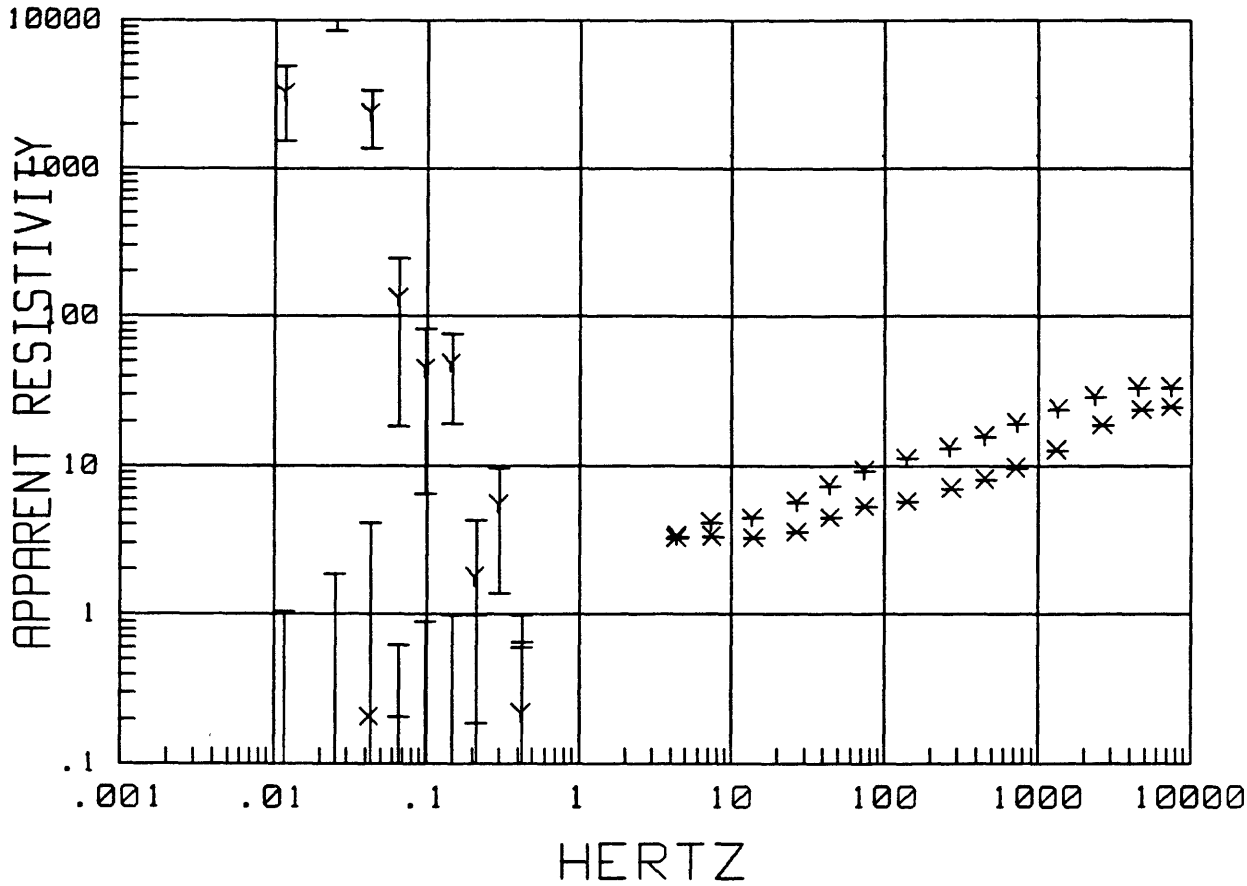

MTHO14 LOCAL H-ref 20:52:57 7 Jul 1988
IMPEDANCE PHASE

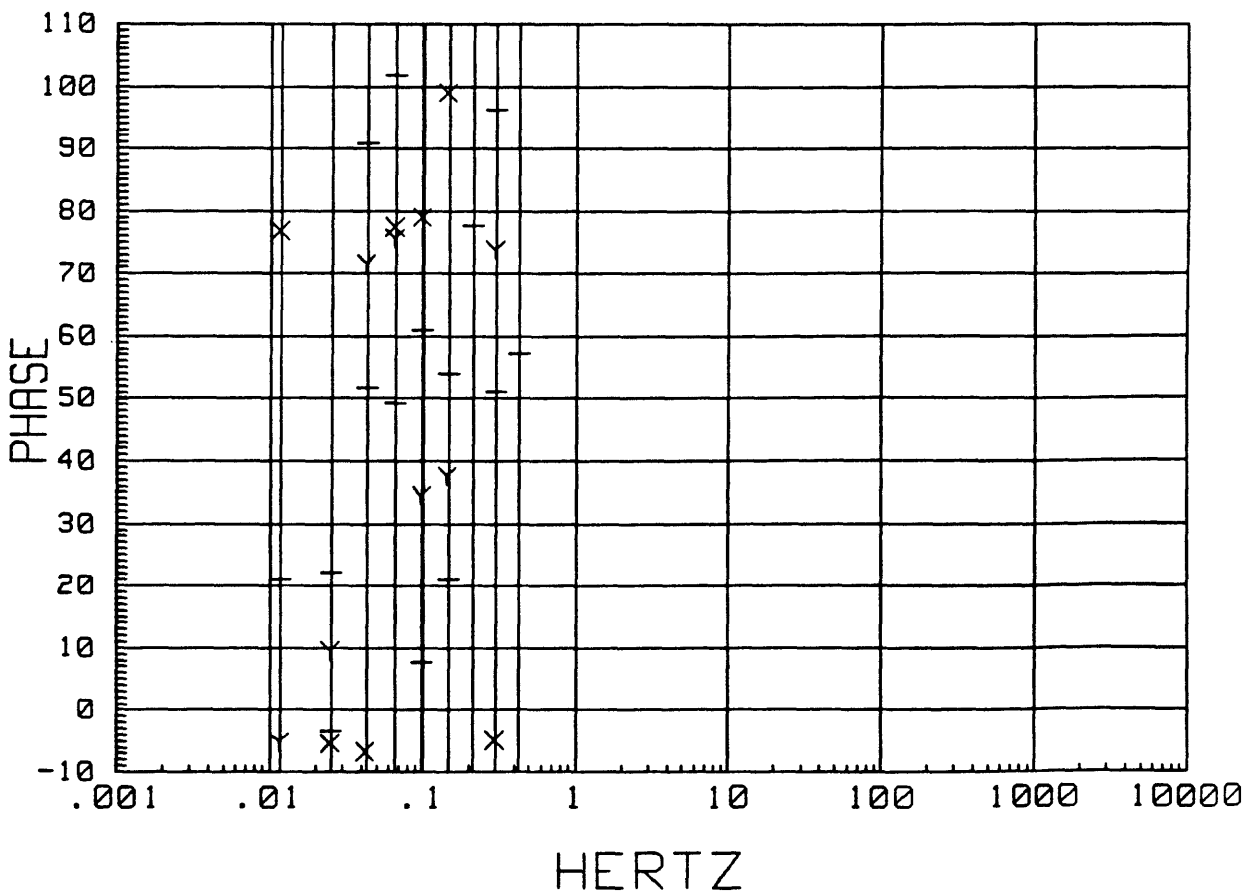

MTHO14 LOCAL H-ref 20:52:57 7 Jul 1988
Z MAXIMUM DIRECTION

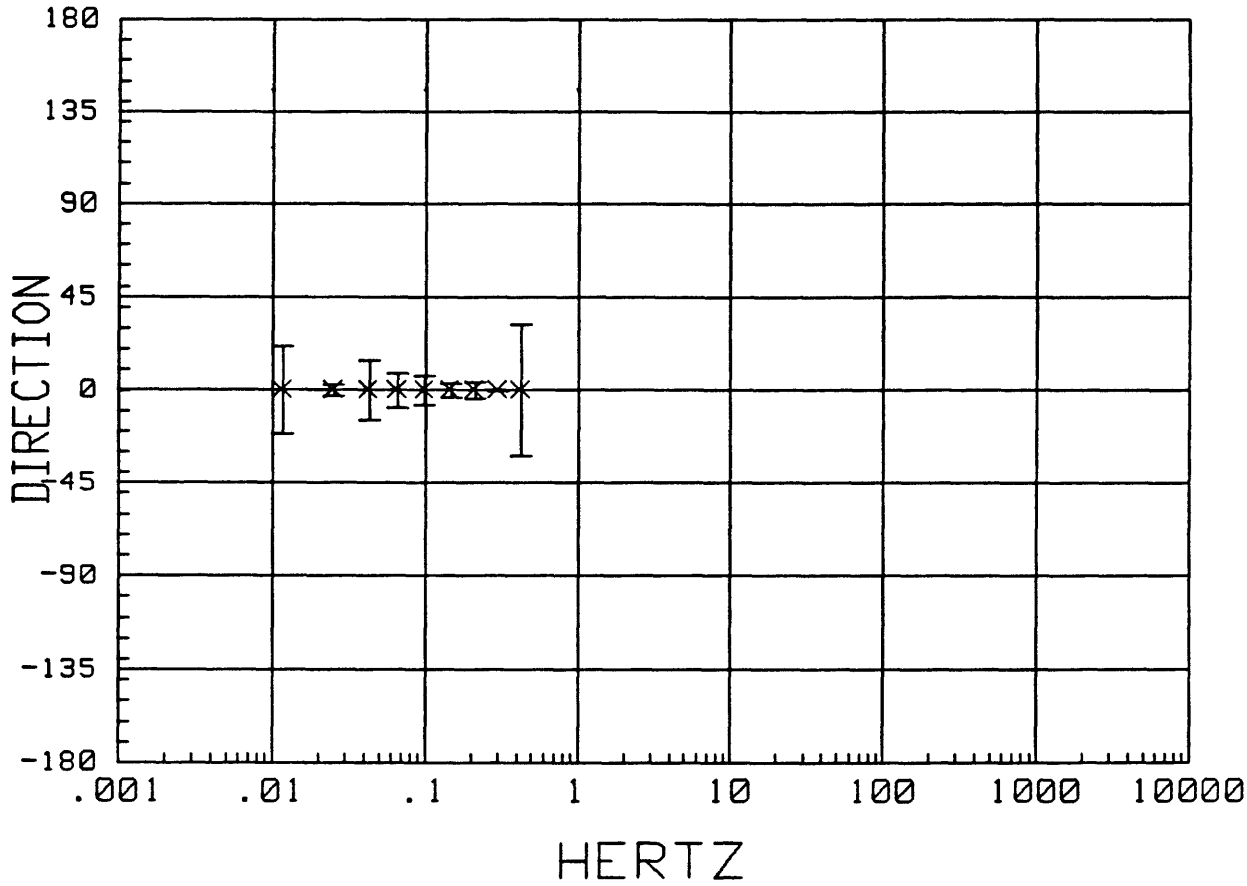

MTHO14 LOCAL H-ref 20:52:57 7 Jul 1988
SKEW

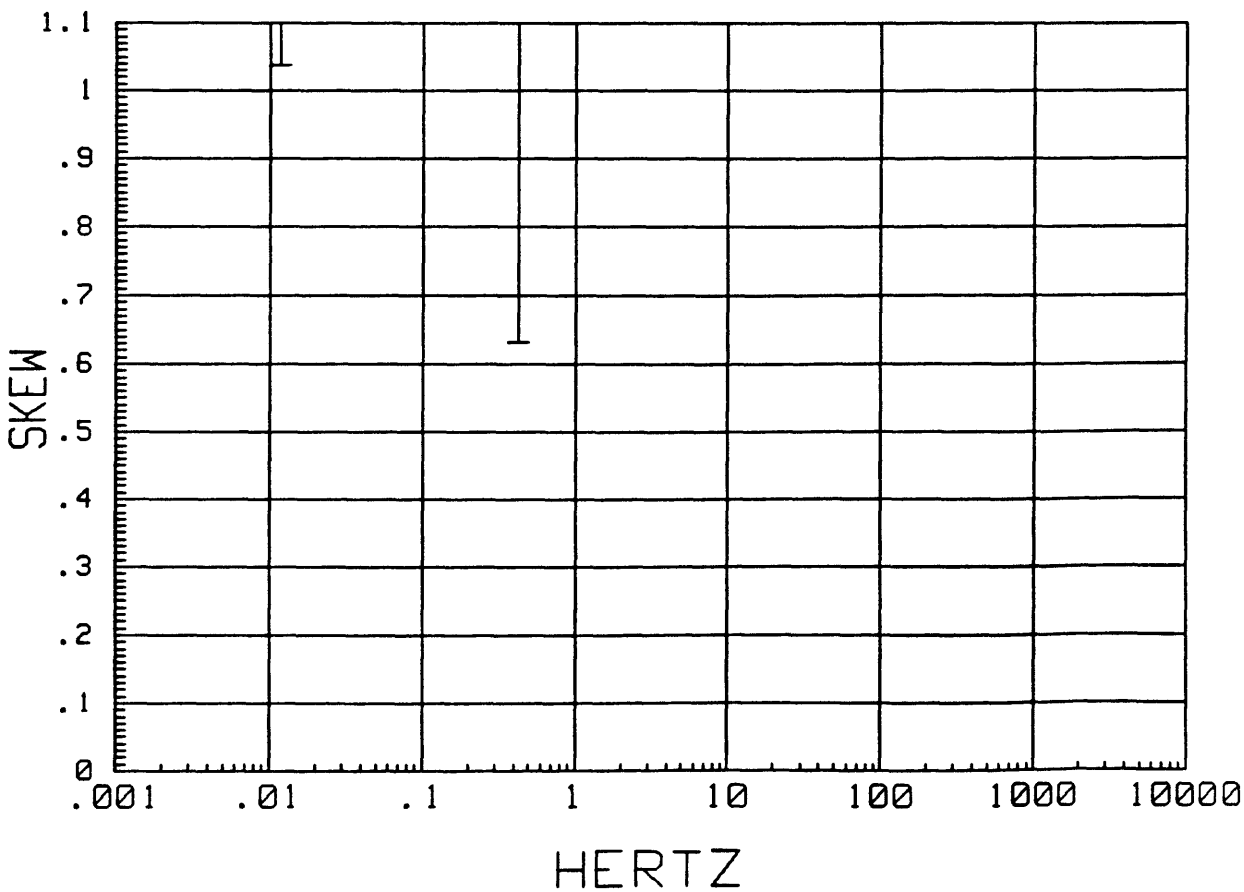

MTHO15 LOCAL H-ref 16:11:59 25 Jul 1988
APPARENT RESISTIVITY

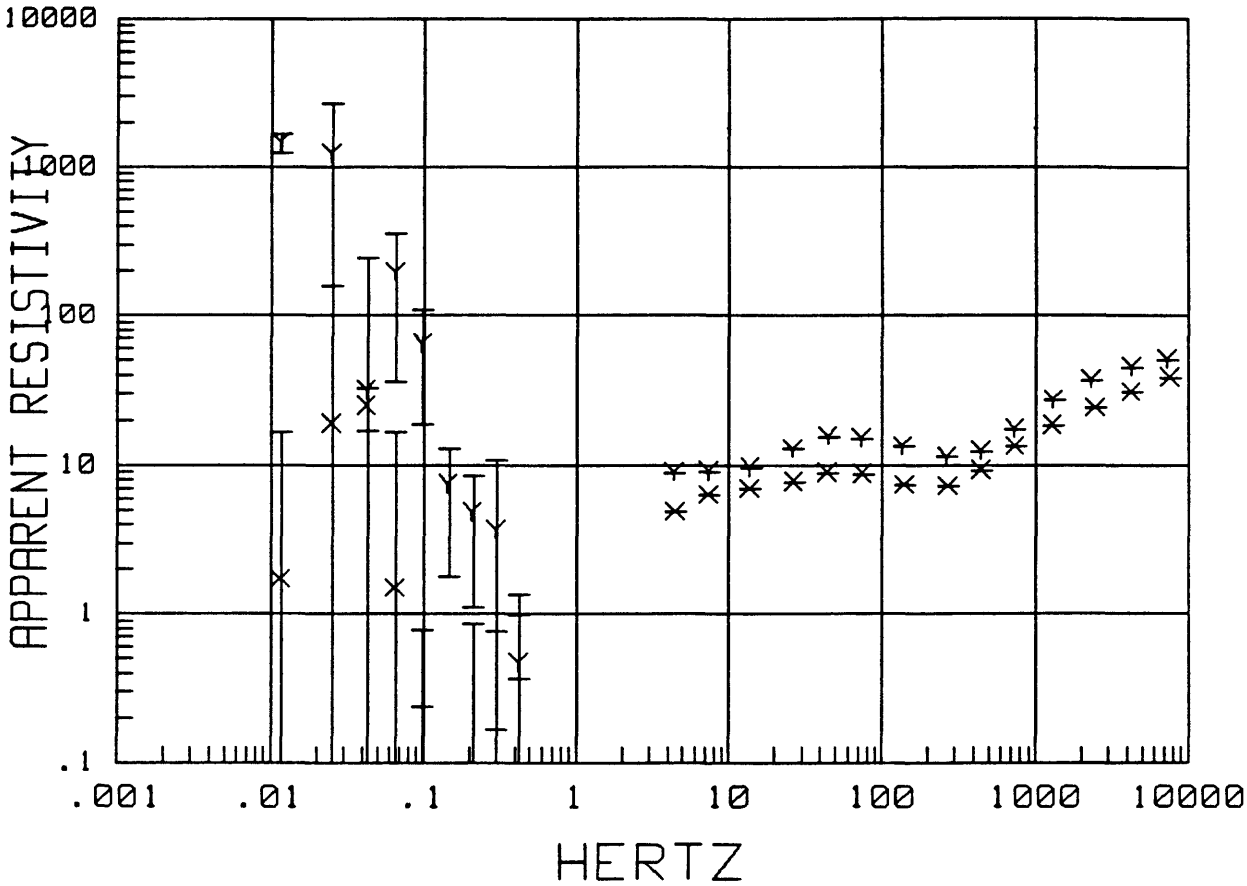

MTHO15 LOCAL H-ref 16:11:59 25 Jul 1988
IMPEDANCE PHASE

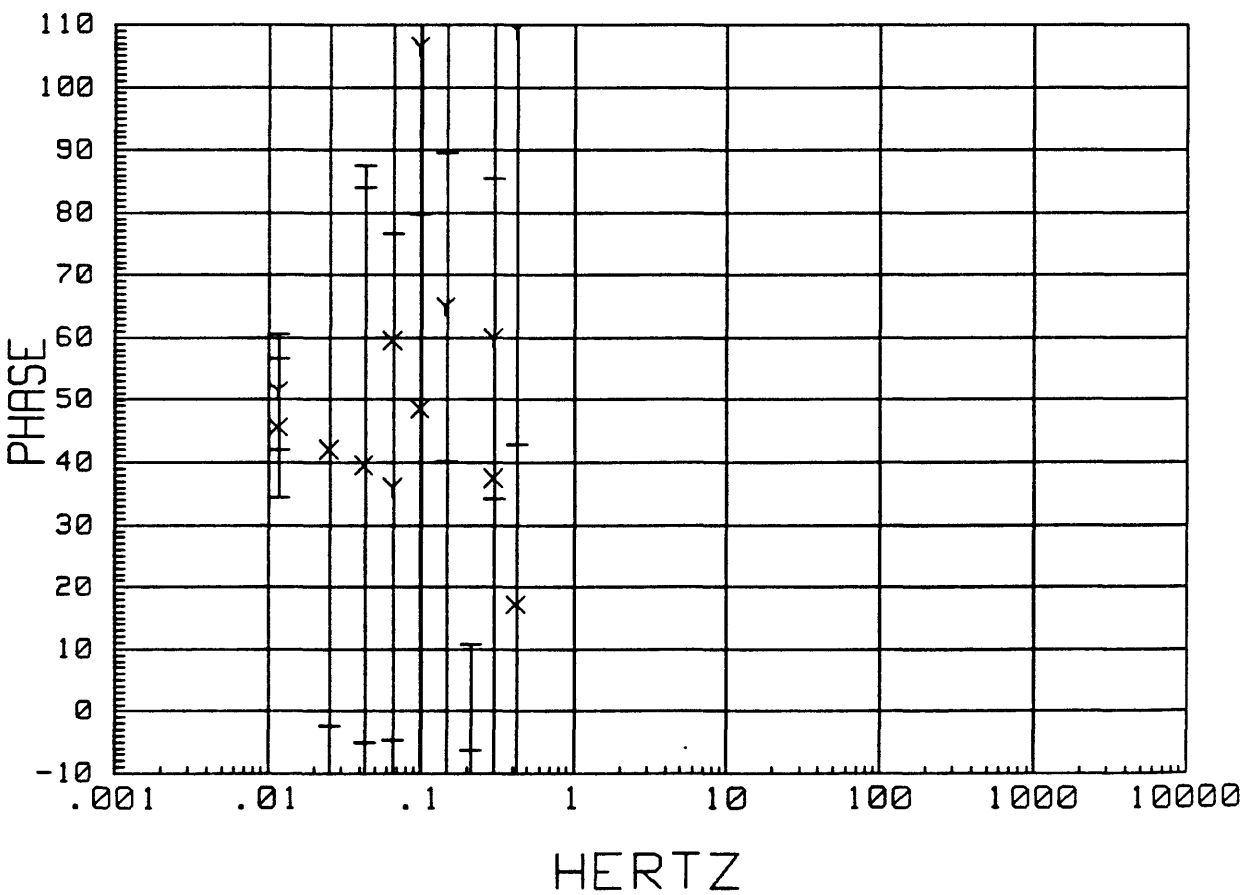

MTHO15 LOCAL H-ref 16:11:59 25 Jul 1988
Z MAXIMUM DIRECTION

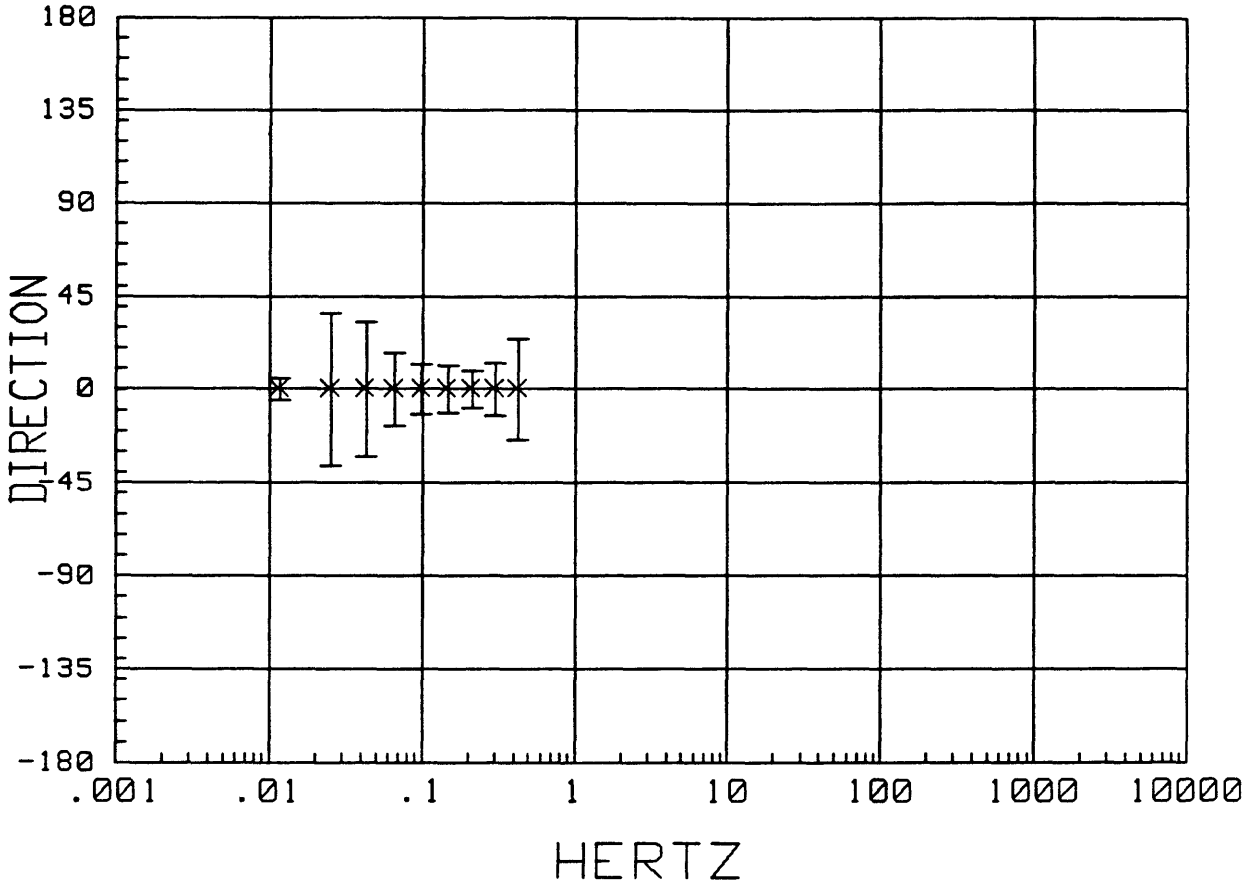

MTHO15 LOCAL H-ref 16:11:59 25 Jul 1988
SKEW

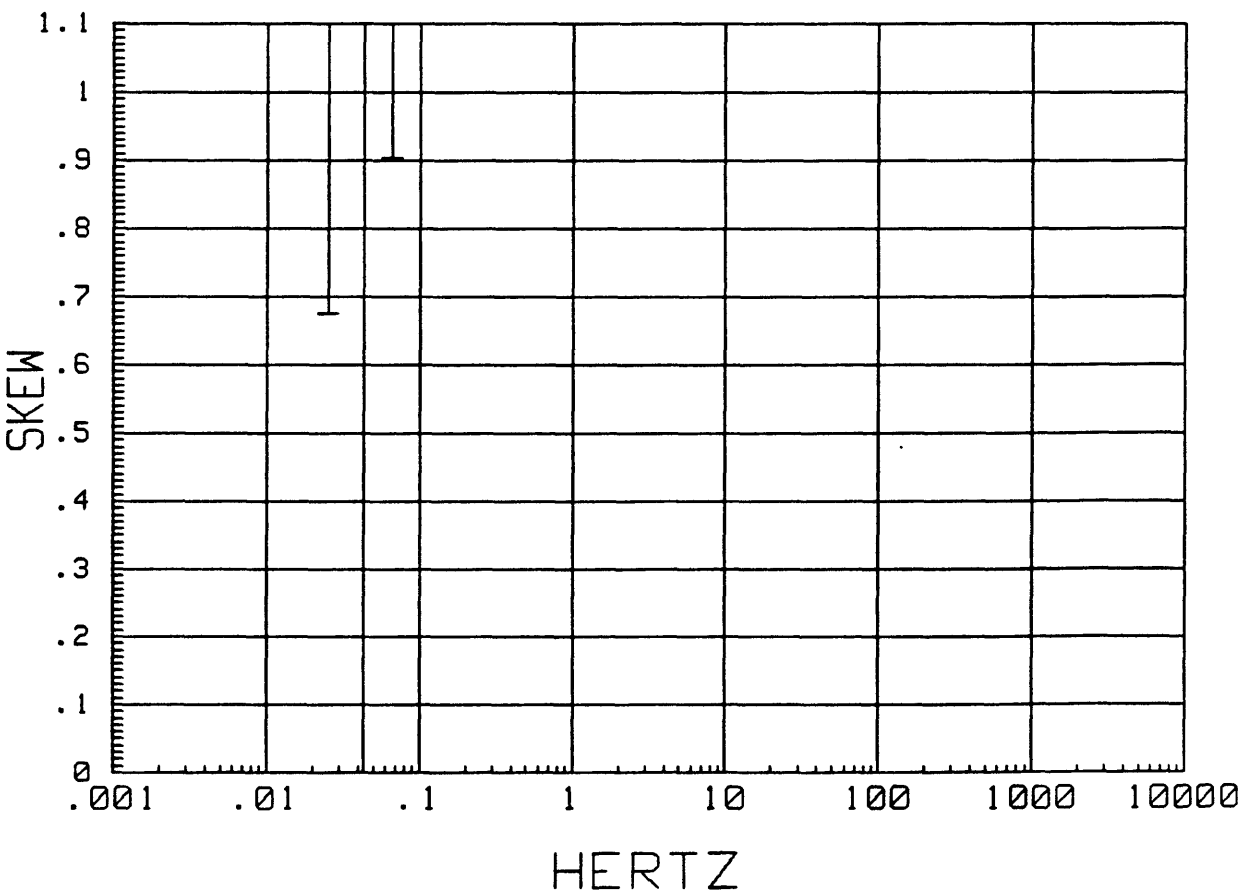

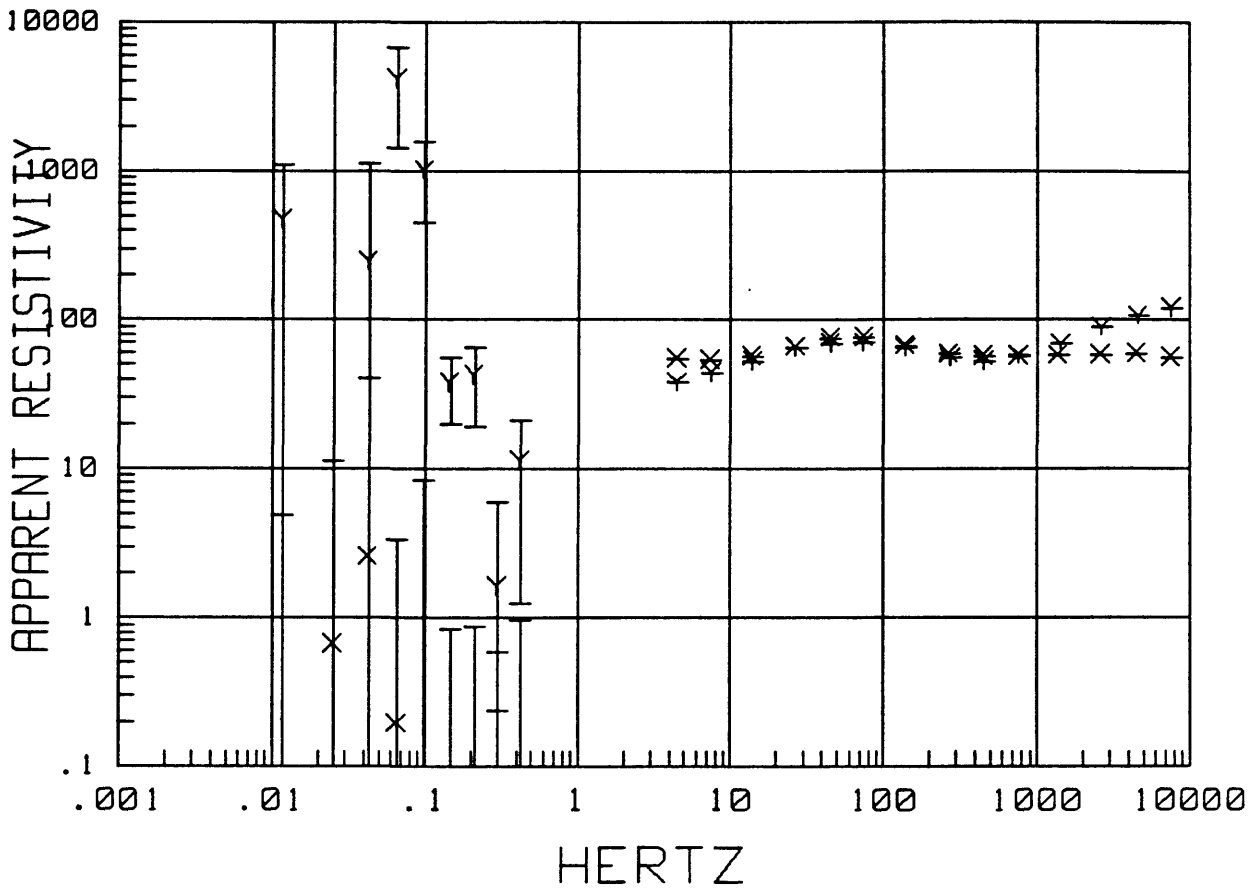
MTHO16 LOCAL H-ref 16:22:01 25 Jul 1988
APPARENT RESISTIVITY
10000
1000
100
10
1
.1
APPARENT RESISTIVITY
.001
.01
.1
1
10
100
1000
10000
HERTZ

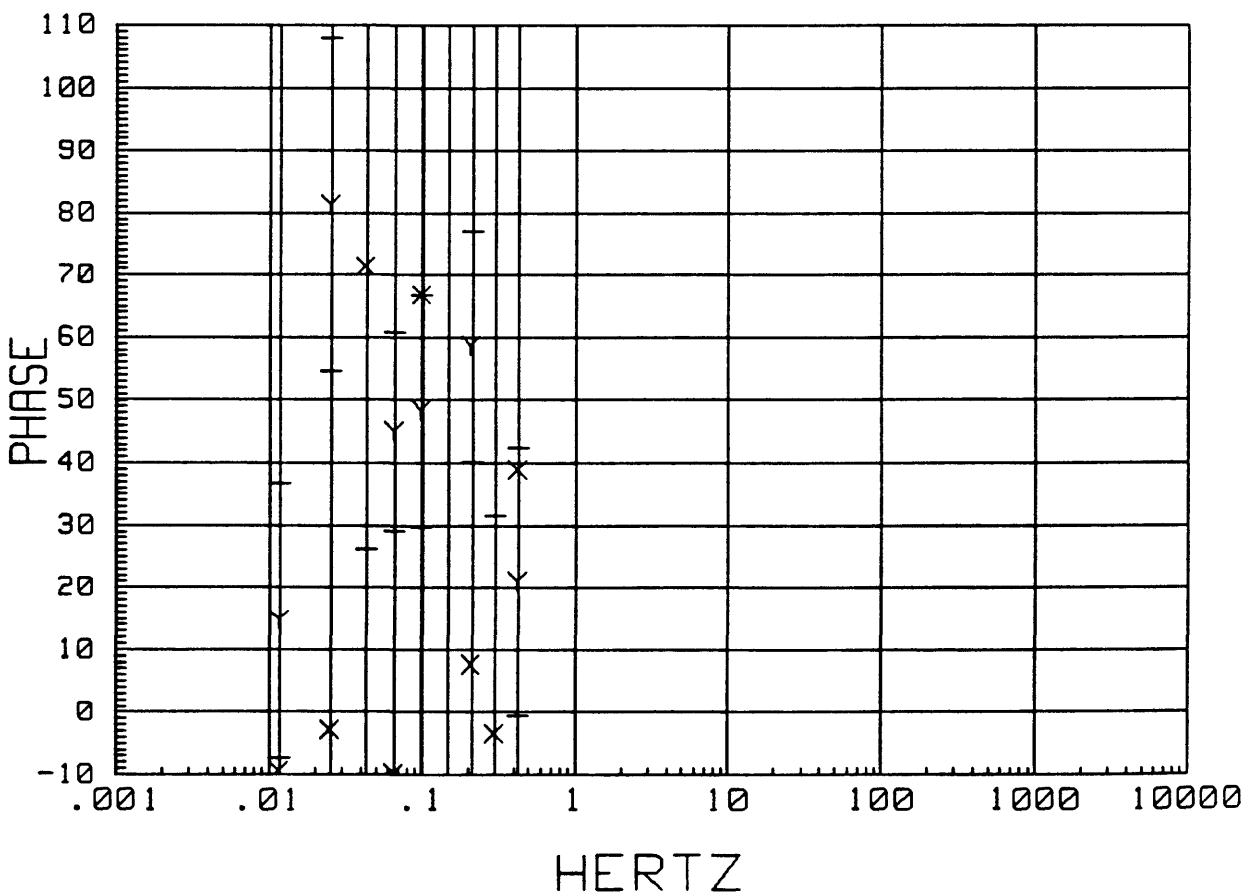
MTHO16 LOCAL H-ref 16:22:01 25 Jul 1988
IMPEDANCE PHASE
110
100
90
80
70
60
50
40
30
20
10
0
-10
PHASE
.001
.01
.1
1
10
100
1000
10000
HERTZ

MTH016 LOCAL H-ref 16:22:01 25 Jul 1988
Z MAXIMUM DIRECTION

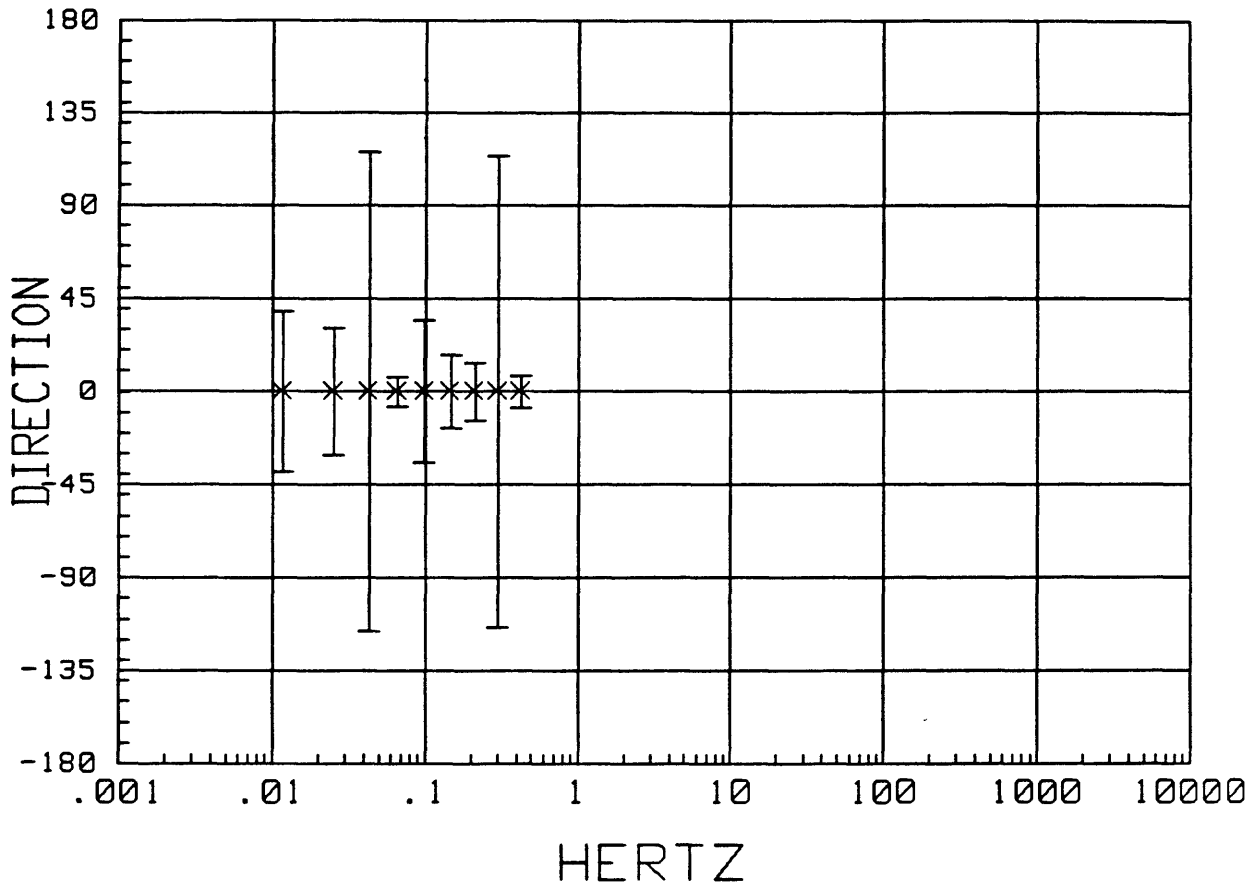

MTH016 LOCAL H-ref 16:22:01 25 Jul 1988
SKEW

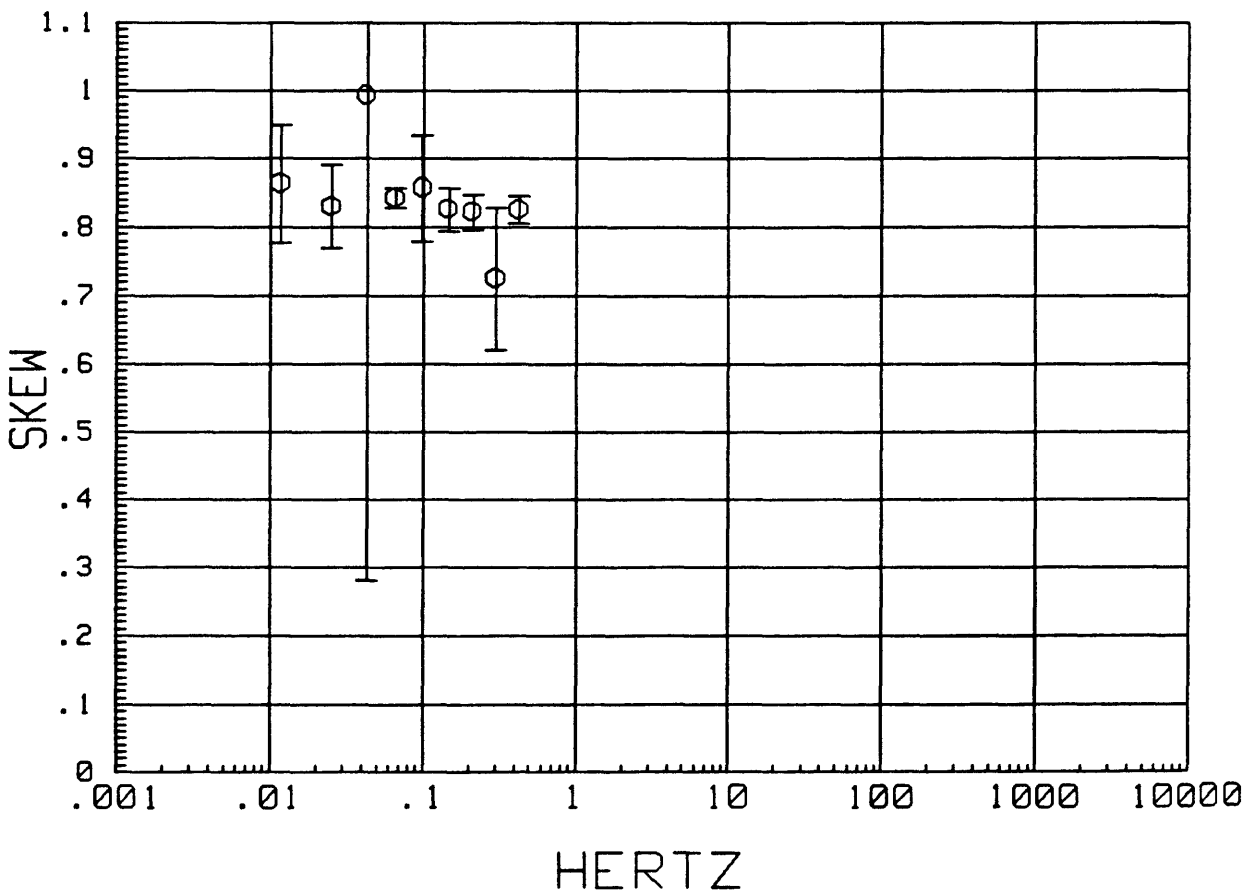

MTH017 LOCAL H-ref 16:32:25 25 Jul 1988
APPARENT RESISTIVITY

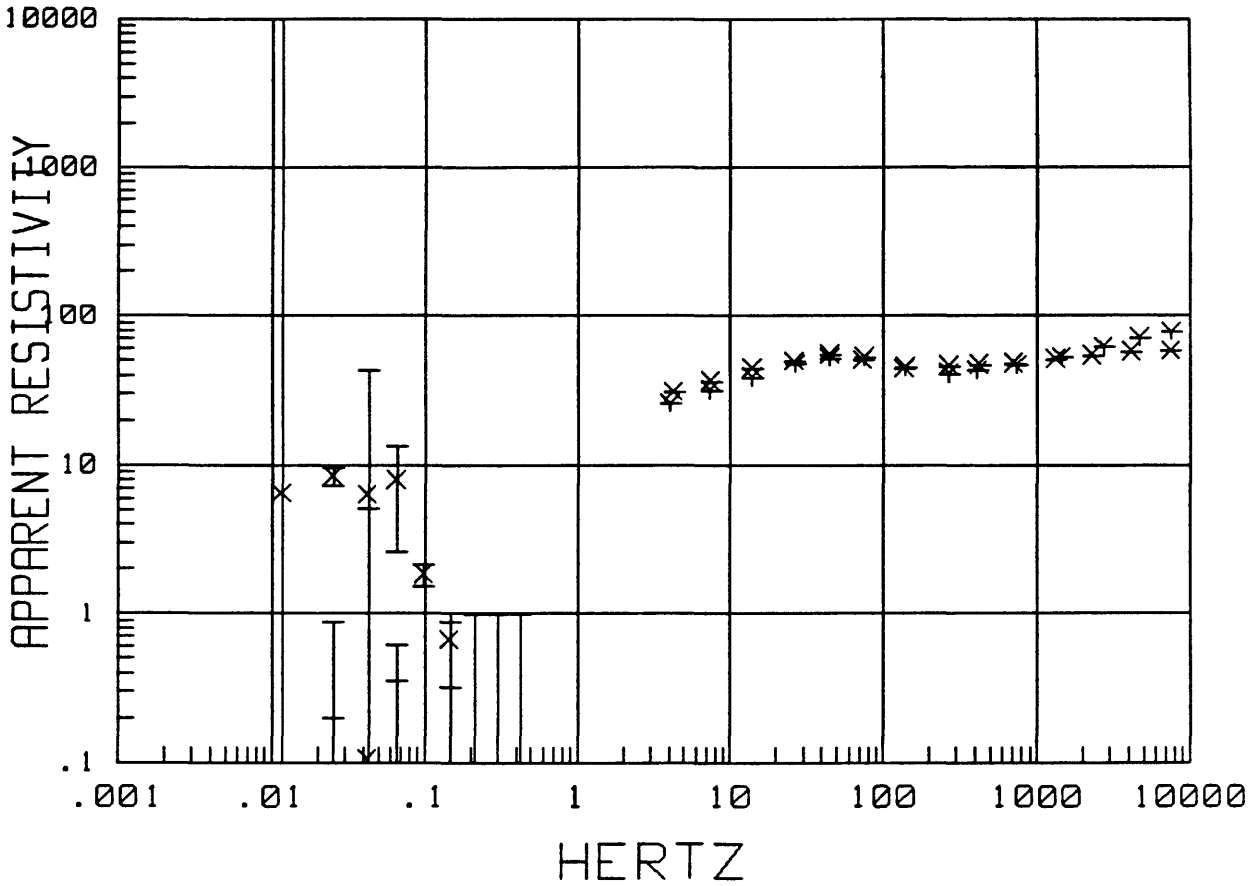

MTH017 LOCAL H-ref 16:32:25 25 Jul 1988
IMPEDANCE PHASE

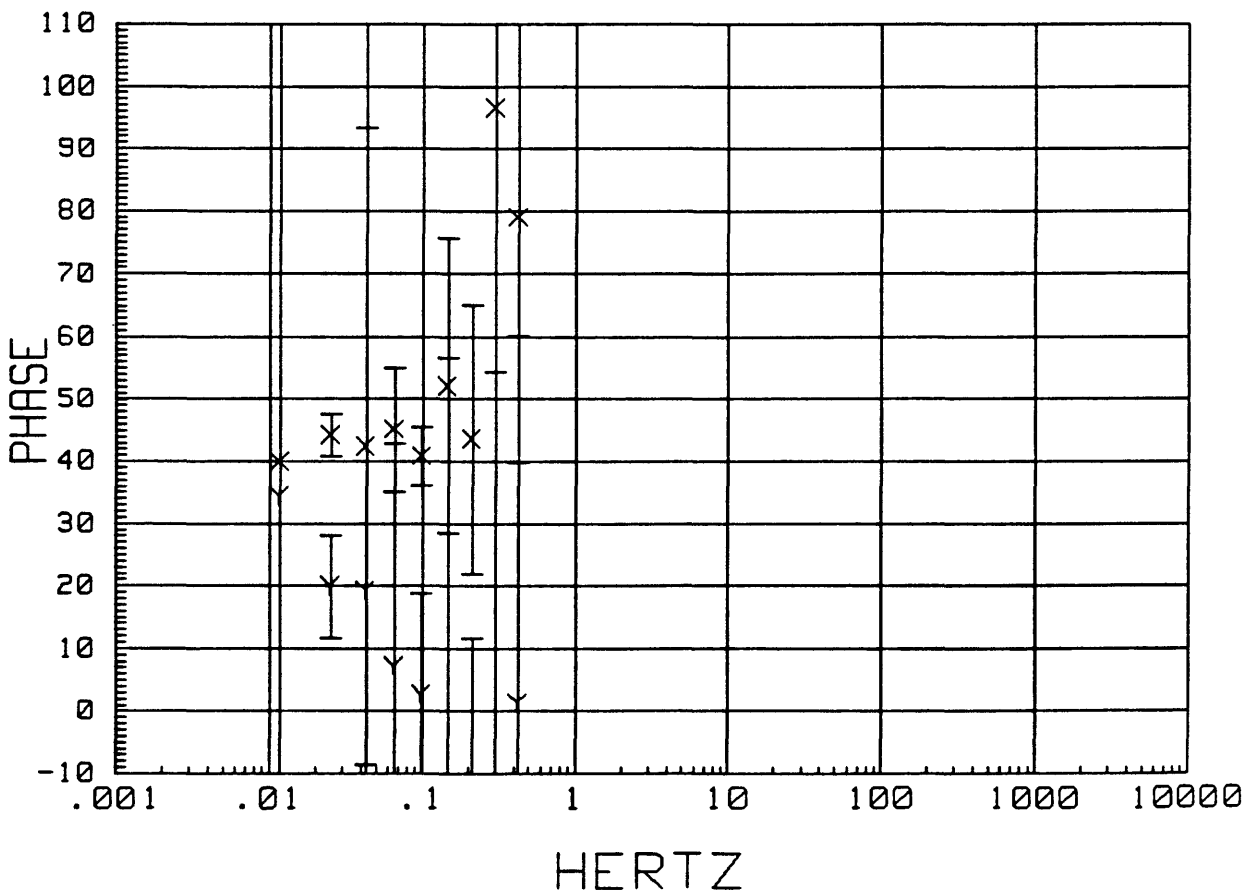

MTHO17 LOCAL H-ref 16:32:25 25 Jul 1988
Z MAXIMUM DIRECTION

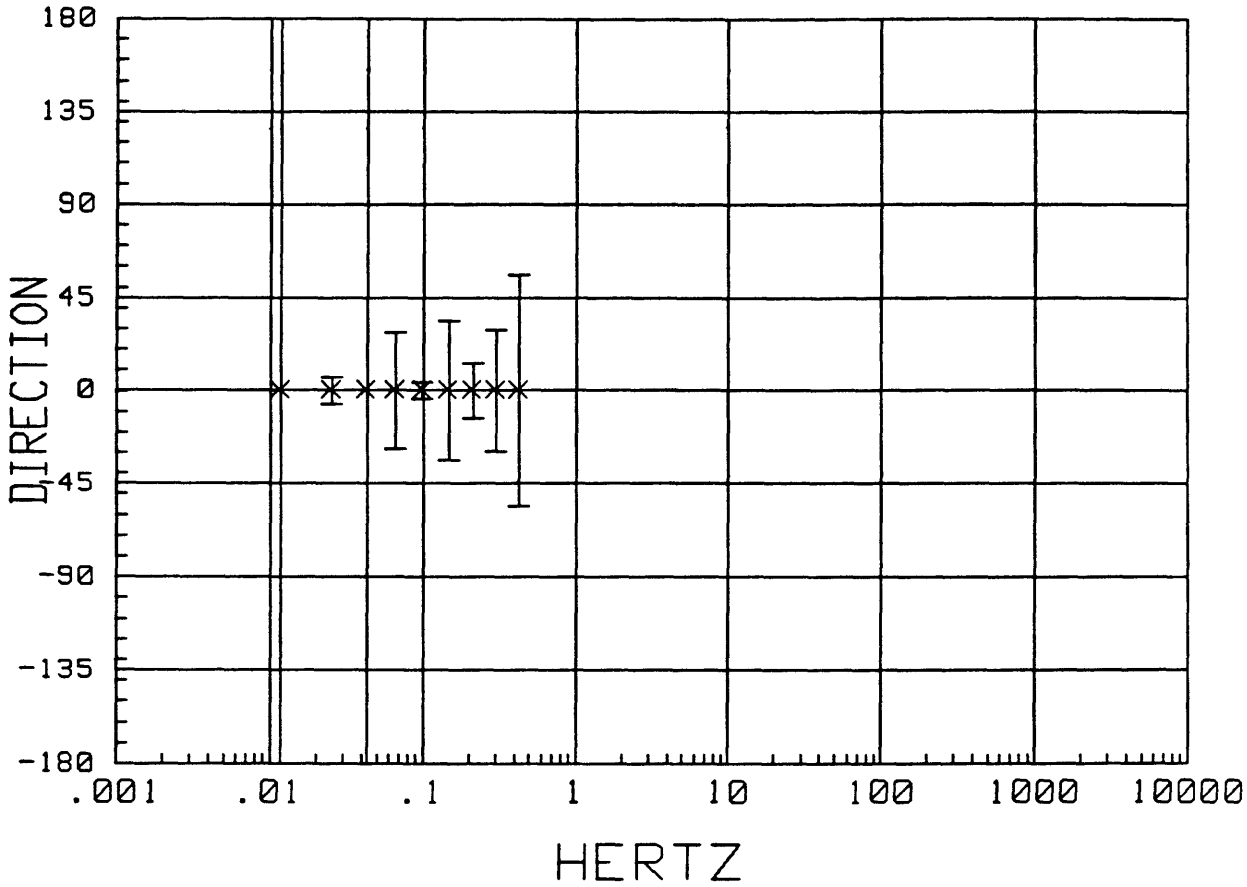

MTHO17 LOCAL H-ref 16:32:25 25 Jul 1988
SKEW

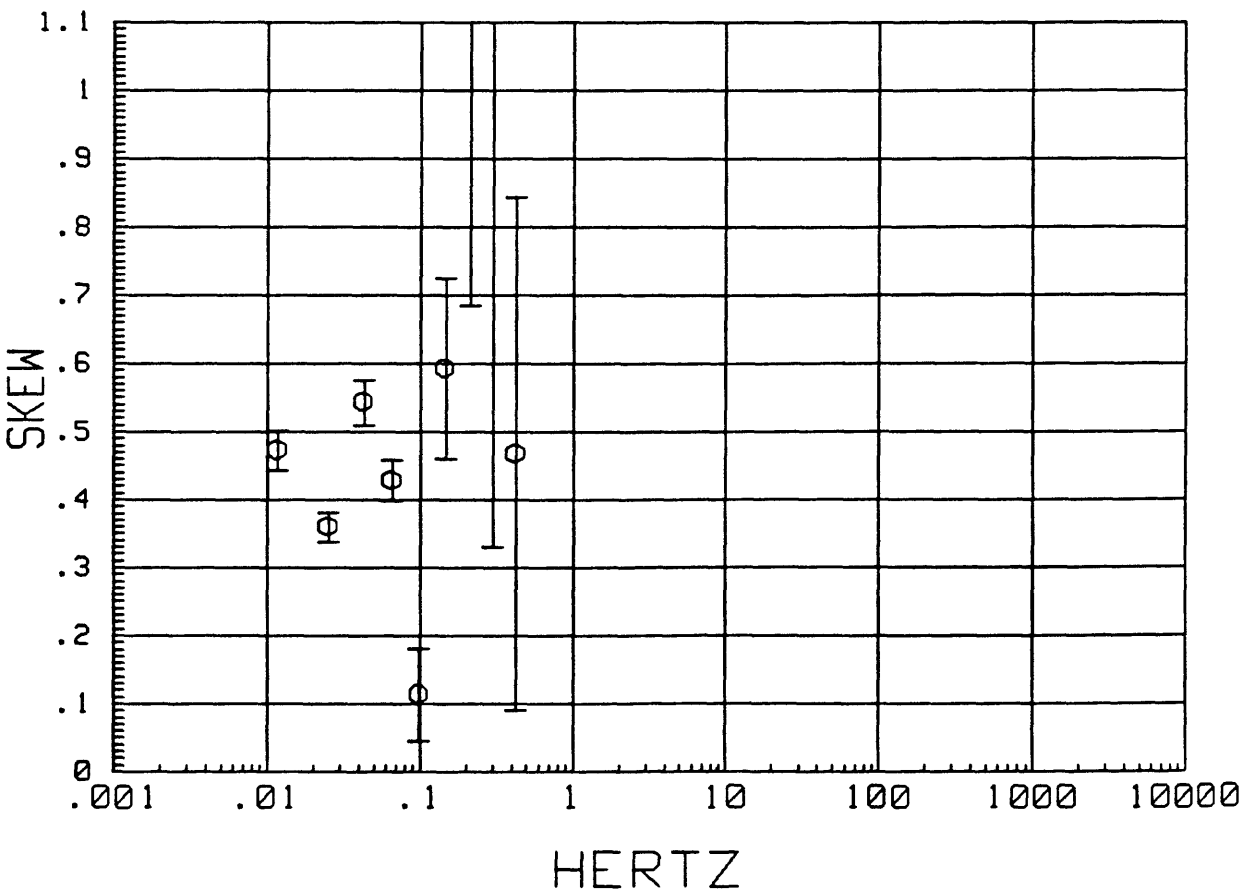

Appendix 3

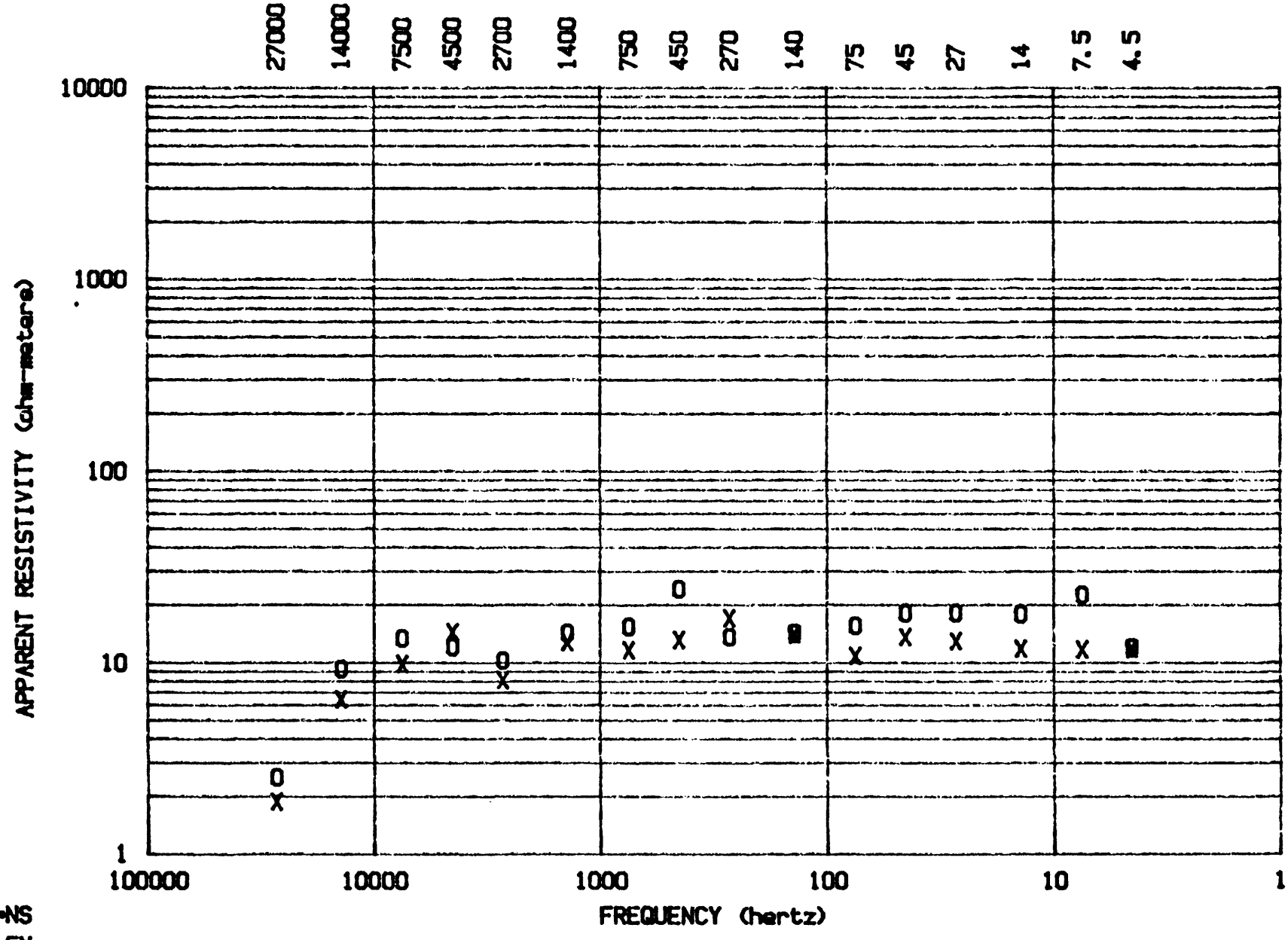
27000
14000
7500
4500
2700
1400
750
450
270
140
75
45
27
14
7.5
4.5
10000
1000
100
10
1
APPARENT RESISTIVITY (ohm-meters)
100000
10000
1000
100
10
1
FREQUENCY (hertz)
O=NS
X=EW
STA# AH001
PROJECT- HONEY LAKE

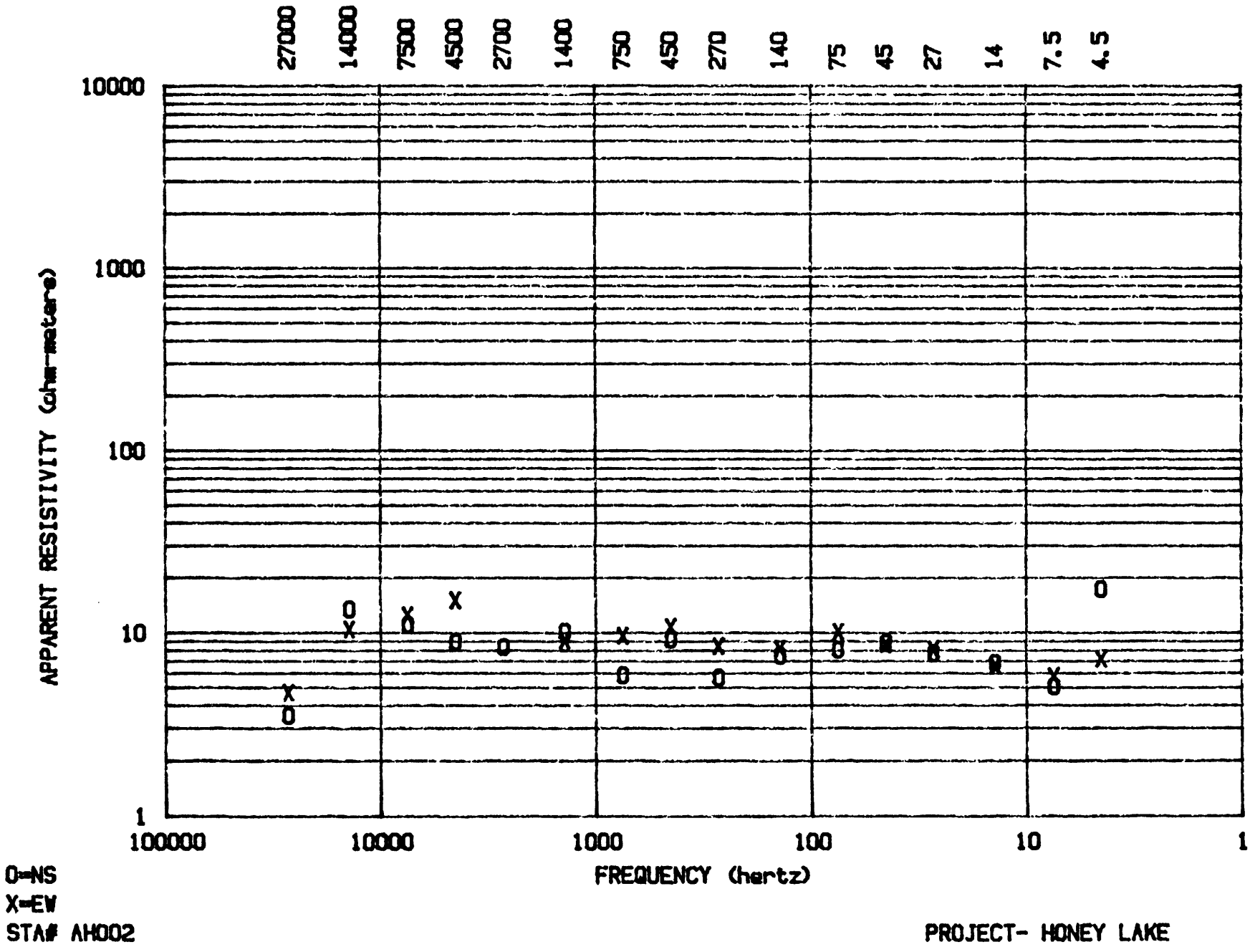
27000
14000
7500
4500
2700
1400
750
450
270
140
75
45
27
14
7.5
4.5
10000
1000
100
10
1
APPARENT RESISTIVITY (ohm-meters)
100000
10000
1000
100
10
1
FREQUENCY (hertz)
O=NS
X=EW
STA# AH002
PROJECT- HONEY LAKE

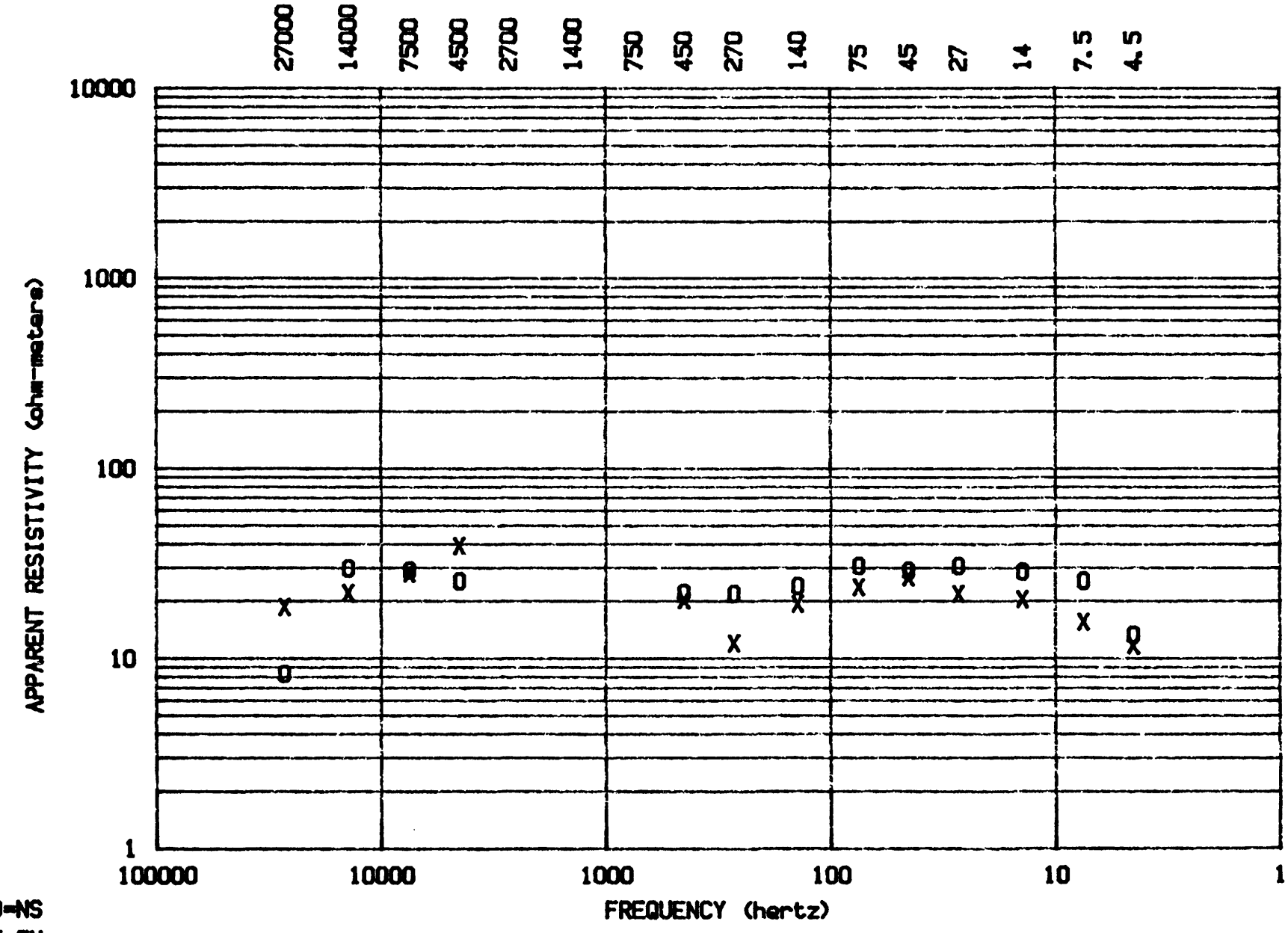
27000
14000
7500
4500
2700
1400
750
450
270
140
75
45
27
14
7.5
4.5
10000
1000
100
10
1
APPARENT RESISTIVITY (ohm-meters)
100000
10000
1000
100
10
1
FREQUENCY (hertz)
O=NS
X=EW
STA# AH003
PROJECT- HONEY LAKE

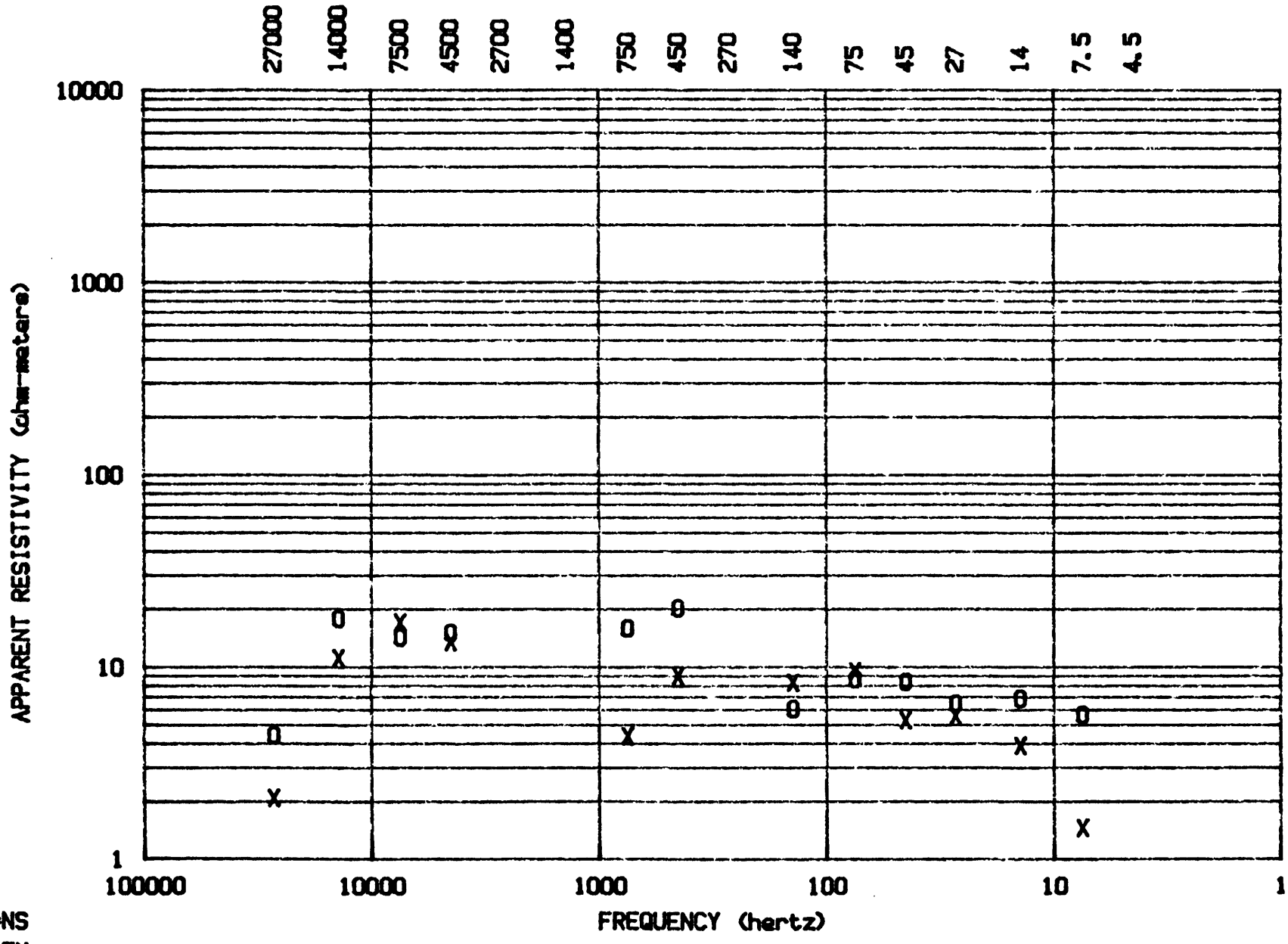
27000
14000
7500
4500
2700
1400
750
450
270
140
75
45
27
14
7.5
4.5
10000
1000
100
10
1
APPARENT RESISTIVITY (ohm-meters)
100000
10000
1000
100
10
1
FREQUENCY (hertz)
O=NS
X=EW
STA# AH004
PROJECT- HONEY LAKE

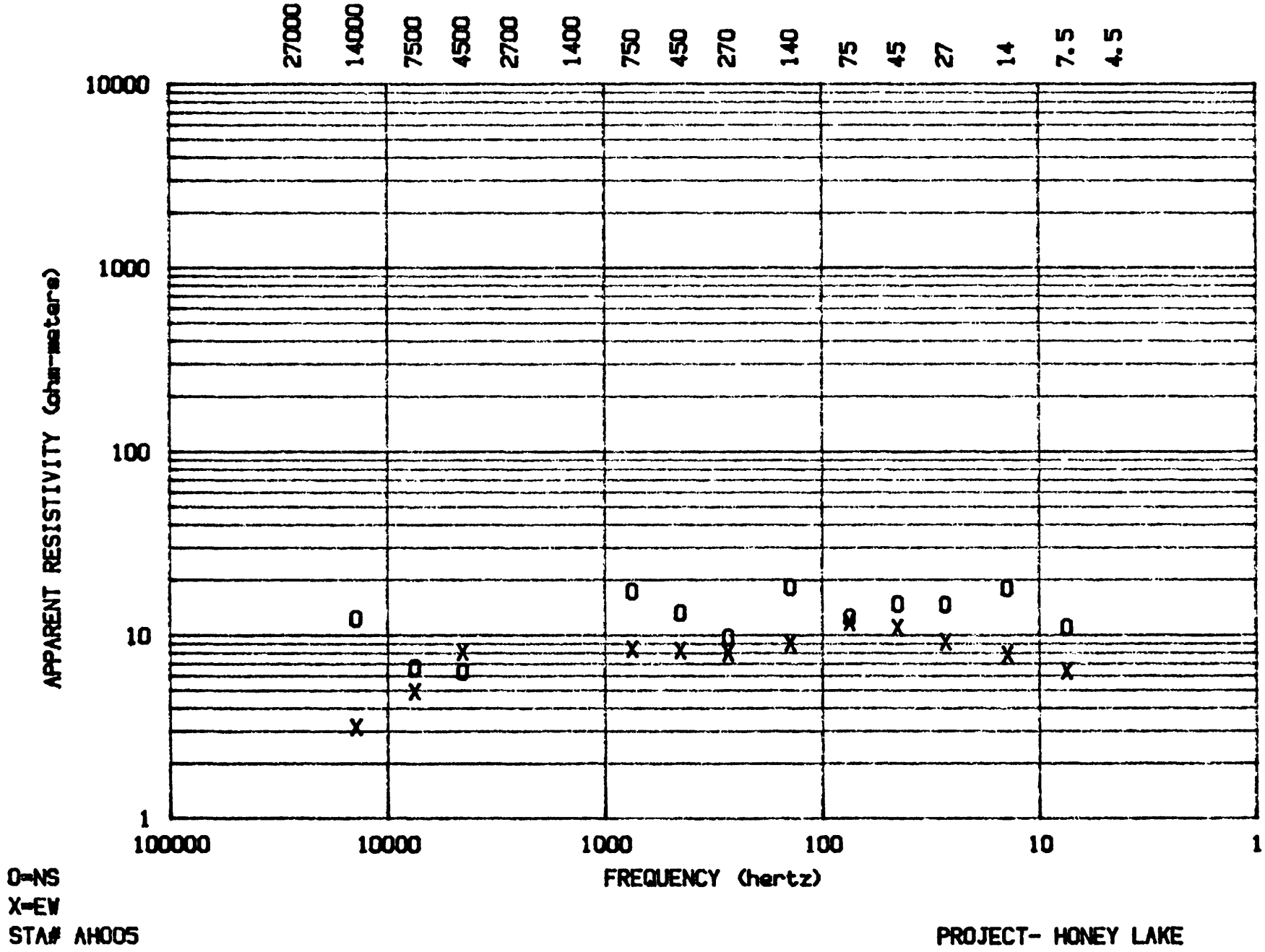
27000
14000
7500
4500
2700
1400
750
450
270
140
75
45
27
14
7.5
4.5
10000
1000
100
10
1
APPARENT RESISTIVITY (ohm-meters)
100000
10000
1000
100
10
1
FREQUENCY (hertz)
O=NS
X=EW
STA# AH005
PROJECT- HONEY LAKE

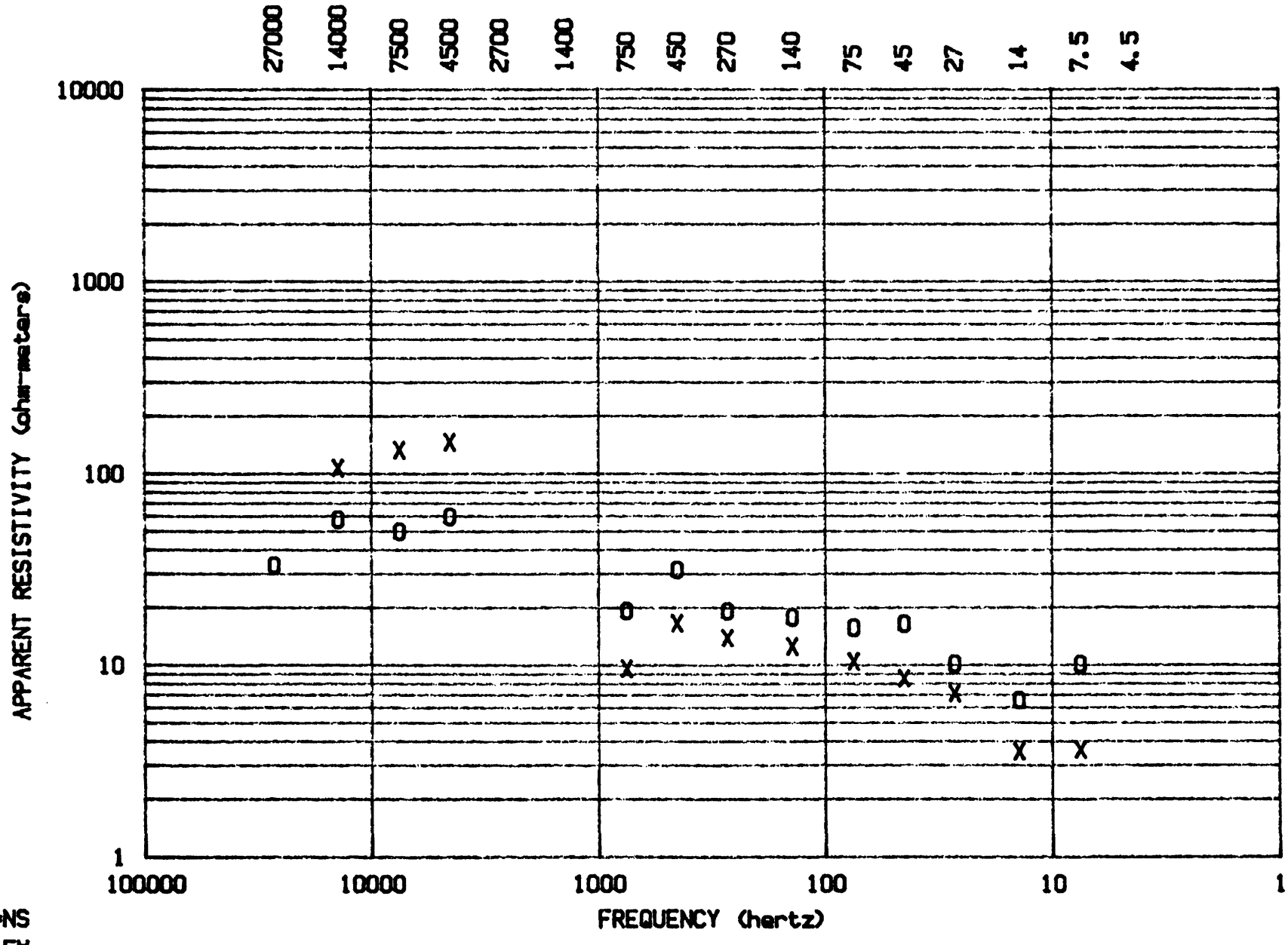

O=NS
X=EW
STA# AH006

PROJECT- HONEY LAKE

PROJECT- HONEY LAKE
STA# AH007
O=NS
X=EW
APPARENT RESISTIVITY (ohm-meters)
10000
1000
100
10
1
FREQUENCY (hertz)
1
10
100
1000
10000
100000
4.5
7.5
14
27
45
75
140
270
450
750
1400
2700
4500
7500
14000
27000

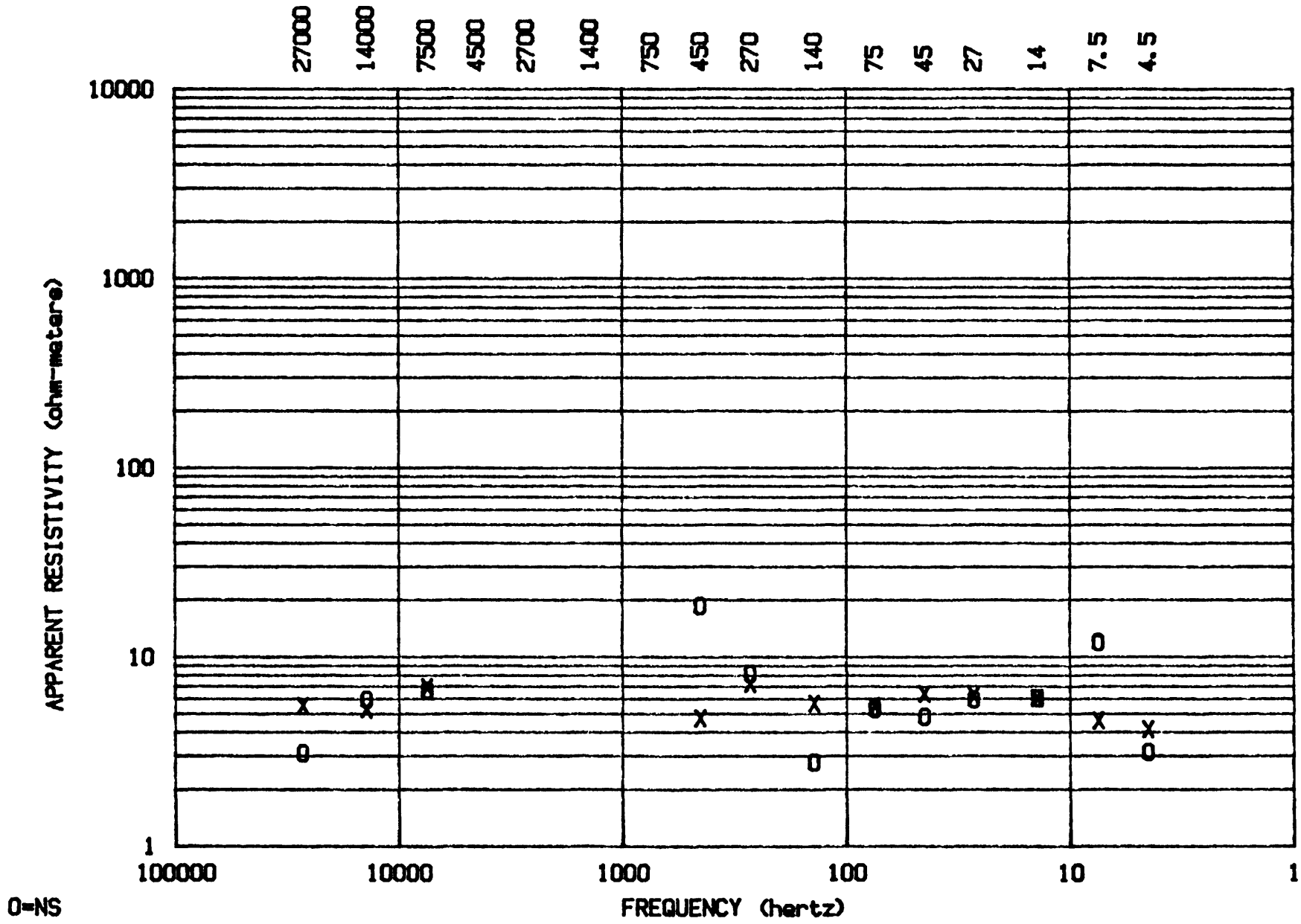
27000
14000
7500
4500
2700
1400
750
450
270
140
75
45
27
14
7.5
4.5
10000
1000
100
10
1
APPARENT RESISTIVITY (ohm-meters)
100000
10000
1000
100
10
1
FREQUENCY (hertz)
O=NS
X=EW
STA# AH008
PROJECT- HONEY LAKE

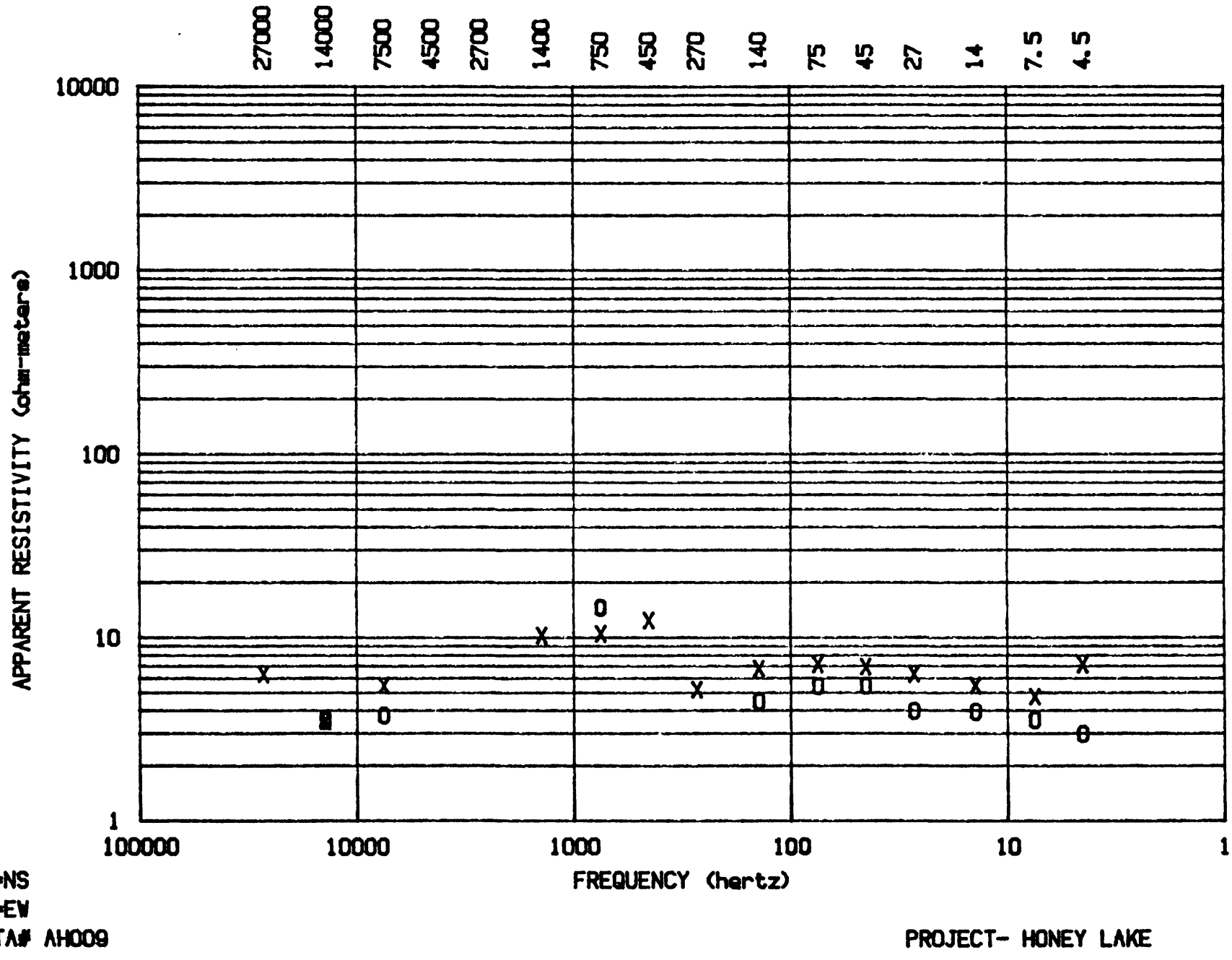
27000
14000
7500
4500
2700
1400
750
450
270
140
75
45
27
14
7.5
4.5
10000
1000
100
10
1
APPARENT RESISTIVITY (ohm-meters)
100000
10000
1000
100
10
1
FREQUENCY (hertz)
O=NS
X=EW
STA# AH009
PROJECT- HONEY LAKE

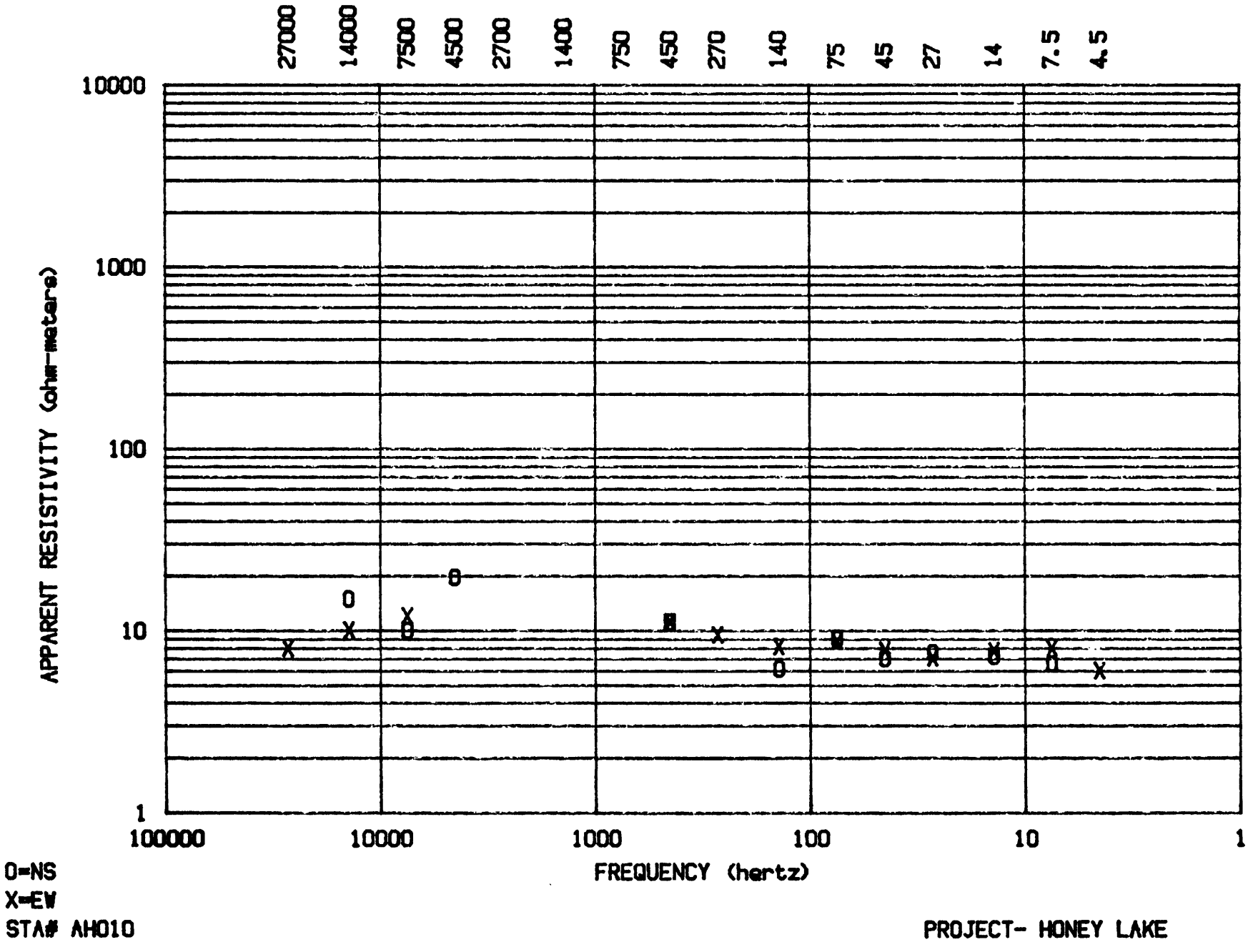
27000
14000
7500
4500
2700
1400
750
450
270
140
75
45
27
14
7.5
4.5
10000
1000
100
10
1
APPARENT RESISTIVITY (ohm-meters)
100000
10000
1000
100
10
1
FREQUENCY (hertz)
O=NS
X=EW
STA# AH010
PROJECT- HONEY LAKE

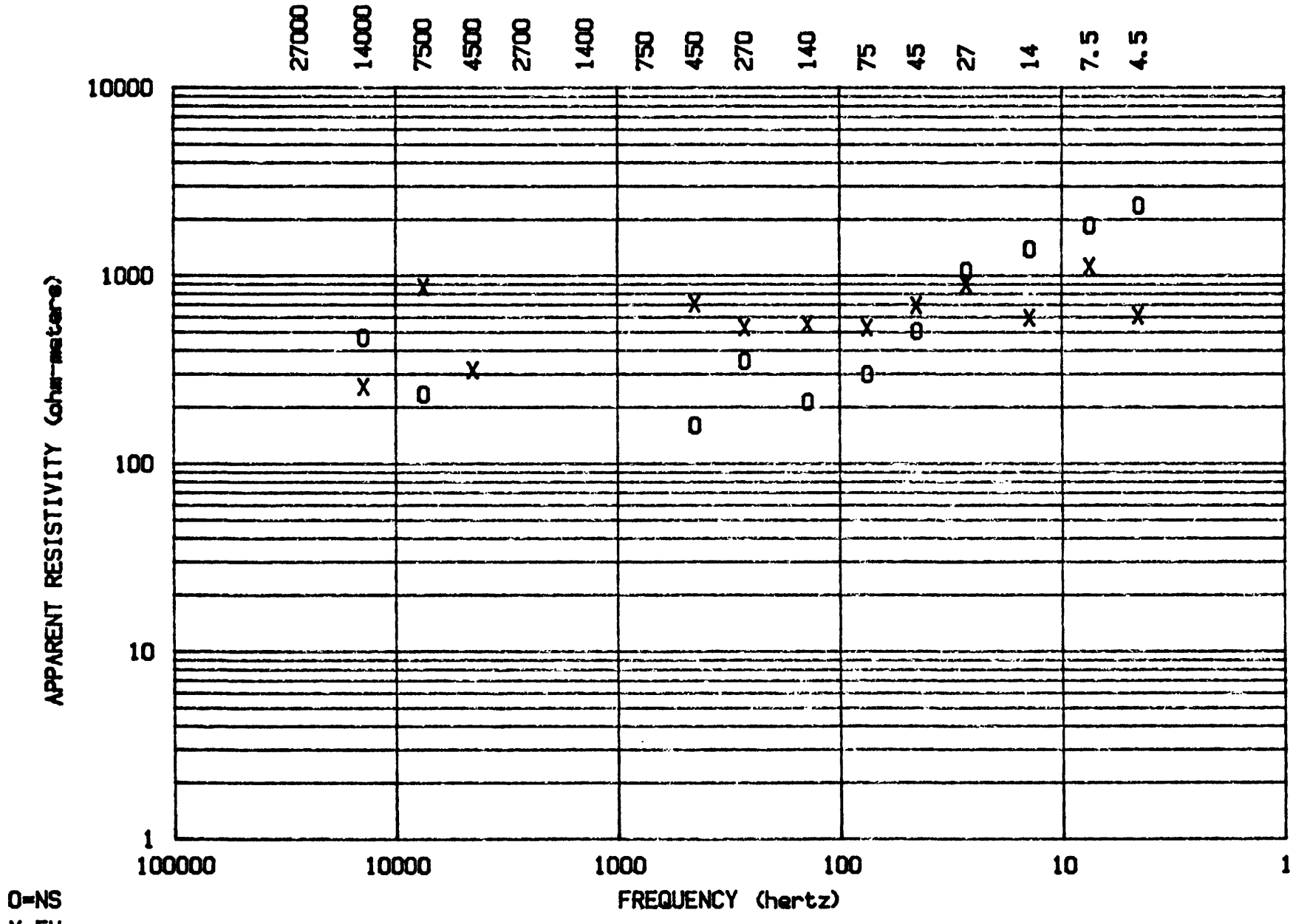
27000
14000
7500
4500
2700
1400
750
450
270
140
75
45
27
14
7.5
4.5
10000
1000
100
10
1
APPARENT RESISTIVITY (ohm-meters)
100000
10000
1000
100
10
1
FREQUENCY (hertz)
O=NS
X=EW
STA# AH011
PROJECT- HONEY LAKE

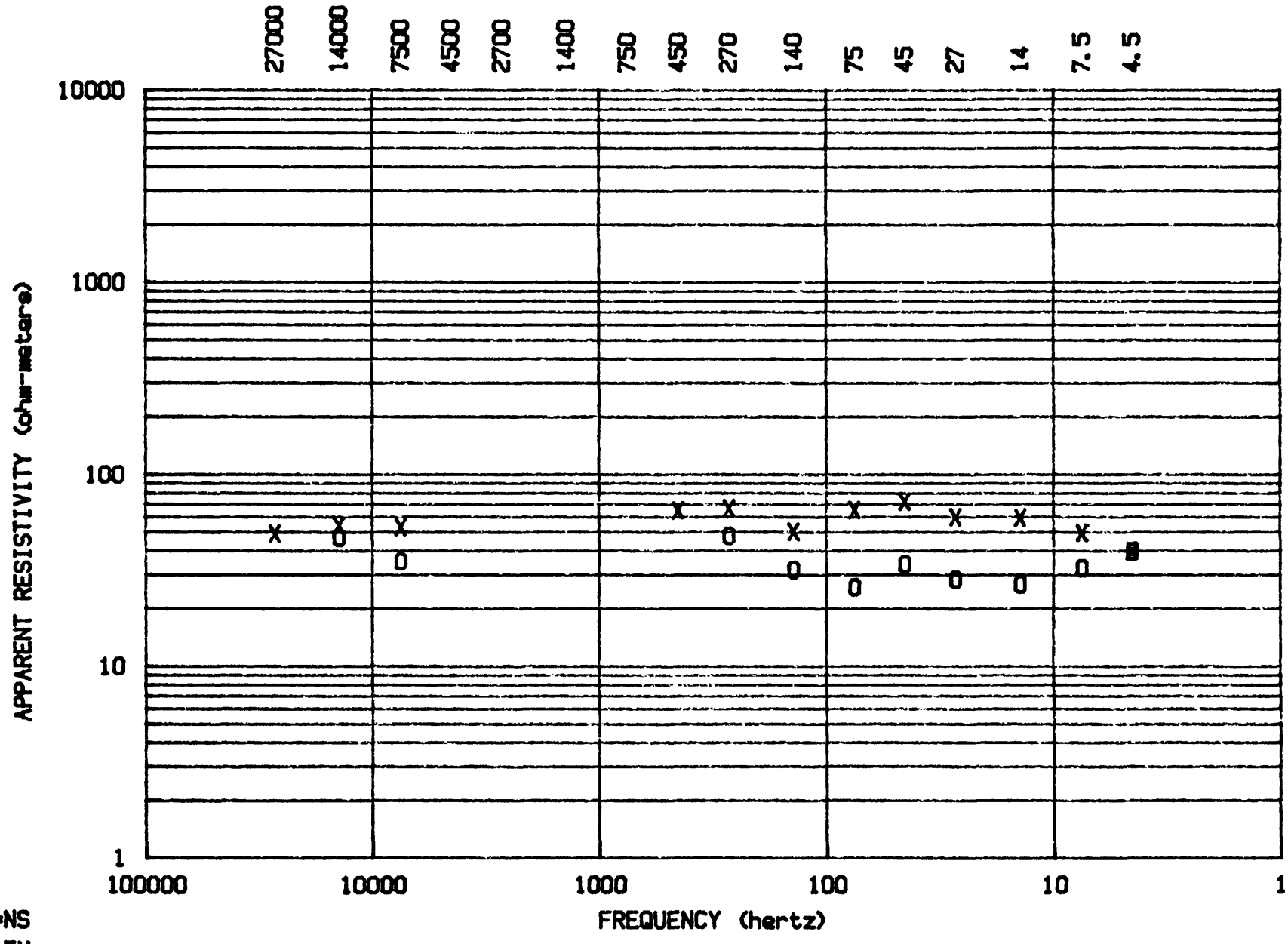

O=NS
X=EW
STA# AH012

PROJECT- HONEY LAKE

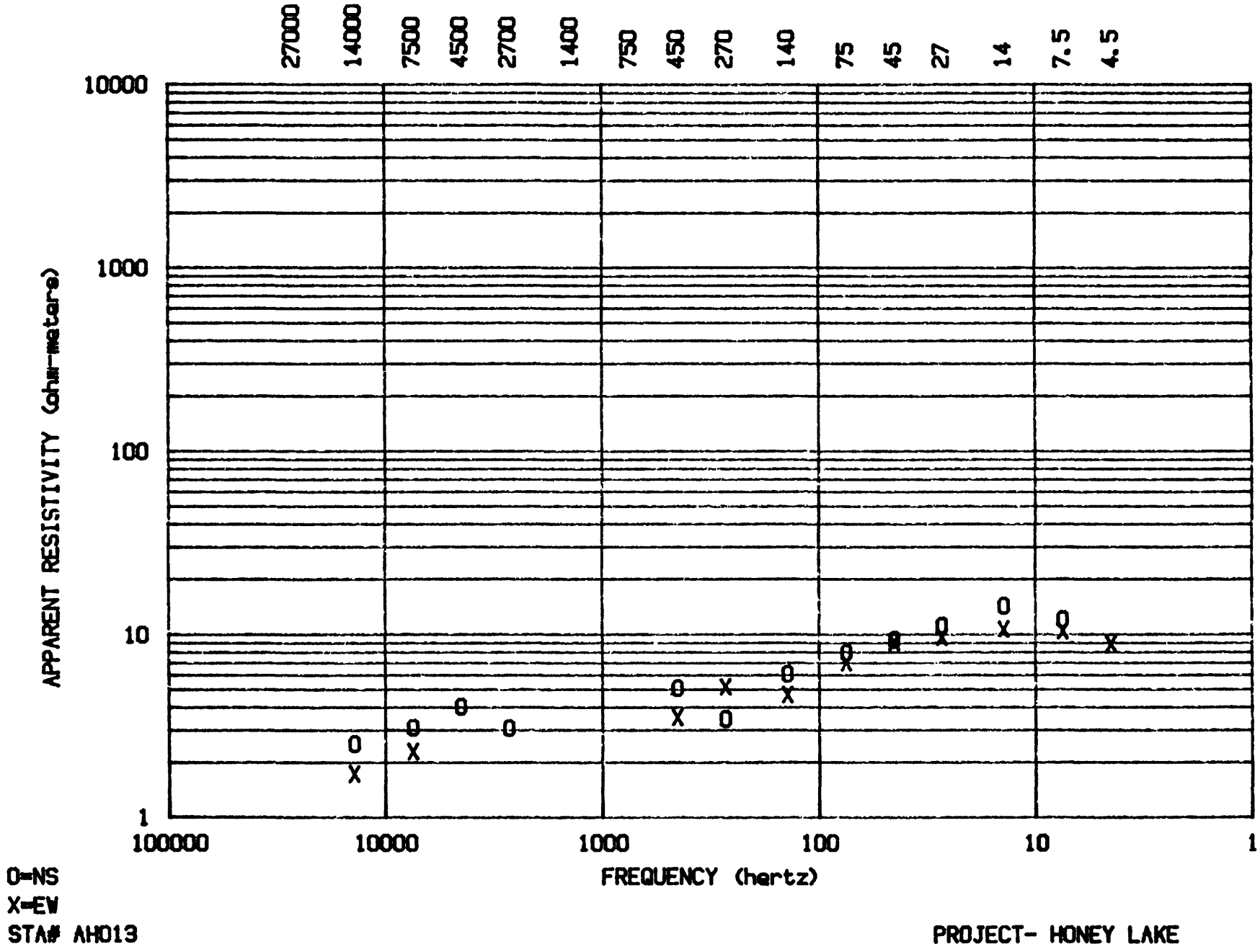
27000
14000
7500
4500
2700
1400
750
450
270
140
75
45
27
14
7.5
4.5
10000
1000
100
10
1
APPARENT RESISTIVITY (ohm-meters)
100000
10000
1000
100
10
1
FREQUENCY (hertz)
O=NS
X=EW
STA# AH013
PROJECT- HONEY LAKE

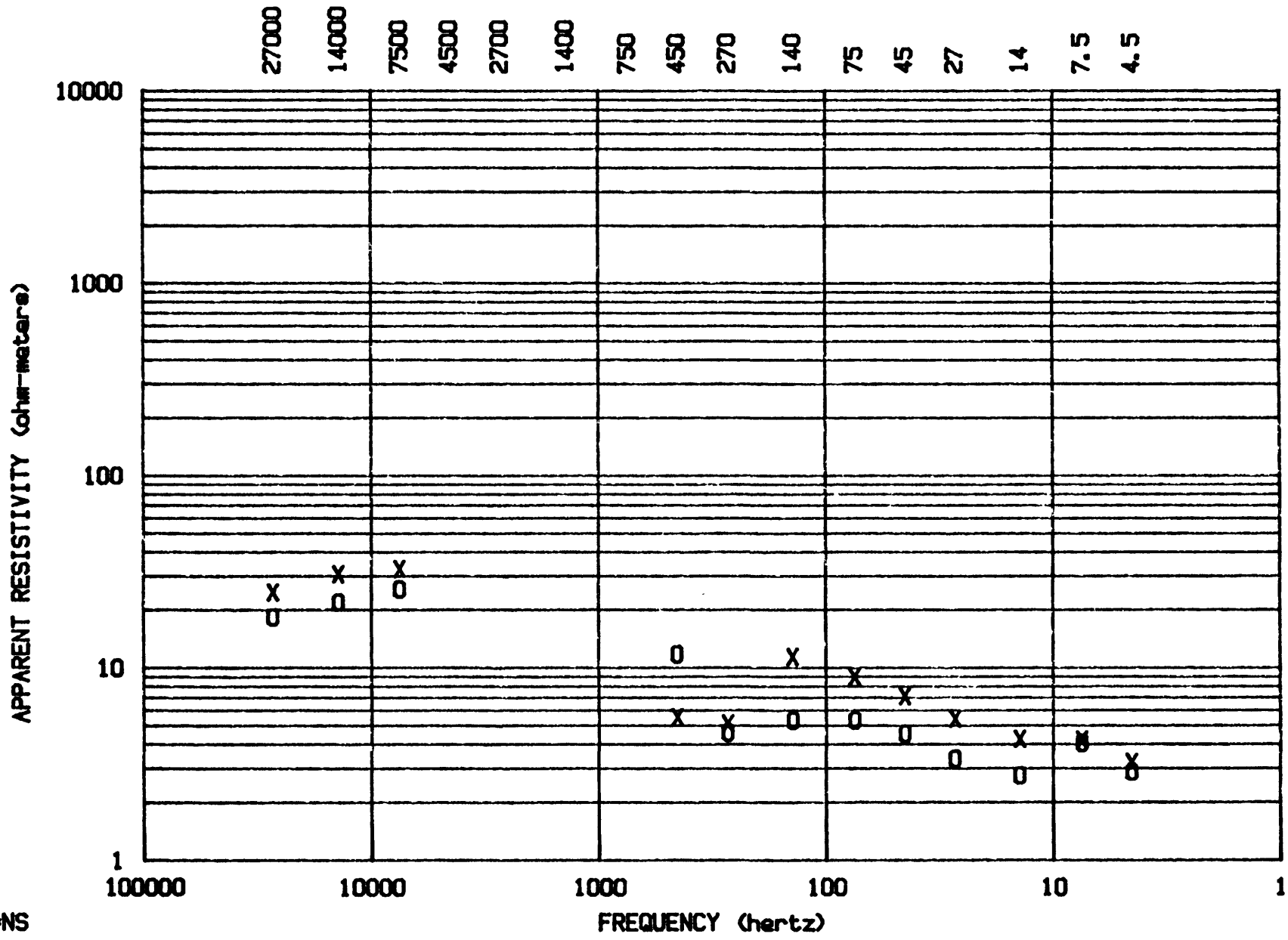

O=NS
X=EW
STA# AH014

PROJECT- HONEY LAKE

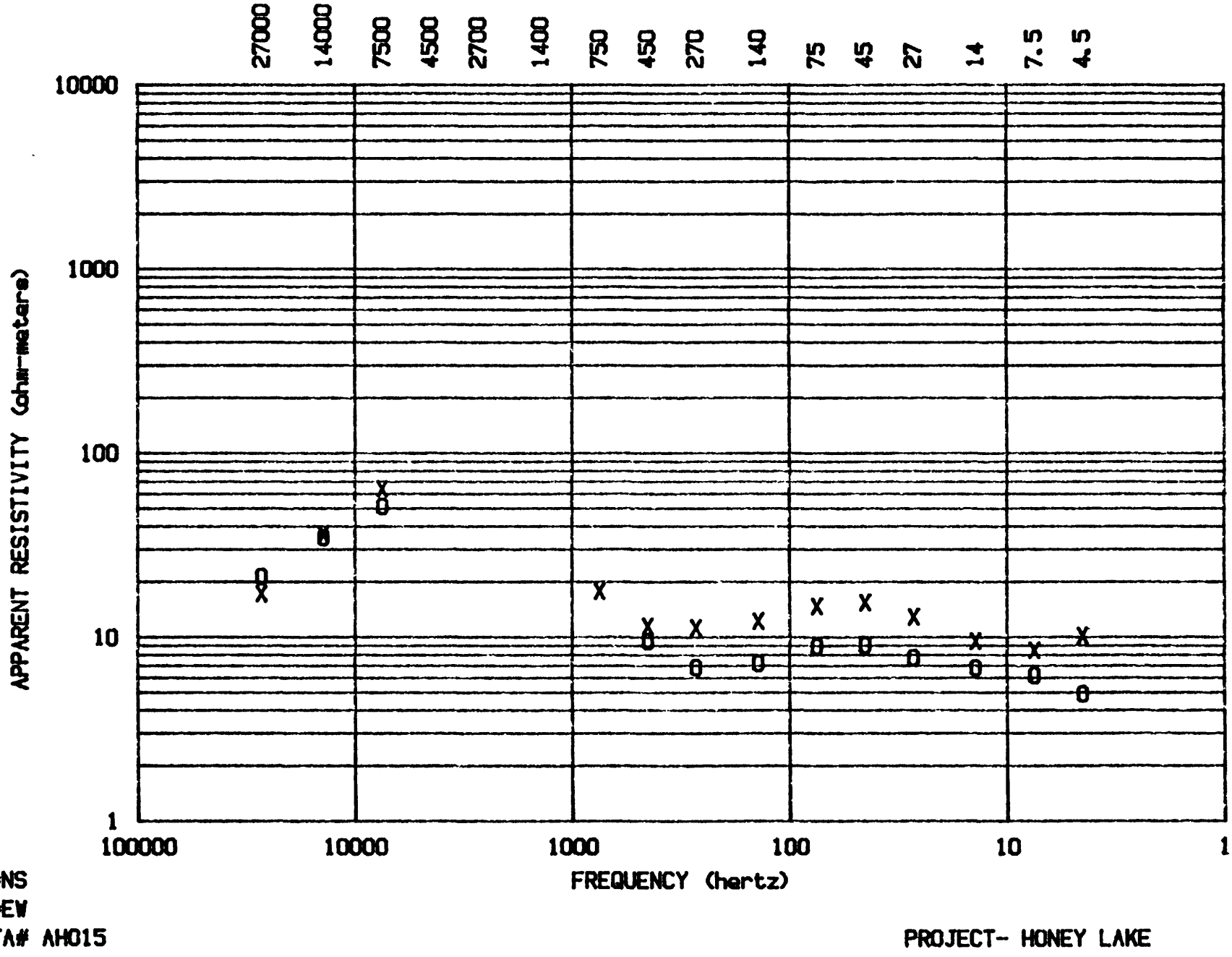
27000
14000
7500
4500
2700
1400
750
450
270
140
75
45
27
14
7.5
4.5
10000
1000
100
10
1
APPARENT RESISTIVITY (ohm-meters)
100000
10000
1000
100
10
1
FREQUENCY (hertz)
O=NS
X=EW
STA# AH015
PROJECT- HONEY LAKE

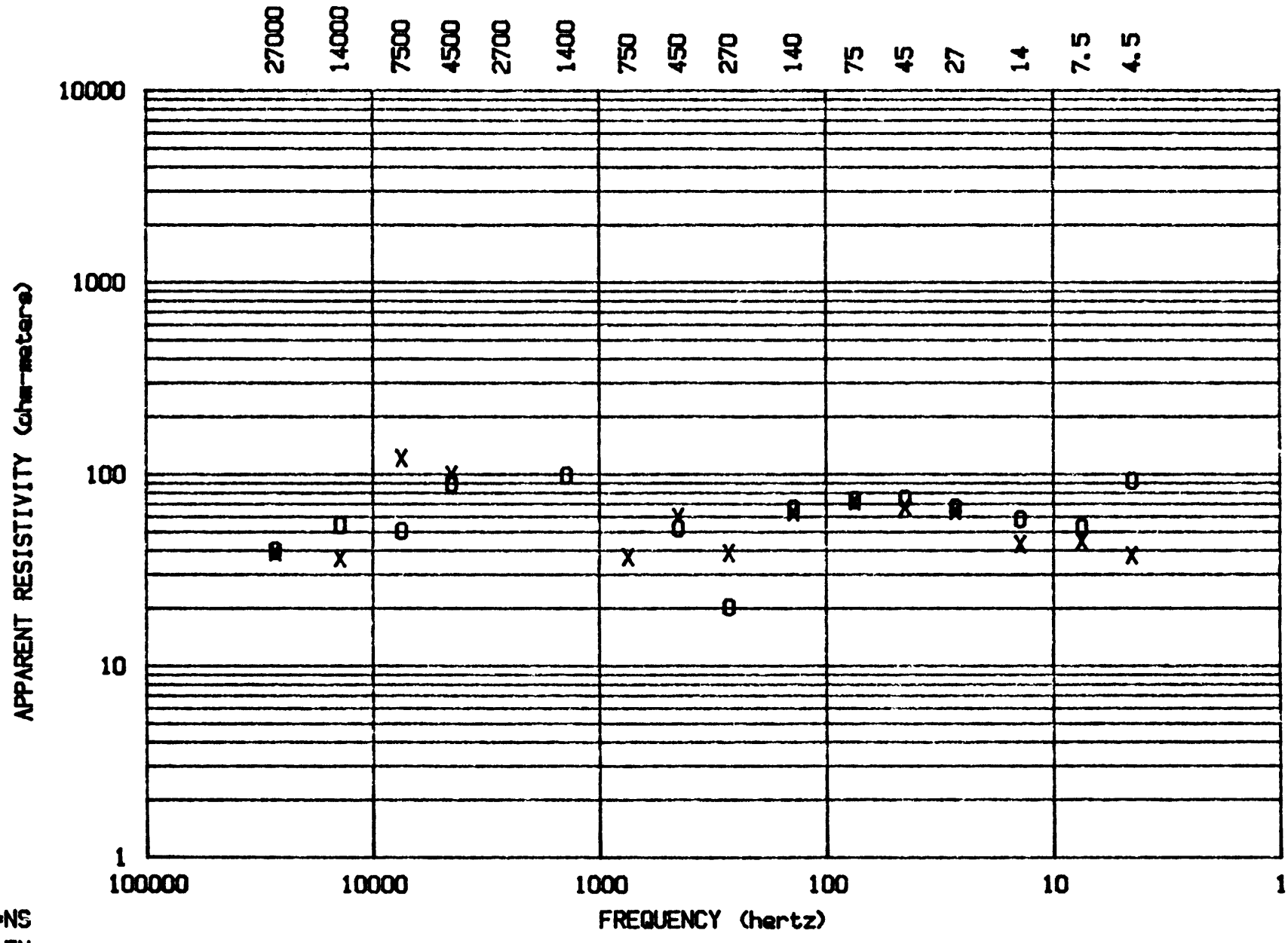

O=NS
X=EW
STA# AH016

PROJECT- HONEY LAKE

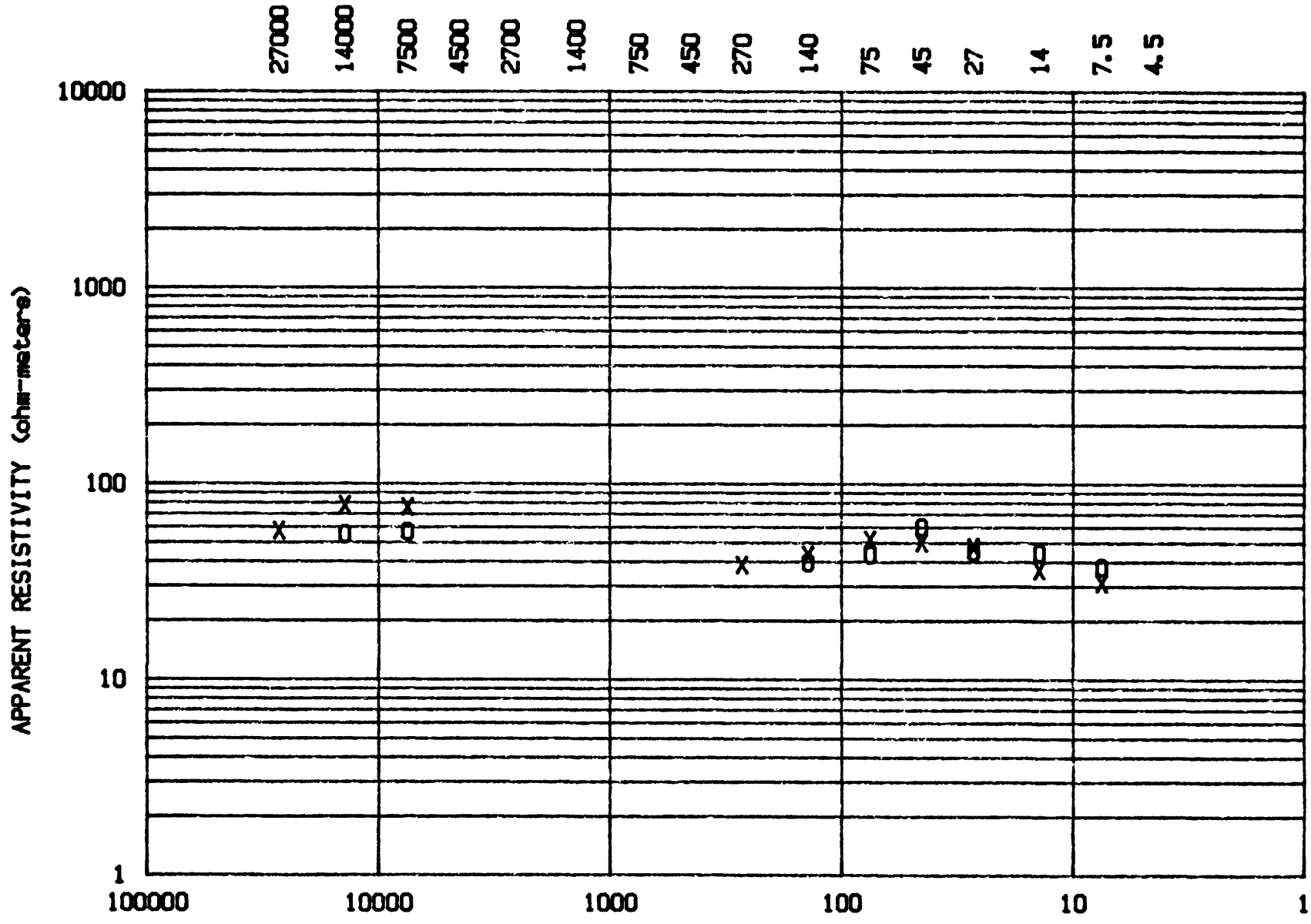

O=NS
X=EW
STA# AH017

PROJECT- HONEY LAKE

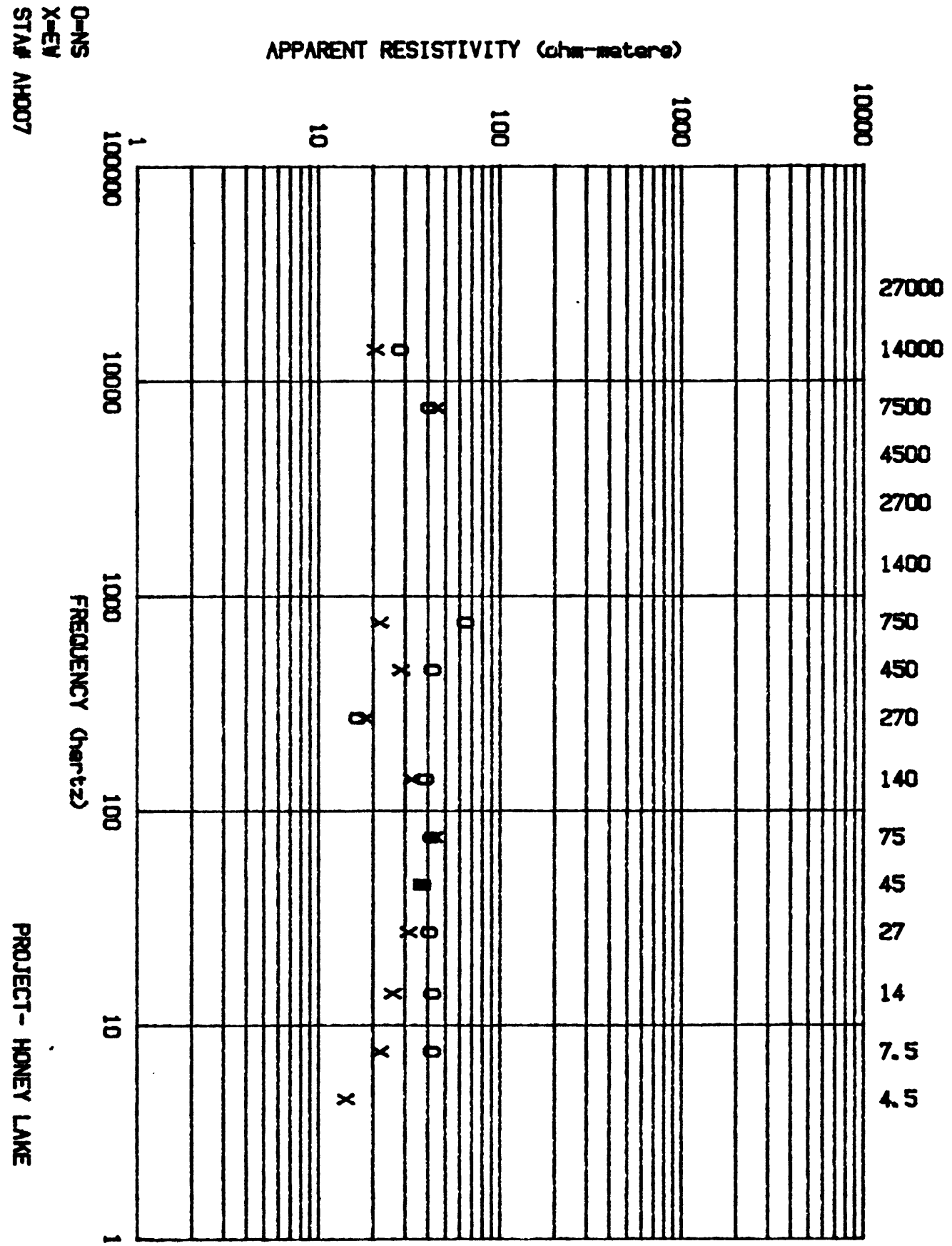
O=NS
X=EW
STA# AH007
APPARENT RESISTIVITY (ohm-meters)
1
10
100
1000
10000
100000
10000
1000
100
10
1
FREQUENCY (hertz)
27000
14000
7500
4500
2700
1400
750
450
270
140
75
45
27
14
7.5
4.5
PROJECT- HONEY LAKE

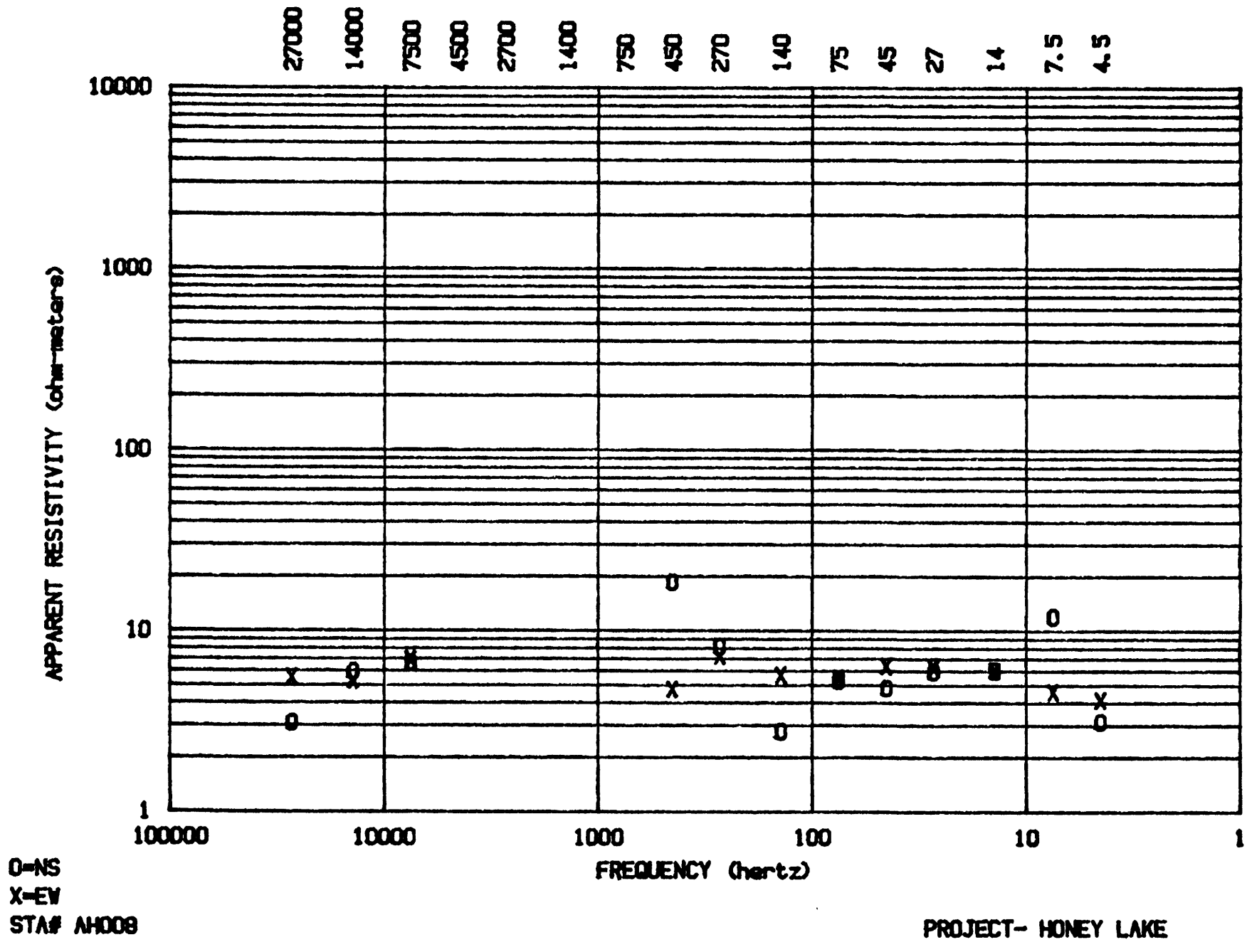
27000
14000
7500
4500
2700
1400
750
450
270
140
75
45
27
14
7.5
4.5
10000
1000
100
10
1
APPARENT RESISTIVITY (ohm-meters)
100000
10000
1000
100
10
1
FREQUENCY (hertz)
O=NS
X=EW
STA# AH008
PROJECT- HONEY LAKE

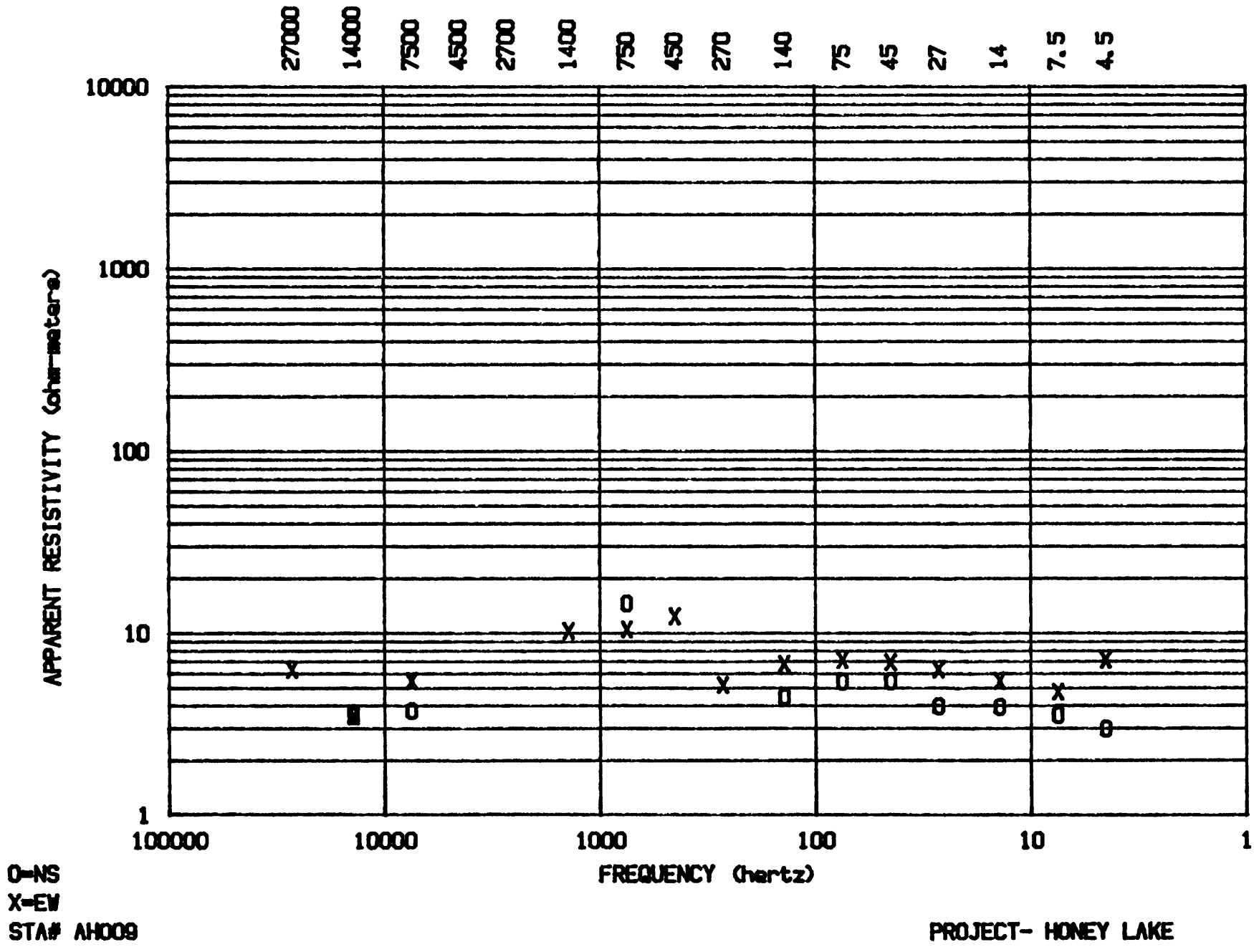
27000
14000
7500
4500
2700
1400
750
450
270
140
75
45
27
14
7.5
4.5
10000
1000
100
10
1
APPARENT RESISTIVITY (ohm-meters)
100000
10000
1000
100
10
1
FREQUENCY (hertz)
O=NS
X=EW
STA# AH009
PROJECT- HONEY LAKE

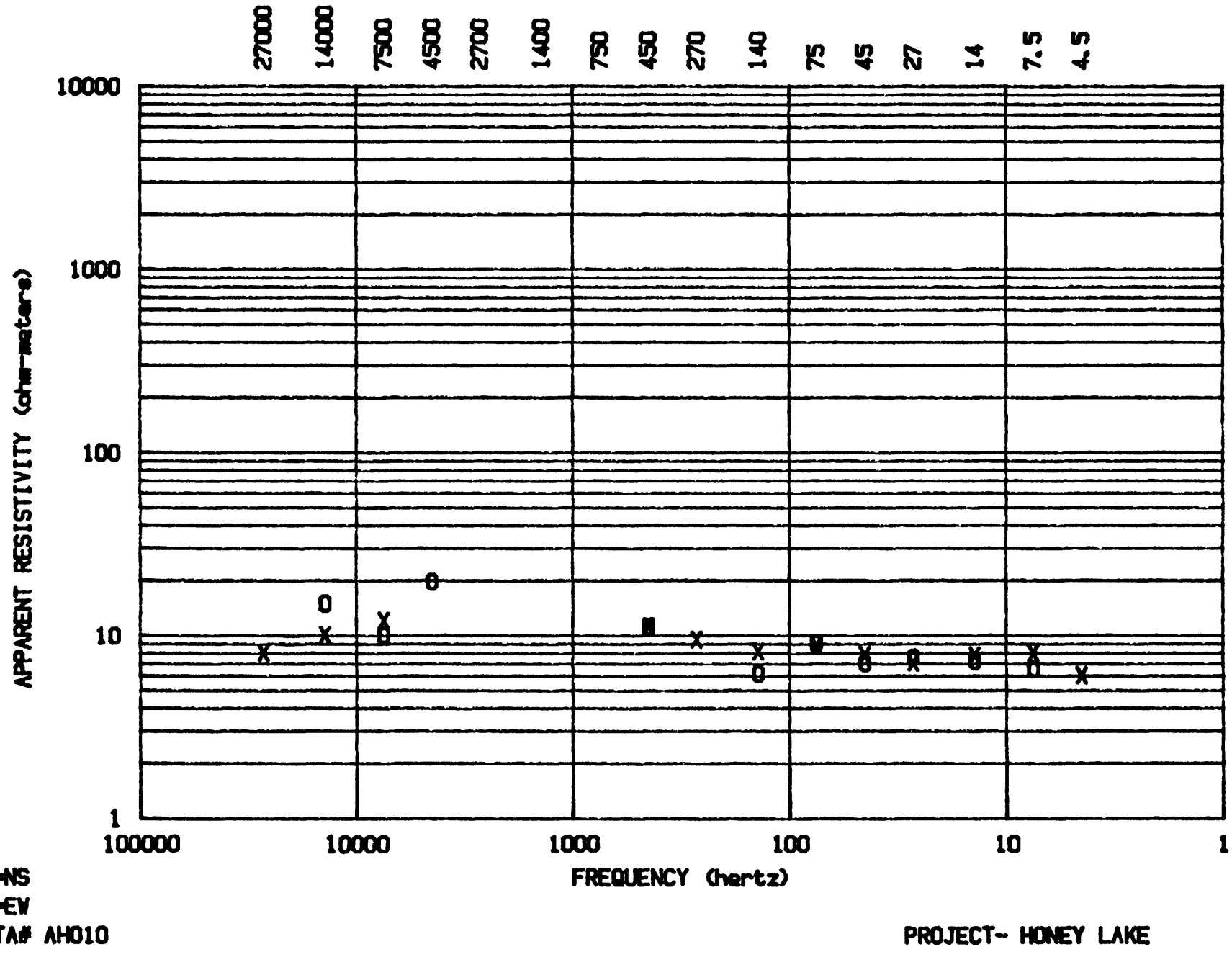
27000
14000
7500
4500
2700
1400
750
450
270
140
75
45
27
14
7.5
4.5
10000
1000
100
10
1
APPARENT RESISTIVITY (ohm-meters)
100000
10000
1000
100
10
1
FREQUENCY (hertz)
O=NS
X=EW
STA# AH010
PROJECT- HONEY LAKE

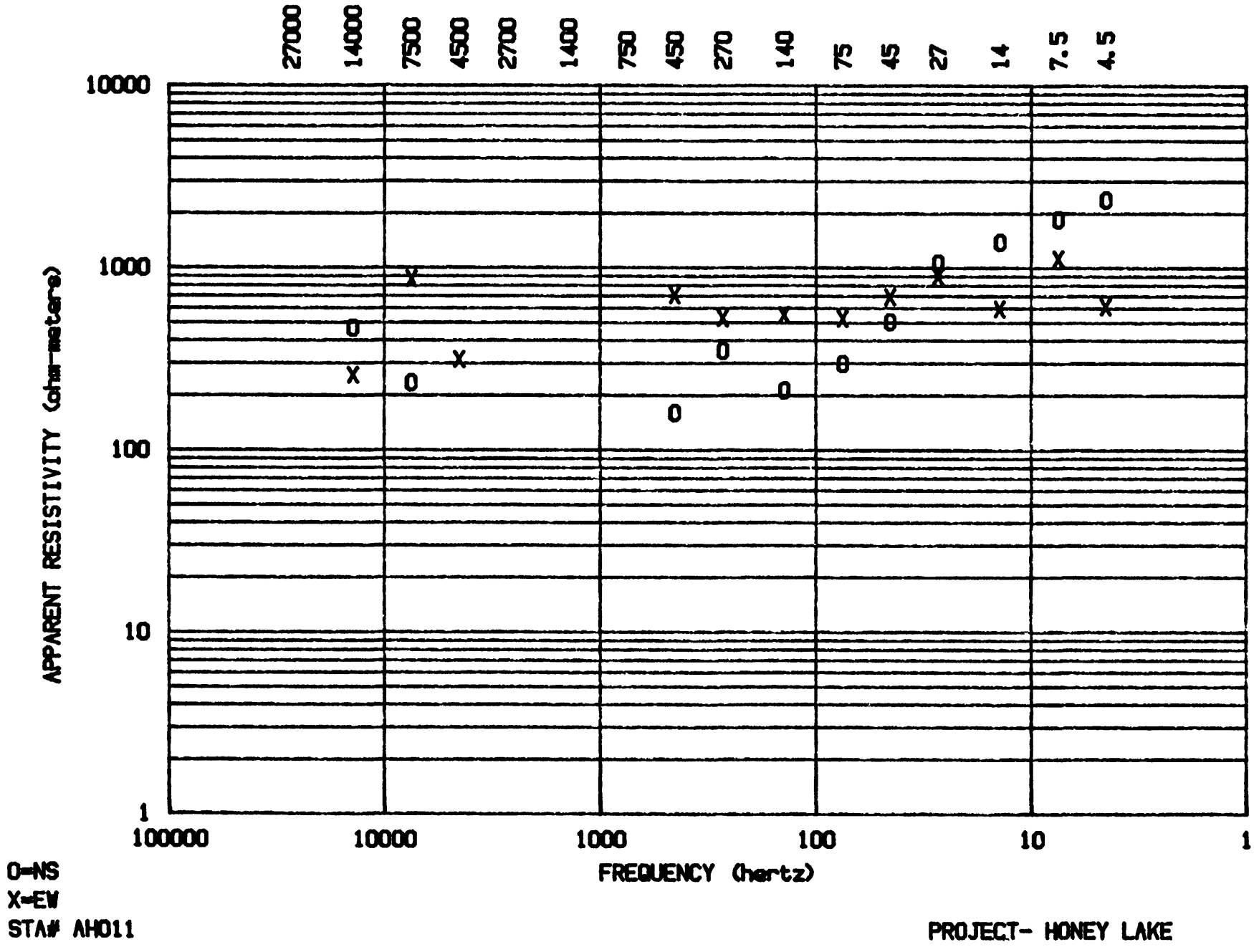
27000
14000
7500
4500
2700
1400
750
450
270
140
75
45
27
14
7.5
4.5
10000
1000
100
10
1
APPARENT RESISTIVITY (ohm-meters)
100000
10000
1000
100
10
1
FREQUENCY (hertz)
O=NS
X=EW
STA# AH011
PROJECT- HONEY LAKE

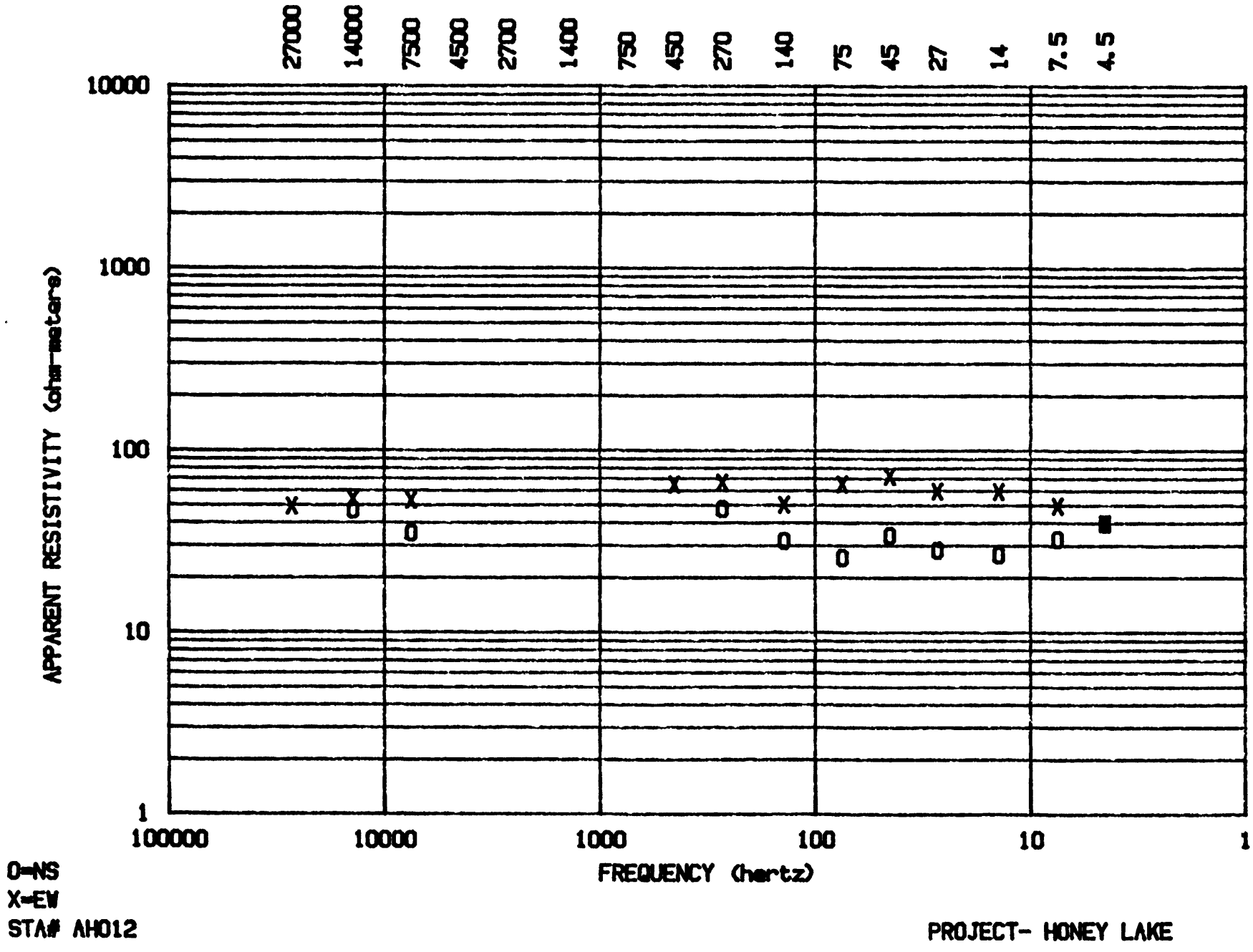
27000
14000
7500
4500
2700
1400
750
450
270
140
75
45
27
14
7.5
4.5
10000
1000
100
10
1
APPARENT RESISTIVITY (ohm-meters)
100000
10000
1000
100
10
1
FREQUENCY (hertz)
O=NS
X=EW
STA# AH012
PROJECT- HONEY LAKE

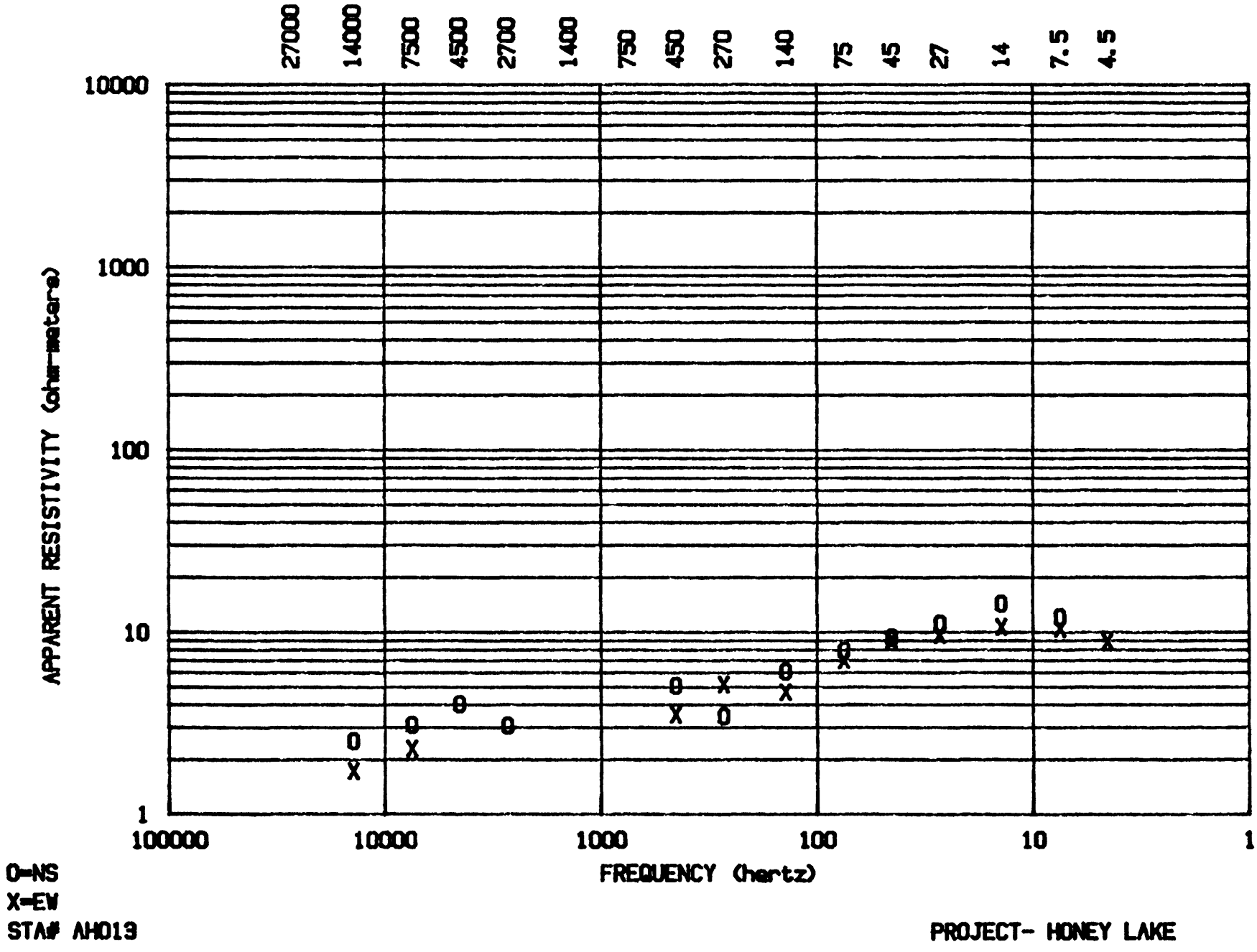
27000
14000
7500
4500
2700
1400
750
450
270
140
75
45
27
14
7.5
4.5
10000
1000
100
10
1
APPARENT RESISTIVITY (ohm-meters)
100000
10000
1000
100
10
1
FREQUENCY (hertz)
O=NS
X=EW
STA# AH013
PROJECT- HONEY LAKE

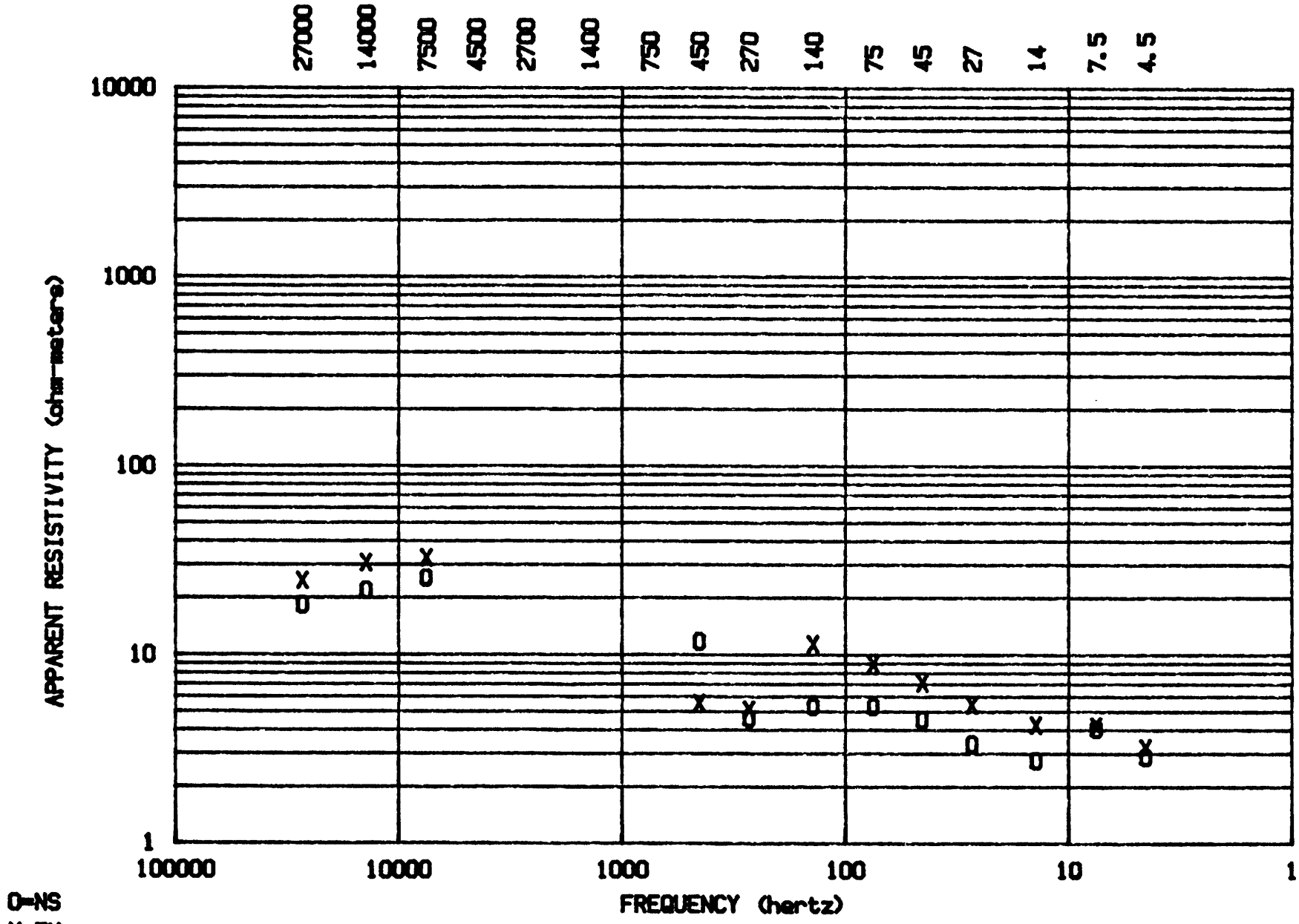
27000
14000
7500
4500
2700
1400
750
450
270
140
75
45
27
14
7.5
4.5
10000
1000
100
10
1
APPARENT RESISTIVITY (ohm-meters)
100000
10000
1000
100
10
1
FREQUENCY (hertz)
O=NS
X=EW
STA# AH014
PROJECT- HONEY LAKE

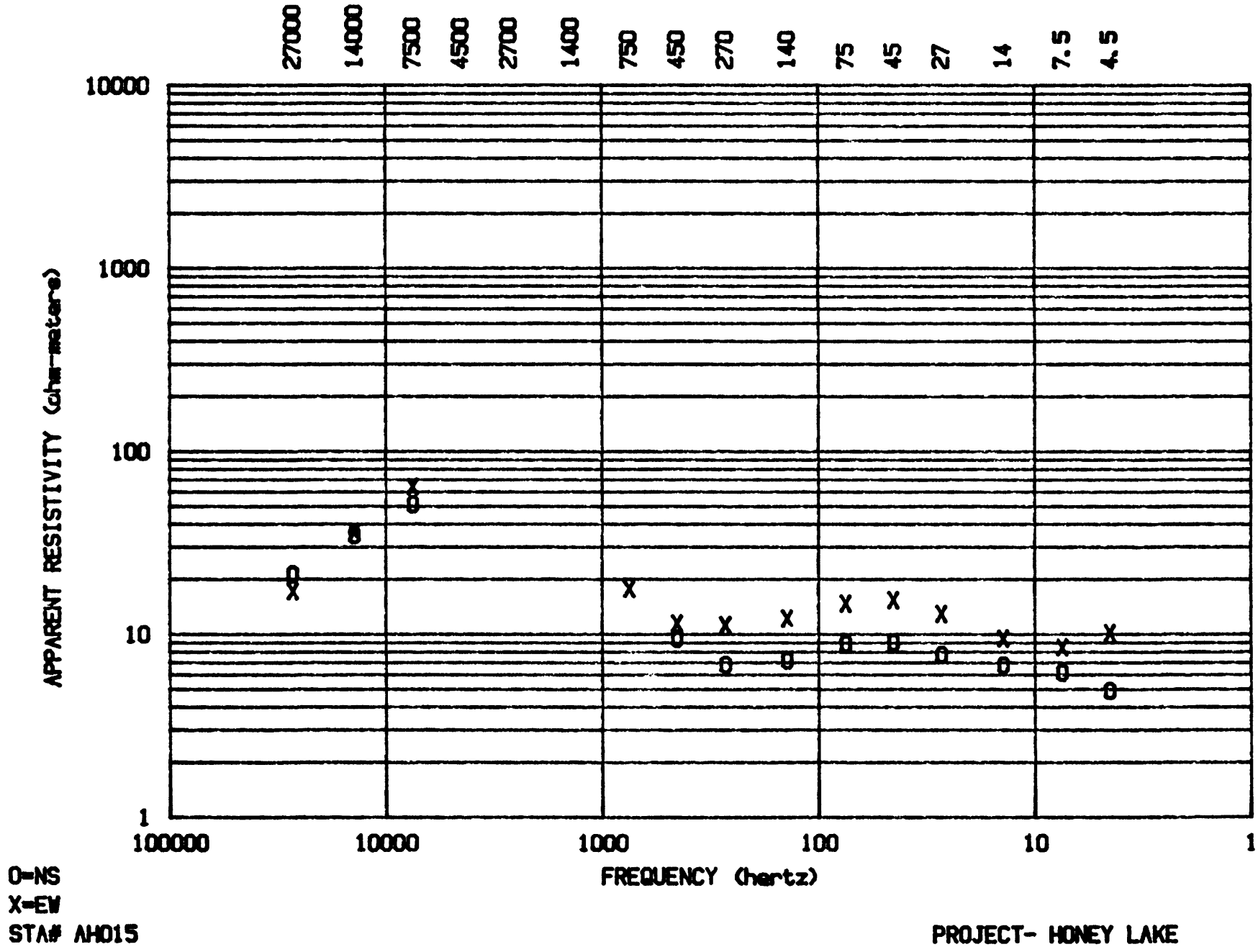
27000
14000
7500
4500
2700
1400
750
450
270
140
75
45
27
14
7.5
4.5
10000
1000
100
10
1
APPARENT RESISTIVITY (ohm-meters)
100000
10000
1000
100
10
1
FREQUENCY (hertz)
O=NS
X=EW
STA# AH015
PROJECT- HONEY LAKE

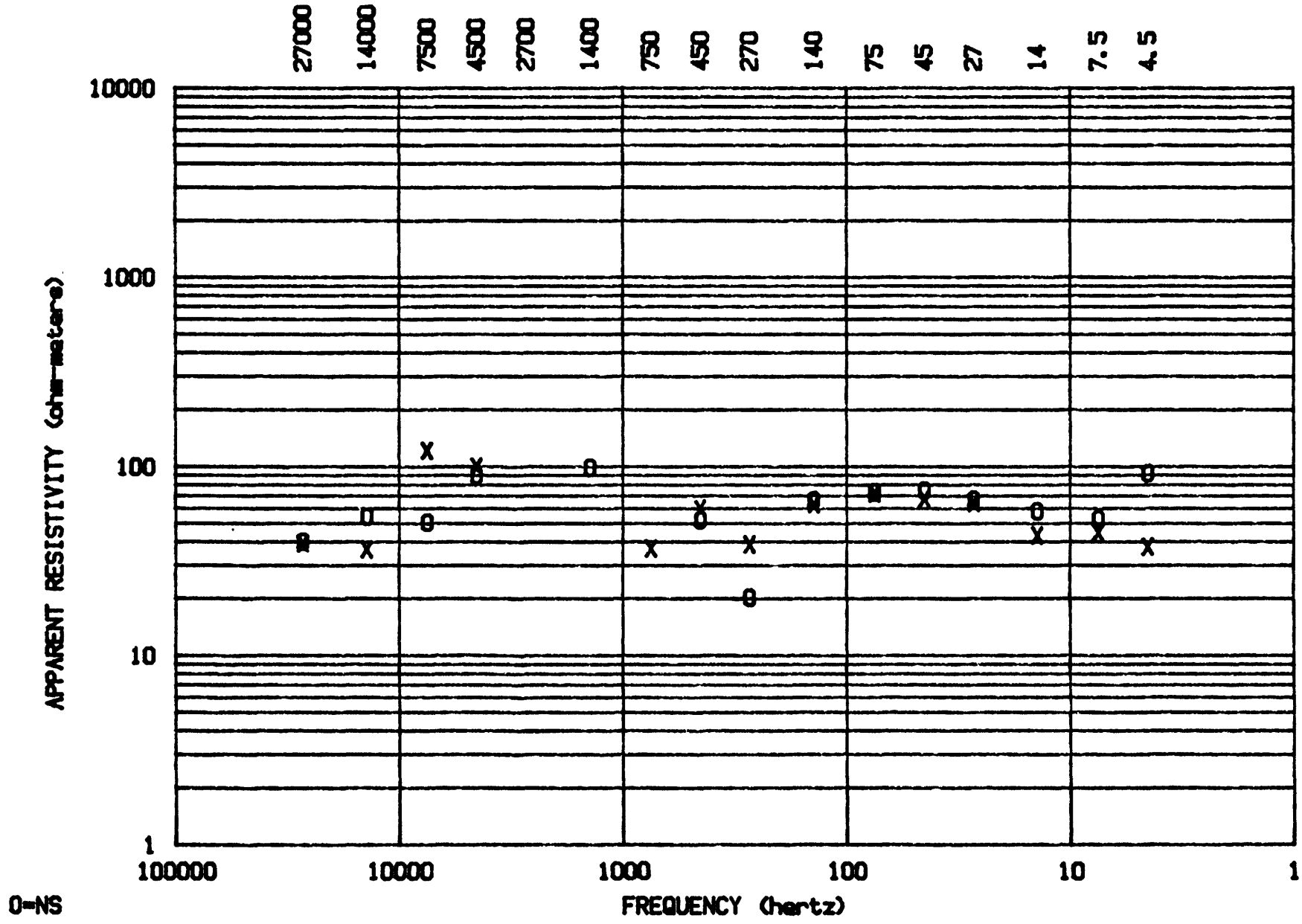
27000
14000
7500
4500
2700
1400
750
450
270
140
75
45
27
14
7.5
4.5
10000
1000
100
10
1
APPARENT RESISTIVITY (ohm-meters)
100000
10000
1000
100
10
1
FREQUENCY (hertz)
O=NS
X=EW
STA# AH016
PROJECT- HONEY LAKE

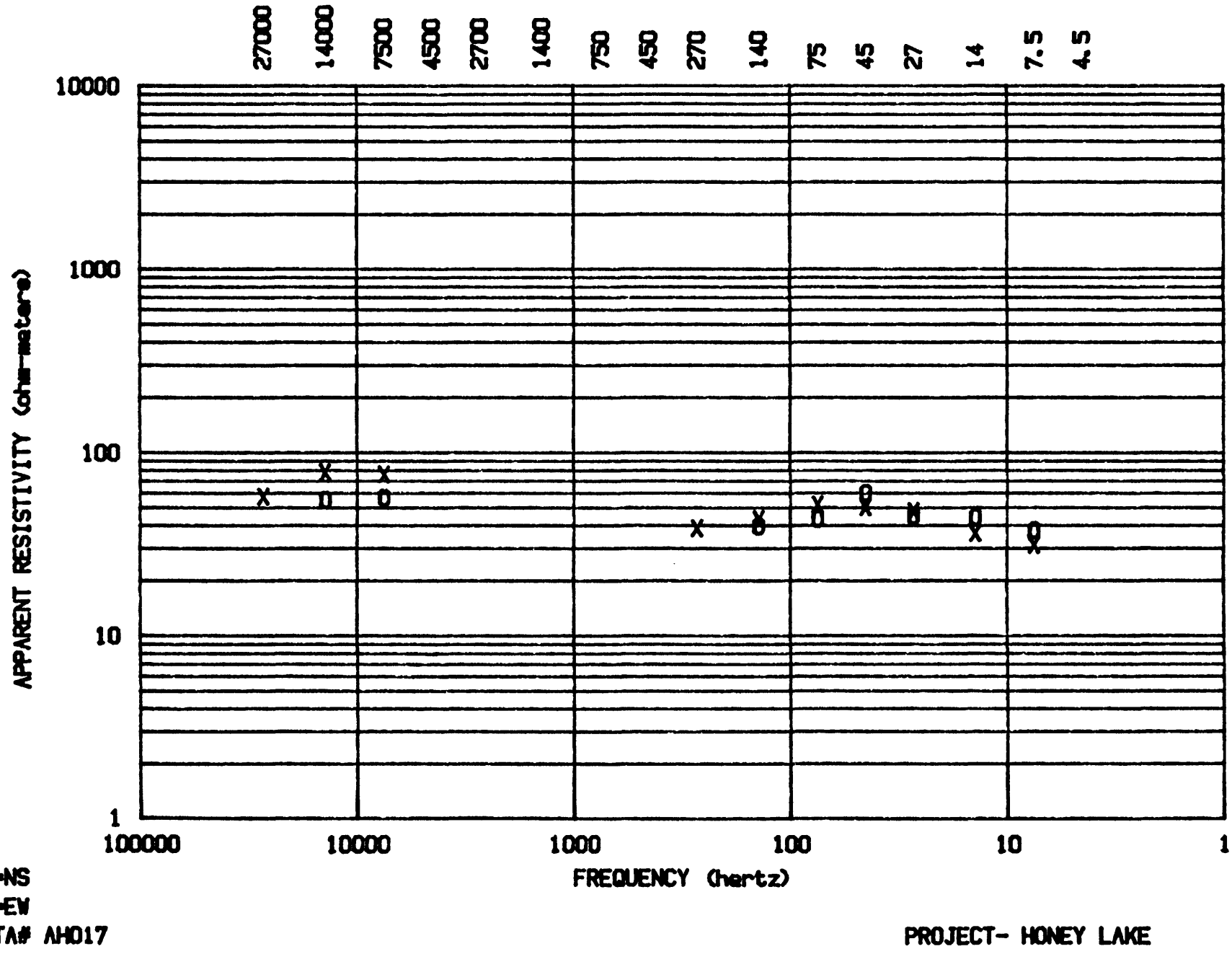
27000
14000
7500
4500
2700
1400
750
450
270
140
75
45
27
14
7.5
4.5
10000
1000
100
10
1
APPARENT RESISTIVITY (ohm-meters)
100000
10000
1000
100
10
1
FREQUENCY (hertz)
O=NS
X=EW
STA# AH017
PROJECT- HONEY LAKE

Appendix 4

TELLURIC TRAVERSE DATA
HONEY LAKE, LINE 1
500m DIPOLES

STATION NUMBER	FREQUENCY in Hz	RATIO	NUMBER of OBS.	STANDARD ERROR	DIPOLE POSITION	RELATIVE VOLATGE
0	.025	.60	8	.020	-500 to 0	1.00
0	7.500	.41	5	.005	-500 to 0	1.00
0	27.000	.42	5	.007	-500 to 0	1.00
500	.025	.40	10	.040	0 to 500	.60
500	7.500	.45	7	.021	0 to 500	.41
500	27.000	.42	5	.018	0 to 500	.42
1000	.025	.42	6	.070	500 to 1000	.24
1000	7.500	.58	5	.086	500 to 1000	.18
1000	27.000	.51	5	.160	500 to 1000	.17
1500	.025	.90	10	.060	1000 to 1500	.10
1500	7.500	.98	5	.013	1000 to 1500	.11
1500	27.000	.85	5	.014	1000 to 1500	.09
2000	.025	.84	9	.050	1500 to 2000	.09
2000	7.500	.66	5	.026	1500 to 2000	.10
2000	27.000	.82	5	.035	1500 to 2000	.08
2500	.025	.87	11	.030	2000 to 2500	.08
2500	7.500	.95	5	.029	2000 to 2500	.07
2500	27.000	.80	5	.043	2000 to 2500	.06
3000	.025	1.04	9	.040	2500 to 3000	.07
3000	7.500	.94	7	.063	2500 to 3000	.06
3000	27.000	1.02	5	.057	2500 to 3000	.05
3500	.025	.81	7	.030	3000 to 3500	.07
3500	7.500	.93	5	.007	3000 to 3500	.06
3500	27.000	.96	5	.019	3000 to 3500	.05
4000	.025	1.02	10	.010	3500 to 4000	.06
4000	7.500	1.01	6	.006	3500 to 4000	.06
4000	27.000	1.02	5	.041	3500 to 4000	.05
4500	.025	.88	11	.020	4000 to 4500	.06
4500	7.500	.91	5	.062	4000 to 4500	.06
4500	27.000	1.02	5	.016	4000 to 4500	.05
5000	.025	1.00	9	.020	4500 to 5000	.05
5000	7.500	1.01	5	.006	4500 to 5000	.05
5000	27.000	1.01	5	.018	4500 to 5000	.05
5500	.025	.96	12	.010	5000 to 5500	.05
5500	7.500	.97	5	.005	5000 to 5500	.05
5500	27.000	.96	5	.017	5000 to 5500	.05
6000	.025	1.15	11	.020	5500 to 6000	.05
6000	7.500	1.00	5	.013	5500 to 6000	.05
6000	27.000	.96	5	.024	5500 to 6000	.05
6500	.025	.84	8	.030	6000 to 6500	.06
6500	7.500	.93	5	.020	6000 to 6500	.05
6500	27.000	.96	5	.019	6000 to 6500	.05
7000	.025	1.00	11	.010	6500 to 7000	.05
7000	7.500	.94	7	.027	6500 to 7000	.05
7000	27.000	.99	5	.018	6500 to 7000	.05
7500	.025	1.15	10	.010	7000 to 7500	.05

7500	7.500	.91	6	.057	¦	7000	to	7500	.05
7500	27.000	1.00	6	.029	¦	7000	to	7500	.04
8000	.025	1.28	10	.010	¦	7500	to	8000	.05
8000	7.500	.96	5	.018	¦	7500	to	8000	.04
8000	27.000	.93	6	.029	¦	7500	to	8000	.05
8500	.025	1.47	10	.010	¦	8000	to	8500	.07
8500	7.500	1.01	5	.041	¦	8000	to	8500	.04
8500	27.000	1.09	5	.031	¦	8000	to	8500	.04
9000	.025	1.03	10	.010	¦	8500	to	9000	.10
9000	7.500	1.04	5	.022	¦	8500	to	9000	.04
9000	27.000	1.19	5	.070	¦	8500	to	9000	.05
	.025				¦	9000	to	9500	.10
	7.500				¦	9000	to	9500	.04
	27.000				¦	9000	to	9500	.05

TELLURIC TRAVERSE DATA
HONEY LAKE, LINE 1
500m DIPOLES

STATION NUMBER	FREQUENCY in Hz	RATIO	NUMBER of OBS.	STANDARD ERROR	DIPOLE POSITION	RELATIVE VOLATGE
3500	270.000	1.02	5	.010	3000 to 3500	1.00
4000	270.000	.93	5	.006	3500 to 4000	1.02
4500	270.000	1.03	5	.008	4000 to 4500	.94
5000	270.000	.95	5	.013	4500 to 5000	.98
5500	270.000	1.08	5	.007	5000 to 5500	.92
6000	270.000	.96	5	.012	5500 to 6000	.99
6500	270.000	.99	5	.004	6000 to 6500	.96
7000	270.000	.97	5	.011	6500 to 7000	.94
7500	270.000	1.03	5	.014	7000 to 7500	.91
8000	270.000	.88	5	.019	7500 to 8000	.94
8500	270.000	1.09	5	.008	8000 to 8500	.83
9000	270.000	1.27	5	.025	8500 to 9000	.91
	270.000				9000 to 9500	1.15

TELLURIC TRAVERSE DATA
HONEY LAKE, LINE 2
500m DIPOLES

STATION NUMBER	FREQUENCY in Hz	RATIO	NUMBER of OBS.	STANDARD ERROR	DIPOLE POSITION	RELATIVE VOLATGE
0	.025	1.22	6	.100	-500 to 0	1.00
0	7.500	1.25	6	.042	-500 to 0	1.00
0	27.000	1.33	6	.035	-500 to 0	1.00
0	270.000	1.18	7	.121	-500 to 0	1.00
500	.025	1.00	9	.040	0 to 500	1.22
500	7.500	.82	5	.025	0 to 500	1.25
500	27.000	.87	5	.024	0 to 500	1.33
500	270.000	.87	7	.016	0 to 500	1.18
1000	.025	1.37	10	.040	500 to 1000	1.22
1000	7.500	.90	7	.038	500 to 1000	1.03
1000	27.000	.93	7	.040	500 to 1000	1.16
1000	270.000	.90	7	.029	500 to 1000	1.03
1500	.025	.57	10	.040	1000 to 1500	1.67
1500	7.500	.73	7	.041	1000 to 1500	.92
1500	27.000	.74	7	.031	1000 to 1500	1.08
1500	270.000	.69	7	.019	1000 to 1500	.92
2000	.025	.96	9	.020	1500 to 2000	.95
2000	7.500	.95	8	.058	1500 to 2000	.67
2000	27.000	.98	7	.017	1500 to 2000	.80
2000	270.000	.89	7	.039	1500 to 2000	.64
2500	.025	.46	8	.060	2000 to 2500	.91
2500	7.500	.80	7	.028	2000 to 2500	.64
2500	27.000	.90	7	.016	2000 to 2500	.78
2500	270.000	.88	8	.016	2000 to 2500	.57
3000	.025	.61	8	.130	2500 to 3000	.42
3000	7.500	.89	4	.020	2500 to 3000	.51
3000	27.000	1.06	7	.038	2500 to 3000	.71
3000	270.000	1.06	7	.012	2500 to 3000	.50
3500	.025	.93	11	.080	3000 to 3500	.26
3500	7.500	.97	7	.011	3000 to 3500	.46
3500	27.000	.89	8	.021	3000 to 3500	.74
3500	270.000	.89	7	.019	3000 to 3500	.53
4000	.025	1.39	12	.060	3500 to 4000	.24
4000	7.500	.98	7	.018	3500 to 4000	.44
4000	27.000	.97	7	.017	3500 to 4000	.67
4000	270.000	1.06	7	.017	3500 to 4000	.47
4500	.025	.99	8	.020	4000 to 4500	.33
4500	7.500	1.16	9	.044	4000 to 4500	.43
4500	27.000	1.00	5	.009	4000 to 4500	.65
4500	270.000	.96	6	.025	4000 to 4500	.50
5000	.025	.79	8	.080	4500 to 5000	.33
5000	7.500	.64	7	.030	4500 to 5000	.50
5000	27.000	.62	6	.034	4500 to 5000	.65
5000	270.000	.57	5	.016	4500 to 5000	.48
5500	.025	1.86	8	.070	5000 to 5500	.26
5500	7.500	.90	7	.015	5000 to 5500	.32

5500	27.000	.86	7	.025	5000	to	5500	.40
5500	270.000	.74	6	.009	5000	to	5500	.27
6000	.025	1.30	8	.020	5500	to	6000	.48
6000	7.500	.99	6	.035	5500	to	6000	.29
6000	27.000	.92	7	.022	5500	to	6000	.34
6000	270.000	.99	6	.007	5500	to	6000	.20
6500	.025	1.25	9	.020	6000	to	6500	.63
6500	7.500	1.12	12	.059	6000	to	6500	.29
6500	27.000	1.06	6	.021	6000	to	6500	.31
6500	270.000	.94	6	.048	6000	to	6500	.20
	.025				6500	to	7000	.78
	7.500				6500	to	7000	.32
	27.000				6500	to	7000	.33
	270.000				6500	to	7000	.19